


UNIVERSITEIT GENT

FACULTY OF PHARMACEUTICAL SCIENCES

Ghent University

Faculty of Pharmaceutical Sciences

Department of Bioanalysis

Laboratory for Medical Biochemistry and Clinical Analysis

Characterizing hepatic clearance in early life: PBPK as modeling tool and tramadol as guide

Apr. Huybrecht T'jollyn

Thesis submitted to obtain the degree of Doctor in Pharmaceutical Sciences

Promotors

Prof. Dr. J. Van Bocxlaer

Prof. Dr. K. Boussery

Prof. Dr. A. Vermeulen

Copyright

SAMENVATTING

Het hoofdobjectief van dit doctoraatsproject was om fysiologisch-gebaseerde farmacokinetische (PBPK) modellen te evalueren m.b.t. hun betrouwbaarheid aangaande de 'bottom-up' voorspelling van de klaring in kinderen. Verder was het ons doel de hiaten te identificeren die mogelijks oorzaak zijn van onnauwkeurigheden in deze voorspellingen. In deze context werd tramadol gebruikt als modelgeneesmiddel om de 'bottom-up' en 'top-down' maturatiefuncties van de klaring te vergelijken in de volledige kinderpopulatie, en meer specifiek in neonaten en zuigelingen. De 'top-down' klaringsmaturatie werd geschat d.m.v. een populatie-farmacokinetisch (popPK) model in een gepoolde dataset gaande van neonaten tot volwassenen.

Hoofdstukken 3 & 4 behandelen het onderzoek aangaande het *in vitro* metabolisme van tramadol en de daaropvolgende constructie van verschillende tramadol PBPK klaringsmodellen, terwijl hoofdstukken 5 & 6 focussen op het gebruik van het finale tramadol klaringsmodel voor de predictie van de klaring van tramadol in kinderen. In **Hoofdstuk 3** beschrijven we de resultaten van de ***in vitro* metabolisme experimenten met tramadol** en de **contributies van de verschillende enzymen die betrokken zijn in de hepatisch klaring** van dit geneesmiddel. Het metabolisme van tramadol werd onderzocht in humane levermicrosomen (HLM) en humane recombinante CYP-enzymen (rhCYP). Parameters van het *in vitro* metabolisme (CLint, Km, Vmax) werden geschat via niet-lineaire regressieanalyse. Deze *in vitro* metabolismeparameters van tramadol werden geëxtrapoleerd naar een *in vivo* hepatische klaring, gebruik makend van het ***in vitro-in vivo* extrapolatieprincipe** (IVIVE), reeds geïmplementeerd in de Simcyp® PBPK Simulator. Terzelfdertijd werd een **retrograad klaringsmodel** opgesteld in Simcyp®, gebaseerd op *in vivo* klaringsdata. Dit model voorspelt de *in vivo* klaring, wat werd onderbouwd d.m.v. een accurate voorspelling van hepatische enzym- en renale contributies. De IVIVE-klaringsmodellen (opgebouwd uit de HLM en rhCYP data) werden vergeleken met het retrograad klaringsmodel wat betreft de absolute klaringsvoorspelling en de contributies van de hepatische enzymen. Op theoretische gronden werd voor de IVIVE-klaringsmodellen een factor van 1.58 geïncorporeerd, die rekening houdt met de opstapeling van tramadol in het intracellulair milieu ('ion trapping'). De resultaten tonen aan dat de **voorspelling van de totale tramadolklaring binnen een factor 2** van de geobserveerde klaring valt, echter met **verschillen in enzymcontributies** in vergelijking met de *in vivo* situatie. Daarboven toonde een sensitiviteitsanalyse aan dat de bloed-plasma ratio en de intracellulaire accumulatie in de levercel de predictie van de leverklaring sterk beïnvloedden.

In **Hoofdstuk 4** onderzochten we de **oorzaak van de verschillen tussen *in vitro*** en *in vivo* **hepatische enzymcontributies** (Hoofdstuk 3). We stelden een algemene **strategie op om correcte enzymcontributies**

te implementeren in de opschaling van de *in vitro* naar de *in vivo* klaring. Eerst werden de referentiestoffen dextrometorphan en midazolam geïncubeerd - naast tramadol - in dezelfde HLM batch om de activiteit van de CYP2D6 en CYP3A4 enzymen te bepalen. Ten tweede, een retrograad model voor beide referentiestoffen liet ons toe om te berekenen wat de *in vitro* CYP activiteit had moeten zijn, teruggerekend vanuit hun respectievelijke *in vivo* data. Ten derde, een 'activity-adjustment factor' (AAF) werd berekend als de ratio van de *in vitro* gemeten/*in vitro* teruggerekende CYP activiteit voor CYP2D6 en CYP3A4. De AAF die werd bekomen voor CYP2D6 en CYP3A4 was 1.97 en 0.91, respectievelijk. Dit impliceert dat de *in vitro* CYP2D6 activiteit circa 2-voud lager ligt dan de teruggerekende CYP2D6 activiteit. Deze daling in *in vitro* CYP2D6 activiteit werd reeds voorheen beschreven in de literatuur. De verklaring die werd gegeven was dat het CYP2D6 enzym leidt aan enzyminstabiliteit. De correctie van de tramadol IVIVE-klaringsmodellen met de AAF voor CYP2D6 en CYP3A4, zorgde ervoor dat de CYP contributies in deze modellen gealigneerd waren met hun *in vivo* contributies (zoals geïncorporeerd in het retrograad klaringsmodel). Er dienen echter nog meer geneesmiddelen bestudeerd te worden om deze strategie meer algemeen te valideren.

Hoofdstuk 5 beschrijft de kwalificatie van het tramadol retrograad klaringsmodel voor volwassenen en de evaluatie van de 'bottom-up' klaringsvoorspelling in kinderen, gebruik makend van de Simcyp® Simulator, t.o.v. de *in vivo* observaties van de tramadolklaring in kinderen. Het retrograad klaringsmodel incorporeert op mechanistische wijze de enzymcontributies van CYP2D6, CYP3A4, CYP2B6 evenals de renale klaring. Dit model werd gekwalificeerd op basis van beschikbare *in vivo* PK parameters van tramadol in volwassenen. Als eerste controlestap werden 2 pediatrische HLM batchen (van 1 en 3 maand oude kinderen) geïncubeerd met tramadol en de referentiestoffen dextrometorphan (CYP2D6) en midazolam (CYP3A4). Dit experiment bevestigde de hypothese dat O-desmethyltramadol voor het overgrote deel door CYP2D6 wordt gemetaboliseerd, terwijl de vorming van NDT niet gecorreleerd was met de CYP3A4 activiteit. CYP2B6 speelt inderdaad ook nog een rol in de vorming van NDT. In een volgende stap werd de tramadol klaringsmaturatie in pediatrische subjecten voorspeld d.m.v. virtuele populaties. Twee gepubliceerde popPK modellen die de maturatie van de totale en CYP2D6 tramadolklaring in neonaten/zuigelingen (exponentieel model) en over de volledige humane leeftijdsrange (Hill model) beschrijven, werden geselecteerd als referentie. Echter, het Hill model werd verkozen boven het exponentieel model in termen van totale en CYP2D6 klaring zowel voor neonaten/zuigelingen als voor de rest van de pediatrische leeftijdscategorieën. Additioneel werd de maturatie in renale klaring bekomen door het individueel fitten van urinaire tramadolconcentraties bij 9 subjecten a.d.h.v. WinNonlin®. Door het visueel vergelijken van de voorspelde Simcyp® 'bottom-up' klaringswaarden met de bekomen klaringswaarden uit het Hill maturatiemodel, werd besloten dat de 'bottom-up' methode de maturatie in de klaring goed capteert. Desalniettemin werd een algemene

onderpredictie geobserveerd in de totale en CYP2D6 klaringen, echter niet in de renale klaring. Een verschil in fysiologie (bvb. levergewicht) werd verantwoordelijk geacht voor deze discrepantie, gezien de totale en de CYP2D6 klaring een gelijkaardige onderpredictie vertoonden.

Hoofdstuk 6 bouwt verder op het open einde van Hoofdstuk 5 door de invloed van variaties in systeem-gerelateerde (biologie/fysiologie) informatie te bestuderen op de 'bottom-up' voorspelling van de hepatische klaring in pediatrische virtuele subjecten. In deze context werden drie commercieel beschikbare PBPK softwarepaketten (PK-Sim®, Simcyp®, en Gastroplus®) onderzocht m.b.t. hun verschillende systeem-gerelateerde informatie en de consequentie hiervan op de voorspelling van de klaring. In elke software werd een retrograad klaringsmodel opgesteld dat de renale en de hepatische tramadol klaring mechanistisch voorspelde in volwassenen. Deze keer werden de retrograde modellen gecalibreerd aan de populatiepredictie van het Hill model voor volwassenen, zodat elk verschil tussen 'bottom-up' (PBPK) en 'top-down' (Hill) voorspelde klaringswaarden enkel te wijten kon zijn aan een verschil in maturatiefuncties. Elk retrograad model werd gekwalificeerd in termen van totale, CYP2D6, en renale tramadol klaringen. De pediatrische tramadol klaringen werden vergeleken tussen de verschillende PBPK modellen (bottom-up) en het Hill model (top-down) in de range van neonaten tot adolescenten. Door de aanwezige variaties in fysiologische data, zoals gebruikt door elke PBPK tool, werden relevante verschillen in de voorspelling van de hepatische klaring in kinderen vastgesteld. Interessant is dat in het geval van CYP2D6, het PBPK model met het kortste maturatiehalfleven resulteerde in de beste predictie van de *in vivo* tramadol CYP2D6 klaring. Consensus over welke fysiologische data het best dienen gebruikt te worden in deze PBPK modellen, zou pediatrische klaringsvoorspelling kunnen harmoniseren en optimaliseren. Daarenboven, de combinatie van 'bottom-up' en 'top-down' technieken, gebruik makend van een gepaste referentiestof, bezit potentieel om systeem-gerelateerde parameters aan te passen om op die manier de pediatrische fysiologie beter te capteren. Analoog onderzoek met bijkomende geneesmiddelen is aangewezen om deze resultaten verder te confirmeren.

SUMMARY

The main aim of this PhD project was to evaluate a physiologically-based pharmacokinetic (PBPK) approach for a reliable bottom-up clearance prediction in pediatric life, and to identify the gaps that underlie potential prediction inaccuracies. In this light, tramadol was used as a model compound to compare the bottom-up to the top-down clearance maturation function across pediatric life, with a particular focus on neonates/infants. The top-down clearance maturation was estimated from a population PK investigation in a pooled data set, ranging from neonates to adults.

Chapter 3 & 4 outline the investigation of tramadol's *in vitro* metabolism and the subsequent construction of different tramadol adult PBPK clearance models, while Chapters 5 & 6 focus on using this adult PBPK model for the prediction of the pediatric tramadol clearance. In Chapter 3, we describe the results from ***in vitro*** **metabolism experiments for tramadol** and the associated **enzyme contributions to the hepatic clearance** of this compound. Tramadol metabolism was investigated in human liver microsomes (HLM) and human recombinant enzyme systems (rhCYP). Based on the formation rates of tramadol metabolites, *in vitro* metabolism parameters (CLint, Km, Vmax) were estimated via non-linear regression analysis. These *in vitro* tramadol metabolism parameters were extrapolated to achieve the *in vivo* hepatic clearance, using the so-called ***in vitro*****-to-*****in vivo*** **extrapolation** (IVIVE) method, implemented in the **Simcyp®** PBPK Simulator. In parallel, a **retrograde clearance model** in Simcyp® was set up, built from *in vivo* clearance data. This model predicts the *in vivo* clearance, substantiated with accurate predictions of the involvement of enzymes and renal processes. The IVIVE clearance models (from HLM data and from rhCYP data) were compared to the retrograde clearance model in terms of absolute clearance and hepatic enzyme contributions. For the IVIVE clearance models, a factor of 1.58 was incorporated based on theoretical grounds, which accounts for tramadol accumulation in the intracellular milieu due to ion trapping. The results indicate that the **prediction of tramadol clearance is within two-fold** of the observed clearance value, albeit with **differences in hepatic enzyme contributions**, compared to *in vivo*. In addition, a sensitivity analysis indicated that especially the blood-plasma ratio and the hepatic accumulation were factors influencing the bottom-up prediction of the clearance.

In Chapter 4, we describe our efforts to **identify the reason for the *in vitro* inaccuracies** in the CYP enzyme contributions described in Chapter 3, and propose a general **strategy to implement correct enzyme contributions** in the IVIVE clearance models. First, the probe substrates dextromethorphan and midazolam were incubated alongside tramadol in the same HLM batch to determine the *in vitro* activity of CYP2D6 and CYP3A4, respectively. Second, a retrograde clearance model for both compounds allowed to calculate what the *in vitro* CYP activities should have been, by back-calculation from the *in*

vivo clearance in the population. Third, an activity-adjustment factor (AAF) was calculated as the ratio of the *in vitro* measured/*in vitro* back-calculated activity for CYP2D6 and CYP3A4. The AAF for CYP2D6 and CYP3A4 were determined as 1.97 and 0.91. This implies that for pooled HLM assays, the *in vitro* CYP2D6 activity is approximately 2-fold lower compared to the expected value. A decrease in HLM CYP2D6 activity has already been observed in literature. Enzyme instability seemed to be responsible for this phenomenon. Hence, correction of the existing IVIVE models with the AAF provided CYP contributions, which were aligned in both *in vitro* systems and agreed well with *in vivo* contributions. However, more compounds should be investigated with this approach to validate our results.

Chapter 5 outlines the qualification of the adult retrograde clearance model and the evaluation of the bottom-up prediction of pediatric clearance , using the Simcyp® Simulator, against *in vivo* pediatric data. The adult retrograde model for tramadol mechanistically incorporated enzyme contributions for CYP2D6, CYP3A4, CYP2B6 and renal clearance. This model was qualified based on available tramadol *in vivo* PK parameters in adults. As a first checkpoint, 2 pediatric HLM samples (originating from a 1 and a 3 month old child) were incubated with tramadol and probe substrates dextromethorphan (CYP2D6) and midazolam (CYP3A4). This experiment confirmed our belief that O-desmethyltramadol, as in adults, is mainly CYP2D6 mediated, while CYP3A4 activity did not seem to correlate with NDT formation. CYP2B6 might indeed also be involved in this conversion step. In a next step, the maturation of tramadol clearance was predicted by letting Simcyp® generate virtual pediatric subjects. Two published population PK models that respectively described the maturation of total and CYP2D6 tramadol clearance in neonates/infants (exponential model) and over the complete lifespan in a pooled population (Hill model), were considered as reference. However, the Hill model was preferred over the exponential model in terms of total and CYP2D6 clearance in early life as well as over the complete pediatric life span. In addition, the maturation of the renal clearance was obtained by fitting urinary data for 9 subjects in a one-by-one WinNonlin® modelling effort. By visually comparing the Simcyp® bottom-up predicted clearance values to the *in vivo* Hill maturation model, the bottom-up approach seemed to capture the overall maturation trend well. However, a general underprediction was apparent in the total and CYP2D6 clearance maturation, but not in the renal clearance. A difference in physiology (e.g. liver size) between the real and virtual pediatric subjects was assumed to be the reason, both affecting predicted total and CYP2D6 clearance in a similar way.

Chapter 6 addresses the open ending of Chapter 5 by comparing the influence of variations in system-related information on the bottom-up prediction of the hepatic clearance using pediatric virtual subjects. To this end, three commercially available PBPK softwares (PK-Sim®, Simcyp®, Gastroplus®) were investigated for differences in system-related information and their effects on prediction of the clearance. In each software tool, a retrograde clearance model was constructed to mechanistically

describe hepatic and renal tramadol clearance in adults. This time, the retrograde clearance models were calibrated to the population prediction of the Hill model in adults, so that any difference in predicted and *in vivo* pediatric clearance would be solely attributable to differences in maturation. Each retrograde clearance model was qualified in terms of **total, CYP2D6, and renal clearance.** Pediatric tramadol clearance predictions were compared between the different PBPK (bottom-up) models and the Hill (top-down) model in the range from neonates to adolescents. Since variations were present in physiological data used by the PBPK softwares, **relevant differences were picked up in the hepatic clearance prediction** in children. Interestingly, in the case of **CYP2D6**, the PBPK model with the shortest maturation half-life agreed best with the *in vivo* CYP2D6 maturation. **Consensus on the selection of the best pediatric data** to use, should help to further harmonize and optimize pediatric clearance predictions. Moreover, the **combination of bottom-up and top-down** approaches, using a carefully selected probe substrate, holds potential in **updating system-related parameters** to better represent pediatric physiology. Investigations using additional compounds need to be performed to further strengthen these results.

DANKWOORD

Het dankwoord. Het enige deel van het doctoraat dat niet onder review staat, maar toch door iedereen wordt gelezen. Daarom wil ik mij nu reeds excuseren mocht ik iemand vergeten zijn! Ik ervaarde een doctoraat als een confrontatie. Een confrontatie met andere wetenschappers, je naasten, maar voornamelijk met jezelf. Door deze periode weet ik beter wie ik ben en wat ik waard ben op professioneel én peri-professioneel gebied. Ik ben dan ook erg dankbaar dat ik deze kans heb gekregen.

Mijn dank gaat uit naar mijn promotoren Jan Van Bocxlaer, Koen Boussery en An Vermeulen. Bedankt voor deze mooie opportuniteit en het in mij gestelde vertrouwen om dit project tot een goed eind te brengen. De initiële voorbereidingen voor het IWT, verschillende buitenlandse cursussen & workshops, de zomerstage bij Model-Based Drug Development in Janssen Pharmaceutica, Beerse, het finaal reviewen van de doctoraatsthesis (met strakke deadline, volgens An mijn *signature mark*), zijn geselecteerde voorbeelden waar een welgemeende 'dankuwel' op z'n plaats is. Ook een welgemeende dank aan de leden van mijn examenjury om het manuscript grondig door te nemen en van de nodige commentaren te voorzien.

Tijdens de eerste paar maanden, mocht ik ervaring opdoen in het DMPK departement in Janssen Pharmaceutica, Beerse. Hier heb ik leren incuberen en stalen analyseren. De plejade aan beschikbare technieken (LC-massaspectrometrie, LC-radiometrie, liquid scintillation counting (with and without combustion)) en de analysten die altijd op mijn vele vragen antwoord hadden, gaven een reële boost aan het hele project. Er zijn teveel mensen die ik zou moeten bedanken, dus vergeef mij enige dwaling. Bedankt Peter, Veronique, Sofie, Aline, Ivo, Dirk, Willy, Helga, Lieve, Filip om mij te ondersteunen in deze initiële fase van het project. Geert Mannens, jij was voor mij een katalysator in dit hele gebeuren. Ik wil je bedanken voor de opportuniteit om mijn onderzoeksstage 1e Master geneesmiddelenontwikkeling onder jouw supervisie te mogen doorbrengen. Door je ongebreideld enthousiasme en onze succesvolle samenwerking (+publicatie in DMD!), heb je wel degelijk de ADME-bacterie laten overslaan. Nog steeds is dit vakgebied voor mijeen onuitputbare bron van wetenschappelijk uitdaging en verwondering, dank daarvoor! Achiel Van Peer, ook jou wil ik bedanken voor je efforts in de eerste draft (!) van dit project, je oprechte en continue interesse, en kritische blik in dit project, het ga je goed! Jan Snoeys, jouw visie op en expertise in in vitro drug metabolisme en de implementatie ervan in PBPK modellen, liet een nieuwe (virtuele) wereld voor mijn ogen ontvouwen. Ik ben je erg dankbaar voor je inzichten, je bereikbaarheid en wetenschappelijke integriteit.

Karel Allegaert, bedankt voor uw kritisch visie, uw beschikbaarheid en uw betrokkenheid in het pediatrisch (neonataal) onderzoek. Ik ben ervan overtuigd dat uw initiatieven in dit vakgebied zullen leiden tot betere 'dose precision' bij ons meest kwetsbare populatie. Pieter Annaert wil ik oprecht bedanken voor het kritisch nalezen van mijn verschillende publicaties.

Graag wil ik ook mijn collega's bedanken van het LMBKA in Gent die steeds voor een aangename sfeer zorgden. Bedankt, Lisl voor het betere secretariaatswerk, Wim voor hulp bij de analyses en het practicum, doorspekt met een gezonde portie ironie, en Sofie voor je betrokkenheid en hulp in het practicum en bij de vele LC-MS projecten! Bedankt collega's Robin, Elien en Feifan voor jullie inzet tijdens het practicum en in de verschillende projecten die lopende zijn. Bedankt Julie, voor het wegwijs maken in het labo en de bij momenten hilarische verbeteringen van de cases medische biochemie. Bedankt Lies en Pieter en Eline, voor alle hulp die ik van jullie kon krijgen tijdens mijn PhD en de amusante debatten tijdens de lunch. Pieter, De wetenschappelijke discussies gingen soms ver en tot laat, maar leidden wel tot inzichten (+publicatie) waar ik nog steeds dankbaar voor ben. Ook de verschillende thesisstudenten wens ik te bedanken voor hun inzet tijdens hun masterproef: Hanne, Charlotte, Elien en Somaya

Het leven naast mijn doctoraat was nu niet bepaald een bron van rust, maar wel één waaruit ik dag na dag kracht en weerbaarheid kon putten. Mama en papa, alles wat ik tot op heden heb bereikt en kan/mag doen, komt door jullie onvoorwaardelijke steun en stabiliteit. Opgroeien in een nest waar liefde, warmte en respect centraal staan, is een onmisbaar goed weinigen gegund. Bedankt voor alles wat jullie voor mij gedaan hebben! Broertjes Linze en Flinze, ik ben erg trots dat ik jullie grotere broer mag zijn en hoop dat we mekaar nooit uit het oog verliezen. Opa en oma, bedankt om altijd klaar te staan voor mij (ons). Geen moeite was jullie teveel. Indicatief zijn dan ook de quicheverslavingen bij alle kleinkinderen en mijn onuitwisbare herinnering aan het stratenplan van Kaprijke.

De kameraderie. Een op zichzelf staand concept. Het is een biotoop, meer nog, een soort symbiose waarin elkeen zijn eigen rol met verve lijkt te vervullen. Gaande van avondlijke verbroederingen, wilde ritjes op de WWB, een welkome after-work pint toe Geuzes, of een helpende hand bij het verbouwen van mijn huis. Een betere vriendengroep kan men zich niet wensen. Ik heb dikwijls verstek moeten geven en vaak was er een poos radiostilte, maar toch kon ik steeds op jullie rekenen. Jacky, Pepe (Daddy T), Marnix 2, Jurgen, Boris, Tijlke, Messiang, merci! Of zoals groot poëet ooit verwoorde:

En daar in het diepste van de tuin
verscholen in de Sleinse lommerte
zat een man
een vokke
getroost door een glaasje pastis
zijn eindeloos hongerig proefschrift te voeden
met woorden van dank,
krolse pennenstreken over kameraadschap,
grenzeloze liefde en onvoorwaardelijke steun
"Dank u kameraden, eenvoudigweg dank u,
welk genot ik ervaar,
tintelende vingers bij het neerschrijven van jullie liefde voor mijn proefschrift,
jullie eeuwige steun in deze ellenlange calvarietocht

naar het eindpunt van dit werk,
de dubbele maatstreep"

-DT

De bafana's. Bedankt voor de vriendschap, de vele onvergetelijke avonden tijdens onze farma- en doctoraats-jaren en de prachtige reizen die we samen gemaakt hebben. Mr. Wes, Koenan, Wellie en Tank, ik hoop dat we elkaar regelmatig blijven zien!

Vrienden die mij op elke mogelijke manier geholpen hebben in de voorbije drukke periode, vrienden van 't muziek, vrienden waarbij ik altijd terecht kan, bedankt! In het bijzonder Sander, merci om ons gezin zoveel warmte te geven en er steeds te zijn! Het doet goed om een vriend als u te hebben, Lele voor de nachtelijke ingevingen bij een goed glas wijn en uw eeuwige bereidheid, Quinten omdat ge Quinten zijt en we mekaar te weinig zien, Jolientje om steeds de berg naar Mozes te laten komen, Pieter & Loore, Guillaume & Rosa, Katelijn, Evelien voor de hulp en de interessante gesprekken over sliced dogs, Tom & Jive Cats om mijn gezever te aanhoren & te fungeren als muzikale uitlaatklep, Tanguy & Katrien, David & Anne, Angie & Sarah & Sarah voor alle hulp, leuke avonden en jaren '90 herinneringen.

Ook deze keer moet ik het cliché alle eer aandoen. Achter elk mannelijk succes, staat een sterke vrouw. Laurien, wat een geluk dat ik je 10 jaar geleden leerde kennen. De laatste jaren waren op z'n zachtst

uitgedrukt een turbulente periode. Doctoreren betekende voor jou het aanhoren van geraaskal over practica en experimenten, een immer aanwezig laptopscherm dat vaak onze avondrite verstoorde, gevloek over mislukte experimenten, en af en toe een uitstapje naar het ffw om te kijken of de stalen nog aan het lopen waren. Bewonderenswaardig vind ik je inzet om mijn steeds te lange en veel te uitgebreide uiteenzetting over massaspectrometrie, chromatografie of PBPK modelling te incasseren, en vervolgens nog in staat te zijn om het toch enigszins te reproduceren! Dit doe je. Je steunt me in alles wat ik maar wil doen en zet jezelf heel vaak opzij om mij kansen te geven mezelf te ontplooien, in dit doctoraat, in muziek, etc. Op momenten wanneer ik weer eens “caught up” geraakte, was jij er om mij terug met beide voeten in de aarde te zetten en me opnieuw moed in te spreken om toch maar door te doen. Bedankt om mij zoveel te geven, ik hoop dat ik in de komende jaren een even grote steun mag zijn voor jou. Ik kijk er ongelofelijk naar uit om samen met jou en ons persoonlijk pediatrisch projectje, Roman, de toekomst vorm te geven.

TABLE OF CONTENTS

LIST OF ABBREVIATIONS

AAF: Activity-adjustment factor

ADME: Absorption, distribution, metabolism, excretion

BCRP: Breast cancer resistance protein

BPCA: Best Pharmaceuticals Act for Children

BW: Bodyweight

CL: Clearance

CV: Coefficient of Variation

CLint: Intrinsic clearance

CYP450: Cytochrome P450

DEX: Dextromethorphan

EM: Extensive metabolizer

EMA: European Medicines Agency

E.U.: European Union

FDA: U.S. Food and Drug Administration

FMO: Flavin mono-oxygenases

Fu_p: Fraction unbound in plasma

GFR: Glomerular filtration rate

HCl: Hydrochloric Acid

HLM: Human liver microsomes

ISEF: Inter-system extrapolation factor

IIV: Inter-individual variability

i.v.: Intravenous

IVIVE: In vitro-in vivo extrapolation

Km: Michaelis-Menten constant (µM)

Kp: Tissue-plasma partition coefficient

M&S: Modelling and simulation

MDZ: Midazolam

MeOH: Methanol

MP: Microsomal protein

MPPGL: Microsomal protein per gram liver

MRP: Multi-drug resistance protein

Mw: Molecular weight

NADPH: Reduced Nicotinamide adenine dinucleotide phosphate

NDT: N-desmethyltramadol

NODT: N,O-didesmethyltramadol

NONMEM: Non-linear mixed effects model

OATP: Organic anion transporting peptide

OCT/OAT: Organic cation/anion transporter

ODT: O-desmethyltramadol

PAH: Para-aminohippuric acid

PBPK: Physiologically-based pharmacokinetics (model)

PDCO: Pediatric Committee

P-gp: P-glycoprotein

PIP/PSP: Pediatric investigational plan/Pediatric study plan

PK/PD: Pharmacokinetics/pharmacodynamics

PM: Poor metabolizer

PMA: Postmenstrual age

PNA: Postnatal age

PopPK: Population pharmacokinetic (model)

PREA: Pediatric Research Equity Act

Q_H: Hepatic blood flow

RAF/REF: Relative activity/expression factor

RG: Retrograde (model)

rhCYP: Human recombinant CYP450 enzyme systems

RUV: Residual unexplained variability

STS: Standard two-stage approach

SULT: Sulfotransferase

Tmax: Time of maximal plasma concentration

TPMT: Thiopurine methyltransferase

UGT: UDP-glucuronosyltransferase

UM: Ultra-extensive metabolizer

U.S.: United States (of America)

Vd: Volume of distribution

Vmax: Maximal velocity of an enzymatic reaction (pmol/min)

Vss: Steady-state volume of distribution

CHAPTER 1

GENERAL INTRODUCTION

TABLE OF CONTENTS

1

1 MEDICINE AND THE CHILD, A COMPLEX RELATIONSHIP

Before a new drug is approved to enter the market, supportive evidence has to be provided that it is safe, effective and of high quality. Therefore, during the end-to-end drug development process, preclinical and clinical studies are designed to prove that the drug indeed complies with these criteria and is eligible for marketing. In the preclinical phase, the drug is investigated *in vitro* and *in vivo* in different animal species to obtain information on its mechanism of action, its drug disposition characteristics and its safety. Clinical studies are carried out first in healthy volunteers to assess drug safety, pharmacokinetics/pharmacodynamics (PKPD) and dosage requirements. Afterwards, the drug is given to patients to assess the drug's efficacy and safety profile [1].

Intuitively, when a drug is to be developed for pediatric patients, there are practical and ethical issues associated with the clinical testing of drugs in children. Because of this, there is a historic shortage of data on the safety, dosing requirements and efficacy of drugs used in children that were previously approved in adults, especially in the neonate/infant population. The term "therapeutic orphans" was coined in 1968 by Shirkey to describe this phenomenon [2]. This leads to the paradox of clinicians having to treat our most vulnerable population with off-label and unlicensed drugs. In off-label drug use, the drug is prescribed for a different indication, or is given at a different dose or in a different way as opposed to what the label instructs. When a drug is used unlicensed, the drug is imported from another country where it is has obtained a license for marketing. Off-label drug use in the pediatric population ranges from 60 to 90% of patients, the highest percentage being in infants <1 year of age [3]. Since this situation brings about delays, costs and risks for both patients and clinicians, regulatory authorities have established strategies and installed regulations to promote clinical research in children [4]. In 2002, the Best Pharmaceuticals for Children Act (BPCA) was adopted by the Food and Drug Administration (FDA), which provided incentives for pharmaceutical companies to conduct pediatric studies (the carrot). Furthermore, the Pediatric Research Equity Act (PREA), passed in 2003, defines the legal framework (the stick) in which to develop Pediatric Study Plans (PSP) [5]. Not long thereafter, in 2007, the European Pediatric Regulation was developed by the European Medicines Agency (EMA). Its objective is to improve the health of children in Europe by facilitating the development and availability of medicines for children. The main impact was the establishment of the Pediatric Committee (PDCO) overseeing the Agency's work on a sponsor's Pediatric Investigational Plan (PIP) [6]. The incentive in both continents is a six month extension of the sponsor's patent protection, even in the case of a negative outcome in pediatrics.

In the drug development process (Figure 1), the phase 1 clinical trials expose 20 to 100 healthy volunteers/patients to the drug to document safety & tolerability, pharmacokinetics and dose

requirements. Phase 2 trials expose several hundreds of patients to the drug to assess efficacy, the side effect profile and perform dose finding, while up to several thousands of patients are enrolled in phase three trials to confirm the efficacy and safety profile. Timeline differences with respect to the pediatric investigation exist between E.U. (EMA) and U.S. (FDA). The Pediatric Investigational Plan (PIP, EMA) has to be submitted at the end of phase 1, while for the Pediatric Study Plan (PSP, FDA) this needs to take place at the end of phase 2. Several contact moments occur between the sponsor and the regulatory authority leading to potential adaptations of the sponsor's pediatric plans. This is necessary since an initial pediatric plan is submitted as early as after phase 1. At that time, a lot of preclinical data (e.g. *in vitro* ADME, animal pharmacology/toxicology data) and minimal clinical data pertaining to the adult dose regimen and safety are available to inform the pediatric plan. As more clinical information is generated, newly obtained insights in the adult population should allow to better inform the design of the pediatric clinical trials [5]. The question of when to perform pediatric clinical trials is of the essence and should always be governed by a risk/benefit analysis. At the time new compounds enter phase 1 clinical trials, this ratio is high. To initiate a pediatric clinical trial, there should minimally be some adult *in vivo* PK, safety and/or efficacy data available in order to lower this ratio. Therefore, Shaddy et al. [7] suggested that pediatric clinical trials may be deferred until after phase 3, with the risk/benefit ratio being typically much lower at that moment in the drug development process. However, if e.g. disease progression, or the drug's PKPD relationship is not similar in children and adults or the disease exclusively occurs in children, clinical trials in adults will minimally affect this risk/benefit ratio. In such cases, it might become relevant to investigate (predictive) juvenile animal models or use model-based approaches on limited adult data to optimize first-time-in-pediatric studies.

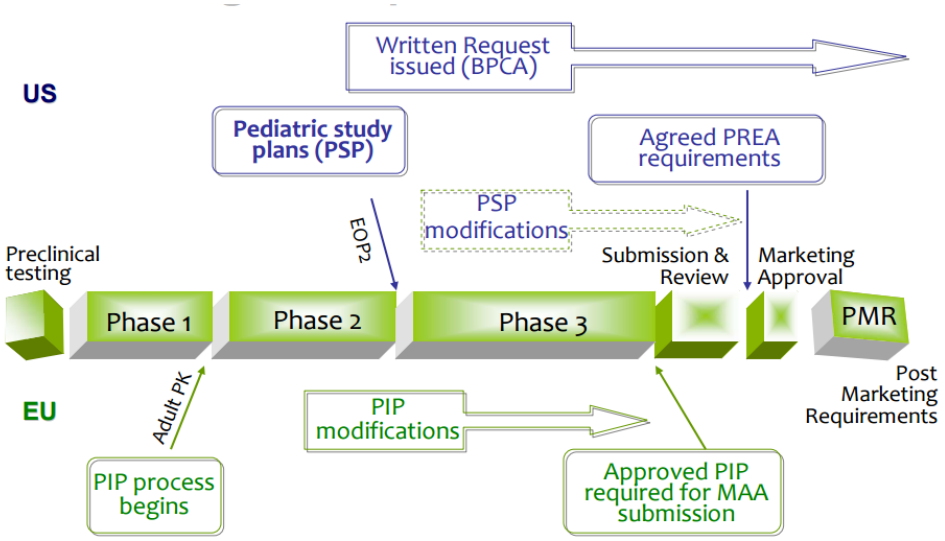

FIGURE 1: OVERVIEW OF THE DRUG DEVELOPMENT PROGRAM, WITH AN EMPHASIS ON PEDIATRIC DEVELOPMENT [8]

2 CURRENT KNOWLEDGE ON PEDIATRIC ADME

Developing appropriate drugs for children is a daunting task. Children constitute a vulnerable and heterogeneous population in which the physiology is changing rapidly, especially in the younger ages. Therefore, the pediatric population really consists of several subpopulations, mostly stratified in the following largely arbitrary age categories: term newborn infants (0-27 days), infants and toddlers (28 days to 23 months), children (2 to 11 years), and adolescents (12 to 16-18 years). Because of this changing physiology, it is impossible to apply a one-dose-fits-all approach across the whole pediatric age range. The following section provides an overview of the most important changes affecting drug disposition, with a possible implication for drug therapy. When drugs are dosed extravascularly to patients, the processes determining the concentrations of the drug in several tissues and blood are absorption, distribution, metabolism, and excretion (ADME).

2.1 ABSORPTION

Given the focus of this thesis on drug disposition after i.v. administration, the physiological changes affecting absorption will only be described high level. In short, parameters determining the rate and extent of oral absorption are gastric emptying time, gastrointestinal pH, and gastro-intestinal transit time. The fasted/fed state may also affect drug absorption, certainly given the high and very frequent milk intake [9]. As Bowles et al. [10] summarize, the oesophageal transit time of liquids seems similar in children and in adults, whereas gastric emptying is delayed, gastric pH elevated due to the low acid secretion, and intestinal transit reduced and irregular. Gastrointestinal enzyme activities of α-amylase and other pancreatic enzymes in the duodenum are low up to 4 months of age. Also concentrations of bile acids and lipase are typically low in neonates. This may decrease the absorption of lipid-soluble drugs [11]. Globally, absorption seems to be slower in children than in adults and bioavailability is strongly influenced by all these factors. Absorption from intramuscular and subcutaneous injection sites may be limited due to reduced peripheral blood flow in neonates and may suddenly increase due to physiological changes with subsequent toxic drug levels. Skin absorption is enhanced in neonates/young infants. In addition, the ratio of the BSA relative to body mass in pediatric life exceeds the adult ratio. As a consequence, drugs dosed per surface area may induce toxic effects more rapidly (Figure 2) [10-12].

2.2 DISTRIBUTION

Drug distribution describes the reversible mass transfer of drug from plasma (blood) to the different tissues. The pharmacokinetic parameter associated with drug distribution is the volume of distribution (Vd). The Vd represents the hypothetical volume that is needed to dissolve the drug dose to achieve the concentrations measured in plasma. Drug distribution alters with organ composition, organ blood flow, and drug plasma protein binding. In neonates, extracellular spaces and total body water content are higher, compared to adults. As a consequence, the volume of distribution for compounds mainly distributing in extracellular water will be higher (such as aminoglycosides). In addition, the adipose tissue consists of a relatively higher water content and a lower lipid fraction (Figure 2) [12]. In preterm infants, the lipid fraction even goes down to about 1%, compared to 15% of total body weight in term neonates. Therefore, lipid-soluble drugs may accumulate less in these premature infants [11]. As an example, the Vd for gentamycin and sufisoxazole is twice or more that in adults, while diazepam and flunitrazepam display a reduction in Vd [13].

Compounds highly bound to plasma proteins may display altered fractions of unbound drug, because the concentration of plasma proteins (albumin and α_1-acid glycoprotein) is decreased in early life. Typically, albumin levels in adults reach 40 g/L, while there is a higher variation in α_1-acid glycoprotein levels (400-1000 mg/L). This is because the latter is increased in conditions such as stress and inflammation, while it is decreased in renal and hepatic disease. In early life, albumin levels are reduced by 20%, while α_1-acid glycoprotein levels are approximately halved [14]. Because oftentimes it is hard to obtain a sufficient number and volume of blood samples, which is typically needed for equilibrium dialysis, McNamara and Alcorn provided a method for calculating the unbound fraction of a drug, based on the difference in protein levels in adults versus neonates/infants. This approach offers a way to predict the unbound fraction of a drug in early life [15].However, plasma protein binding may be decreased further due to changes in affinity as a result of a lower blood pH and conformational changes in the fetal protein, and competition with endogenous compounds, such as bilirubin and free fatty acids that compete for binding. This however, does not necessarily imply that the drug effect will have increased, since unbound drug concentrations may be unchanged. Situations in which altered unbound plasma concentrations of a drug are anticipated, are mostly due to changes in elimination capacity or driven by saturation kinetics of plasma protein binding [16, 17]. However, because the bound drug fraction is decreased, a rise in the unbound fraction in plasma may be observed with an increased distribution of the drug in the tissues as a consequence. For theophylline, reduced protein binding implied a different therapeutic range for this drug in neonates. For this group, serum concentrations should be between 6-13 mg/L, while in older patients 10-20 mg/L is targeted [13].

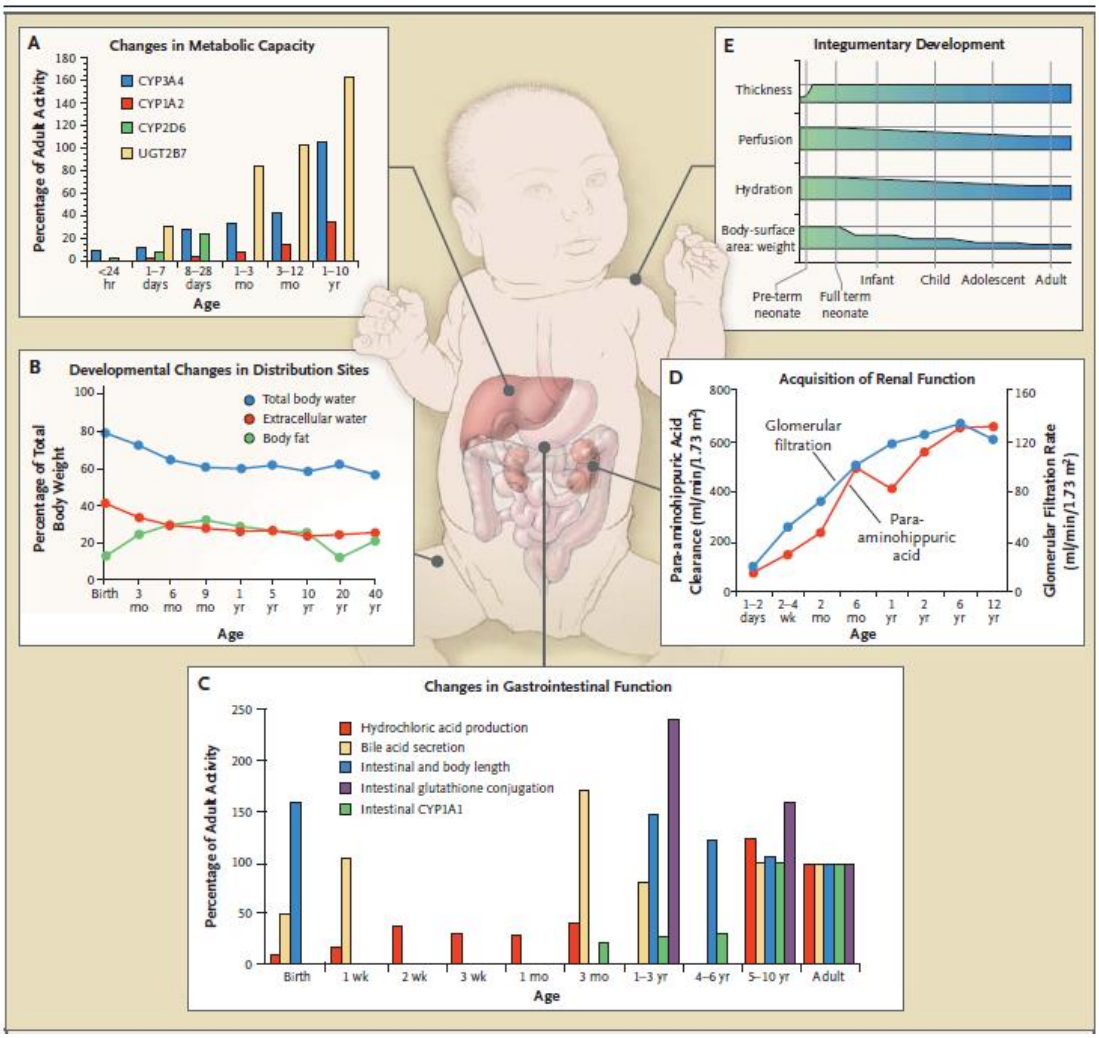

FIGURE 2: CLEAR ILLUSTRATION DISPLAYING THE KEY CHANGES IN PHYSIOLOGICAL PARAMETERS THAT GOVERN AGE RELATED DIFFERENCES IN DRUG DISPOSITION, FROM KEARNS ET AL. [12]. (A) PANEL A SHOWS CHANGES IN METABOLIC CAPACITY OF DIFFERENT CYP AND UGT ENZYMES AS A FUNCTION OF POSTNATAL AGE. THE METABOLIC ACTIVITY IS CLEARLY REDUCED AT BIRTH AND MATURES FOLLOWING AN ENZYME-SPECIFIC PATTERN; (B) IN PANEL B, THE CHANGE OF BODY COMPOSITION WITH AGE IS DISPLAYED. THE HUMAN BODY CAN BE SUBDIVIDED INTO MAINLY 3 DISTRIBUTION SITES: TOTAL BODY WATER, EXTRACELLULAR WATER, AND BODY FAT. IN THE FIRST 6 MONTHS, THE TOTAL AND EXTRACELLULAR WATER ARE HIGHER. (C) PANEL C INDICATES THE CHANGES OF THE GASTROINTESTINAL STRUCTURE AND FUNCTION OVER AGE, NORMALIZED TO ADULTS; (D) IN PANEL D THE ACQUISITION OF RENAL FUNCTION IS ILLUSTRATED FOR GLOMERULAR FILTRATION (GFR) AND PARA-AMINOHIPPURIC ACID (PAH) CLEARANCE. THE GFR IS A MEASURE OF THE FILTRATION CAPACITY OF THE KIDNEY, WHILE PAH EXCRETION INDICATES ACQUISITION OF ACTIVE TUBULAR SECRETION; (E) AS REFLECTED IN PANEL E, THE THICKNESS, PERFUSION, AND HYDRATION OF THE SKIN AND THE RELATIVE SIZE OF THE SKIN SURFACE AREA ALL FOLLOW SPECIFIC PATTERNS WITH AGE. CLEARLY, PARAMETERS STEADILY DECLINING OVER AGE ARE THE PERFUSION AND HYDRATION OF THE SKIN, WHILE THE THICKNESS VASTLY INCREASES AROUND PRE-TERM AGE AND STAGNATES THEREAFTER. IN ADDITION, THE BODY-SURFACE AREA/WEIGHT RATIO IS HIGH AT FIRST BUT THEN DIMINISHES RAPIDLY TO ADULTHOOD

Membrane differences exist between neonates/infants and adults, which affects drug binding to erythrocytes and membrane permeability. The erythrocyte:plasma concentration ratio of digoxin is reported to be 3 times higher, compared to adults. Apparently, neonatal erythrocytes have about three times more digoxin-binding sites, compared to adults [14]. Membrane permeability in neonates and infants is higher than for older children, and has an important consequence for drugs crossing the blood-brain barrier. This would be, in part, related to the still immature myelinization, counteracting drug passage. This observation is underpinned by the occurrence of kernicterus, which is caused by excessive plasma levels of bilirubin crossing the blood-brain barrier. Lipophilic H1-receptor antagonists also cross the blood-brain barrier and cause fatigue, somnolence, lethargy and impairment of cognitive function [11, 13].

For most low molecular weight drugs, distribution is governed by passive diffusion along the concentration gradients. However, for drugs with low permeation through biological membranes, drug distribution (and elimination as well) may be influenced by an active transport system. Transporters may transfer the drug out of cells (efflux, e.g. P-gp, MRP, BCRP) or into the cells (influx, e.g. OCT, OAT, OATP). In addition, due to a significant overlap between drugs being substrates for transporters and CYP enzymes, the disposition of these drugs is not only often times complex but also makes them prone to potential drug-drug interactions [18]. In pediatrics, functional transporter activity changes as a function of age. Although the importance of active transport is well-recognized and developmental patterns for transporter-specific expression and activity emerge, a lot remains to be clarified [19].

2.3 METABOLISM

Metabolism describes the process of degrading a drug substance and is typically divided in phase I and phase II reactions. In general, these reactions serve to convert hydrophobic chemicals into more hydrophilic products that can easily be excreted in urine or bile. Phase I reactions are functionalization reactions and involve oxidation, reduction and hydrolysis reactions, while phase II reactions are conjugation reactions. Many drugs are prone to metabolism by the sequence of phase I then II, while others only undergo either of the 2 phases. Drug metabolizing enzymes that catalyze phase I reactions include the Cytochrome P450 enzyme family (CYP), alcohol dehydrogenases (ADH), and flavin monooxygenases (FMO). Enzymes that catalyze phase II reactions include UDP-glucuronosyltransferases (UGT), sulfotransferases (SULT), glutathione-S-transferases (GST), N-acetyltransferases (NAT), and methyltransferases (MT). Phase I reactions mostly result in inactive drug metabolites, which no longer exert an effect, while phase II reactions vastly improve water solubility and hence ‘excretion’ of the drug. Prodrugs are an exception to this principle, as they require *in vivo*

conversion of the drug substance to the active metabolite in order to be biologically active (e.g. carbamazepine, enalapril and oseltamivir). Some metabolites may be as active as their parent drugs (e.g. morphine-6-glucuronide and desvenlafaxine), while others are responsible for adverse events (e.g. the reactive NAPQI-metabolite of paracetamol) [20-23].

The major site of human metabolism is the liver, for both endogenous compounds (e.g. steroid hormones, cholesterol, fatty acids, and proteins) as well as exogenous drugs. Circulating drug is efficiently exposed to liver cells, which is assured by the liver architecture. About 80% of liver cells, called hepatocytes, are responsible for uptake, metabolism, and excretion of drug substance. In addition, upon oral delivery, most drugs are absorbed by the gut and taken to the liver through the portal vein. In the enterocytes lining the gut wall, high concentrations of drug metabolizing enzymes, such as CYP3A4, are present as well. Significant metabolism may occur at these two sites for susceptible drug substrates, causing a substantial decrease in the oral bioavailability of these drugs. These two tissues are involved in what is called the 'first-pass effect' [20].

2.3.1 The cytochrome P450 enzyme system

The Cytochrome P450 enzyme system (CYP) is the major detoxifying system for the majority of clinically used drugs in humans. It is a superfamily, divided into families (by gene family), subfamilies (amino acid similarity) and individual enzymes (individual genes). Although most tissues express CYP enzymes, their activity and expression is highest in the liver and the intestines. Clinically relevant CYP members are indicated in Figure 3, adapted from Zanger et al. [24]. For every relevant CYP enzyme, the relative contribution of the enzyme is mentioned, based on data from 248 clinically used drugs. There are a number of factors affecting the CYP's activity or expression, including sex, inflammation, age, interaction, and polymorphisms. It is well known that several endogenous compounds, as well as other drugs may affect the activity of CYPs (inhibition vs. induction). Polymorphism is the term signifying allelic variation resulting in altered enzyme activity or expression. In this way, different 'phenotypes' exist in the population. Important phenotypic polymorphisms have been described for CYP2B6, CYP2C9, CYP2C19, and CYP2D6 [22, 25].

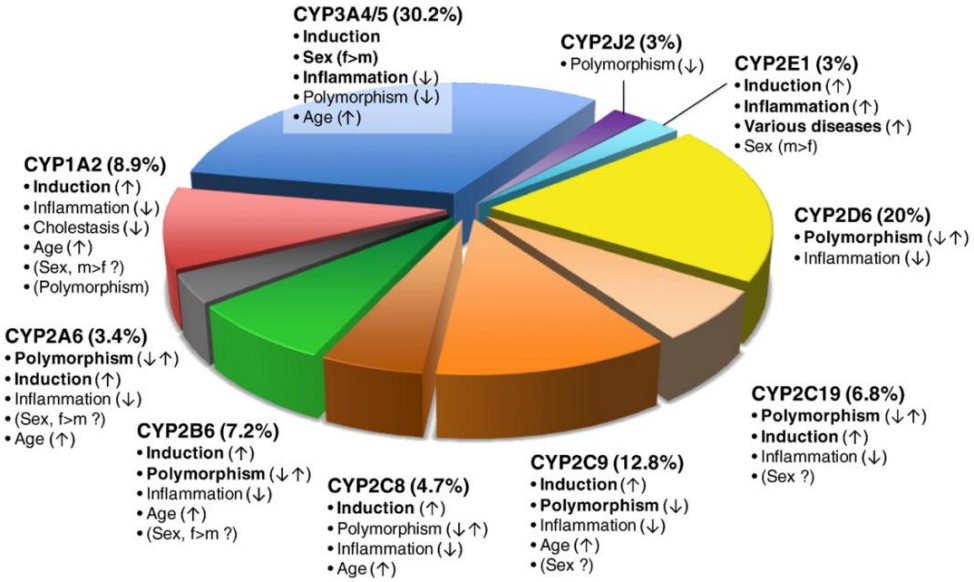

FIGURE 3: PIE CHART FROM ZANGER ET AL. [24] INDICATING THE FRACTION OF CLINICALLY USED DRUGS METABOLIZED BY THE DIFFERENT CYP ENZYMES AND FACTORS INFLUENCING VARIABILITY. THE 2 MAJOR CYP ENZYMES ARE CYP3A4 AND CYP2D6, WHICH COVER ALREADY 50% OF THE METABOLIZED COMPOUNDS. IMPORTANT VARIABILITY FACTORS ARE INDICATED IN BOLD. ARROWS INDICATE THE DIRECTION OF POSSIBLE INFLUENCE (↑ , INCREASED ACTIVITY; ↓ , DECREASED ACTIVITY; ↑ ↓ , INCREASED OR DECREASED ACTIVITY).

2.3.2 Enzyme Ontogeny

In the developing infant, systemic clearance is mainly determined by hepatic and renal elimination mechanisms. Hepatic clearance is determined by the efficiency with which metabolic conversions are executed. In the first two years of life, there is a dramatic increase in the activity of phase I and II reactions, when normalized to milligram of hepatic microsomal protein present. This makes hepatic clearance strongly age-dependent. On top of this, this so-called 'ontogeny' is different for the different phase I and II enzymes and cannot be described by one function (Figure 4) [13, 26, 27].

In Figure 4, maturation of phase I and II enzymes is subdivided into 3 classes, based on the work of Hines et al. [28]. The first class represents enzymes, which are expressed at high levels during prenatal life and drop after birth, e.g. CYP3A7, FMO1, SULT1A3. A second class of enzymes show consistent levels throughout *in utero* development and postnatal life, i.e. CYP3A5, SULT1A1, thiopurine methyltransferase (TPMT). A third class of enzymes primarily develop after birth, i.e. most CYP and UGT

enzymes [29]. Typically these enzymes will also display increased weight-normalized clearance values, compared to adults.

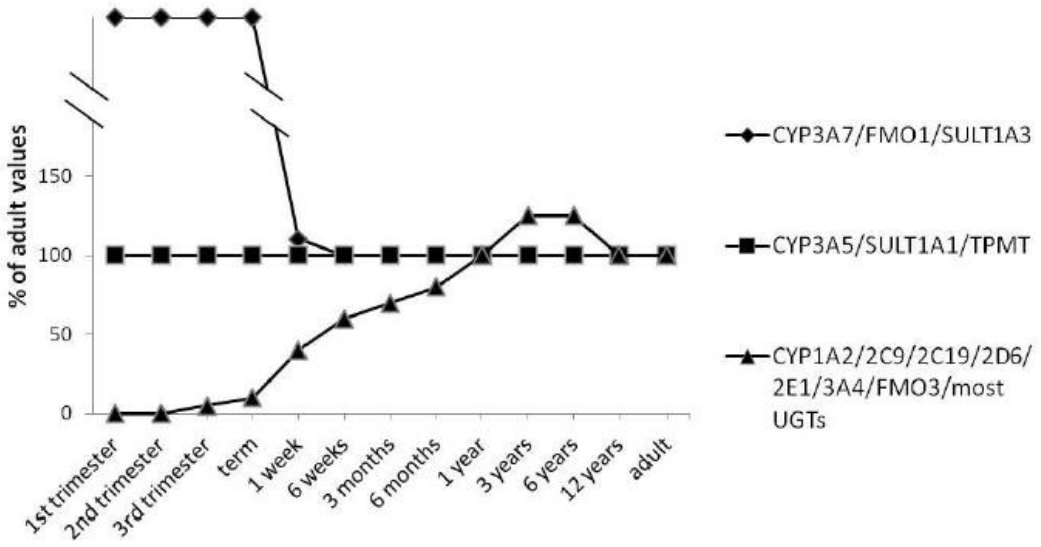

FIGURE 4: THREE CLASSES OF ENZYME MATURATION MAY BE DISCERNED. CLASS 1 REPRESENTS ENZYMES THAT ARE EXPRESSED AT HIGH LEVELS DURING PRENATAL LIFE AND DROP AFTER BIRTH, E.G. CYP3A7. CLASS 2 ENZYMES SHOW A CONSISTENT EXPRESSION THROUGHOUT PRE- AND POSTNATAL LIFE, E.G. SULT1A1. CLASS 3 ENZYMES DISPLAY A MATURATION PATTERN THAT IS INITIALLY LOW AT BIRTH BUT INCREASES THROUGHOUT POSTNATAL LIFE., ADAPTED FROM DE BOCK ET AL. [30]

An update to these developmental classes has already been published by Hines in 2013 [31], and is represented in Table 1. Next to the addition of some enzymes (e.g. Carboxylesterases CES1/2), the most important update concerns some of the CYP enzymes that have switched from class 3 to class 2 (class 2 meaning that enzymes show consistent levels throughout pre- and postnatal life, e.g. CYP2C19 and CYP3A5).

TABLE 1: AN UPDATED VISION ON THE CLASSES OF HUMAN HEPATIC DRUG METABOLIZING ENZYME DEVELOPMENTAL TRAJECTORIES., REPRESENTED IN FIGURE 4, ADAPTED FROM HINES ET AL. [31].

Class 1	Class 2	Class 3	
ADH1A[a]	CYP2C19[a]	ADH1B[a]	EPHX1[a]
CYP3A7[a]	CYP2B6[c]	ADH1C[a]	EPHX2[a]
FMO1[a]	CYP3A5[a]	AOX1[a]	FMO3[a]
GSTP[a]	GSTA1[a]	CES1[d,e]	GSTM1[a]
SULT1E1[a]	GSTA2[a]	CES2[d,e]	GSTZ1[g]
SULT1A3[b]	SULT1A1[a]	CYP1A2[a]	SULT2A1[a]
		CYP2C9[a]	UGT1A1[a,h]
		CYP2D6[a,f]	UGT1A6[a,h]
		CYP2E1[a]	UGT2B7[a,h]
		CYP3A4[a]	

[a] Reviewed in Hines (2008).
[b] Cappiello et al. (1991).
[c] Croom et al. (2009).
[d] Yang et al. (2009).
[e] Zhu et al. (2009).
[f] Stevens et al. (2008).
[g] Li et al. (2011).
[h] de Wildt et al. (1999).

1

Moreover, each CYP enzyme seems to have its own individual ontogeny function (Figure 5). As Zanger et al. [24] described, individual CYP expression is influenced by a unique combination of genetic polymorphisms, induction by xenobiotics, regulation by cytokines and hormones, disease states, as well as sex, age, and other factors. Some CYP enzymes are already mature at birth, while others take a longer time to develop. The ontogeny profiles in Figure 5 were taken from the Simcyp® M&S platform (Simcyp® v14, Certara, CA), which are based on an extensive literature search. Most enzyme ontogeny information available to date, is derived from *in vitro* sources (*ex vivo* human liver tissue) [31]. Some reports, however, noted a potential difference in *in vitro* vs. *in vivo* derived maturation functions [32-34]. The CYP1A2 curve in Figure 5 is an example of an *in vivo* derived ontogeny function. It increases to about 1.6-fold of the adult activity at 2 years of age. Figures 4 and 5 however, need to be interpreted with caution, since often times this type of figure is subject to misinterpretation. The y-axis represents the fraction of adult activity on the (sub)cellular level, being the 'maturation' of cellular differentiation and organization. However, 'growth', represented by the gain in liver mass, is also affecting the total elimination capacity of eliminating organs. Although the latter process is as important as the enzyme-specific maturation functions, this is not taken into account in this graphic. In essence, this means that for e.g. the CYP2C8 liver enzyme, activity at the cellular level is mature around 0.5 years, but the total liver size still is only ca.15% of the adult liver size. Taken together, the total hepatic elimination capacity of CYP2C8 will still be much lower compared to the adult elimination. This understanding is essential when tailoring the drug dose for pediatrics.

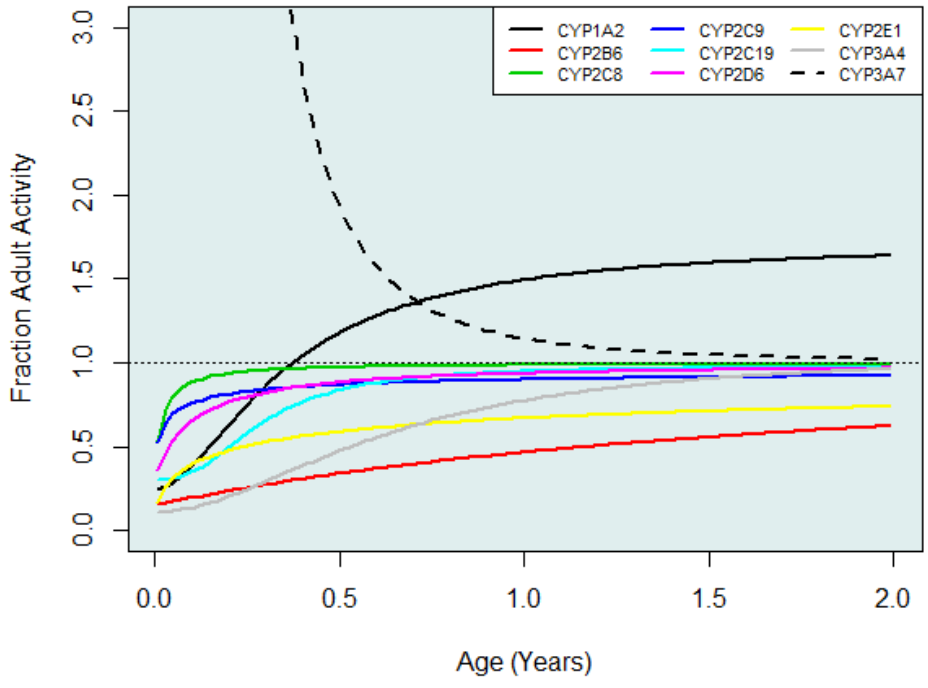

FIGURE 5: OVERVIEW OF THE DIFFERENT MATURATION TRAJECTORIES FOR THE MOST IMPORTANT CYP ENZYMES. MATURATION FUNCTIONS WERE EXTRACTED FROM THE SIMCYP® PBPK PLATFORM, SET UP AFTER AN EXHAUSTIVE LITERATURE RESEARCH

The authors hypothesized that this increased CYP1A2 activity might be due to specific hormonal or dietary influences [33]. Although *in vivo*-derived ontogeny is preferred over *in vitro* ontogeny, the *in vivo* metabolic activity is obscured by protein binding, hepatic blood flow and liver size. Unless these physiological parameters are measured in the different individuals, they need to be predicted which involves some level of uncertainty. This may eventually be reflected into the ontogeny function [33].

Maturation of CYP activity in early life may obscure underlying CYP-specific polymorphisms, described for e.g. CYP2C19 and CYP2D6. For CYP2C19, different genotypes result in phenotypically different (poor – intermediate – extensive metabolizer) subgroups. Adult patients who are CYP2C19 PM are reported to have a higher pantoprazole exposure and a longer elimination half-life. In neonates/infants, a significant difference in pantoprazole exposure for CYP2C19 PM could not be detected [35]. However, a study conducted in children, from 5 years of age and older, reported pantoprazole plasma concentrations that were 6 times higher in CYP2C19 PM. Based on these findings, the pantoprazole drug label includes the following statement, "For known pediatric poor metabolizers, a dose reduction should be considered" [36]. In contrast, a genotype – phenotype concordance for CYP2D6 could already be observed 2 weeks after birth [37]. For atomoxetine and pimozide, a dosage adjustment is also recommended in the label whenever this drug is co-administered with a strong CYP2D6 inhibitor or given to CYP2D6 PM patients [23, 36]. This means that depending on the maturation half-life and the activity difference between PM and EM of a specific CYP enzyme, the polymorphic status is only becoming apparent some time after birth.

When normalizing the clearance per kg bodyweight, an increased clearance capacity of toddlers versus adults is often identified [23, 38, 39]. This phenomenon implies that the dose needed, expressed as mg/kg, is higher for toddlers compared to adults. To date there has been no compelling evidence suggesting increased drug metabolizing enzyme activity. Two possible theories are now postulated. The first theory attributes this phenomenon to the ratio of the liver to the total body weight, which is higher in children between 2 to 4 years of age [40]. The second theory originates from the allometric principle. When dosing mg/kg, in essence a linear scaling is applied to predict a child's drug dose from adults. However, it is well accepted that metabolic weight ($BWT^{0.75}$) is recommended for extrapolating adult drug doses to children [38]. This principle holds true for the different pediatric age categories, except for neonates and infants due to ontogeny-related aspects [41]. Dosing issues related to this finding may go two directions. On the one hand, underexposure has been reported for the anti-HIV drug efavirenz, which was dosed to children on a per kg basis from adult doses. After some years, a PK assessment revealed that no less than 40% of efavirenz levels were subtherapeutic for children, dosed following the initial WHO guidelines [23]. On the other hand, increased activity of CYP enzymes (CYP3A and CYP1A2) may increase the formation of potentially toxic metabolites. This scenario would occur if an increased

bioactivation is not accompanied by a corresponding increase in detoxifying capacity (typically glutathione conjugation) [39].

2.4 EXCRETION

An important organ, involved in the excretion of many endogenous compounds and xenobiotics is the kidney. Kidney function too is not fully mature at birth and displays a distinct maturation profile. Nephrogenesis starts in the embryo at week 5–6 of gestation and is completed at week 36. Hemodynamic changes at birth lead to a rapidly rising GFR during the first weeks of life. The adult GFR is approached at approximately 6–12 months of age (per unit of body surface area). Maturation in GFR has been studied for a long time (e.g. Rubin in 1949), with the most recent effort by De Cock et al. [42]. In this study, maturation in GFR was derived from *in vivo* data in neonates with a model-based approach using amikacin as probe substrate. This semi-physiological GFR maturation function was further investigated using probe substrates gentamicin, tobramycin and vancomycin [43]. In line with what was described in the metabolism section, the renal clearance, expressed as clearance per kg body weight, is much higher in toddlers than adults. Consequently, drugs that are primarily renally excreted need a higher dose, in mg/kg [44]

In addition, the active tubular transport process, measured by para-aminohippuric acid (PAH), also matures in the first months after birth. This mainly depends on renal blood flow and ontogeny of organic anion transporters. There is consensus that maturation of OAT transporters is slower than the GFR maturation and reaches adult values around 7 months of age, though the relative contribution of tubular secretion might be higher in children aged 3-12 years compared to adults. P-glycoprotein expression and function seems to follow maturation in GFR [11, 13]. The third process involved in the renal elimination is the tubular reabsorption, which mainly acts as a passive process for xenobiotics, determined by their physicochemical properties. In neonatal life, urinary pH is typically lower and may influence the reabsorption of acids and bases [45]. It is documented that extreme situations (i.e. undernutrition, energy excess, and sustained stress) during perinatal life increase the chances of developing chronic kidney disease, hypertension, diabetes mellitus, obesity, and atherosclerosis later on in life [46].

Biliary excretion is a major elimination pathway in which intact drug or glucuronidated metabolites are actively transported from hepatocyte into the bile canaliculus. Once released in the intestines, the drug may undergo enterohepatic recirculation. Measuring biliary excretion is not often done, since it is difficult to do and experimental procedures are often invasive. Therefore, age-related changes are not

well documented for this elimination route and it is highly unlikely that this situation would change in the near future [47, 48]. Key transporters involved in the transport of drugs from hepatocytes in to the bile canaliculus, are P-glycoprotein (P-gp), multidrug resistance–associated protein 2 (MRP2), and breast cancer resistance protein (BCRP). The abundance of transporter proteins appears to be lower compared to adults [19, 49], although the impact on biliary excretion remains uncertain. However, a very recent study from Johnson et al [48] applied a 'bottom-up' approach to assess the maturation of these key transporters, using 'top-down' data from dedicated probe substrates. In general, biliary excretion appears to develop rapidly and reaches adult capacities soon after birth. The authors conclude that this finding is in line with recent reports on transporter ontogeny in humans, although a lot of contradictory information is present as well.

1

3 CURRENT TECHNOLOGIES USED IN PEDIATRIC DRUG RESEARCH

The challenges and limitations associated with determining the correct dose for pediatric use, together with the scarcity of clinical studies supporting pediatric indications and labeling, created a public awareness that safe and efficacious drug therapy for children is largely lacking. By the different regulatory authorities in the U.S. and E.U., legislative frameworks as well as financial incentives were adopted to push pediatric drug development forward. Parallel to the increased interest in pediatric research, pharmaceutical industry committed to implement model-based drug development in its drug development programs. Modelling and simulation are two different techniques but are always mentioned in conjunction (as M&S), since they are always combined in model-based drug development. 'Modelling' comprises the mathematical description of the behavior of a biological process or system under consideration. 'Simulation' indicates the application of the constructed model to explore other situations, initially not used to build the model. M&S aligns hypotheses and experimental observations while transitioning from a pharmacotherapeutic problem to its solution (Figure 6). It fulfills, as Sheiner stated [50], a so-called 'learn-confirm' paradigm and by consequence, offers a way to transcend empiricism in drug research. [51-53]. The modelling approaches used in pediatric model-based drug development can be divided into two distinct but complimentary domains: a 'top-down' and a 'bottom-up' approach.

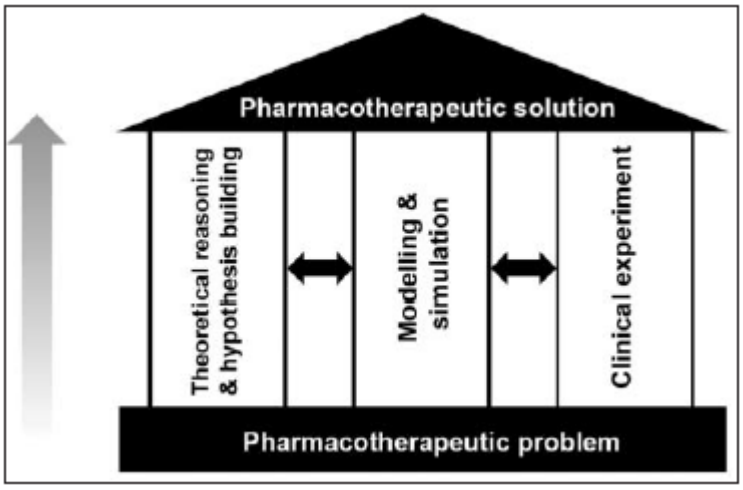

FIGURE 6: TRANSITING FROM PHARMACOTHERAPEUTIC PROBLEM TO SOLUTION BY THEORETICAL REASONING AND CLINICAL EXPERIMENTS, INTERCONNENCTED BY MODELLING & SIMULATION [51]

3.1 TOP-DOWN APPROACH

3.1.1 BACKGROUND

The **top-down approach** has the longest track record in PKPD drug development. Based on observed data (e.g. plasma or biomarker concentrations, clinical signs, …) from actual healthy volunteers or patients, the modeler takes an assumption in the form of a mathematical description (model) that is fitted to the data. The most common top-down approach is the compartmental pharmacokinetic analysis. The description of how the drug is absorbed and distributed in the human body is simplified in terms of a number of hypothetical or 'lumped' compartments (Figure 7). They mostly have no physiological meaning but are appropriate to describe the evolution of plasma concentrations as a function of time after dosing [54] .

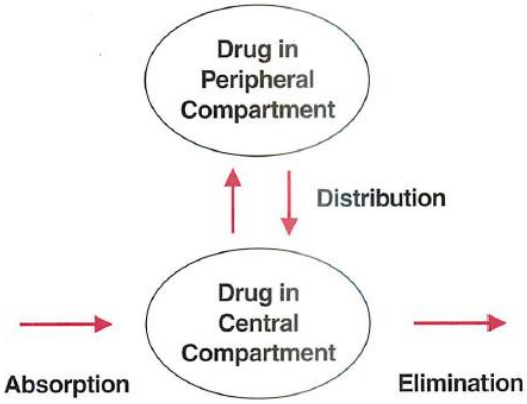

FIGURE 7: REPRESENTATION OF A SIMPLE TWO-COMPARTMENTAL MODEL. DRUG IS ASSUMED ABSORBED INTO THE CENTRAL COMPARTMENT, REVERSIBLY DISTRIBUTED TO THE PERIPHERAL COMPARTMENT AND ELIMINATED (METABOLISED AND/OR EXCRETED) FROM THE CENTRAL COMPARTMENT, ADAPTED FROM ROWLAND TOZER [45]

In compartmental pharmacokinetics, there are mainly 2 approaches: the standard two-stage (STS) approach and the population pharmacokinetic (popPK) approach. In the STS approach, individual PK parameters are estimated subject-by-subject and then summarized as means with their associated spread. A weakness of this approach is that it needs intense sampling in all subjects and the observed variability cannot be assigned to either inter-individual variability (IIV) or residual unexplained variability (RUV). IIV is the true variability originating from differences in PK parameters between different subjects, while RUV is the random noise that consists of variability within one subject, measurement error, bioanalytical error, or model misspecification. In population PKPD models, the structural model component (i.e. the compartmental model) is supplemented with a stochastic, and a covariate model component. The stochastic model describes the variability (or random effects) in the observed data and allows to distinguish the IIV on different PK parameters from the RUV. Finally, in the covariate model,

the IIV on some estimated PK parameters might be explained by variables, related to the studied subjects, e.g. weight, height, age, sex, race, genotype (the fixed effects) [55, 56]. In essence, population PKPD models are non-linear mixed-effects models that attempt to assign observed variability in the observations to random effects (IIV and RUV) and fixed effects (covariates). In pediatric research, ethical and practical constraints limit the volume and number of PK samples that one can draw, often leaving no choice but sparse, unbalanced, and fragmented sampling schemes. However, the population approach is a data-driven approach and is based on a simultaneous analysis of all data of the entire population, while still accounting for the fact that different observations come from different patients. Therefore, it is the method of choice for analyzing pediatric pharmacokinetic data [57, 58].

3.1.2 Clearance estimation in pediatrics

Drug clearance may be seen as the most important pharmacokinetic parameter determining pharmacological response [26, 27]. It determines the exposure after a single intravenous dose, as well as the steady-state plasma concentration after i.v. infusion/multiple i.v. doses. Given the importance of this parameter, it is often used to extrapolate the dose in the pediatric age range [59].

In defining appropriate functions to describe clearance maturation across the pediatric age range, mainly 3 different approaches are distinguished: allometric scaling, allometric scaling with maturation functions, and systematic covariate analysis. Allometry, in biology, is a concept that links size to a physiological process (e.g. metabolic rate, GFR, cardiac output). In PK, it is used to estimate or predict the evolution of a certain PK parameter with bodyweight. In population PK, an allometric relationship is built into the model using the following equation :

$$\theta_i = \theta_{std} * \left(\frac{BW_i}{BW_{std}}\right)^{exp}$$

EQUATION 1

Where θ is a PK parameter of interest (e.g. clearance (CL), volume of distribution (Vd), or half-life) for the individual *i*. The individual PK parameter is assumed to be related to the standardized population parameter (θ_{std}) multiplied with the ratio of individual (BW_i) and standardized bodyweight (BW_{std}, i.e. 70 kg). The exponent of this ratio (*exp*) may be fixed, based on theoretical principles, or estimated directly from the data. For scaling drug clearance from adults to children, the fixed exponent is assumed to be 0.67 or 0.75, based on the universal relationship between basal metabolic rate and body surface area or bodyweight, respectively [59, 60]. The estimation of the allometric exponent directly from the data, which may change across the age range, is more data-driven and does not assume an *a priori* value for the allometric exponent. Some authors reported on issues regarding pediatric extrapolation for drug clearance using a single fixed exponent for the complete pediatric age

range, especially in neonates and infants [61, 62]. In their vision, when using a fixed or single allometric exponent for BW, an additional age-related exponential or sigmoidal **maturation function** is required that accounts for the maturation in early life. Here again some issues have arisen with the predictive performance of these models, and the inclusion of 2 collinear covariates (BW and age) in the model structure [63, 64]. In a **systematic covariate analysis**, no *a priori* relationship between a covariate and the drug clearance is assumed. It is a much cleaner data-driven approach in which empirical Bayes estimates (the individual parameter estimates in non-linear mixed effects are estimated using Bayesian methodology) are plotted against different covariates (if shrinkage allows), in order to obtain the most appropriate covariate relationship for drug clearance. There is some evidence that the covariate relationships, estimated this way, would be applicable across drugs sharing the same metabolic pathways [65]. This finding, however, still does not make allometry the method of choice for clearance extrapolations to children.

3.2 BOTTOM-UP APPROACH

3.2.1 BACKGROUND

The **bottom-up approach** is relatively new to this specific area, but has gained a lot of interest from regulators, academia and industry [66]. The general concept is to mathematically describe the relevant underlying physiological, physicochemical, and biochemical processes that explain the observed pharmacokinetic behavior in clinical studies. In order to do so, bottom-up physiologically-based pharmacokinetic (PBPK) models make an *a priori* distinction between the properties of the organism or 'system' and those of the drug. Regarding the **system's properties**, the anatomical structure of a human body is represented by physiologically relevant compartments that are interconnected via the blood circulation (Figure 8)

Every tissue is represented by a single compartment, supplied by the arterial blood and debouching in the venous blood pool. Only the lung is an exception, which is supplied by the venous blood. The differential equations describing (reversible) drug (mass) transfer from and to the tissues are derived from the law of mass action. In specific organs (by default liver, kidney, and intestines), the drug may be eliminated from the tissue, hence an extra term in the differential equation should account for the disappearance of mass over time. The differential equations below exemplify the mass balance principle from plasma to a perfusion rate-limited tissue without (equation 2) and with (equation 3) elimination [67, 68].

1

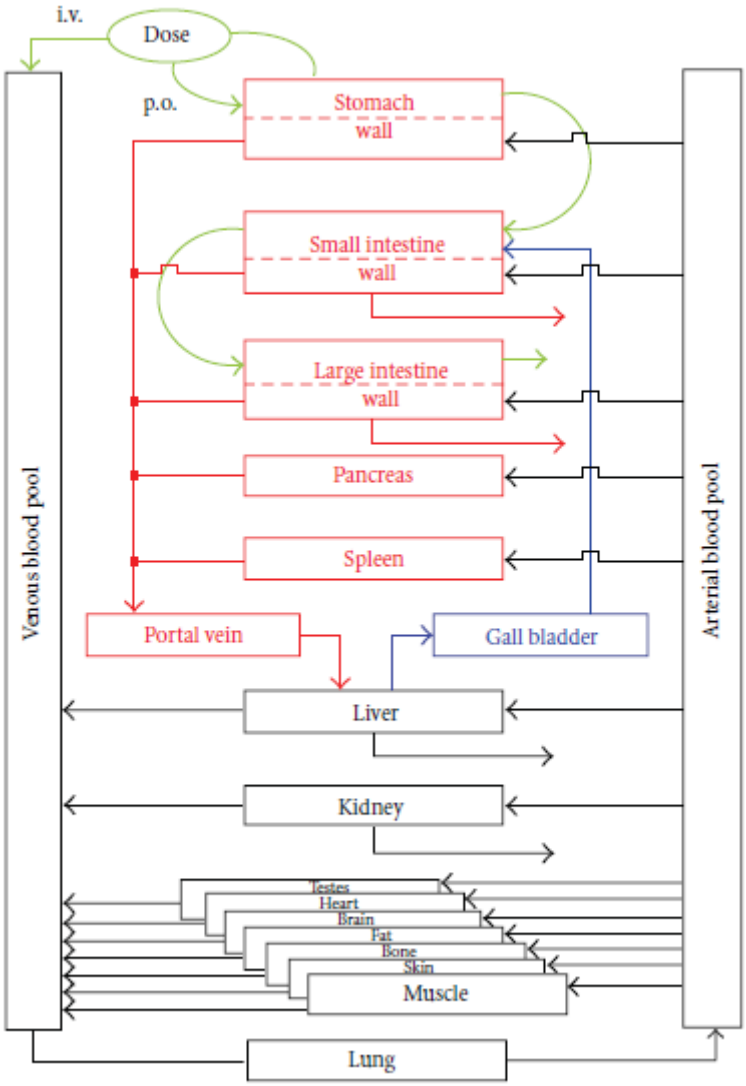

FIGURE 8: GENERIC PBPK MODEL STRUCTURE THAT REPRESENTS EVERY TISSUE AS A SINGLE COMPARTMENT. COMPARTMENTS IN RED ARE INVOLVED IN ORAL DRUG ABSORPTION, AND IN BLUE THE COMPARTMENT INVOLVED IN BILIARY EXCRETION TO THE SMALL INTESTINE (ENTEROHEPATIC RECIRCULATION). ALL COMPARTMENTS (BLACK, RED, BLUE) ARE INVOLVED IN DISTRIBUTION. ELIMINATION MAY OCCUR FROM THE SMALL AND LARGE INTESTINE, LIVER AND KIDNEY COMPARTMENTS. FIGURE ADOPTED FROM WILLMANN ET AL. [69]

$$Vt * \frac{dCt}{dt} = Q * \left(C_{art} - \frac{C_t}{Kp}\right)$$

EQUATION 2

$$Vt * \frac{dCt}{dt} = Q * C_{art} - Q * \frac{C_t}{Kp} - Clint_u * \frac{C_t * fu_p}{Kp}$$

EQUATION 3

Where *Vt* is the tissue volume, *dCt/dt* the change of the tissue concentration over time, *Q* the tissue perfusion, C_{art} the arterial concentration, C_t the tissue concentration, *Kp* the tissue-plasma partition coefficient, fu_p the unbound fraction in plasma, and $CLint_u$ the unbound intrinsic clearance.

On top of the anatomical structure depicted in Figure 8, tissues are provided with tissue-specific properties derived from physiological knowledge pertaining to e.g. tissue volumes and composition, cardiac output to the tissues, surface area, intracellular pH, etc. Tissues may even be divided into cellular and subcellular spaces, as far as the physiological knowledge is available to do so and depending on the level of detail required to get reliable bottom-up predictions. This is often done for liver tissue as a drug's (sub)cellular location may influence its transport or elimination [67, 69].

In parallel, **drug-specific properties** should be provided, which create a molecular fingerprint for *in silico* bottom-up simulation of the expected PK behaviour. Table 2 provides an overview of drug-specific parameters, necessary for bottom-up predictions. Some parameters may be obtained from *in vitro* assays, e.g. permeability from Caco-2 or Vmax/Km from metabolism assays [70, 71]. Others may be predicted *in silico* from published models, e.g. microsomal binding from physicochemistry [72, 73].

TABLE 2: DRUG-SPECIFIC PARAMETERS THAT ARE USED AS DRUG-RELATED INPUT FOR PBPK MODELLING AND SIMULATION PLATFORM

Drug-specific parameter	Description
B:P	Blood-to-plasma ratio
fu_p	Fraction unbound in plasma
K_D	Dissociation constant from binding proteins
P*SA	Permeability-Surface Area product
logP	Lipophilicity
MW	Molecular Weight
pKa	Acid dissociation constant
S	Solubility in reference medium
CLint	Intrinsic elimination clearance
Km Vmax	Michaelis-Menten kinetic constants

In the next step, information on the **'system' and the 'drug' is integrated** into a very specific set of models that yield essential parameters, which represent the interaction of the drug with the system. These parameters are incorporated in the differential equations and govern the disposition of the drug in the *in silico* organism. **Tissue-to-plasma partition coefficients** (Kp) are calculated based on the compound's physicochemistry and the tissue' composition. Kp's determine the extent of distribution to each tissue, as illustrated in equations 2 and 3, and may be derived using a variety of published methodologies by e.g. Rodgers [74, 75], Poulin [76], Schmitt [77]. The choice of method depends on the compound's physicochemical properties and the assumptions underlying these models. For example, the Rodgers and Rowland distribution model was well-suited to predicted tramadol volume of distribution, since it

takes into account the electrostatic interactions of positively-charged basic amines and negatively-charged phospholipids in biological membranes. The **intrinsic liver clearance** ($CLint_H$) is calculated based on the drug's *in vitro* metabolism parameters (Km, Vmax, CLint), the *in vivo* abundance of the responsible liver enzymes and the overall liver architecture. $CLint_H$ is the determinant of liver clearance and, as illustrated in equation 3, determines the loss of mass from the system [78]. More information on how to obtain *in vitro* metabolism parameters from *in vitro* assays is provided in the section '*In vitro*-to-*in vivo* extrapolation'.

Although drug distribution and elimination are strictly separate processes, their prediction depends on a given set of physiological parameters. Given the naturally occurring variation in the physiological parameters, e.g. organ volumes, blood flows, enzyme abundances, etc. in a given population, this information can be used to create physiologically plausible **variability in the bottom-up predictions** of drug distribution and elimination. The most attractive concept of the bottom-up approach is, that it allows to predict changes in drug PK that are due to physiological variation. Therefore, with the increasing availability of physiological information for specific subpopulations, such as pediatrics, geriatrics, cirrhotic or renally impaired patients, PBPK creates a scientific platform and stimulates integrated research in these populations. It enables the mechanistic exploration of the effect of physiology on drug disposition and allows to simulate any 'what-if' scenarios to anticipate the drug's behavior in vulnerable patient populations. In the context of pediatrics, PBPK is ideally positioned to integrate the *a priori* known physiological and biochemical changes occurring in childhood into a meaningful model to predict ADME changes with age. PBPK makes pediatric clinical trials 'confirmatory' rather than 'exploratory' [79-81].

3.2.2 *IN VITRO*-TO-*IN VIVO* EXTRAPOLATION OF DRUG CLEARANCE

In order to assess the rate at which a drug compound is metabolized *in vitro* and to identify the responsible enzymes involved, metabolism parameters CLint/Vmax/Km can be estimated from *in vitro* studies mainly using human liver microsomes, hepatocytes or recombinantly expressed enzymes. Human hepatocytes are regarded as the gold standard for the prediction of human drug clearance, since they possess the whole armamentarium of enzymes and transporters participating in the hepatic clearance of most drugs and represent the most relevant system physiologically. However, given the low enzyme selectivity of this *in vitro* model, human liver microsomes (HLM) or human recombinantly expressed enzyme systems (rhCYP) may be used instead. HLM are obtained by differential centrifugation of liver homogenate and only contain enzymes present in the endoplasmic reticulum, i.e. CYPs, Flavin monooxygenases (FMO) and UDP-glucuronosyltransferases (UGT). Recombinant enzyme systems are microsomes prepared from systems (mostly insect cells) infected with a virus (baculovirus) engineered to express a specific CYP enzyme. Although these subcellular systems may add to the

uncertainty of extrapolation to the *in vivo* situation, the system's complexity is lower and the enzyme selectivity higher. Therefore, these systems allow a more accurate assessment of a particular enzyme's involvement [70, 82, 83].

Michaelis-Menten parameters Km and Vmax may be estimated by fitting a non-linear regression model to the *in vitro* clearance rate (metabolite formation or substrate depletion) as a function of the substrate concentration (equation 4). Alternatively, the intrinsic clearance (CLint) may be estimated at substrate concentrations well below the Km (equation 5). This is often done in high-throughput analyses when only one low substrate concentration is incubated to provide an estimate of the maximal enzyme efficiency (CLint). In this setting, data do not allow to estimate Km and no information is available regarding when the substrate concentration will start to saturate the enzyme under study [80].

$$CL_{invitro} = \frac{Vmax}{Km + [S]}$$

EQUATION 4

$$CLint = \frac{Vmax}{Km} \quad if\ [S] \ll Km$$

EQUATION 5

Subsequently, *in vitro* metabolism parameters may be extrapolated to an *in vivo* hepatic clearance by multiplication with the total abundance of each enzyme in the liver, the so-called *in vitro*-to-*in vivo* extrapolation (IVIVE). It is important to correct the Km for microsomal drug binding using the unbound fraction in the assay (fu_{mic}), since only the unbound drug can be metabolized. equation 6 and 7 represent the calculation of the unbound hepatic intrinsic clearance ($CLint_{H,u}$) from *in vitro* estimated Vmax/Km values in HLM and rhCYP, respectively.

$$CLint_{H,u} = \left[\sum_{j=1}^{n}\left(\frac{Vmax}{Km * fu_{mic}} * CYP_j\ abundance\right)\right] * MPPGL * liver\ weight$$

EQUATION 6

$$CLint_{H,u} = \left[\sum_{j=1}^{n}\left(ISEF_j * \frac{Vmax}{Km * fu_{mic}} * CYP_j\ abundance\right)\right] * MPPGL * liver\ weight$$

EQUATION 7

Where *j* represents each of the *n* CYPs, CYP*j* abundance the *in vivo* abundance of each of the *n* CYP enzymes, the MPPGL the microsomal protein per gram liver, and the *ISEF* the inter-system

extrapolation factor; a scaling factor that compensates for any difference in the activity per unit of enzyme between recombinant systems and hepatic enzymes. The resulting hepatic intrinsic clearance is now ready to be implemented in the differential equations from the PBPK model. The liver may be considered to act as a well-stirred compartment interacting with parameters describing liver blood flow and fraction unbound in plasma (dynamic well-stirred liver model). The static form of the well stirred liver model is well-known and is represented in equation 8 [84-86].

$$CL_H = \frac{Q_H * fu_p * CLint_{H,u}}{Q_H + fu_p * \frac{CLint_{H,u}}{B:P}}$$

EQUATION 8

Where Q_H represents hepatic blood flow, fu_p the unbound fraction in plasma, $CLint_{H,u}$ the unbound hepatic intrinsic clearance, and *B:P* the blood-to-plasma ratio. Alternatively, the parallel tube or dispersion model for the liver may be used, although their mathematical complexity is higher. Moreover, the difference between the well-stirred and the other hepatic liver models is only apparent for intermediate to high extraction compounds [82, 87].

3.2.3 CLEARANCE PREDICTION IN PEDIATRICS

In the bottom-up prediction of drug clearance, the knowledge of physiological changes occurring in childhood is essential in the prediction of the clearance evolution across the pediatric age span. In predicting the drug clearance within the context of PBPK modelling and simulation, a rigorous workflow should be followed for the successful construction of an adequate pediatric PBPK model (Figure 9). First, an adult PBPK model needs to be developed, and then iteratively verified and refined. Verification of the model predictions is accomplished by using the results from *in vitro* ADME experiments and clinical studies. In this model, the different relevant drug disposition pathways need to be captured and sources of variability understood even before this model is to be used for pediatric predictions. In the next step, the pediatric drug clearance is predicted by the PBPK platform by using the drug-specific information, which has been verified in adults in the first step, and the pediatric physiology in an integrated, mechanistic framework. Then, the pediatric PBPK model should be verified and refined using the available pediatric data. Verification may be obtained i) by comparing PK parameters from top-down (*in vivo*) and bottom-up (PBPK) methodologies, or ii) by comparing observed and predicted plasma concentration-time profiles. Depending on the age group, one or the other approach may be used (e.g. sparsely sampled infants may provide popPK-estimated PK parameters which can be compared to PBPK-predicted ones). In adequate pediatric microdosing studies, PK parameters are informative about the drug's disposition at therapeutic doses [88]. Possible mismatches between PBPK-predicted and estimated *in vivo* clearances may guide subsequent experiments, i.e. the 'learning-confirming' paradigm

should be followed. Relevant pathways, specific to pediatrics, may be identified or anatomical/physiological variables carrying a high degree of uncertainty in the pediatric population may be adjusted to match the observed data. Additional drug-specific PBPK investigations may then confirm these anatomical/physiological variables [3, 71]. The incorporation of pediatric, and by extension any subpopulation's physiological information in such PBPK M&S platforms is a time and resource-costly task. However, once created, this population library can be used repeatedly for any drug under any study design. Moreover, libraries can be updated and expanded as the knowledge of the system improves [89].

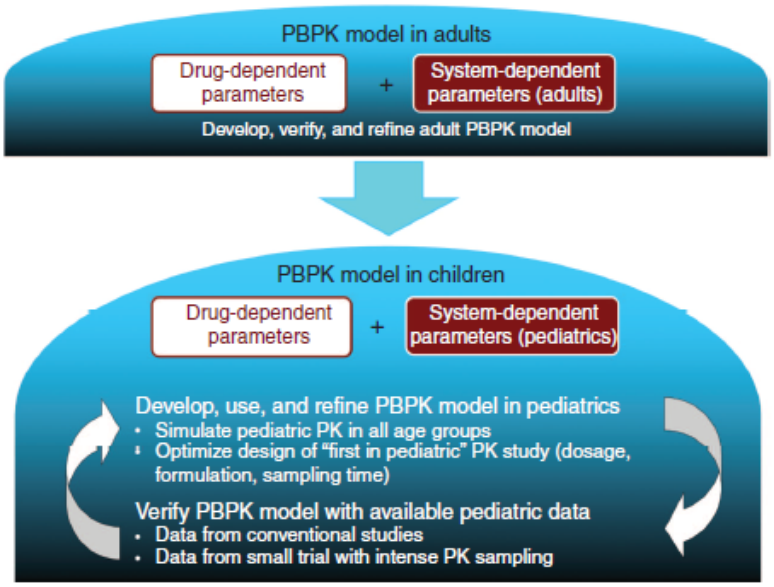

FIGURE 9: RIGOROUS WORKFLOW TO SET UP A PEDIATRIC PBPK MODEL. FIRST, THE PBPK MODEL NEEDS TO BE DEVELOPED, VERIFIED AND REFINED IN ADULTS. IN THE NEXT STEP, THIS VERIFIED PBPK MODEL IS USED TO MECHANISTICALLY PREDICT PEDIATRIC PK. VERIFICATION OF THE PEDIATRIC PBPK PREDICTIONS WITH OBSERVED PEDIATRIC DATA IS NECESSARY. THE FURTHER REFINEMENT OF THIS MODEL MAY BE NECESSARY IN THE SIMULATION OF CLINICAL TRIALS OR DIFFERENT DOSING SCENARIOS, ADAPTED FROM LEONG ET AL. [3]

To date, there are several PBPK M&S platforms commercially available (Simcyp® by Certara, PK-Sim® by Bayer, Gastroplus® by SimulationsPlus) that allow end-users (PKPD scientists) to put in experimentally determined drug-specific data and simulate the PK(PD) for a given drug in virtual patient populations that are built from system-specific information. These tools are provided as platforms on which a user-defined PBPK model can be constructed by combining building blocks in an appealing graphical user interface.

1

4 STATE-OF-ART BOTTOM-UP CLEARANCE PREDICTION IN CHILDREN AND FOCUS OF THIS DISSERTATION

The area in which PBPK models may really provide added value is for children below 2 years of age, i.e. neonates/infants. Typically in the first 2 years of life, processes 'maturation' and 'growth' occur side-by-side, impacting drug clearance in such a way that a single allometric exponent is no longer appropriate [59]. Given their physiological nature, PBPK models predict the changing elimination capacity based on the knowledge of the changing biology/physiology in these early years. PBPK models that successfully predict changes in the pediatric clearance for several drugs from very early life to adulthood, were published. Influential publications were provided by Johnson et al. [90] for 11 drugs (midazolam, caffeine, carbamazepine, cisapride, theophylline, diclofenac, omeprazole, S-warfarin, phenytoin, gentamicin, and vancomycin) and Edginton [81] for a training set of 8 (gentamicin, isepamicin, alfentanil, midazolam, caffeine, ropivacaine, morphine, lorazepam) and a test set of 6 drugs (fentanyl, theophylline, acetaminophen, ciprofloxacin, lidocaine, buprenorphine) after i.v. administration. Although both publications contrast bottom-up clearance predictions with observed pediatric clearances, both share a similar weakness. Predicted and observed total clearances are compared, even if the compounds were eliminated by different pathways. Hence, biases in pathway-specific contributions may cancel out in the predicted total clearance. The consequence is that if these models are to be used for situations in which the renal or metabolic route is impaired, the predicted clearance may be completely erroneous since the underlying contributions could be incorrect. Therefore, an in-depth analysis of different pathways involved in the bottom-up prediction and top-down estimation of the clearance is provided in this work. To this end, tramadol was used as the model compound. Tramadol is an excellent probe substrate because of 3 reasons. First, tramadol is clinically implemented as an analgesic drug, used over the entire pediatric age range from premature neonates to adults. Moreover, relatively much data is available coming from tramadol's clinical use in the pediatric population. The analgesic effect of tramadol is mediated through noradrenaline re-uptake inhibition, increased release of serotonin, and decreased re-uptake of serotonin in the spinal cord [91]. Concerning the opioid effect, tramadol itself has weak μ-opioid activity (~6000 times weaker than morphine), but the CYP2D6 metabolite, O-desmethyltramadol, has a μ-opioid-receptor affinity approximately 300 times larger than tramadol [92]. Consequently, CYP2D6 poor metabolizer status is highly correlated with an increased non-response rate to pain medication, making individualized treatment highly necessary [93]. Second, the different pathways involved in the disposition of tramadol include a renal component, as well as CYP enzymes CYP2D6, CYP3A4, and CYP2B6. As was already outlined in the section on pediatric ADME, these are relevant disposition routes for the majority of drugs. By investigating the ontogeny and activity of tramadol's disposition routes in a PBPK-M&S environment, indirectly the prediction of many drugs, eliminated by

at least one of these disposition routes, will be enhanced. Third, given the low hepatic extraction of tramadol, its *in vivo* hepatic clearance is sensitive to changes in the activity of the involved CYP enzymes. Any alterations in CYP activity will be reflected in the hepatic clearance, e.g. immature clearance in pediatrics, and CYP2D6 poor-extensive metabolizers. Taken all together, tramadol is well-suited to investigate pediatric bottom-up clearance maturation, particularly focusing on children below 2 years of age.

1

5 PKPD OF TRAMADOL

5.1 INTRODUCTION

In this PhD dissertation, tramadol is the model compound that allowed us to investigate the maturation of CYP2D6 and renal clearance from birth to adulthood. Tramadol is a centrally acting analgesic drug, which is structurally related to morphine and codeine. It is known to exhibit enantioselective metabolism and pharmacodynamics properties. Tramadol has weak μ-opioid activity and inhibits serotonin and norepinephrine reuptake, thereby inhibiting pain transmission in the spinal cord. O-desmethyltramadol, the CYP2D6 metabolite of tramadol, has a μ-opioid activity 300-times higher than that of tramadol. It was first registered as analgesic drug in Germany in 1977, and later on in the UK (1994) and US (1995) with many other countries to follow. Given the unique PD profile of this drug, it has been classified as a nontraditional centrally acting analgesic by the FDA. This section aims to provide a brief overview of the PKPD properties of this drug and its clinical implementation, with a focus on pediatrics. The reason why tramadol was chosen as a model compound is discussed in section 4 "State-of-art bottom-up clearance prediction in children and focus of this dissertation".

5.2 PHYSICOCHEMICAL INFORMATION

Tramadol, or (1RS,2RS)- 2-[(dimethylamino)methyl]- 1 -(3-methoxyphenyl)- cyclohexanol has a molecular weight of 263.4 g/mol and is depicted alongside its metabolites in Figure 10. It is a weak base with a pKa of 9.41, which makes that tramadol is ionized and caries a positive charge on its amine residue at physiological pH. The logP-value is 1.35, showing a moderate tendency of tramadol towards the lipid phase. Tramadol has 2 chiral centers and is formulated as racemic mixture, mostly as the tramadol hydrochloride salt [94].

5.3 PHARMACOKINETICS

5.3.1 ABSORPTION

Tramadol is formulated as a solution for injection, immediate and sustained release capsules, drops, and suppositories for different administration routes (intravenous, intramuscular, subcutaneous, and per os). After a single oral dose, tramadol attains a bioavailability of 70%, and is subject to first-pass metabolism. Upon multiple administration the bioavailability reaches 90-100%, probably due to saturation of first-pass metabolism. Plasma concentrations and AUC increase linearly over a dose range of 50-400 mg. No food effect was observed in tramadol's PK. Bioavailability of tramadol in drops with or without ethanol, remains similar. After rectal administration, absolute bioavailability is higher,

probably due to (partial) avoidance of first-pass. Intramuscular injection and infusion are bio-equivalent [92, 95-97].

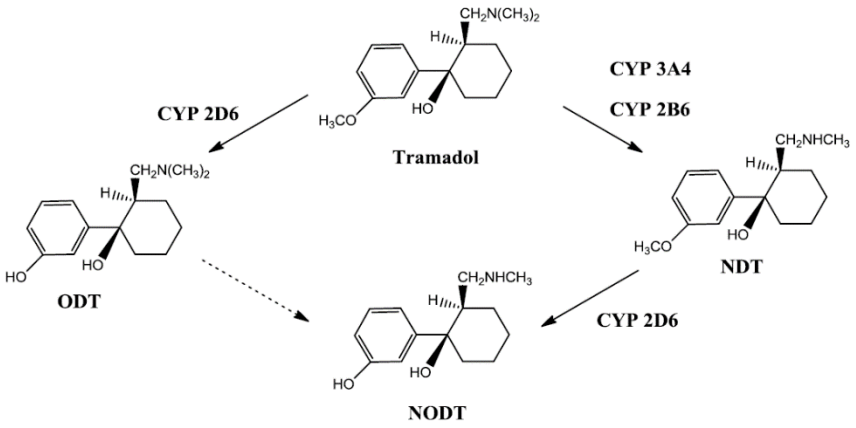

FIGURE 10: MOLECULAR STRUCTURE OF TRAMADOL AND ITS PRIMARY PHASE I METABOLITES O-DESMETHYLTRAMADOL (ODT), N-DESMETHYLTRAMADOL (NDT), AND THE SECONDARY NODT (N,O-DIDESMETHYLTRAMADOL).

5.3.2 DISTRIBUTION

Tramadol displays extensive tissue distribution and distributes widely throughout the body, especially in the lungs, spleen, liver, kidneys and brain. This is readily observed by the initial drop in tramadol plasma concentrations after an i.v. bolus dose (Figure 11), leading to a typical two-compartmental pharmacokinetic profile. The volume of distribution is estimated at 210 L for a 70 kg individual. Due to the fact that tramadol is a weak base, many charge-charge interactions are possible between tramadol and the constituents of biological membranes, i.e. acidic phospholipids. In addition, weak bases tend to accumulate intracellularly (and in lysosomes in particular) because of the more acidic pH at the intracellular side of the cell membrane.

Plasma protein binding for tramadol is reported to be 20% of the total tramadol plasma concentration and typical plasma concentrations are in the region of 5 to 10 µM (1.3 to 2.6 µg/mL). In addition, *in vitro* studies indicate that tramadol and its metabolite, O-desmethyltramadol (ODT), are substrates for OCT transporters. However, tramadol plasma concentrations *in vivo* are unaffected by the OCT1-genotype, while ODT concentrations are [92, 98].

1

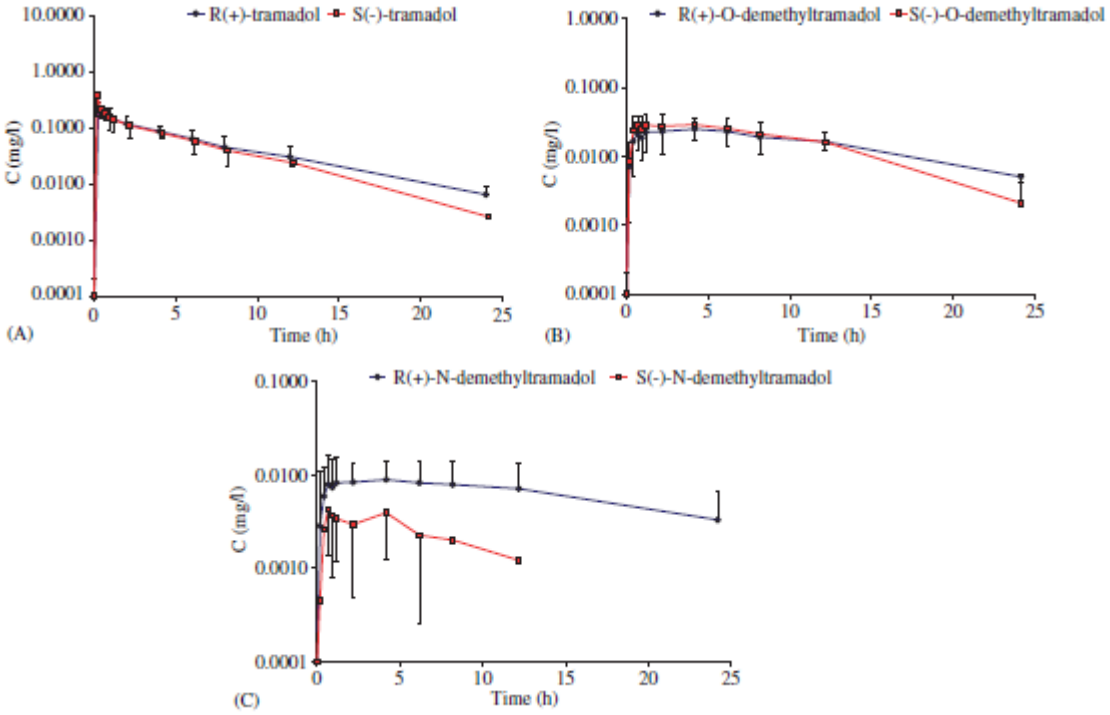

FIGURE 11: SEMILOGARITHMIC PLOTS OF TRAMADOL, ODT, AND NDT MEAN PLASMA CONCENTRATION VS. TIME PROFILES AFTER A 100MG RACEMIC TRAMADOL I.V. DOSE, ADAPTED FROM GARCIA QUETGLASS, ET AL. [99].

5.3.3 EXCRETION

Ninety percent of a tramadol dose (unchanged tramadol and metabolites) may be traced back in urine, while only 10% is excreted via the faeces. The kidney accounts for 25% of the tramadol plasma clearance that is mainly governed by glomerular filtration. Tramadol has an extensive metabolite profile (23 metabolites from phase I & II reactions have been identified in man) but is considered a low clearance drug [100]. The plasma clearance is 30 L/h, of which 75% is hepatically cleared. The metabolism of tramadol to its primary metabolites, ODT and N-desmethyltramadol (NDT), is governed by CYP enzymes. *In vitro* metabolism studies of tramadol indicated that CYP2D6, CYP3A4 and CYP2B6 are mainly responsible for tramadol phase I metabolism. As indicated in Figure 10, Tramadol metabolism to ODT is mainly governed by CYP2D6, while the N-demethylation to NDT is governed by CYP2B6 and CYP3A4. There is a common secondary metabolite as well, N,O-didesmethyltramadol (NODT), although its formation is believed to be mainly driven by CYP2D6 from NDT [100-102]. The formation of ODT is slow *in vivo*, with reported Tmax values of 1.4h later than tramadol Tmax. The half-lives of the metabolites ODT and NDT are similar to the one of tramadol, making the metabolites kinetics formation-rate dependent [92].

CYP2D6 is an enzyme known to exhibit genetic polymorphisms, leading to different phenotypes in the patient population. Poor metabolizers have two null-alleles leading to a non-functional CYP2D6 protein, while intermediate and extensive metabolizers have at least one allele that leads to functional CYP2D6. Ultra-rapid metabolizers even have more than two alleles. This phenotypic variation does not only lead to a difference in tramadol clearance in the population, it also results in pharmacodynamic variation since the CYP2D6 metabolite has stronger opioid activity than tramadol itself (see later) [25, 93].

In addition, tramadol displays stereoselective metabolism. The O-demethylation appeared to be 2-fold greater for (-)-tramadol than for (+)-tramadol. On the other hand, N-demethylation occurs faster for the (+)-enantiomer. The kidney preferably eliminates (-)-tramadol and (+)-ODT. In terms of total exposure, the AUC for (+)-tramadol and (+)-NDT is greater than the AUC for their (-)-enantiomers [92].

5.4 PHARMACODYNAMICS

Tramadol possesses a moderate affinity for the μ-opioid receptor. Compared to morphine and codeine, tramadol's affinity is respectively 6000- and 10-times lower. In a way, tramadol may be considered a prodrug since the metabolic reaction via CYP2D6 releases the ODT metabolite that has 300-times more affinity for the μ-opioid receptor than tramadol itself. The CYP2D6-polymorphism has led to the observation that treatment efficacy *in vivo* is associated with CYP2D6 genotype [93]. In addition, tramadol also inhibits the neuronal reuptake of norepinephrine and serotonin, neurotransmitters involved in antinociceptive effects of the descending inhibitory pathways of the central nervous system. This dual mode of action provides tramadol its status of nontraditional centrally acting analgesic. Stereoselectivity is also observed in tramadol's mechanism of action. (+)-Tramadol binds to the μ-opioid receptor with a 20-fold higher affinity than (-)-tramadol. In addition, (+)-tramadol mainly blocks serotonin reuptake, while (-)-tramadol is the main blocker for norepinephrine reuptake [92, 103].

5.5 TRAMADOL CLINICAL USE

Tramadol is mainly used in patients, suffering from postoperative pain. It is effective in providing adequate analgesia in acute pain, being superior to placebo in many studies. In some cases however, tramadol's analgesic effects are not distinguishable from placebo, depending on the baseline pain intensity. Therefore, tramadol may be combined with other analgesics (e.g. paracetamol, or dipyrone) to broaden its clinical applications [92, 104]. Oral or intravenous tramadol administration may be preferred, since intramuscular injection is painful and the absorption may delay Tmax, thereby hampering fast pain relief. Tramadol shares some common features of opioids as typical adverse events include nausea and vomiting. However, a major advantage of tramadol over opioids is that it minimally affects respiratory function, making it an often-used analgesic drug in children for moderate to severe

pain. In addition, given the pathways involved in its elimination, impairment of one route will not directly lead to safety concerns, as the others take over. However, in patients suffering from severe liver cirrhosis or renal failure, the drug dose should be adapted.

5.6 TRAMADOL PKPD IN PEDIATRICS

Earlier reports claiming there is no age-dependency in tramadol's PK [92, 105] are contradicted by new insights in the field. A study by Allegaert et al [106] pooled the available pediatric and adult studies that describe tramadol disposition after i.v. administration. The raw data from different individual authors was gathered and used to construct a population PK model. Differences in pediatric tramadol and ODT PK vs. adults are mainly explained by weight and age differences, requiring the use of an allometric exponent when extrapolating from adult data. The tramadol clearance that is attributable to CYP2D6, is even considered to mature in very early life and reaches 50% of the adult-normalized value at 39.8 weeks PMA, i.e. shortly before term birth. Thereafter, mainly the increase in body weight explains the increasing clearance of tramadol. The maturation in renal function occurs slower (50% of adult-normalized activity at 47.7 weeks), so that clearance of the ODT metabolite as well as tramadol urinary excretion is delayed in early life as compared to the CYP2D6 maturation. In the Allegaert study, it could be estimated that in subjects with low CYP2D6 activity, the formation clearance of ODT was 19.4% of that in extensive metabolizers at the population level. In this analysis, not more than two phenotypic groups could be identified, i.e. poor and extensive metabolizers. It should be noted, however, that the formation and elimination of ODT in this analysis is considered to be the result of CYP2D6 activity and renal filtration. Information regarding the influence of organic cationic transporter (OCT1)-activity on ODT disposition still is lacking and should be supplemented to better understand the disposition of this metabolite. The volume of distribution can be scaled from children to adults based solely on weight. Looking at the dosing protocols that are used in children (table 2 from the reference article), it stands out that different loading and maintenance doses are provided to these children in different studies. Since this popPK analysis determines how the clearance changes with age, a consensus should be made on the appropriate dosing regimen, which is to be used in the clinic for tramadol use in pediatrics. In addition, it needs mentioning that tramadol still is used off-label in the pediatric population because of the risk for respiratory depression. FDA is currently investigating the use of tramadol in pediatrics and will communicate their findings upon completion of the review [107].

6 REFERENCES

1. Umscheid CA, Margolis DJ, Grossman CE. Key Concepts of Clinical Trials: A Narrative Review. Postgrad med. 2011;123(5):194-204.
2. Shirkey H. Therapeutic orphans. J Pediatr. 1968;72(1):119-20.
3. Leong R, Vieira MLT, Zhao P, Mulugeta Y, Lee CS, Huang SM, et al. Regulatory Experience With Physiologically Based Pharmacokinetic Modeling for Pediatric Drug Trials. Clin Pharmacol Ther. 2012.
4. Corny J, Lebel D, Bailey B, Bussieres JF. Unlicensed and Off-Label Drug Use in Children Before and After Pediatric Governmental Initiatives. J Pediatr Pharmacol Ther. 2015;20(4):316-28.
5. FDA website. CDER World- Pediatric Regulations. [cited; Available from: https://www.accessdata.fda.gov/scripts/cderworld/index.cfm?action=newdrugs:main&unit=4&lesson=1&topic=8
6. EMA website. EMA- Paediatric Regulation. [cited; Available from: http://www.ema.europa.eu/ema/index.jsp?curl=pages/regulation/document_listing/document_listing_000068.jsp
7. Shaddy RE, Denne SC. Guidelines for the Ethical Conduct of Studies to Evaluate Drugs in Pediatric Populations. Pediatrics. 2010;125(4):850-60.
8. Tassinari M. Pediatric Regulations 2012: Permanent Laws and New Provisions under FDASIA. 2012.
9. Schmidt LE, Dalhoff K. Food-drug interactions. Drugs. 2002;62(10):1481-502.
10. Bowles A, Keane J, Ernest T, Clapham D, Tuleu C. Specific aspects of gastro-intestinal transit in children for drug delivery design. Int J Pharm. 2010;395(1-2):37-43.
11. 't Jong G. Pediatric Development: Physiology. Enzymes, Drug Metabolism, Pharmacokinetics and Pharmacodynamics. In: Bar-Shalom DK, R, editor. Pediatric Formulations: A Roadmap. AAPS Advances in the Pharmaceutical Sciences Series: American Association of Pharmaceutical Scientists; 2014. p. 9-23.
12. Kearns GL, Abdel-Rahman SM, Alander SW, Blowey DL, Leeder JS, Kauffman RE. Developmental pharmacology--drug disposition, action, and therapy in infants and children. N Engl J Med. 2003;349(12):1157-67.
13. Strolin Benedetti M, Baltes EL. Drug metabolism and disposition in children. Fundam Clin Pharmacol. 2003;17(3):281-99.
14. Mahmood I. Developmental Pharmacology: Impact on Pharmacokinetics and Pharmacodynamics of Drugs. In: Mahmood IB, G., editor. Fundamentals of Pediatric Drug Dosing. Switzerland: Springer International Publishing Switzerland 2016; 2016. p. 23-44.
15. McNamara PJ, Alcorn J. Protein binding predictions in infants. AAPS PharmSci. 2002;4(1):E4.
16. MacKichan J. Influence of protein binding and use of unbound (free) drug concentrations. In: Burton MS, LM; Schentag, JJ; Evans, WE, editor. Applied Pharmacokinetics and Pharmacodynamics Principles of Therapeutic Drug Monitoring. Baltimore: Lippincott Wiliams & Wilkins; 2006. p. 82-120.
17. Toutain PL, Bousquet-Melou A. Free drug fraction vs free drug concentration: a matter of frequent confusion. J Vet Pharmacol Ther. 2002;25(6):460-3.

18. Lin JH. Transporter-mediated drug interactions: clinical implications and in vitro assessment. Expert Opin Drug Metab Toxicol. 2007;3(1):81-92.

19. Brouwer KL, Aleksunes LM, Brandys B, Giacoia GP, Knipp G, Lukacova V, et al. Human Ontogeny of Drug Transporters: Review and Recommendations of the Pediatric Transporter Working Group. Clin Pharmacol Ther. 2015;98(3):266-87.

20. Gonzalez F, Robert T. Chapter 3: Drug metabolism. In: Brunton LB, Lazo JS, Parker KL, editors. Goodman & Gilman's The Pharmacological Basis of Therapeutics. 11th ed. New York: McGraw-Hill; 2005.

21. Nebert DW, Russell DW. Clinical importance of the cytochromes P450. Lancet. 2002;360(9340):1155-62.

22. Zhou SF, Liu JP, Chowbay B. Polymorphism of human cytochrome P450 enzymes and its clinical impact. Drug Metab Rev. 2009;41(2):89-295.

23. de Wildt SN, Tibboel D, Leeder JS. Drug metabolism for the paediatrician. Arch Dis Child. 2014;99(12):1137-42.

24. Zanger UM, Schwab M. Cytochrome P450 enzymes in drug metabolism: regulation of gene expression, enzyme activities, and impact of genetic variation. Pharmacol Ther. 2013;138(1):103-41.

25. Zhou SF. Polymorphism of Human Cytochrome P450 2D6 and Its Clinical Significance Part I. Clin Pharmacokinet. 2009;48(11):689-723.

26. Alcorn J, McNamara PJ. Ontogeny of hepatic and renal systemic clearance pathways in infants: part I. Clin Pharmacokinet. 2002;41(12):959-98.

27. Alcorn J, McNamara PJ. Ontogeny of hepatic and renal systemic clearance pathways in infants: part II. Clin Pharmacokinet. 2002;41(13):1077-94.

28. Hines RN. The ontogeny of drug metabolism enzymes and implications for adverse drug events. Pharmacol Ther. 2008;118(2):250-67.

29. de Wildt SN. Profound changes in drug metabolism enzymes and possible effects on drug therapy in neonates and children. Expert Opin Drug Metab Toxicol. 2011;7(8):935-48.

30. De Bock L. Pharmacokinetics in children with liver disease: can ex vivo obtained population-specific CYP450 characteristics bridge the knowledge gap? [Doctoral Dissertation]. Ghent: Ghent University; 2014.

31. Hines RN. Developmental expression of drug metabolizing enzymes: impact on disposition in neonates and young children. Int J Pharm. 2013;452(1-2):3-7.

32. Ince I, Knibbe CA, Danhof M, de Wildt SN. Developmental changes in the expression and function of cytochrome P450 3A isoforms: evidence from in vitro and in vivo investigations. Clin Pharmacokinet. 2013;52(5):333-45.

33. Salem F, Johnson TN, Abduljalil K, Tucker GT, Rostami-Hodjegan A. A re-evaluation and validation of ontogeny functions for cytochrome P450 1A2 and 3A4 based on in vivo data. Clin Pharmacokinet. 2014;53(7):625-36.

34. Upreti VV, Wahlstrom JL. Meta-analysis of hepatic cytochrome P450 ontogeny to underwrite the prediction of pediatric pharmacokinetics using physiologically based pharmacokinetic modeling. J Clin Pharmacol. 2016;56(3):266-83.

35. Ward RM, Tammara B, Sullivan SE, Stewart DL, Rath N, Meng X, et al. Single-dose, multiple-dose, and population pharmacokinetics of pantoprazole in neonates and preterm infants with a clinical diagnosis of gastroesophageal reflux disease (GERD). Eur J Clin Pharmacol. 2010;66(6):555-61.

36. Green DJ, Mummaneni P, Kim IW, Oh JM, Pacanowski M, Burckart GJ. Pharmacogenomic information in FDA-approved drug labels: Application to pediatric patients. Clin Pharmacol Ther. 2016;99(6):622-32.

37. Blake MJ, Gaedigk A, Pearce RE, Bomgaars LR, Christensen ML, Stowe C, et al. Ontogeny of dextromethorphan O- and N-demethylation in the first year of life. Clin Pharmacol Ther. 2007;81(4):510-6.

38. Anderson BJ, Holford NH. Understanding dosing: children are small adults, neonates are immature children. Arch Dis Child. 2013;98(9):737-44.

39. Leeder JS. Translating pharmacogenetics and pharmacogenomics into drug development for clinical pediatrics and beyond. Drug Discov Today. 2004;9(13):567-73.

40. Johnson TN, Tucker GT, Tanner MS, Rostami-Hodjegan A. Changes in liver volume from birth to adulthood: a meta-analysis. Liver Transpl. 2005;11(12):1481-93.

41. Calvier EA, Krekels EH, Valitalo PA, Rostami-Hodjegan A, Tibboel D, Danhof M, et al. Allometric Scaling of Clearance in Paediatric Patients: When Does the Magic of 0.75 Fade? Clin Pharmacokinet. 2016.

42. De Cock RF, Allegaert K, Schreuder MF, Sherwin CM, de Hoog M, van den Anker JN, et al. Maturation of the glomerular filtration rate in neonates, as reflected by amikacin clearance. Clin Pharmacokinet. 2012;51(2):105-17.

43. De Cock RF, Allegaert K, Brussee JM, Sherwin CM, Mulla H, de Hoog M, et al. Simultaneous pharmacokinetic modeling of gentamicin, tobramycin and vancomycin clearance from neonates to adults: towards a semi-physiological function for maturation in glomerular filtration. Pharm Res. 2014;31(10):2643-54.

44. Chen N, Aleksa K, Woodland C, Rieder M, Koren G. Ontogeny of drug elimination by the human kidney. Pediatr Nephrol. 2006;21(2):160-8.

45. Rowland MT, T. Clinical Pharmacokinetics and Pharmacodynamics: Concepts and Apllications. 4th ed. Philadelphia, PA: Lippincott Williams & Wilkins, a Wolters Kluwen business; 2011.

46. Bagby S. Prenatal Origins of Chronic Kidney Disease. In: Kimmel PR, M, editor. Chronic Renal Disease. USA: Elsevier; 2014. p. 783-99.

47. Ghibellini G, Leslie EM, Brouwer KL. Methods to evaluate biliary excretion of drugs in humans: an updated review. Mol Pharm. 2006;3(3):198-211.

48. Johnson TN, Jamei M, Rowland-Yeo K. How Does In Vivo Biliary Elimination of Drugs Change with Age? Evidence from In Vitro and Clinical Data Using a Systems Pharmacology Approach. Drug Metab Dispos. 2016;44(7):1090-8.

49. Rollins DE, Klaassen CD. Biliary excretion of drugs in man. Clin Pharmacokinet. 1979;4(5):368-79.

50. Sheiner LB. Learning versus confirming in clinical drug development. Clin Pharmacol Ther. 1997;61(3):275-91.

51. Laer S, Barrett JS, Meibohm B. The in silico child: using simulation to guide pediatric drug development and manage pediatric pharmacotherapy. J Clin Pharmacol. 2009;49(8):889-904.

52. Lalonde RL, Kowalski KG, Hutmacher MM, Ewy W, Nichols DJ, Milligan PA, et al. Model-based drug development. Clin Pharmacol Ther. 2007;82(1):21-32.

53. Milligan PA, Brown MJ, Marchant B, Martin SW, van der Graaf PH, Benson N, et al. Model-based drug development: a rational approach to efficiently accelerate drug development. Clin Pharmacol Ther. 2013;93(6):502-14.

54. Laer S, Meibohm B. Study Design and Simulation Approach. In: Seyberth H, Rane A, Schwab M, editors. Pediatric Clinical Pharmacology. 205 ed. Berlin Heidelberg: Springer Berlin Heidelberg; 2011. p. 125-48.

55. Mould DR, Upton RN. Basic concepts in population modeling, simulation, and model-based drug development. CPT Pharmacometrics Syst Pharmacol. 2012;1:e6.

56. Ette EI, Williams PJ. Population pharmacokinetics I: background, concepts, and models. Ann Pharmacother. 2004;38(10):1702-6.

57. De Cock RF, Piana C, Krekels EH, Danhof M, Allegaert K, Knibbe CA. The role of population PK-PD modelling in paediatric clinical research. Eur J Clin Pharmacol. 2011;67 Suppl 1:5-16.

58. Sun H, Fadiran EO, Jones CD, Lesko L, Huang SM, Higgins K, et al. Population pharmacokinetics. A regulatory perspective. Clin Pharmacokinet. 1999;37(1):41-58.

59. Mahmood I. Dosing in children: a critical review of the pharmacokinetic allometric scaling and modelling approaches in paediatric drug development and clinical settings. Clin Pharmacokinet. 2014;53(4):327-46.

60. Anderson BJ, Holford NH. Mechanism-based concepts of size and maturity in pharmacokinetics. Annu Rev Pharmacol Toxicol. 2008;48:303-32.

61. Mahmood I. Application of fixed exponent 0.75 to the prediction of human drug clearance: an inaccurate and misleading concept. Drug Metabol Drug Interact. 2009;24(1):57-81.

62. Johnson TN. The problems in scaling adult drug doses to children. Arch Dis Child. 2008;93(3):207-11.

63. Bonate PL. The effect of collinearity on parameter estimates in nonlinear mixed effect models. Pharm Res. 1999;16(5):709-17.

64. Mahmood I. Evaluation of sigmoidal maturation and allometric models: prediction of propofol clearance in neonates and infants. Am J Ther. 2013;20(1):21-8.

65. Krekels EH, Neely M, Panoilia E, Tibboel D, Capparelli E, Danhof M, et al. From pediatric covariate model to semiphysiological function for maturation: part I-extrapolation of a covariate model from morphine to Zidovudine. CPT Pharmacometrics Syst Pharmacol. 2012;1:e9.

66. Zhao P, Zhang L, Grillo JA, Liu Q, Bullock JM, Moon YJ, et al. Applications of physiologically based pharmacokinetic (PBPK) modeling and simulation during regulatory review. Clin Pharmacol Ther. 2011;89(2):259-67.

67. Khalil F, Laer S. Physiologically based pharmacokinetic modeling: methodology, applications, and limitations with a focus on its role in pediatric drug development. J Biomed Biotechnol. 2011;2011:907461.

68. Nestorov IA, Aarons LJ, Arundel PA, Rowland M. Lumping of whole-body physiologically based pharmacokinetic models. J Pharmacokinet Biopharm. 1998;26(1):21-46.

69. Willmann S, Lippert J, Sevestre M, Solodenko J, Fois F, Schmitt W. PK-Sim®: a physiologically based pharmacokinetic 'whole-body' model. BIOSILICO. 2003;1(4):121-4.

70. Pelkonen O, Turpeinen M, Raunio H. In vivo-in vitro-in silico pharmacokinetic modelling in drug development: current status and future directions. Clin Pharmacokinet. 2011;50(8):483-91.

71. Maharaj AR, Edginton AN. Physiologically based pharmacokinetic modeling and simulation in pediatric drug development. CPT Pharmacometrics Syst Pharmacol. 2014;3:e150.

72. Austin RP, Barton P, Cockroft SL, Wenlock MC, Riley RJ. The influence of nonspecific microsomal binding on apparent intrinsic clearance, and its prediction from physicochemical properties. Drug Metab Dispos. 2002;30(12):1497-503.

73. Hallifax D, Houston JB. Binding of drugs to hepatic microsomes: comment and assessment of current prediction methodology with recommendation for improvement. Drug Metab Dispos. 2006;34(4):724-6.

74. Rodgers T, Leahy D, Rowland M. Physiologically based pharmacokinetic modeling 1: Predicting the tissue distribution of moderate-to-strong bases. J Pharm Sci. 2005;94(6):1259-76.

75. Rodgers T, Rowland M. Physiologically based pharmacokinetic modelling 2: Predicting the tissue distribution of acids, very weak bases, neutrals and zwitterions. J Pharm Sci. 2006;95(6):1238-57.

76. Poulin P, Theil FP. Prediction of pharmacokinetics prior to in vivo studies. 1. Mechanism-based prediction of volume of distribution. J Pharm Sci. 2002;91(1):129-56.

77. Schmitt W. General approach for the calculation of tissue to plasma partition coefficients. Toxicology in Vitro. 2008;22(2):457-67.

78. Jamei M, Marciniak S, Feng K, Barnett A, Tucker G, Rostami-Hodjegan A. The Simcyp population-based ADME simulator. Expert Opin Drug Metab Toxicol. 2009;5(2):211-23.

79. Johnson TN, Rostami-Hodjegan A. Resurgence in the use of physiologically based pharmacokinetic models in pediatric clinical pharmacology: parallel shift in incorporating the knowledge of biological elements and increased applicability to drug development and clinical practice. Paediatr Anaesth. 2011;21(3):291-301.

80. Rostami-Hodjegan A, Tucker GT. Simulation and prediction of in vivo drug metabolism in human populations from in vitro data. Nat Rev Drug Discov. 2007;6(2):140-8.

81. Edginton AN, Schmitt W, Voith B, Willmann S. A mechanistic approach for the scaling of clearance in children. Clin Pharmacokinet. 2006;45(7):683-704.

82. Fagerholm U. Prediction of human pharmacokinetics--evaluation of methods for prediction of hepatic metabolic clearance. J Pharm Pharmacol. 2007;59(6):803-28.

83. Stringer RA, Strain-Damerell C, Nicklin P, Houston JB. Evaluation of recombinant cytochrome P450 enzymes as an in vitro system for metabolic clearance predictions. Drug Metab Dispos. 2009;37(5):1025-34.

84. Howgate EM, Rowland Yeo K, Proctor NJ, Tucker GT, Rostami-Hodjegan A. Prediction of in vivo drug clearance from in vitro data. I: impact of inter-individual variability. Xenobiotica. 2006;36(6):473-97.

85. Proctor NJ, Tucker GT, Rostami-Hodjegan A. Predicting drug clearance from recombinantly expressed CYPs: intersystem extrapolation factors. Xenobiotica. 2004;34(2):151-78.

86. Yang J, Jamei M, Yeo KR, Rostami-Hodjegan A, Tucker GT. Misuse of the well-stirred model of hepatic drug clearance. Drug Metab Dispos. 2007;35(3):501-2.

87. Pang KS, Rowland M. Hepatic clearance of drugs. I. Theoretical considerations of a "well-stirred" model and a "parallel tube" model. Influence of hepatic blood flow, plasma and blood cell binding, and the hepatocellular enzymatic activity on hepatic drug clearance. J Pharmacokinet Biopharm. 1977;5(6):625-53.

88. Turner MA, Mooij MG, Vaes WH, Windhorst AD, Hendrikse NH, Knibbe CA, et al. Pediatric microdose and microtracer studies using 14C in Europe. Clin Pharmacol Ther. 2015;98(3):234-7.

89. Jamei M, Dickinson GL, Rostami-Hodjegan A. A framework for assessing inter-individual variability in pharmacokinetics using virtual human populations and integrating general knowledge of physical chemistry, biology, anatomy, physiology and genetics: A tale of 'bottom-up' vs 'top-down' recognition of covariates. Drug Metab Pharmacokinet. 2009;24(1):53-75.

90. Johnson TN, Rostami-Hodjegan A, Tucker GT. Prediction of the clearance of eleven drugs and associated variability in neonates, infants and children. Clin Pharmacokinet. 2006;45(9):931-56.

91. Allegaert K, van den Anker J, de Hoon J, van Schaik R, Debeer A, Tibboel D, et al. Covariates of tramadol disposition in the first months of life. BJA. 2008;100(4):525-32.

92. Grond S, Sablotzki A. Clinical pharmacology of tramadol. Clin Pharmacokinet. 2004;43(13):879-923.

93. Stamer UM, Musshoff F, Kobilay M, Madea B, Hoeft A, Stuber F. Concentrations of Tramadol and O-desmethyltramadol Enantiomers in Different CYP2D6 Genotypes. Clin Pharmacol Ther. 2007;82(1):41-7.

94. WHO. Tramadol Update Review Report Agenda item 6.1: World Health Organization; 2014.

95. Lintz W, Barth H, Becker R, Frankus E, Schmidt-Bothelt E. Pharmacokinetics of tramadol and bioavailability of enteral tramadol formulations - 2nd communication: Drops with ethanol. Arzneimittel-Forschung. 1998;48(5):436-45.

96. Lintz W, Barth H, Osterloh G, Schmidt-Bothelt E. Bioavailability of Enteral Formulations 1st communication: Capsules. Arzneimittel-Forschung. 1986;36-2(8):1278-83.

97. Lintz W, Barth H, Osterloh G, Schmidt-Bothelt E. Pharmacokinetics of tramadol and bioavailability of enteral tramadol formulations - 3rd communication: Suppositories. Arzneimittel-Forschung. 1998;48(9):889-99.

98. Tzvetkov MV, Saadatmand AR, Lotsch J, Tegeder I, Stingl JC, Brockmoller J. Genetically Polymorphic OCT1: Another Piece in the Puzzle of the Variable Pharmacokinetics and Pharmacodynamics of the Opioidergic Drug Tramadol. Clin Pharmacol Ther. 2011;90(1):143-50.

99. Quetglas EG, Azanza JR, Cardenas E, Sadaba B, Campanero MA. Stereoselective pharmacokinetic analysis of tramadol and its main phase I metabolites in healthy subjects after intravenous and oral administration of racemic tramadol. Biopharm Drug Dispos. 2007;28(1):19-33.

100. Wu WN, Mckown LA, Liao S. Metabolism of the analgesic drug ULTRAM (R) (tramadol hydrochloride) in humans: API-MS and MS/MS characterization of metabolites. Xenobiotica. 2002;32(5):411-25.

101. Abdel-Rahman SM, Leeder JS, Wilson JT, Gaedigk A, Gotschall RR, Medve R, et al. Concordance between tramadol and dextromethorphan parent/metabolite ratios: the influence of CYP2D6 and non-CYP2D6 pathways on biotransformation. J Clin Pharmacol. 2002;42(1):24-9.

102. Subrahmanyam V, Renwick AB, Walters DG, Young PJ, Price RJ, Tonelli AP, et al. Identification of Cytochrome P-450 Isoforms Responsible for cis-Tramadol Metabolism in Human Liver Microsomes. Drug Metab Dispos. 2001;29(8):1146-55.

103. Gillen C, Haurand M, Kobelt DJ, Wnendt S. Affinity, potency and efficacy of tramadol and its metabolites at the cloned human mu-opioid receptor. Naunyn Schmiedebergs Arch Pharmacol. 2000;362(2):116-21.

104. Wiebalck A, Zenz M, Tryba M, Kindler D, Donner B, Czekalla U. [Are tramadol enantiomers for postoperative pain therapy better suited than the racemate? A randomized, placebo- and morphine-controlled double blind study]. Anaesthesist. 1998;47(5):387-94.

105. Bamigbade TA, Langford RM. Tramadol hydrochloride: an overview of current use. Hosp Med. 1998;59(5):373-6.

106. Allegaert K, Holford N, Anderson BJ, Holford S, Stuber F, Rochette A, et al. Tramadol and o-desmethyl tramadol clearance maturation and disposition in humans: a pooled pharmacokinetic study. Clin Pharmacokinet. 2015;54(2):167-78.

107. FDA website. FDA Drug Safety Communication: FDA evaluating the risks of using the pain medicine tramadol in children aged 17 and younger. 21-09-2015 [cited; Available from: http://www.fda.gov/Drugs/DrugSafety/ucm462991.htm

1

CHAPTER 2

OBJECTIVES

2

2

An often used phrase in pediatric pharmacology is that “children are not small adults”. Hence, the pediatric drug dose is often not a miniature adult dose, but should be tailored to this specific population in order to obtain the adequate exposure, ensuring acceptable efficacy/safety profiles in children. In drug development as well as in the clinic, children’s drug doses are typically calculated based on several scaling approaches, using easily accessible covariates. These include the scaling of the adult drug dose (or clearance & volume) using bodyweight, body surface area, or some empirically-derived exponent to the pediatric dose [1]. Any of these methods failed to reliably predict the drug dose that should be given over the complete pediatric age range for certain classes of compounds. The main problem is that these approaches do not consistently take into account organ maturation, changes in body composition, and the ontogeny of drug elimination pathways across the pediatric life span. Because these changes are often non-linear, a simple linear or exponential model frequently fails to predict an adequate pediatric drug dose, especially in children below 2 years of age. The population pharmacokinetic (popPK) approach is a ‘top-down’ model-based approach in which the changes in pharmacokinetic parameters (mainly clearance or volume of distribution) and their variability are assessed over the pediatric life span, based on measured plasma-concentration time profiles. These models may provide a much better quantitative description of the changes in drug disposition that affect the drug plasma concentration. A disadvantage, however, is that they remain drug-dependent *per se,* which limits their extrapolatibility, although some groups are putting efforts in circumventing these constraints [2].

An approach in which physiological changes occurring in early life implicitly affect the prediction of a drug’s pharmacokinetic (PK) profile, is physiologically-based pharmacokinetic modelling and simulation (PBPK-M&S). This makes the method very attractive and appropriate to predict drug clearance over the complete human life span, since it assimilates the physiological knowledge in each particular age stage to predict changes in a drug’s PK (bottom-up). Additionally, these models may also be applied to anticipate or explain a drug’s behavior in pathophysiological conditions, e.g. liver cirrhosis [3], or drug-drug interactions [4]. The fact that PBPK models are drug-independent, allows ‘extrapolatibility’ of many drugs to many (virtual) clinical situations [5]. Practically, however, there are some limitations in the approach that need further evaluation and optimization in order to better predict the pediatric clearance. The emphasis of this work is on drug clearance since it is the most important pharmacokinetic parameter determining pharmacological response [1, 6, 7].

The main aim of this PhD project was twofold:

I. Evaluate the PBPK approach for a reliable bottom-up clearance prediction in pediatric life, and
II. Identify the gaps that underlie prediction inaccuracies.

In this light, tramadol was used as a model compound to compare the bottom-up to the top-down clearance maturation function across pediatric life, with a particular focus on neonates/infants. The top-down clearance maturation was estimated from a population PK investigation in a pooled data set, ranging from neonates to adults. In order to achieve the main aim of this project, four objectives were defined as separate subprojects:

1. Investigate tramadol ***in vitro*** **metabolism** and investigate ***in vitro*****-to-*****in vivo*** **extrapolation** of CYP enzyme activity [Chapter 3 & 4]
2. Construct and qualify the tramadol **adult i.v. PBPK clearance model** in terms of absolute total clearance, and CYP2D6 and renal contributions [Chapter 5]
3. Use the adult model to mechanistically **predict pediatric clearance (bottom-up)** and **evaluate against *in vivo* pediatric data (top-down)** [Chapter 5]
4. Construct the adult model in **different commercially available PBPK software tools,** mechanistically **predict pediatric clearance (bottom-up)** for each and **evaluate their strengths/ weaknesses against *in vivo* pediatric data (top-down)** [Chapter 6]

REFERENCES

1. Mahmood I. Dosing in children: a critical review of the pharmacokinetic allometric scaling and modelling approaches in paediatric drug development and clinical settings. Clin Pharmacokinet. 2014;53(4):327-46.

2. Krekels EH, Tibboel D, Knibbe CA. Pediatric pharmacology: current efforts and future goals to improve clinical practice. Expert Opin Drug Metab Toxicol. 2015;11(11):1679-82.

3. Johnson TN, Boussery K, Rowland-Yeo K, Tucker GT, Rostami-Hodjegan A. A semi-mechanistic model to predict the effects of liver cirrhosis on drug clearance. Clin Pharmacokinet. 2010;49(3):189-206.

4. Moj D, Hanke N, Britz H, Frechen S, Kanacher T, Wendl T, et al. Clarithromycin, Midazolam, and Digoxin: Application of PBPK Modeling to Gain New Insights into Drug-Drug Interactions and Co-medication Regimens. AAPS J. 2016.

5. Jamei M, Dickinson GL, Rostami-Hodjegan A. A framework for assessing inter-individual variability in pharmacokinetics using virtual human populations and integrating general knowledge of physical chemistry, biology, anatomy, physiology and genetics: A tale of 'bottom-up' vs 'top-down' recognition of covariates. Drug Metab Pharmacokinet. 2009;24(1):53-75.

6. Alcorn J, McNamara PJ. Ontogeny of hepatic and renal systemic clearance pathways in infants: part I. Clin Pharmacokinet. 2002;41(12):959-98.

7. Alcorn J, McNamara PJ. Ontogeny of hepatic and renal systemic clearance pathways in infants: part II. Clin Pharmacokinet. 2002;41(13):1077-94.

2

CHAPTER 3

PHYSIOLOGY-BASED IVIVE PREDICTIONS OF TRAMADOL FROM IN VITRO METABOLISM DATA

This chapter is based on:

T'jollyn, Huybrecht; Snoeys, Jan; Colin, Pieter; Van Bocxlaer, Jan; Annaert, Pieter; Cuyckens, Filip; Vermeulen, An; Van Peer, Achiel; Allegaert, Karel; Mannens, Geert & Boussery, Koen¨ Physiology-Based IVIVE Predictions of Tramadol from in Vitro Metabolism Data. Pharm Res. 2015 Jan;32(1):260-74

3

TABLE OF CONTENTS

3

1 ABSTRACT

Objective

To predict the tramadol *in vivo* pharmacokinetics in adults by using *in vitro* metabolism data and an *in vitro-in vivo* extrapolation (IVIVE)-linked physiologically-based pharmacokinetic (PBPK) modeling and simulation approach (Simcyp®).

Methods

Tramadol metabolism data was gathered using metabolite formation in human liver microsomes (HLM) and recombinant enzyme systems (rhCYP). Hepatic intrinsic clearance ($CLint_H$) was (i) estimated from HLM corrected for specific CYP contributions from a chemical inhibition assay (model 1); (ii) obtained in rhCYP and corrected for specific CYP contributions by study-specific intersystem extrapolation factor (ISEF) values (model 2); and (iii) scaled back from *in vivo* observed clearance values (model 3). The model-predicted clearances of these 3 models were evaluated against observed clearance values in terms of relative difference of their geometric means, the fold difference of their coefficients of variation, and relative CYP2D6 contribution.

Results

Model 1 underpredicted, while model 2 overpredicted the total tramadol clearance by -27% and +22%, respectively. The CYP2D6 contribution was underestimated in both models 1 and 2. Also, the variability on the clearance of those models was slightly underpredicted. Additionally, blood-to-plasma ratio and hepatic uptake factor were identified as most influential factors in the prediction of the hepatic clearance using a sensitivity analysis.

Conclusion

IVIVE-PBPK proved to be a useful tool in combining tramadol's low turnover *in vitro* metabolism data with system-specific physiological information to come up with reliable PK predictions in adults.

3

2 INTRODUCTION

Tramadol is a centrally acting analgesic drug with weak opioid activity and has an established use in the clinical setting [1]. Tramadol is metabolized by different cytochrome P450 enzymes (CYP), of which CYP3A4 and CYP2D6 are deemed to be the most important ones [2, 3] (Figure 1). CYP3A4 governs the metabolism of about 50% of clinically used drugs and is characterized by large interindividual variability [4]. Also for CYP2D6 genetic polymorphisms have been described that can lead to large interindividual variation in substrate pharmacokinetics [5]. Tramadol, which inhibits neuronal uptake of norepinephrine and serotonine, is bio-activated by CYP2D6 to its O-demethylated metabolite that has 300 times more affinity for the μ-opioid receptor than tramadol [1]. Therefore, CYP2D6 activity and metabolizer status may have implications on the pharmacokinetics and on the extent of μ-opioid effect after administration of this drug [6, 7]. The above described metabolism properties make this drug an interesting compound to study the performance of bottom-up physiologically-based pharmacokinetic (PBPK) modeling, relying on *in vitro* drug metabolism kinetics to predict *in vivo* pharmacokinetics.

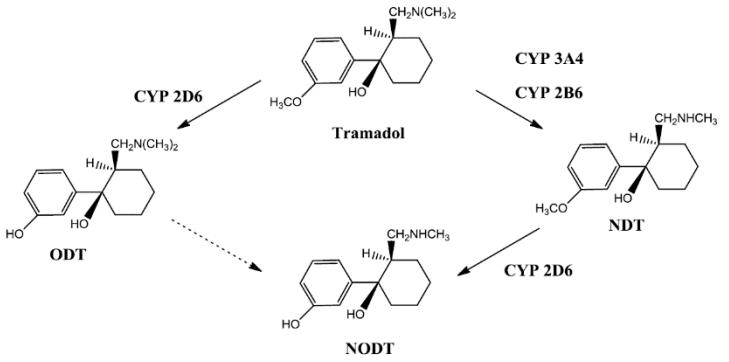

FIGURE 1: TRAMADOL CYP METABOLISM PATHWAYS (O-DESMETHYLTRAMADOL (ODT); N-DESMETHYLTRAMADOL (NDT); NODT (N,O-DIDESMETHYLTRAMADOL))

In the past, the use of PBPK models was limited due to their complexity and high computational requirements. Therefore, simpler, empirical methods such as sums of exponentials and compartmental models, were commonly chosen to 'describe' the (plasma) concentration-time profiles [8]. PBPK models represent the studied organism as a closed circulatory system in which organs and different tissues make up the physiologically relevant compartments, interconnected by the blood circulation, independent of the drug under investigation [9]. In order to make compound-specific PBPK predictions, compound-specific information, such as molecular descriptors logP, pKa, molecular weight (Mw), and *in vitro* measured values intrinsic clearance (CLint), Km, Vmax, blood-plasma ratio, fraction unbound in plasma have to be provided [10]. The mechanistic extrapolation of *in vitro* pharmacokinetic data to *in vivo* is the so-called bottom-up IVIVE-linked PBPK approach and allows to predict first-in-man

pharmacokinetic exposure, anticipate major drug-drug interactions, and predict drug clearance in subject populations at risk (e.g. renal/hepatic impaired, pediatric populations) [11, 12]. Furthermore, this bottom-up PBPK approach is able to *a priori* identify disposition covariates of a new drug candidate through *in vitro* investigation, and can provide mechanistic insight in the observed absorption, distribution, metabolism, and excretion properties of the studied compound. Nevertheless, the classical 'top-down' approach will remain a vital complementary tool to adequately describe the observed data obtained in clinical studies [13].

In IVIVE, it is extremely important that the metabolic enzyme kinetic data are obtained under optimal conditions to build a robust quantitative PBPK model. Intrinsic metabolic drug clearance values can be determined by using metabolite formation or substrate depletion assays. In substrate depletion assays, the *in vitro* half-life of the drug is determined [14] and at least 20% compound turnover is required for analytical reasons. In such assays, especially for low clearance drugs, long incubation times and relatively high protein concentrations are needed. This may lead to issues such as loss in enzyme activity over time, end product inhibition, and binding problems, thus preventing reliable prediction of drug clearance. However, other methods (such as the hepatocyte relay method) are now available that allow accurate and precise measurement of compounds with low *in vitro* turnover [15]. Metabolite formation assays use initial rates, enabling the use of shorter incubation times and lower protein concentrations. However, reference standards for metabolites are needed for the bioanalysis. Underprediction of clearance can occur if not all metabolic pathways are accounted for [16]. As an alternative, formation of all metabolites originating from a parent compound can be studied by using a radiolabel in the incubation experiments.

In this manuscript we present an extended case study on the IVIVE-PBPK prediction of tramadol. The hepatic intrinsic clearance ($CLint_H$) was estimated using 3 different clearance models: $CLint_H$ from human liver microsomal (HLM) metabolism data corrected for specific CYP contributions from a chemical inhibition assay (model 1, HLM model); $CLint_H$ obtained from recombinant enzyme systems corrected for specific CYP contributions by study-specific intersystem extrapolation factor (ISEF) values (model 2, rhCYP model); and $CLint_H$ scaled back from *in vivo* observed clearance values (model 3, retrograde model). Besides, we highlight a number of essential aspects regarding the design of the *in vitro* enzyme kinetic experiments and discuss the role of PBPK in the bottom-up scaling of these data to *in vivo* PK.

3

3 MATERIALS AND METHODS

3.1 CHEMICALS AND MATERIALS

All chemicals and reagents used were of the highest available grade: Na_2HPO_4, KH_2PO_4, KCl, $MgCl_2$, NADP, HCl (Merck, Darmstadt, Germany), glucose-6-phosphate, glucose-6-phosphate dehydrogenase (Roche Diagnostics GmbH, Manheim, Germany), Tramadol (TRC inc, Toronto, Canada), O-desmethyltramadol (ODT) (TRC inc, Toronto, Canada), N-desmethyltramadol (NDT) (LGC GmbH, Luckenwalde, Germany), N,O-didesmethyltramadol (NODT) (TRC inc, Toronto, Canada), O-desmethyltramadol-D6 (TRC inc, Toronto, Canada), ^{14}C-tramadol (Isotope Synthesis, Janssen, Beerse, Belgium).

3.2 INCUBATIONS WITH HUMAN LIVER MICROSOMES

A human liver microsomal pool (BD Biosciences, Woburn, USA), used for tramadol enzyme kinetics investigation, consisted of 50 adult donors and was stored at -80°C in an Ultra Freezer (New Brunswick scientific, Rotselaar, Belgium). Incubation mixtures (total volume 600 µl) consisted of 297 µl microsomal protein, 3 µl of a tramadol solution, and 300 µl cofactor mix containing an NADPH-regenerating system consisting of 1 mg of glucose-6-phosphate, 0.50 units of glucose-6-phosphate dehydrogenase, 0.25 mg of NADP and 1 mg of $MgCl_2.6H_2O$ in 1 ml of 0.5 M Na,K-phosphate buffer pH 7.4. Final microsomal protein concentrations ranged from 0.5 to 2 mg protein/ml. A preincubation with cofactor mix was done for 5 minutes in a shaking water bath at 37°C (100 oscillations/min) (Thermo, Waltham, USA). Incubations were started by adding 3 µl of a tramadol solution (in water), resulting in a final concentration of 0.5, 1, 5, 20, 50, 100, 150, and 200 µM. Reactions were stopped at 2, 5, 7, 10, 20, and 30 min by transferring 100 µl aliquots into 96-well plates containing 10 µl ice-cold 4N HCl and 10 µl of internal standard (O-desmethyltramadol-D6, 6 ng/ml in DMSO). For each substrate and protein concentration level, samples were incubated in duplicate or triplicate and boiled control incubates were run in parallel to correct for non-enzymatic degradation. 96-well plates were then stored at -20°C waiting to be analyzed by UPLC-MS/MS.

3.3 INHIBITION ASSAYS WITH HUMAN LIVER MICROSOMES

Incubation mixtures were essentially the same as described above but relative volumes differed due to the addition of inhibitors, and contained 294 µl of microsomal protein, 300 µl of cofactor mix, 3 µl of inhibitor, and 3 µl of a tramadol solution. The final concentration of microsomal protein and tramadol in the incubations was 0.5 mg/ml and 1 µM, respectively. Inhibitors, which were dissolved in methanol in order to minimize solvent effects (0.5%), were ketoconazole (CYP3A inhibitor, 1 µM), SR-9186 (CYP3A4 inhibitor, 2.5 µM), quinidine (CYP2D6 inhibitor, 1 µM), and thioTEPA (CYP2B6 inhibitor, 10 µM).

Incubations with the mechanism-based inhibitors SR-9186 (TRC inc, Toronto, Canada) and N,N',N''-triethylenethiophosphoramide (thioTEPA; Sigma Aldrich, Overijse, Belgium) were equilibrated in a shaking water bath at 37°C (100 oscillations/min) (Thermo, Waltham, USA) for 5 and 15 min, respectively, and were then started by the addition of tramadol. A 5 min equilibration time was used for the reversible inhibitors ketoconazole and quinidine. All samples were stopped at 10 min in 96-well plates, containing 10 µl ice-cold 4N HCl and 10 µl of internal standard. Linearity controls (incubation mixtures without inhibitors; tramadol 1 µM, 0.5 mg protein/ml, 10 min) as well as boiled controls were run in parallel to allow determination of the inhibited fraction and to correct for background, respectively. 96-well plates were then stored at -20°C waiting to be analyzed by UPLC-MS/MS.

3.4 INCUBATIONS WITH RECOMBINANT CYP ENZYMES

Supersomes™ are membrane fractions derived from baculovirus infected insect cells expressing a specific (selection of) drug metabolizing enzyme(s), i.e. CYP enzymes with or without NADPH cytochrome P450 reductase and cytochrome *b*5. Supersomes™ (BD Biosciences, Woburn, USA) were used in order to investigate the enzyme kinetic behavior of tramadol for the isolated CYPs. Incubation mixtures contained 297 µl of a given recombinant isoform at a final 100 pmol/ml (CYP isoform) concentration, together with 300 µl of the cofactor mix containing an NADPH-regenerating system (composition cfr Materials and Methods 2nd paragraph). These mixtures were preincubated in a shaking water bath at 37°C (100 oscillations/min) (Thermo, Waltham, USA) for 5 min and incubations were started by adding 3 µl of a tramadol solution. Tramadol final test concentrations were 1, 5, 150, and 250 µM. Reactions were stopped at 2, 5, 7, and 10 min by transferring 100 µl aliquots into 96-well plates containing 10 µl ice-cold 4N HCl and 10 µl of internal standard. For each substrate and each recombinant isoform, samples were incubated in duplicate and Supersome^{TM} insect controls, consisting of membrane fractions containing all proteins from the insect cell line except the CYP component, were run in parallel to correct for background. 96-well plates were then stored at -20°C waiting to be analyzed by UPLC-MS/MS.

3.5 BIOANALYSIS

Tramadol's main metabolites O-desmethyl tramadol (ODT, M1),N-desmethyl tramadol (NDT, M2), and N,O-didesmethyl tramadol (NODT, M5) [1] were quantified by a sensitive UPLC-MS/MS method. The Nexera UHPLC system (Shimadzu, Kyoto, Japan), consisting of a RackChanger II, SIL-30AC autosampler, CTO-30A column oven, and LC30AD pump units was linked via a Valco switching valve to an API 4000 QTRAP (AB Sciex, Toronto, Canada) equipped with a Turbo V^{TM} ion source in ESI+ mode. For the chromatographic separation, a gradient was run -with solvents A (0.025M ammonium acetate, pH 8.5)

and B (acetonitrile:methanol 80:20, v/v)- from 5% to 50% B in 3 min, to 100% B in an immediate step gradient, held for 0.3 min, and back to 5% B, allowing 2 min re-equilibration, at a flow rate of 0.6 ml/min. The column was an Acquity UPLC BEH C18 1.7µm 50x2.1mm column (Waters, Milford, USA) packed with 1.7 µm particles and maintained at 60°C.

Metabolite formation was quantified by use of a calibrator set and quality control samples that were prepared by spiking 25 µl of reference standard solutions N-desmethyl tramadol (NDT), O-desmethyl tramadol (ODT), N,O-didesmethyl tramadol (NODT) containing O-desmethyltramadol-D6 as internal standard (6 ng/ml) to a mixture of 250 µl microsomal matrix and stopped with 25 µl 4N HCl. Depending on the expected extent of metabolite formation 10 calibrator levels (ranging 200-fold) and 3 QC levels (low, medium, high; made in duplicate) were selected for each analytical batch. Runs were accepted based on recommendations from the FDA's "Guidance for Industry– Bioanalytical Method Validation". An overview of the specific criteria that were used for run acceptance are provided as an Appendix to this chapter. At least 4 out of 6 QC samples were within 15% of their nominal value, for the calibration curve simple linear regression was applied with a weighting factor 1/x. Standards deviated not more than 15% from the nominal concentration, except for the LLOQ where 20% deviation was allowed. Samples in 96-well plates were thawed while shaking, submersed in an ultrasone bath, and centrifuged using an Allegra^{TM} 25R ultracentrifuge (Beckman Coulter, Suarlée, Belgium). Depending on the expected degree of metabolite formation, between 1 and 10 µl supernatant was directly injected onto the column to assess concentrations of ODT, NDT, and NODT in the incubation samples.

3.6 TRAMADOL ENZYME KINETICS AND IVIVE

Concentrations of metabolites in the incubation samples were corrected for protein concentration (mg microsomal protein/ml), reaction time (min), and initial substrate concentration (µM) in order to calculate the apparent *in vitro* clearance (CL_{app}) for every metabolite. CL_{app} was plotted vs. tramadol incubation concentration and a nonlinear model –with the model structure provided in equation 1- was fitted to the data, using the R statistics program [17]. Models were evaluated by visually inspecting residual plots for bias. In equation 1 CL_{app} is the apparent *in vitro* clearance, expressed as µl/min/mg microsomal protein, v_o is the initial rate of metabolite formation in the incubate (pmol/min/mg protein), *[S]* is tramadol concentration (µM), *Km* and *Vmax* are the Michaelis-Menten constant (µM) and maximum velocity (pmol/min/mg protein), respectively. This equation allowed estimation of the parameters Km and Vmax, and hence the calculation of CLint.

$$CL_{app} = \frac{v_o}{[S]} = \frac{Vmax}{Km + [S]}$$

EQUATION 1

When the substrate concentration in the incubate is substantially below the Km (in practice [S]< Km/10), the intrinsic clearance (CLint) can be approximated from the ratio of Vmax/Km. When the substrate concentration is at Km, the CL_{app} approximates the half maximal CLint.

Tramadol incubation concentrations (0.5 to 250 µM) were chosen to be near the therapeutic plasma concentrations observed *in vivo* (C_{max} 2.25 µM [1]) in order to define the enzyme kinetic parameters of tramadol at a therapeutically relevant concentration test range. An unbound fraction in microsomes (fu_{mic}) of ~0.96 was estimated *in silico* using the prediction toolbox in Simcyp® V12.1 [18].

By scaling up an *in vitro* obtained (unbound) intrinsic clearance ($CLint_u$) with mechanistic information on the liver abundance of each CYP, the amount of microsomal protein per gram liver (MPPGL), and liver weight, a determination of the *in vivo* hepatic intrinsic clearance ($CLint_H$) can be obtained. Additionally, known variability in demographic and biological components is incorporated in order to predict drug disposition in relevant individuals with realistic variability. Additionally, for the scaling from recombinant systems, an intersystem extrapolation factor (ISEF) corrects for the inherent activity difference between recombinant systems and HLM [19, 20].

Equations 2 and 3 are used for the mechanistic scaling of unbound intrinsic clearance to hepatic intrinsic clearance , obtained from HLM and recombinant systems, respectively. For scaling up HLM unbound CLint, the amount of microsomal protein per gram liver (MPPGL), and liver weight are needed to provide an estimate of the *in vivo* hepatic intrinsic clearance ($CLint_H$) (equation 2). For scaling up the unbound CLint determined from rhCYP systems, the CYP isoform abundance *in vivo* and the ISEF value are additional factors needed to calculate the hepatic CLint (equation 3) [19].

$$CLint_H = CLint_{u,HLM} * MPPGL * g\ liver$$

EQUATION 2

$$CLint_H = CLint_{u,rCYP} * ISEF * [isoform]_{in\ vivo} * MPPGL * g\ liver$$

EQUATION 3

Subsequently, the hepatic intrinsic clearance ($CLint_H$) is integrated with the fraction unbound in plasma (fu_p), blood-to-plasma ratio (B:P) and the hepatic blood flow (Q_H) in the commonly used well-stirred liver model in order to obtain an estimate of the hepatic plasma clearance (CL_H), as illustrated in equation 4:

$$CL_H = \frac{Q_H * fu_p * Clint_{\mathrm{H}}}{Q_H + fu_p * CLint_{\mathrm{H}}/B:P}$$

EQUATION 4

3.7 BLOOD DISTRIBUTION

The blood distribution of tramadol was investigated by incubating a tramadol concentration range (0.1 – 10 µM) in whole blood. Fresh whole blood was collected from 3 healthy male volunteers in EDTA-coated tubes to which ^{14}C-tramadol was spiked (no organic solvents were used). Spiked whole blood was left to equilibrate for 30 min in a shaking water bath Grant (type OLS200) (Grant instruments, Cambridge, UK) at 37°C and was gently homogenized every 10 min. After 30 min, 3 homogenous aliquots of 100 µl were pipetted to oxidation cups and the rest of the whole blood sample was centrifuged for 10 min at 1700g in a Hettich Rotixa (type 50S) (Hettich AG, Tuttlingen, Germany). 2 aliquots of 100 µl plasma were placed in counting vials together with scintillation fluid Ultima Gold (PerkinElmer, Waltham, USA) and were counted by liquid scintillation counting (LSC) in a Tri-carb® 2900 TR (PerkinElmer, Waltham, USA). Whole blood samples were combusted in a Packard Sample Oxidizer 307 (PerkinElmer, Waltham, USA), released $^{14}CO_2$ was trapped with Carbosorb and mixed with scintillation fluid, and submitted to LSC. The radioactivity was measured in an aliquot of whole blood as well as in plasma from the same sample in order to assess the ratio of the whole blood concentration vs. the plasma concentration (blood-to-plasma or B:P ratio).

3.8 SIMULATIONS

An intravenous full PBPK model was selected in the Simcyp® Simulator V12.1 (Sheffield, UK) to predict pharmacokinetics as a function of time. In order to verify the simulations, PK parameters were compared to *in vivo* data [21-24].

The virtual clinical trial design was set to capture the pharmacokinetics as a function of time for a 100 mg tramadol i.v. bolus up to 24h post-dose, in line with the *in vivo* observed AUC's which were also obtained from 0 to 24h. Following molecular descriptors were extracted from literature and used as input for the PBPK model: molecular weight 264.4; logP 1.35; pKa 9.41; B:P ratio 1.09 (own experiments); fu_p 0.8.

The virtual population was set to mimic the reference population in terms of the proportion male-female (30% female), the age range (23-57 years), and CYP2D6 metabolizer status (8.2% PM – 86.5% EM – 5.3% UM).

The distribution component of the PBPK model was represented by the Rodgers & Rowland model (method 2 in Simcyp®). The Rodgers and Rowland equation was used since this equation, in contrast to the Poulin and Theil equation (method 1 in Simcyp®), takes into account a tissue's acidic phospholipid fraction and takes explicit account of the extent of ionization of a compound at the pH of the compartment concerned. Since tramadol is almost completely ionized at pH 7.4, the Rodgers and

Rowland equation will assume that binding to acidic phospholipids controls the distribution within the body [25]. The elimination component of the PBPK model involved a renal and a hepatic clearance part. The renal plasma clearance was mechanistically predicted at 6.6 L/h (110 ml/min) using the permeability-limited mechanistic kidney model. Since this value was in good agreement with *in vivo* observations the renal clearance was fixed at 6.6 L/h for further simulations. The hepatic plasma clearance was investigated by means of an IVIVE-linked elimination model using kinetic data from *in vitro* experiments, further elaborated hereunder in the section "Hepatic clearance investigation". In addition, a sensitivity analysis was conducted to assess model robustness to changing input parameters other than CLint values, as well as a population simulation comparing the geometric means of clearance and volume of distribution and their associated variabilities with the reference data set used in this study [21-24].

3.8.1 Hepatic clearance investigation

The CYP-isoform specific CLint values that were used in the 3 different clearance modeling approaches, described hereunder, can be found in Table 1. A factor of 1.58 was used to account for hepatic accumulation of the basic amine tramadol (see discussion for details).

The HLM model (model 1) represents input from intrinsic clearance values obtained in HLM for the two main tramadol CYP-mediated metabolites ODT and NDT (Table 2). The contribution of different CYP enzymes to the total intrinsic clearance per metabolite is estimated based on the effect of different chemical inhibitors (Table 1). The rhCYP model (model 2) consists of intrinsic clearance values obtained in isolated recombinant enzyme systems CYP3A4, 2D6, and 2B6 for the two main tramadol CYP-mediated metabolites ODT and NDT (Table 1). ISEF values for CYP3A4 and CYP2D6 were determined for scaling up tramadol rhCYP kinetic data using probe substrates midazolam and dextromethorphan, respectively. CLint values for both probes were obtained in HLM as well as in rhCYP systems, and specific CYP abundances of 137 and 8 pmol/mg microsomal protein were used to calculate the ISEF values for CYP3A4 and CYP2D6 (Table 1), respectively [26, 27]. For CYP2B6, an ISEF-value of 0.43 was used as provided by Simcyp® V12.1. The retrograde model (model 3) calculates a retrograde hepatic intrinsic clearance per CYP isoform based on apparent *in vivo* CYP contributions in the total metabolism (Table 1). Therefore, it can serve as a reference model next to the 2 other models in evaluating the prediction of the population clearance. Simulations were performed using a study design and healthy volunteer population that resembled the study design and covariate characteristics of the reference study, respectively [21-24]. The simulations were executed using virtual populations of 1000 subjects

The CYP2D6 contribution in the current clearance models was assessed by comparing the fold increase in hepatic clearance between PM and EM with observed data from a study conducted by Pedersen et

al. [28]. Patients from this study were genotyped as *1/*1 (EM; n=8) and *4/*4 (n=7) or *4/*6 (PM) (n=1). The PBPK trial design was set to resemble the actual trial design as closely as possible by taking into account the actual age range, administered dose, proportion of male-female, and metabolizer phenotype in the 2 groups. One thousand virtual patients were simulated for every run.

3.8.2 Population simulation

In Simcyp®, known covariates or correlations of different specifications of the population as well as the observed variability associated with each parameter involved in the bottom-up approach is considered to generate virtual subjects representative of those in the real world [10]. Therefore, a population simulation was set up to investigate how well the 3 IVIVE-linked PBPK models could predict the population values of the clearance (CL) and volume of distribution (Vss) as well as their associated variability. In that respect the relative difference of the predicted and observed geometric means, calculated as (predicted-observed)/observed*100%, was used to compare the population values of CL and Vss. To compare the predicted and observed variability in the population, the fold difference of the predicted and observed coefficients of variation (CV) was used, assuming that these PK parameters follow log-normal distributions (Table 3). Evaluation was based on visual inspection of observed and predicted 95% prediction intervals, calculated as suggested by Johnson et al (29). The simulated virtual population consisted of 1000 patients that mimicked the dosage, age range and male-female proportion of the reference studies[21-24].

3.8.3 Sensitivity Analysis

A sensitivity analysis was undertaken in order to define to what extent other input parameters than intrinsic clearance would influence the prediction of clearance (CL) using the clearance model 1 (based on HLM values) and volume of distribution (Vss) using the distribution model based on the Rodgers equations [25]. Five input parameters of interest (logP, pKa, fraction unbound in plasma (fu), B:P ratio (BP), drug accumulation in hepatocyte (ACC)) were varied within the PBPK model (full factorial design (2^5)), using the Simcyp® Batch processor, between the lowest and the highest value published in literature or own experimental results. Following values (low level – high level) were used as input to the PBPK model: logP (1.35- 2.41), pKa (9.14 – 9.44), fu (0.74 – 0.80), BP (1.09 – 1.20), ACC (1.5 – 3). The reason for varying the ACC factor 2-fold can be found in the discussion. PBPK simulations were performed using a healthy volunteer population that resembled the study population of the reference studies [21-24]. One hundred virtual patients were simulated for every run. The prediction results were interpreted by means of a generalized linear model (glm) that was fitted to the PBPK prediction results, so as to disentangle the effects of the input parameters and their interactions on the prediction of CL and Vss.

4 RESULTS

4.1 *IN VITRO* RESULTS

4.1.1 CLINT FROM HLM ASSAYS

The metabolism kinetics of 0.5 µM to 250 µM tramadol to its two primary metabolites O-desmethyl tramadol (ODT) and N-desmethyl tramadol (NDT) was determined in pooled human liver microsomes. The secondary metabolite N,O-didesmethyl tramadol (NODT) was always about 1% and < 3% of the amount of NDT and ODT formed, respectively, implying negligible underestimation of enzyme kinetic parameters due to secondary metabolism. Furthermore, preliminary experiments using ^{14}C-tramadol (data not shown) it was demonstrated that no other metabolites were formed than the ones described in this paper. The aim was to identify the intrinsic clearance for both metabolites at concentrations well below Km values, previously reported by Subrahmanyam et al. [29] (Km_{ODT} 116 µM; Km_{NDT} 1021 µM). Linearity of metabolite formation to ODT and NDT in relation to time and protein content was investigated at 0.5 µM tramadol, and seemed to be linear up to 10 min and up to 1 mg of microsomal protein per ml.

Considering only linear kinetic data (initial velocities), the CL_{app} was calculated, as described in the previous section. The intrinsic clearance (CLint) is the apparent *in vitro* clearance that is maximal and constant at the lower end of the substrate concentration test range (illustrated for ODT and NDT in Figure 2). Estimated enzyme kinetic parameters Km, Vmax, CLint are presented in Table 2 with their 95% confidence intervals.

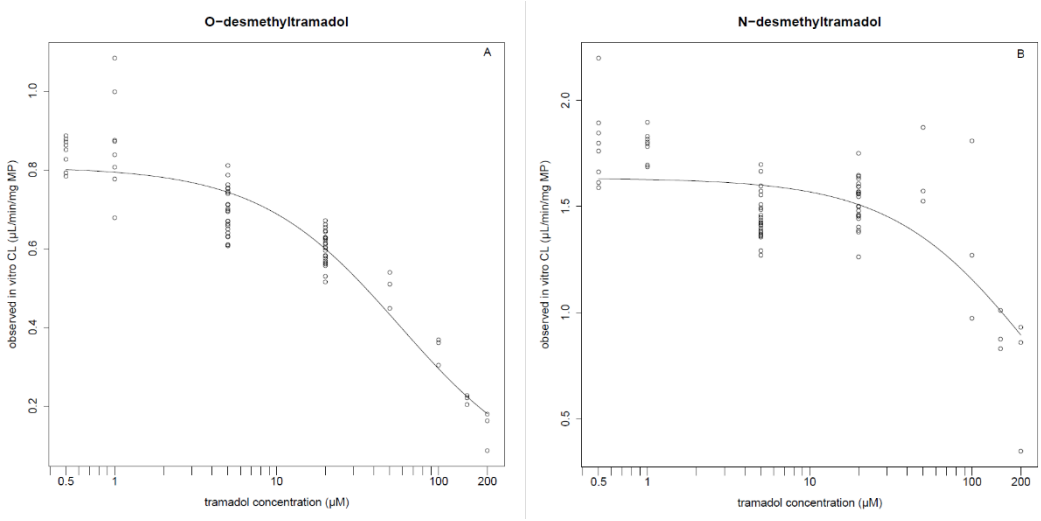

FIGURE 2: THE OBSERVED *IN VITRO* CLEARANCE (µL/MIN/MG MICROSOMAL PROTEIN) IN RELATION TO THE INCUBATION CONCENTRATIONS (µM) OF TRAMADOL FOR ODT (A) AND NDT (B). FOR ODT THE PLATEAU OF INTRINSIC CLEARANCE (CLINT) IS REACHED AT 0.80 µL/MIN/MG PROTEIN, AND FOR NDT THE CLINT WAS ESTIMATED AT 1.63 µL/MIN/MG PROTEIN.

3

TABLE 1: OVERALL SUMMARY OF THE CLINT VALUES OBTAINED IN KINETIC EXPERIMENTS THAT WERE USED AS INPUT FOR PBPK.

SPECIFIC CYP ISOFORM CONTRIBUTION IS INCORPORATED THROUGH CHEMICAL INHIBITION (MODEL 1, HLM) OR ISEF VALUES (MODEL 2, RHCYP) OR BACK-CALCULATED FROM *IN VIVO* (MODEL 3, RG) FOR ODT AND NDT.

Model	Formula	CYP isoform	CLint ODT[a]	CLint NDT[a]
1 HLM [b]	$CLint_{HLM}$ ($CLint_{ODT/NDT}$ * %CYP by chemical inhibition data)	3A4	0.12 (0.80*15%)	1.06 (1.63*65%)
		2D6	0.64 (0.80*80%)	0.08 (1.63*5%)
		2B6	0.04 (0.80*5%)	0.5 (1.63*30%)
2 rhCYP [c]	$CLint_{rhCYP}$ * ISEF	3A4	0.00 *0.23	0.11 *0.23
		2D6	0.57 *0.45	0.054 *0.45
		2B6	0.018 *0.43	0.20 *0.43
3 RG[d]	Retrograde model	2D6	48% of HepCL	
		3A4+2B6	52% of HepCL	

[a] CLint values for model 1 are expressed as µl/min/mg protein, whereas for model 2 CLint is expressed as µl/min/pmol CYP

[b] reported CLint values are obtained by multiplication of the $CLint_{HLM}$ values with % CYP isoform contribution calculated from inhibition assay data

[c] $CLint_{rhCYP}$ obtained from recombinant enzyme systems, are presented with their specific ISEFs

[d] Retrograde model allows the user to set specific CYP contributions based on *in vivo* data in CYP2D6 PM and EM

TABLE 2: OVERVIEW OF ENZYME KINETIC PARAMETERS KM, VMAX AND CLINT AND THEIR ASSOCIATED 95% CONFIDENCE INTERVALS FOR TRAMADOL'S TWO MAIN METABOLITES ODT AND NDT IN POOLED HLM

	ODT	NDT
Km [95% CI] (µM)	57.5 [47.0 ; 71.1]	242 [174 ; 353]
Vmax [95% CI] (pmol/min/mg protein)	46.4 [38.9 ; 56.1]	395 [290 ; 565]
CLint [95% CI] (µl/min/mg protein)	0.80 [0.78 ; 0.84]	1.63 [1.57 ; 1.69]

4.1.2 HLM INHIBITION ASSAYS

Tramadol metabolism to ODT (Figure 3, Table 1) was found to be primarily inhibited (80%) by 1 µM quinidine, which causes a selective inhibition of CYP2D6 [30]. Inhibition of another major CYP enzyme, CYP3A and CYP3A4 by ketoconazole and SR-9186 [31], respectively was derived to be approximately 15%. The rest of the ODT formation (5%) seemed to be mediated by CYP2B6 as indicated by the thioTEPA inhibitory effect.

Tramadol N-demethylation, displayed in Figure 3 and Table 1, is mainly mediated by CYP3A4 because about 60% of the metabolism to NDT is blocked by chemical inhibition with ketoconazole (1 µM) and SR-9186 (2.5 µM). The inhibitory effect of thioTEPA (10 µM) is believed to result from a dual effect on CYP3A4 and CYP2B6. This cross-reactivity was investigated by co-incubating tramadol with the 2 inhibitors. Knowing that SR-9186 causes selective inhibition of CYP3A4, the real contribution of CYP2B6 in the NDT formation can be estimated at 30% by subtracting the inhibition of SR-9186 alone from the inhibition with SR-9186 + thioTEPA, thereby correcting for thioTEPA's inhibitory effect on CYP3A4.

4.1.3 CLINT FROM RHCYP ASSAYS

The kinetics of 1 µM to 250 µM tramadol to metabolites ODT and NDT was determined in recombinantly expressed enzyme systems containing CYP3A4, CYP2D6, CYP2B6, and insect controls (Supersomes™). Linear conditions were determined for both metabolites in relation to time per recombinant isoform at 100 pmol/ml. Enzymatic rates were linear up to 5 or 7 min, depending on the isoform under investigation. Only linear data should be used for calculation of the CL_{app}, yielding a plateau of CLint at tramadol concentrations well below Km (Figure 4). CLint values that were used as input for hepatic clearance model 2, the rhCYP model, can be found in Table 1.

3

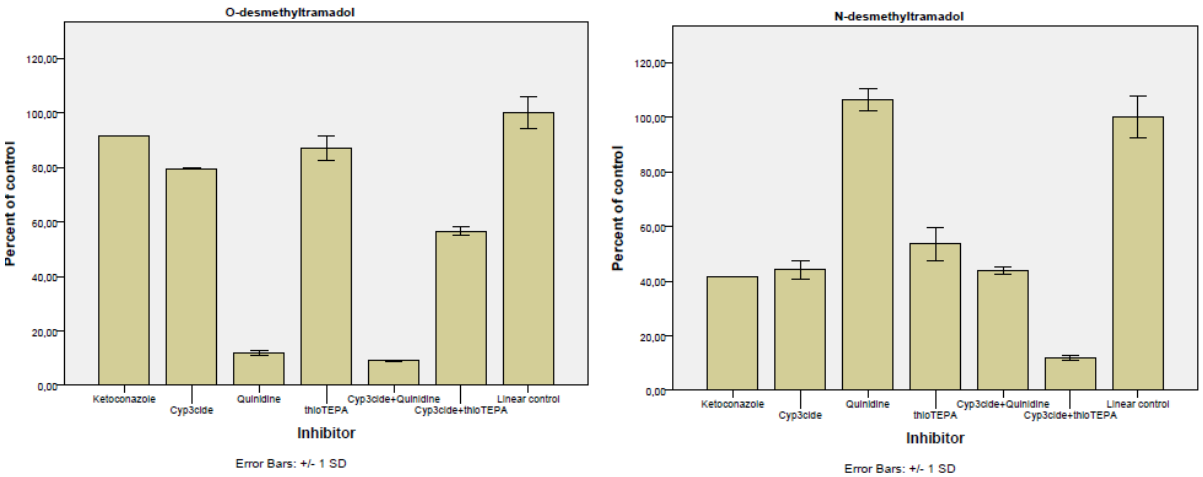

FIGURE 3: THE INHIBITION PLOTS REPRESENT REST FRACTIONS OF METABOLITE ODT (LEFT) AND NDT (RIGHT) IN RELATION TO INHIBITOR(S) PRESENT. A LINEAR CONTROL WAS ALWAYS RUN IN PARALLEL TO THE INHIBITION ASSAYS TO DETERMINE 100% ODT AND NDT FORMATION.

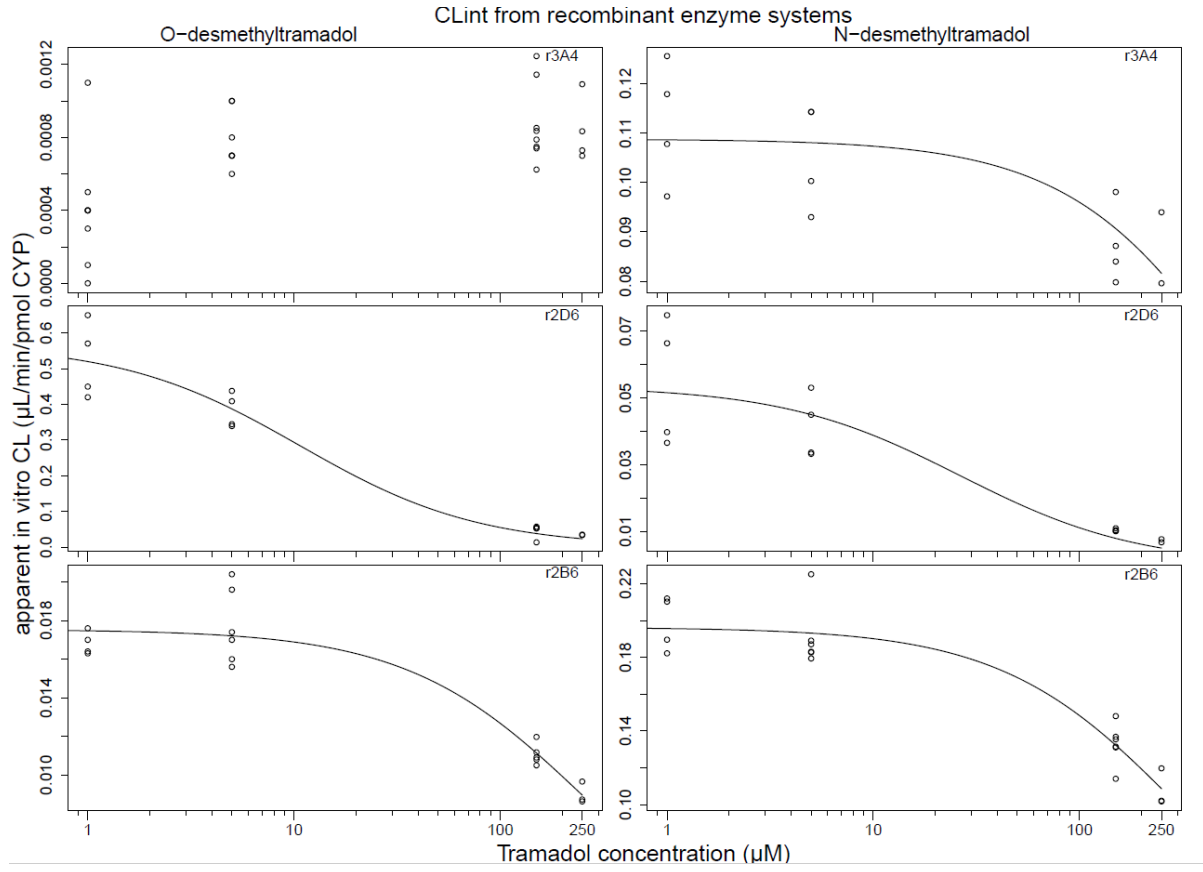

FIGURE 4: THE APPARENT *IN VITRO* CLEARANCE (µL/MIN/PMOL CYP) FOR ODT AND NDT IN RELATION TO THE INCUBATION CONCENTRATIONS (µM) OF TRAMADOL, FOR EVERY RECOMBINANT ENZYME CYP3A4, 2D6 AND 2B6.

4.1.4 Blood distribution

The blood distribution of tramadol appeared to be concentration independent within the test range of 0.1 to 10 µM tramadol and the blood-to-plasma ratio was determined at 1.09 (sd 0.02).

4.2 Simulation results

4.2.1 Hepatic clearance investigation and population simulation

The involvement of the hepatic clearance in the total tramadol clearance was investigated by using the input from two distinct IVIVE-linked PBPK clearance models (HLM and rhCYP model) and the retrograde clearance model as reference model. The results of this analysis are presented in figures 5, 6, and Table 3. Input details for every clearance model are provided in the section Materials and Methods-Simulations.

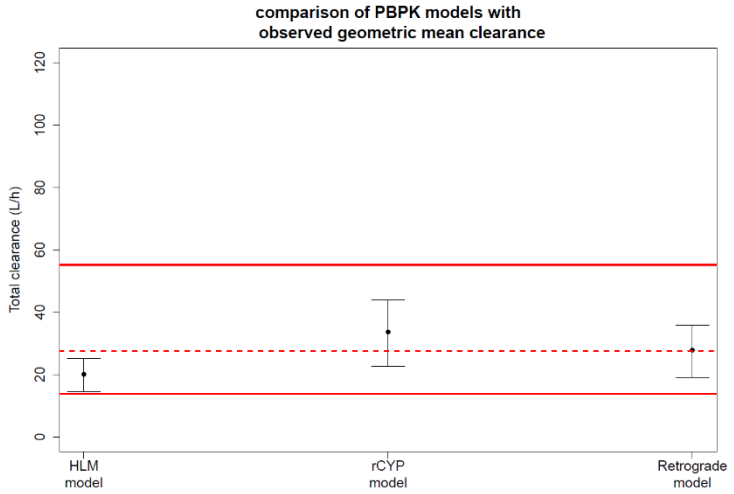

FIGURE 5: THE PREDICTION OF THE TOTAL CLEARANCE PER CLEARANCE MODEL. BLACK DOTS ARE PREDICTED GEOMETRIC MEAN CLEARANCE AND ERROR BARS REPRESENT THE STANDARD DEVIATIONS. DASHED AND DOTTED LINES REPRESENT THE OBSERVED GEOMETRIC MEAN AND THEIR 2 FOLD BOUNDARIES, RESPECTIVELY. HLM MODEL: HEPATIC CLEARANCE MODEL FROM HUMAN LIVER MICROSOMES; RHCYP MODEL: HEPATIC CLEARANCE MODEL FROM RECOMBINANT HUMAN ENZYMES; RETROGRADE MODEL: HEPATIC CLEARANCE MODEL FROM *IN VIVO* OBSERVED CLEARANCE DATA

The HLM model as well as the rhCYP model (models 1 and 2) are predicted within 2 fold of the observed geometric mean clearance, and the retrograde model, as a reference model, coincides with the geometric mean clearance (Figure 5). From Table 3 it is apparent that the geometric mean clearance is slightly underpredicted in the HLM model but is somewhat overpredicted in the rhCYP model. The variability in every model seems to be slightly underpredicted when compared to the observed variability. The CYP2D6 contribution, as illustrated by the fold increase of the hepatic clearance in PM

vs EM (Table 3), is underpredicted by both the HLM and the rhCYP model, compared to the retrograde model and the observed data [28].

TABLE 3: HEPATIC CLEARANCE INVESTIGATION BY COMPARISON OF 3 PBPK MODELS.

FIRST, THE 3 MODELS ARE PRESENTED WITH THEIR RENAL, HEPATIC AND 2D6 INVOLVEMENT, RELATIVE TO THE TOTAL CLEARANCE. SECOND, THE 3 MODELS ARE COMPARED BY THEIR RELATIVE DIFFERENCE IN GEOMETRIC MEAN AND FOLD OF COEFFICIENTS OF VARIATION (CV) VERSUS OBSERVED DATA. FURTHERMORE, THE INCREASE IN HEPATIC CLEARANCE BETWEEN CYP2D6 PM AND EM IS A MEASURE OF CYP2D6 CONTRIBUTION, INDICATING AN UNDERINVOLVEMENT OF CYP2D6 IN BOTH THE HLM AND THE RHCYP MODEL

	HLM model 1	rhCYP model 2	Retrograde model 3
Renal involvement (%)	43	24	29
Hepatic involvement (%)	57	76	71
2D6 involvement in hepatic clearance (%)	29	29	44
2D6 involvement in total clearance (%)	17	22	31
Comparison of geometric mean and coefficient of variation			
Relative difference in geometric Mean	-27%	+22%	+1%
Fold difference in CV	0.73	0.89	0.85
Hepatic clearance fold increase			
HepCL fold increase for CYP2D6 PM to EM	1.39	1.33	1.73[a]

[a] observed hepatic clearance increase was calculated at 1.74 [28]

The steady-state volume of distribution was mechanistically predicted using the Rodgers and Rowland model. Preliminary simulations with the Poulin & Theil distribution model [32] resulted in a clear underprediction of the volume of distribution (data not shown). This is in line with previous reports on the better performing Rodgers & Rowland model, accounting for membrane interaction of ionized basic drugs [25, 33], such as tramadol.

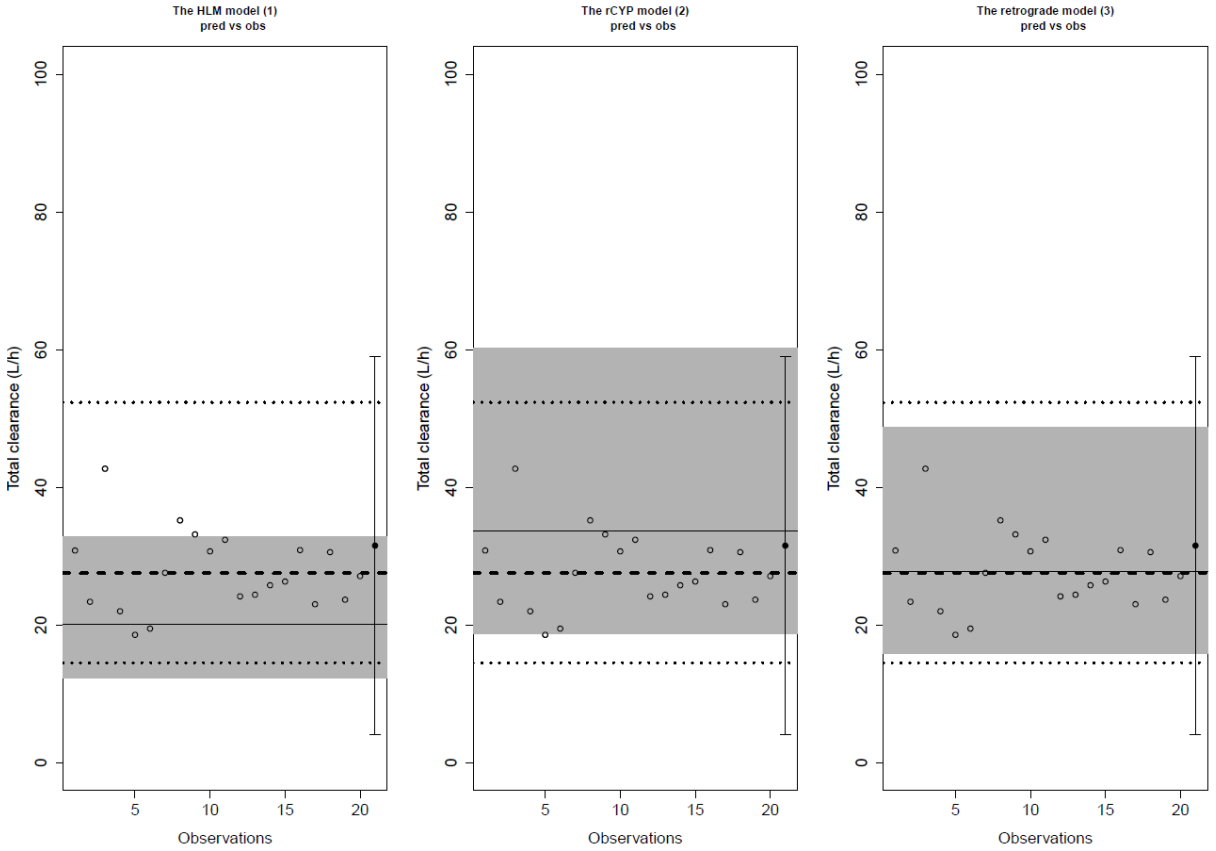

FIGURE 6: POPULATION SIMULATION RESULTS FOR TOTAL CLEARANCE BY THE 3 MODELS CONSIDERED IN THIS PAPER. OPEN CIRCLES (LINTZ DATA [21-23]) AND BLACK CIRCLE (MEAN +- 2*SD) (QUETGLAS DATA [24]) REPRESENT DATA FROM *IN VIVO* STUDIES WITH THE DASHED LINE BEING THEIR OVERALL GEOMETRIC MEAN AND THE DOTTED LINE THEIR 95% PREDICTION INTERVAL. THE GREYED AREA REPRESENTS THE 95% PREDICTION INTERVAL OF THE SIMULATED POPULATION WITH ITS GEOMETRIC MEAN AS SOLID BLACK LINE

In Figure 6 the 3 plots visualize the output from the simulation results by overlaying the *in vivo* observed clearances and PBPK predicted clearances in a plot per considered model. Circles represent data from *in vivo* studies by Lintz et al. and Quetglas et al. [21-24] with the dashed line being their overall geometric mean and the dotted line their 95% prediction interval as calculated by Johnson [34]. Y-axis represents total clearance for the predictions and observations, while the x-axis represents an index for the observations only -sorted per individual (Lintz data [21-23]) or per study population (Quetglas data [24])-. The greyed area represents the 95% prediction interval on the total clearance of the virtual population with its geometric mean as solid black line. Visually, the 95% prediction intervals for the rhCYP and the retrograde model are more in line with the observed interval than for the HLM model, where an underestimation is present. In addition, Figure 7 displays the observed and predicted values of Vss. Although some underprediction of the geometric mean Vss in this case is apparent, the predicted variability is in line with the observed one as can be concluded visually from the 95% prediction intervals.

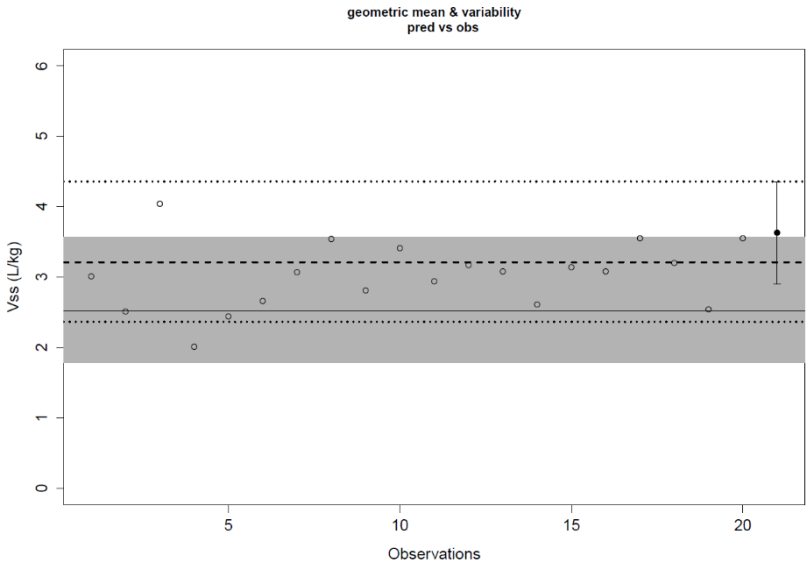

FIGURE 7: POPULATION SIMULATION RESULTS FOR VOLUME OF DISTRIBUTION (VSS). SINCE WE ONLY CONSIDERED 1 DISTRIBUTION MODEL, ONLY 1 PLOT IS PRESENTED. OPEN CIRCLES (LINTZ DATA [21-23]) AND BLACK CIRCLE (MEAN +- 2*SD) (QUETGLAS DATA [24]) REPRESENT DATA FROM *IN VIVO* STUDIES WITH THE DASHED LINE BEING THEIR OVERALL GEOMETRIC MEAN AND THE DOTTED LINE THEIR 95% PREDICTION INTERVAL. THE GREYED AREA REPRESENTS THE 95%PREDICTION INTERVAL OF THE SIMULATED POPULATION WITH ITS GEOMETRIC MEAN AS SOLID BLACK LINE.

4.2.2 SENSITIVITY ANALYSIS

In order to identify those input parameters that significantly affected the PBPK prediction of total clearance (CL) and steady-state volume of distribution (Vss), a generalized linear model (glm) was fitted to the PBPK prediction outcomes. In this sensitivity analysis, effects of input parameters logP, pKa, fraction unbound in plasma (fu), blood:plasma ratio (B:P), and hepatic accumulation (ACC) on PBPK predicted CL and Vss were determined. Isolated effects and interaction effects were distinguished in order to obtain meaningful parameter estimates (Table 4). It is worth noting that CL values were calculated as dose/AUC from Simcyp® output sheets. This means that the predictions of CL in this case (PK profiles mode) are not independent from the prediction of Vss, because we record AUCs over the 24h period post dose. In short, if input parameters that have an impact on the elimination or distribution of the drug are changed, plasma concentrations change, $AUC_{0\text{-}24h}$ changes, and hence CL (=$D/AUC_{0\text{-}24h}$). The "(Intercept)" from the glm output displays the predicted total clearance (19.31 L/h) and volume of distribution (2.77 L/kg) when all five input parameters are at their lower level. Increasing the logP, fu, B:P and ACC to their higher level, increases the predicted total clearance, while increasing pKa has a small but significantly lowering effect on the total clearance. An increase in logP and B:P increases the predicted Vss, while increasing pKa and fu decreases the prediction of Vss. A simultaneous increase in both fu and ACC results in a higher predicted CL than what is to be expected from their isolated effects.

TABLE 4: SENSITIVITY ANALYSIS BY A GENERALIZED LINEAR MODEL (GLM).

THE ISOLATED AND INTERACTION EFFECTS OF INPUT PARAMETERS ON THE GEOMETRIC MEAN TOTAL CLEARANCE (CL) AND VOLUME OF DISTRIBUTION (VSS) ARE DISPLAYED WITH SIGNIFICANCE LEVEL. (INTERCEPT) HAS THE VALUE OF THE CL OR VSS WHEN ALL VARIABLES ARE AT THEIR LOWER INPUT LEVEL. THE ESTIMATE FOR A SPECIFIC VARIABLE REPRESENTS THE INCREASE/DECREASE IN CL OR VSS WHEN THIS VARIABLE IS CHANGED TO THE HIGHER INPUT LEVEL

	Input level	Coefficients for CL (L/h)[a]		Coefficients for Vss (L/kg)[a]	
	low – high	*Estimate*	*Significance*	*Estimate*	*Significance*
(Intercept)		19.31	***	2.77	***
logP	1.35 – 2.41	+0.19	***	+0.070	***
pKa	9.13 – 9.44	-0.020	**	-0.0075	***
fu	0.74 – 0.80	+0.025	**	-0.23	***
BP	1.09 – 1.20	+2.84	***	+1.12	***
ACC	1.5 – 3	+6.32	***	-	-
logP:pKa9.44		-0.098	***	-0.040	***
logP:fu0.8		-	-	+0.010	***
fu:BP1.2		-0.13	***	-	-
fu:ACC3		+0.49	***	-	-
BP:ACC3		-0.17	***	-	-
pKa:fu0.8		-	-	-0.0050	**
pKa:BP1.2		-	-	-0.0050	**

[a] Signif. codes '***' 0 ; '**' 0.001 ; '-' coefficient for this variable did not contribute significantly to the model

It can be concluded from the results in Table 4 that based on the values for these 5 input parameters encountered in the literature or derived from own experimental work, the B:P ratio (BP) and the hepatic accumulation factor (ACC) influenced the prediction of the total clearance most, while mainly the B:P ratio (BP) and the unbound fraction in plasma (fu) seemed to be affecting the value of Vss.

3

5 DISCUSSION

In this paper, we investigated the contribution of the hepatic clearance and the different CYP isoforms in the total clearance of tramadol by considering 3 different clearance models. Model 1 (HLM model) is based on data from HLM systems with specific CYP contributions via a chemical inhibition assay, while model 2 (rhCYP model) uses recombinant *in vitro* clearance data with ad hoc determined ISEF values. Finally, model 3 (retrograde model) was included as a reference model, based on hepatic intrinsic clearances scaled back from *in vivo* hepatic clearance. For every model prediction not only the geometric mean of the total clearance but also the associated variability was evaluated. The difference in total clearance between these models is solely due to their hepatic component since renal clearance was fixed at 6.6 L/h. Apparently, the HLM model underpredicted the total clearance by -27%, while the rhCYP model overpredicted the total clearance by +22% due to the fact that the hepatic clearance is increased in the rhCYP model vs the HLM model (cfr Figure 6 and Table 3). The involvement of CYP2D6 still is underestimated in the HLM model and rhCYP model, as can be concluded from the lower values for hepatic fold increase in Table 3 compared to the retrograde model. Although a large pool of human liver microsomes was used for the experiments, it has been previously shown that CYP2D6 is not the most stable isoform as could be derived from *in vitro* metabolism studies [35], and hence an underestimation of CYP2D6 activity as measured in this HLM batch could be a plausible explanation. Despite the fact that the rhCYP model, based on study-specific ISEFs, somewhat overpredicts hepatic involvement, the CYP2D6 contribution is quite analogous to the one in the HLM model. Although an underprediction of -27% (HLM model) and an overprediction of +22% (rhCYP model) of the total clearance is apparent, the question can be raised how much more accurate these bottom-up clearance models need to be. Are we only and unconditionally satisfied when the model predictions fall within the 2 fold prediction error margins? In our opinion, although our clearance model predictions clearly fall within these boundaries, there is undoubtedly room for improvement since a suboptimal CYP2D6 involvement in our clearance models prevails. Additional research should enable us to fine-tune these models further in their relative CYP contributions.

In the evaluation of the population simulations we found that the variability in all three models tends to be underpredicted, as is readily observed from the CV fold values being smaller than 1 in Table 3. Upon visual inspection of Figure 6 the variability of the rhCYP model predictions seems larger than that of the HLM model predictions. However, when comparing the fold differences of CV between the two models, it is noticed that the difference between the fold differences (0.73 vs 0.89, Table 3) is smaller than what would have been expected based on comparison of the 95% prediction intervals from the plots in Figure 6. This indicates that variability, incorporated in the PBPK predictions, assumes a constant CV model. Having a good prior estimate of the variability associated with the clearance through the use of PBPK

modeling and simulation would definitely facilitate the prospective design and power calculations of an upcoming clinical trial.

In establishing *in vitro* intrinsic clearance values, using whatever *in vitro* system, it is well known that data should be linear with respect to time and protein concentration [36]. Drug-specific HLM and recombinant enzyme kinetic data on tramadol are available in the literature [29]. The data, however, are based on experiments using pools from 5 livers in which linearity was not investigated at the lowest *in vitro* test concentration. Moreover, the experiments were conducted at concentrations beyond those ever reached *in vivo* (intrahepatically). We therefore redesigned these experiments, in order to obtain physiologically relevant *in vitro* enzyme kinetic parameters. From the literature it was anticipated that tramadol would have a very low turnover *in vitro* [37], and our data equally substantiated that after 10 min incubation with 1 mg microsomal protein/ml, only 1% of tramadol at [S] < Km/10 was converted to its respective metabolites. By using appropriate, physiologically relevant incubation conditions, we were able to achieve quantitative estimates for the intrinsic clearances for both metabolites. Additionally, next to CYP2D6 and CYP3A4, a role for CYP2B6 of about 30% in the HLM metabolism of tramadol to NDT could be identified. This contribution however may be overemphasized due to the lower CYP2D6 activity present in this HLM batch. Nevertheless, in the case of CYP2D6 poor metabolizers e.g., the contribution of CYP2B6 and its expected associated variability [38] may become important covariates in the tramadol disposition.

An appealing feature of IVIVE-linked PBPK modeling and simulation is the learning-confirming principle, and consequently, the fact that mechanistic insights into the observed pharmacokinetics can be obtained [39]. In that respect, the sensitivity analysis conducted in this case study clearly revealed that the B:P ratio and hepatic accumulation were factors most influential for the prediction of clearance, while the B:P ratio and fraction unbound in plasma strongly influenced the prediction of steady-state volume of distribution. While it is obvious why e.g. the hepatic accumulation and unbound fraction in plasma determine the prediction of the clearance and volume, respectively, it is not directly evident why the B:P ratio has such a marked effect, while logP and pKa hardly have any effect on the prediction of the tramadol clearance (Table 4). It has to be kept in mind however, that all predictions are based on kinetics as a function of time after a single i.v. dose, recording plasma concentrations up to 24h post dose. Because B:P ratio, logP, and pKa all influence the prediction of the volume of distribution, and hence plasma concentrations, this has a rebound effect on the calculation of the clearance, calculated as dose/$AUC_{0\text{-}24h}$. The influence of the B:P ratio on the Vss was anticipated considering its role in the Rodgers & Rowland model for the prediction of tissue distribution [25]. Therefore, a blood distribution experiment was conducted to ascertain the value of this B:P ratio in the model. Also, the positive effect of hepatic accumulation on the prediction of the hepatic clearance value proved to be a very influential

factor in this PBPK model, which is to be expected for low clearance drugs. Tramadol, as basic amine, is expected to accumulate inside the hepatocyte, solely driven by the existing pH gradient from 7.4 outside the cell, over 7.2 in the cytosol, to 5 in lysosomes [40]. No transporters are thought to be involved in this process [7], which is in line with tramadol's BCS class I. An important issue in this matter is to establish which fraction of drug is available to the CYP enzyme system. The CLint, as determined *in vitro* in hepatocyte suspensions, should provide an indirect measure of the accumulation of unbound drug inside the hepatocyte, that is readily available for biotransformation. Nevertheless, a substantial underestimation of the CLint using hepatocyte incubations is a recognized problem [41, 42] and questions concerning the presence of a comparable pH gradient in such an *in vitro* setup have arisen [43, 44]. Additionally, Poulin and co-workers also stated that the unbound drug fraction inside the hepatocyte could be greater than the unbound fraction in plasma because of binding effects of albumin on the hepatocyte cell surface *in vivo* on the one hand, and the aforementioned pH difference for ionizable compounds on the other hand. Consequently, by using *in vitro* systems in which these effects are unaccounted for, the CLint could be underestimated [45]. Because of the inability to determine this uptake, a hepatic accumulation value of 1.58 [40] was used in all clearance models, based on the pH difference between the hepatocyte's outer (7.4) and inner (7.2) environment. To be able to put this into context, quite recently, equations were published by Berezhkovskiy et al. [44, 46] that can be used to calculate an ionization factor, describing a drug's trapping behavior based on the drug's pKa and the pH difference over the hepatocyte membrane. These equations revealed that for tramadol by varying the intracellular pH between 7.0 and 7.2, the ionization factor takes on values of 1.67 and 2.5, respectively. In analogy, varying the hepatic accumulation factor 2-fold (from 1.5 to 3) in our sensitivity analysis increased prediction of the clearance with 33%. This indicates that small changes in pH can introduce significant changes in tissue-to-plasma concentration ratios. A better characterization of the relevant processes at hand could improve clearance prediction accuracy from an IVIVE perspective.

6 CONCLUSION

In conclusion, based on this work, we document that for quantitative PBPK modeling & simulation, all experiments to determine enzyme kinetic parameters should be performed with concentrations mimicking the *in vivo* obtained concentrations as closely as possible, while at the same time carefully scrutinizing reaction linearity. Tramadol as such displays a low turnover in hepatic *in vitro* systems, but using the physiological integration features of IVIVE-PBPK, i.e. the combination with a high fraction unbound in plasma (80%) and the hepatic accumulation (1.58 fold) of tramadol, leads to a simulation result corresponding with the quite extensive metabolism (approximately 80% of dose) observed *in vivo*. Three distinct clearance models were described in this paper. The HLM model slightly underpredicted, while the rhCYP model slightly overpredicted the geometric mean clearance. The CYP2D6 contribution was underpredicted in both cases. Although the variability also suffered from some underpredicition, the predicted coefficients of variation were in line with observed ones. We clearly illustrated that the use of a retrograde model as reference model facilitates the bottom-up PBPK model building process. The IVIVE-linked PBPK approach has proven to be a very useful tool in integrating available *in vitro*, *in silico*, and *in vivo* data on tramadol to successfully predict the *in vivo* PK and gain mechanistic insight in relevant disposition covariates at hand.

3

7 REFERENCES

1. Grond S. Clinical pharmacology of tramadol. Clin Pharmacokinet. 2004;43(13):879-923.

2. Subrahmanyam V, Renwick AB, Walters DG, Young PJ, Price RJ, Tonelli AP, et al. Identification of Cytochrome P-450 Isoforms Responsible for cis-Tramadol Metabolism in Human Liver Microsomes. Drug Metab Dispos. 2001;29(8):1146-55.

3. Whirl-Carrillo M, McDonagh EM, Hebert JM, Gong L, Sangkuhl K, Thorn CF, et al. Pharmacogenomics Knowledge for Personalized Medicine. Clin Pharmacol Ther. 2012;92(4):414-7.

4. Gonzalez F, Tukey R. Drug Metabolism. In: Goodman L, Gilman A, Brunton L, Lazo J, Parker K, editors. Goodman and Gilman's The Pharmacological Basis of Therapeutics. New York: McGraw Hill; 2006. p. 71-91.

5. Zhou SF. Polymorphism of human cytochrome P450 2D6 and its clinical significance: Part I. Clin Pharmacokinet. 2009;48(11):689-723.

6. Stamer UM, Musshoff F, Kobilay M, Madea B, Hoeft A, Stuber F. Concentrations of Tramadol and O-desmethyltramadol Enantiomers in Different CYP2D6 Genotypes. Clin Pharmacol Ther. 2007;82(1):41-7.

7. Tzvetkov MV, Saadatmand AR, Lotsch J, Tegeder I, Stingl JC, Brockmoller J. Genetically Polymorphic OCT1: Another Piece in the Puzzle of the Variable Pharmacokinetics and Pharmacodynamics of the Opioidergic Drug Tramadol. Clin Pharmacol Ther. 2011;90(1):143-50.

8. Rowland M, Peck C, Tucker G. Physiologically-Based Pharmacokinetics in Drug Development and Regulatory Science. Annu Rev Pharmacol Toxicol. 2011;51(1):45-73.

9. Edginton AN, Theil FP, Schmitt W, Willmann S. Whole body physiologically-based pharmacokinetic models: their use in clinical drug development. Expert Opin Drug Metab Toxicol. 2008;4(9):1143-52.

10. Jamei M, Marciniak S, Feng K, Barnett A, Tucker G, Rostami-Hodjegan A. The Simcyp Population-based ADME Simulator. Expert Opin Drug Metab Toxicol 2009;5(2):211-23.

11. Bouzom F, Walther B. Pharmacokinetic predictions in children by using the physiologically based pharmacokinetic modelling. Fundam Clin Pharmacol. 2008;22(6):579-87.

12. De Bock L, Colin P, Boussery K, Van Bocxlaer J. Development and validation of an enzyme-linked immunosorbent assay for the quantification of cytochrome 3A4 in human liver microsomes. Talanta. 2012;99:357-62.

13. Rostami-Hodjegan A. Physiologically Based Pharmacokinetics Joined With In Vitro-In Vivo Extrapolation of ADME: A Marriage Under the Arch of Systems Pharmacology. Clin Pharmacol Ther 2012;92(1):50-61.

14. Obach RS, Reed-Hagen AE. Measurement of Michaelis Constants for Cytochrome P450-Mediated Biotransformation Reactions Using a Substrate Depletion Approach. Drug Metab Dispos. 2002;30(7):831-7.

15. Di L, Atkinson K, Orozco CC, Funk C, Zhang H, McDonald TS, et al. In Vitro–In Vivo Correlation for Low-Clearance Compounds Using Hepatocyte Relay Method. Drug Metab Dispos. 2013;41(12):2018-23.

16. Fagerholm U. Prediction of human pharmacokinetics–evaluation of methods for prediction of hepatic metabolic clearance. J Pharm Pharmacol. 2007;59(6):803-28.

17. Team RC. R: A Language and Environment for Statistical Computing. R Foundation for Statistical Computing, Vienna, Austria. 2013.

18. Turner D, Rostami-Hodjegan A, Tucker G, Yeo K. Prediction of nonspecific hepatic microsomal binding from readily available physicochemical properties. Drug Metab Rev. 2007;38(S1):162.

19. Crewe HK. Are there differences in the catalytic activity per unit enzyme of recombinantly expressed and human liver microsomal cytochrome P450 2C9? A systematic investigation into inter-system extrapolation factors. Biopharm Drug Dispos. 2011;32(6):303-18.

20. Rostami-Hodjegan A, Tucker GT. Simulation and prediction of in vivo drug metabolism in human populations from in vitro data. Nat Rev Drug Discov. 2007;6(2):140-8.

21. Lintz W, Barth H, Becker R, Frankus E, Schmidt-Bothelt E. Pharmacokinetics of tramadol and bioavailability of enteral tramadol formulations - 2nd communication: Drops with ethanol. Arzneimittel-Forschung. 1998;48(5):436-45.

22. Lintz W, Barth H, Osterloh G, Schmidt-Bothelt E. Bioavailability of Enteral Formulations 1st communication: Capsules. Arzneimittel-Forschung. 1986;36-2(8):1278-83.

23. Lintz W, Barth H, Osterloh G, Schmidt-Bothelt E. Pharmacokinetics of tramadol and bioavailability of enteral tramadol formulations - 3rd communication: Suppositories. Arzneimittel-Forschung. 1998;48(9):889-99.

24. Quetglas EG, Azanza JR, Cardenas E, Sadaba B, Campanero MA. Stereoselective pharmacokinetic analysis of tramadol and its main phase I metabolites in healthy subjects after intravenous and oral administration of racemic tramadol. Biopharm Drug Dispos. 2007;28(1):19-33.

25. Rodgers T, Leahy D, Rowland M. Physiologically based pharmacokinetic modeling 1: Predicting the tissue distribution of moderate-to-strong bases. J Pharm Sci. 2005;94(6):1259-76.

26. Chen Y, Liu L, Nguyen K, Fretland AJ. Utility of Intersystem Extrapolation Factors in Early Reaction Phenotyping and the Quantitative Extrapolation of Human Liver Microsomal Intrinsic Clearance Using Recombinant Cytochromes P450. Drug Metab Dispos. 2011;39(3):373-82.

27. Yeo KR. Abundance of cytochromes P450 in human liver: a meta-analysis. Br J Clin Pharmacol. 2004;57(5):687-8.

28. Pedersen RS, Damkier P, Brosen K. Enantioselective pharmacokinetics of tramadol in CYP2D6 extensive and poor metabolizers. Eur J Clin Pharmacol. 2006;62(7):513-21.

29. Subrahmanyam V, Renwick AB, Walters DG, Young PJ, Price RJ, Tonelli AP, et al. Identification of Cytochrome P-450 Isoforms Responsible for cis-Tramadol Metabolism in Human Liver Microsomes. Drug Metabolism and Disposition. 2001;29(8):1146-55.

30. von Moltke LL, Greenblatt DJ, Duan SX, Daily JP, Harmatz JS, Shader RI. Inhibition of desipramine hydroxylation (cytochrome P450-2D6) in vitro by quinidine and by viral protease inhibitors: Relation to drug interactions in vivo. J Pharm Sci. 1998;87(10):1184-9.

31. Li X, Song X, Kamenecka TM, Cameron MD. Discovery of a Highly Selective CYP3A4 Inhibitor Suitable for Reaction Phenotyping Studies and Differentiation of CYP3A4 and CYP3A5. Drug Metab Dispos. 2012;40(9):1803-9.

32. Poulin P, Theil FP. Prediction of pharmacokinetics prior to in vivo studies. 1. Mechanism-based prediction of volume of distribution. J Pharm Sci. 2002;91(1):129-56.

33. De Buck SS, Mackie CE. Physiologically based approaches towards the prediction of pharmacokinetics: in vitro-in vivo extrapolation. Expert Opin Drug Metab Toxicol. 2007;3(6):865-78.

34. Johnson TN, Rostami-Hodjegan A, Tucker GT. Prediction of the Clearance of Eleven Drugs and Associated Variability in Neonates, Infants and Children. Clin Pharmacokinet. 2006;45(9):931-56.

35. Foti RS, Fisher MB. Impact of incubation conditions on bufuralol human clearance predictions: enzyme liability and nonspecific binding. Drug Metab Dispos. 2004;32(3):295-304.

36. Sjogren E, Nyberg J, Magnusson MO, Lennernas H, Hooker A, Bredberg U. Optimal Experimental Design for Assessment of Enzyme Kinetics in a Drug Discovery Screening Environment. Drug Metab Dispos. 2011;39(5):858-63.

37. Shao L, Hewitt M, Jerussi TP, Wu F, Malcolm S, Grover P, et al. In vitro and in vivo evaluation of O-alkyl derivatives of tramadol. Bioorg Med Chem Lett. 2008;18(5):1674-80.

38. Zhang H, Sridar C, Kenaan C, Amunugama H, Ballou DP, Hollenberg PF. Polymorphic Variants of Cytochrome P450 2B6 (CYP2B6.4–CYP2B6.9) Exhibit Altered Rates of Metabolism for Bupropion and Efavirenz: A Charge-Reversal Mutation in the K139E Variant (CYP2B6.8) Impairs Formation of a Functional Cytochrome P450-Reductase Complex. J Pharmacol Exp Ther. 2011;338(3):803-9.

39. Zhao P, Zhang L, Grillo JA, Liu Q, Bullock JM, Moon YJ, et al. Applications of Physiologically Based Pharmacokinetic (PBPK) Modeling and Simulation During Regulatory Review. Clin Pharmacol Ther. 2011;89(2):259-67.

40. Hallifax D, Houston JB. Saturable uptake of lipophilic amine drugs into isolated hepatocytes: Mechanisms and consequences for quantitative clearance prediction. Drug Metab Dispos. 2007;35(8):1325-32.

41. Foster JA, Houston JB, Hallifax D. Comparison of intrinsic clearances in human liver microsomes and suspended hepatocytes from the same donor livers: clearance-dependent relationship and implications for prediction of in vivo clearance. Xenobiotica. 2011;41(2):124-36.

42. Ito K, Houston JB. Comparison of the use of liver models for predicting drug clearance using in vitro kinetic data from hepatic microsomes and isolated hepatocytes. Pharm Res. 2004;21(5):785-92.

43. Berezhkovskiy L, Wong S, Halladay J. On the maintenance of hepatocyte intracellular pH 7.0 in the in-vitro metabolic stability assay. J Pharmacokinet Pharmacodyn: Springer US; 2013. p. 683-9.

44. Berezhkovskiy LM, Liu N, Halladay JS. Consistency of the novel equations for determination of hepatic clearance and drug time course in liver that account for the difference in drug ionization in extracellular and intracellular tissue water. J Pharm Sci. 2012;101(2):516-8.

45. Poulin P, Hop CECA, Ho Q, Halladay JS, Haddad S, Kenny JR. Comparative assessment of In Vitro–In Vivo extrapolation methods used for predicting hepatic metabolic clearance of drugs. J Pharm Sci. 2012;101(11):4308-26.

46. Berezhkovskiy LM. The Corrected Traditional Equations for Calculation of Hepatic Clearance that Account for the Difference in Drug Ionization in Extracellular and Intracellular Tissue Water and the Corresponding Corrected PBPK Equation. J Pharm Sci. 2011;100(3):1167-83.

8 APPENDIX

The bioanalytical runs were accepted based on the criteria, which are described hereunder. For these criteria, the FDA Guidance document was followed.

- The calibration curve consisted of 10 calibrators. QC samples were present on 3 levels (low, mid, and high), and were made in duplicate. Calibrators and QC samples were always made from dry powder for every new run
- Linearity of the calibration curve was checked. Simple linear regression was applied with a weighting factor 1/x. The coefficient of determination (R^2) was 0.99 or more.
- At least 4 out of 6 QC samples were within 15% of their nominal value. Standards deviated not more than 15% from the nominal concentration, except for the LLOQ where 20% deviation was allowed.
- Within run accuracy and precision was assessed on the three QC levels (n=4) for the different metabolites that were measured in the analysis (as tabulated hereunder).

	ODT		**NDT**		**NODT**	
Level	Conc ng/mL	ACC (PREC)	Conc ng/mL	ACC (PREC)	Conc ng/mL	ACC (PREC)
LQC	3.65	98% (9.4%)	3.95	95% (5.1%)	3.20	96% (5.4%)
MQC	85.17	105% (1.3%)	92.17	107% (2.6%)	74.67	101% (7.2%)
HQC	851.67	102% (0.1%)	921.67	104% (2.5%)	746.67	97% (0.7%)

- Between-run accuracy and precision was assessed at the LLOQ level (n=4) for the different metabolites that were measured in the analysis (as tabulated hereunder).

	ODT		**NDT**		**NODT**	
Level	Conc ng/mL	ACC (PREC)	Conc ng/mL	ACC (PREC)	Conc ng/mL	ACC (PREC)
LLOQ	1.04	99% (6.2%)	1.19	110% (2.4%)	0.24	107% (9.6%)

3

3

3

CHAPTER 4

STRATEGIES FOR DETERMINING CORRECT CYTOCHROME P450 CONTRIBUTIONS IN HEPATIC CLEARANCE PREDICTIONS: IN VITRO-IN VIVO EXTRAPOLATION AS MODELLING APPROACH AND TRAMADOL AS PROOF-OF CONCEPT COMPOUND

This chapter is based on:

T'jollyn H, Snoeys J, Van Bocxlaer J, De Bock L, Annaert P, Van Peer A, et al. Strategies for Determining Correct Cytochrome P450 Contributions in Hepatic Clearance Predictions: In Vitro–In Vivo Extrapolation as Modelling Approach and Tramadol as Proof-of Concept Compound. European Journal of Drug Metabolism and Pharmacokinetics. 2016//:1-7 (AOP)

4

TABLE OF CONTENTS

4

1 ABSTRACT

Background and Objective

Although the measurement of cytochrome P450 (CYP) contributions in metabolism assays is straightforward, determination of actual *in vivo* contributions might be challenging. How representative are *in vitro* for *in vivo* CYP contributions? This article proposes an improved strategy for the determination of *in vivo* CYP enzyme-specific metabolic contributions, based on *in vitro* data, using an *in vitro-in vivo* extrapolation (IVIVE) approach. Approaches are exemplified using tramadol as model compound, and CYP2D6 and CYP3A4 as involved enzymes.

Methods

Metabolism data for tramadol and for the probe substrates midazolam (CYP3A4) and dextromethorphan (CYP2D6) were gathered in human liver microsomes (HLM) and recombinant human enzyme systems (rhCYP). From these probe substrates, an activity-adjustment factor (AAF) was calculated per CYP enzyme, for the determination of correct hepatic clearance contributions. As a reference, tramadol CYP contributions were scaled-back from *in vivo* data (retrograde approach) and were compared with the ones derived *in vitro*. In this view, the AAF is an enzyme-specific factor, calculated from reference probe activity measurements *in vitro* and *in vivo*, that allows appropriate scaling of a test drug's *in vitro* activity to the 'healthy volunteer' population level. Calculation of an AAF thus accounts for any 'experimental' or 'batch-specific' activity difference between *in vitro* HLM and *in vivo* derived activity.

Results

In this specific HLM batch, for CYP3A4 and CYP2D6, an AAF of 0.91 and 1.97 was calculated, respectively. This implies that, in this batch, the *in vitro* CYP3A4 activity is 1.10-fold higher and the CYP2D6 activity 1.97-fold lower, compared to *in vivo*-derived CYP activities.

Conclusion

This study shows that, in cases where the HLM pool does not represent the typical mean population CYP activities, AAF correction of *in vitro* metabolism data, optimizes CYP contributions in the prediction of hepatic clearance. Therefore, *in vitro* parameters for any test compound, obtained in a particular batch, should be corrected with the AAF for the respective enzymes. In the current study, especially the CYP2D6 contribution was found to better reflect the average *in vivo* situation. It is recommended that this novel approach is further evaluated using a broader range of compounds.

2 INTRODUCTION

In setting up a physiologically relevant *in vitro-in vivo* extrapolated physiologically-based pharmacokinetic (IVIVE-PBPK) model, not only must the total clearance be captured well, also the relevant Cytochrome P450 (CYP) contributions used in the model should be representative of the *in vivo* situation [1, 2]. This IVIVE approach assumes that the CYP contributions measured *in vitro* (pooled human liver microsomes (HLM)) are the same as the ones observed *in vivo*. However, *in vitro* activities might not represent healthy adult activity due to e.g. the source of the liver tissue (often diseased patients) [3] or binding competition of the compound under study with free fatty acids [4]. Therefore, methods are needed that ensure this predictability. In the current work, the use of an activity-adjustment factor (AAF) is presented as an alternative method and evaluated against the conventional (uncorrected) approach. The conventional approach consists of IVIVE from HLM and human recombinant (rhCYP) enzyme kinetic data, including determination of the preferred inter-system extrapolation factor (ISEF) [5]. Tramadol is used as a proof-of-concept compound since it is metabolized by different and clinically important CYP enzymes (i.e. CYP3A4, CYP2D6 and CYP2B6) [6]. Besides, clinical data is available concerning the effect of (i) CYP2D6 polymorphisms, and (ii) rifampicin induction on tramadol's clearance. In the current work, the main focus is on the CYP2D6-CYP3A4 interplay, and less on CYP2B6. This is because the initial focus of this project was on the most relevant CYP enzymes and because CYP2B6 plays a minor role in tramadol metabolism, as indicated in the discussion section.

4

3 MATERIALS AND METHODS

3.1 CHEMICALS AND MATERIALS

All chemicals and reagents used were of the highest available grade: Na_2HPO_4, KH_2PO_4, KCl, $MgCl_2$, NADP, HCl (Merck, Darmstadt, Germany), glucose-6-phosphate, glucose-6-phosphate dehydrogenase (Roche Diagnostics GmbH, Mannheim, Germany), midazolam, dextromethorphan, 1-OH midazolam, dextrorphan, deuterated 1-OH midazolam (TRC inc, Toronto, Canada), chlorpropamide (Sigma Aldrich, St. Louis, USA). Human liver microsomal pool (BD Biosciences, Woburn, USA) consisted of 50 adult donors (mixed gender).

3.2 INCUBATIONS IN HLM AND RHCYP OF MIDAZOLAM, DEXTROMETHORPHAN, AND TRAMADOL

For midazolam/dextromethorphan, the incubation mixture consisted of 120 µL diluted microsomes, 100 µL cofactor mix for NADPH regeneration system, and 5 µL test compound (0.5% MeOH in final incubation mixture) for both HLM as well as rhCYP systems. After a preincubation period of 5 min at 37°C and 100 oscillations/min, NADP was added to the preincubation mixture to a final volume of 250 µL to initiate the reaction. Midazolam was incubated in the range of 0.1-16 µM at 0.15 mg protein/mL (HLM) and 10 pmol CYP3A4/mL (rhCYP). The reaction was stopped after 10 min with 250 µL DMSO containing deuterated 1-OH midazolam as the internal standard (0.1 µg/mL). Dextromethorphan was incubated in the range of 0.5-16 µM at 0.3 mg protein/mL (HLM) and 4 pmol CYP2D6*1/mL (rhCYP). The reaction was stopped after 10 min with 250 µL DMSO containing chlorpropamide as the internal standard (0.22 µg/mL). Although these conditions differ from the ones used in the Walsky and Obach paper [7], linearity as a function of time and protein concentration for these probe substrates was demonstrated (data on file). Samples were centrifuged for 10 min at 1711g and the supernatant introduced to the UPLC-MS method. The intrinsic clearance was calculated in the Enzyme Kinetics module of Sigma Plot. For tramadol linearity experiments, incubations, and phenotyping experiments in pooled HLM and rhCYP systems, we refer to our previous publication [8]. The unbound fraction in the incubates for probe substrates midazolam and dextromethorpan was calculated from reported literature values [9, 10]. Details on the determination of these fu values are provided in the *Appendix*.

3.3 BIOANALYSIS

The midazolam metabolite, 1-OH midazolam, was analyzed using a Waters Acquity UPLC system coupled to a Thermo LTQ mass spectrometer (Thermo Fisher Scientific, San Jose, U.S.) in APCI +. The column was an Acquity UPLC BEH C18 (1.7µm) 50 x 2.1 mm held at 60°C with mobile phase constituents 0.1%

HCOOH in ULC water and 0.1% HCOOH in CH_3CN in a linear gradient. Run time was 3 min and flow rate 0.6 mL/min. Mass transitions for 1-OH midazolam and deuterated 1-OH midazolam (internal standard) using a collision energy (CE) of 30 eV were 342>325, and 346>328, respectively. Calibration curves were always made in the same microsomal matrix as the incubates using at least 8 calibrator levels and 3 QC levels for the calibration curve. The dextromethorphan metabolite, dextrorphan, was analyzed using a Waters Acquity UPLC system coupled to a Micromass Quattro Ultima triple quadrupole, operating in ESI +. The column was an Acquity UPLC BEH C18 (1.7µm) 50 x 2.1 mm at 35°C with mobile phase constituents 0.1% HCOOH in ULC water and 0.1% HCOOH in CH_3CN in a linear gradient. Run time was 5.25 min and flow rate 0.4 mL/min. Mass transitions for dextrorphan and chlorpropamide using a CE of 28 and 25 eV were 258>157, and 277>275. Details about the dextromethorphan and tramadol bioanalysis methods, can be found in De Bock et al, 2012 [11] and T'jollyn et al., 2015 [8], respectively.

3.4 CALCULATION OF ISEF AND ACTIVITY-ADJUSTMENT FACTORS USING PROBE SUBSTRATES

ISEF values were calculated for CYP3A4 (midazolam) and CYP2D6 (dextromethorphan) using the formula below (equation 1).

$$ISEF = \frac{CLint_{u,HLM}}{CLint_{u,rhCYP} * [CYP]_{HLM}}$$

EQUATION 1

$CLint_{u,HLM}$ and $CLint_{u,rhCYP}$ are the unbound intrinsic clearances (determined via metabolite formation) of a specific probe substrate in HLM and rhCYP systems, respectively. $[CYP]_{HLM}$ represents the typical enzyme abundance values of 137 and 8 pmol CYP/mg used for CYP3A4 and CYP2D6, respectively [5, 12].

The activity-adjustment factor (AAF) is calculated as the ratio of the (unbound) *in vivo* back-calculated hepatic CLint and the unbound *in vitro* HLM CLint for a specific enzyme using the specific probe substrate (equation 2 and Table 1).

$$AAF_{CYP} = \frac{CLint_{u,invivo,CYP}}{CLint_{u,HLM,CYP}}$$

EQUATION 2

Then, the AAF, which is calculated for each CYP isozyme, is multiplied with the relevant parameter involved in the IVIVE (i.e. either $CLint_{u,HLM,CYP}$ or $ISEF_{CYP}$. This yields the $CLint_{aa,u,HLM,CYP}$ for HLM data and $ISEF_{aa,CYP}$, for rhCYP data (equation 3 and Table A1 in *Appendix*).

$$CLint_{aa,u,HLM,CYP} = CLint_{u,HLM,CYP} * AAF_{CYP}$$

$$ISEF_{aa,CYP} = ISEF_{CYP} * AAF_{CYP}$$

EQUATION 3

3.5 IVIVE-PBPK MODEL DEVELOPMENT

The unbound intrinsic clearance calculated per *in vitro* system with/without correction (see previous section), is used in the well-stirred liver approach in Simcyp® (v12.1, Certara, Sheffield, UK) to come up with an *in vivo* hepatic clearance. The AAF-corrected hepatic clearance predictions are compared to their uncorrected counterparts, as described in Chapter 3. In the HLM and HLM_{aa} models, CLint values Table A1 in *Appendix*, columns 1 & 2) were provided in the enzyme kinetics tab of the Simcyp® Simulation platform, whereas in the rhCYP and $rhCYP_{aa}$ models, both CLint and ISEF values (Table A1, columns 3 & 4) were provided. In the retrograde model, CLint values were calculated from *in vivo* data, as described below (Table A1, column 5).

3.6 RETROGRADE METHOD: INDIVIDUAL CYP CONTRIBUTIONS FROM TRAMADOL *IN VIVO* DATA

The retrograde-scaled approach calculates a hepatic intrinsic clearance per CYP enzyme based on *in vivo* hepatic clearance values and apparent *in vivo* CYP contributions in the total metabolism. Two different approaches were used to quantitatively define CYP2D6, CYP2B6 and CYP3A4 involvement using tramadol *in vivo* data. For details about the CYP2D6 contribution, we refer to Chapter 3. The CYP2B6-CYP3A4 contribution was assessed by performing a clinical trial simulation in which a tramadol-rifampicin drug-drug interaction (DDI) was considered. To this end, the study population and study design as described by Saarikoski, et al. [13] was matched in a PBPK modelling environment. The rifampicin drug-specific parameters that were used in the PBPK model and that describe its PK and induction effects on CYP2B6 and CYP3A4, are described elsewhere [14]. They were proven to be capable to describe rifampicin's DDI potential. While keeping the CYP2D6 contribution in the tramadol retrograde (RG) model fixed, the CYP2B6 contribution was varied between 0 and 30% at the expense of the CYP3A4 contribution. Simulation results were expressed as the geometric mean ratio of the $AUC_{control}/AUC_{induced}$ for 100 simulated trials and compared to the observed geometric mean ratio from the actual *in vivo* DDI study between tramadol and rifampicin [13].

4 RESULTS

For the calculation of the AAF, the back-calculation of the CYP3A4 $CLint_{u,invivo}$ (probe substrate midazolam) involved a well-stirred liver model and its value is based on 31 investigational midazolam PK studies [15]. This CYP3A4 -specific contribution was assessed by accounting for the conversion midazolam -> 1-OH midazolam, representing 74% of the *in vivo* derived hepatic CLint (Simcyp® midazolam compound file, v12.1) (see *Appendix*). Next, the AAF_{3A4} was calculated and had a value of 0.91 (Table 1). In order to calculate the AAF_{2D6}, the CYP2D6 $CLint_{u,invivo}$ (probe substrate dextromethorphan) was collected from one study [16], using a parallel tube model. In addition, a factor of 1.56 accounts for dextromethorphan's accumulation in the hepatocyte's cytosol [17](see *Appendix*). Next, the AAF_{2D6} was calculated and had a value of 1.97 (Table 1). Final metabolism parameters used in the IVIVE are displayed in Table A1 (*Appendix)*. In addition, Table 1 reports ISEF values per CYP enzyme. Based on midazolam and dextromethorphan metabolism data, an ISEF of 0.23 and 0.45 could be calculated for CYP3A4 and CYP2D6, respectively.

TABLE 1: OVERVIEW OF PROBE SUBSTRATE DATA

THESE VALUES WERE OBTAINED FOR THE PROBE SUBSTRATES MIDAZOLAM (CYP3A4) AND DEXTROMETHORPHAN (CYP2D6). AAF WAS CALCULATED FROM THE RATIO OF THE CLINT VALUES IN THIS TABLE AS DESCRIBED IN THE METHODS SECTION. ISEF WAS CALCULATED PER PROBE SUBSTRATE FROM THE RATIO OF THE CLINTS OBTAINED IN HLM AND RHCYP SYSTEMS.

CYP Enzyme (probe)	CYP3A4 (midazolam)	CYP2D6 (dextromethorphan)
$CLint_{u,in\ vivo,CYP}$ (µL/min/mg)	336 [a]	58.9 [b]
$CLint_{u,HLM,CYP}$ (µL/min/mg)	369	29.9
AAF	0.91	1.97
ISEF	0.23	0.45

[a] [15] ; [b] [16]

CLint: intrinsic clearance; $CLint_{u,in\ vivo,CYP}$: the unbound *in vivo* CLint for a specific CYP enzyme; $CLint_{u,HLM,CYP}$: the unbound HLM CLint for a specific CYP enzyme: AAF: activity-adjustment factor; ISEF: inter-system extrapolation factor

The different hepatic clearance models were evaluated based on prediction errors (calculated as $(CL_{obs}-CL_{pred})/CL_{obs}$x100%) and the different CYP enzyme contributions (Table 2). Tramadol's *in vitro* CYP

contributions (with and without AAF correction) were compared with the ones calculated from the RG method. Tramadol's CYP contributions from activity-adjusted models (HLM_{aa} and $rhCYP_{aa}$ model; Table 2) agree well with those from the tramadol retrograde-scaled clearance approach (RG model, Table 2), although the absolute values of total clearance display some prediction bias (indicated by the prediction error). The CYP2D6 contribution (HLM_{aa} 45%; $rhCYP_{aa}$ 44.6%; RG 45.6%) corresponds very well between the AAF models and is more accurate as compared to the HLM and rhCYP models without AAF. The contributions of CYP3A4 (HLM_{aa} 39.2%; $rhCYP_{aa}$ 39.9%; RG 45.1%) and CYP2B6 (HLM_{aa} 15.8%; $rhCYP_{aa}$ 15.5%; RG 9.3%) differ by maximum 5% with the RG approach.

TABLE 2: MODEL PERFORMANCE AND CHARACTERISTICS PRESENTED PER CLEARANCE MODEL.

THE HLM AND RHCYP MODELS ARE BUILT-UP FROM *IN VITRO* DATA IN HLM AND RHCYP SYSTEMS, RESPECTIVELY. THE HLMAA AND RHCYPAA MODELS ARE CORRECTED WITH THE AAF. THE RETROGRADE MODEL CAN BE CONSIDERED THE REFERENCE MODEL IN TERMS OF TOTAL CLEARANCE AND CYP CONTRIBUTIONS IN THE HEPATIC CLEARANCE.

	prediction error (%)	% hepatic clearance	% CYP2D6 in hep CL	% CYP3A4 in hep CL	% CYP2B6 in hep CL
HLM model	*- 27%*	56.9%	29.1%	51.9%	19.0%
HLMaa model	*- 19%*	61.3%	45.0%	39.2%	15.8%
rhCYP model	*+ 22%*	75.9%	29.2%	51.8%	19.0%
rhCYPaa model	*+ 39%*	78.7%	44.6%	39.9%	15.5%
Retrograde model	*+ 2%*	70.5%	45.6%	45.1%	9.3%

HLM: human liver microsomes; rhCYP: human recombinant CYP enzymes; AAF: activity-adjustment factor; HLM_{aa}: the activity-adjusted HLM model; $rhCYP_{aa}$: the activity-adjusted rhCYP model

In the tramadol RG model, the CYP2D6 contribution was estimated using the dataset from [18] by determining which percentage of the hepatic clearance (48%, Table A1) is required to increase it 1.74-fold between poor and extensive metabolizers. Next, the CYP2B6-CYP3A4 involvement was estimated by comparing geometric mean AUC ratios from a DDI clinical trial simulation approach. The resulting geometric mean AUC ratio with 90% confidence intervals was compared to the observed geometric mean AUC ratio (Figure 1). Only with a CYP2B6 contribution of less than 10% and a CYP3A4 contribution of more than 42% (Table A1), the observed geometric mean AUC ratio fell within the 90% confidence interval of the trial simulations (Figure 1). The main driver of this rifampicin-tramadol DDI is CYP3A4, in view of its important role in tramadol's metabolism. The steady-state rifampicin induction increases CYP2B6's contribution with only 2%, whereas CYP3A4's contribution is increased with 31% (data not

shown). The CYP2B6 contribution was calculated to be maximally 10% of tramadol's hepatic intrinsic clearance (Table A1).

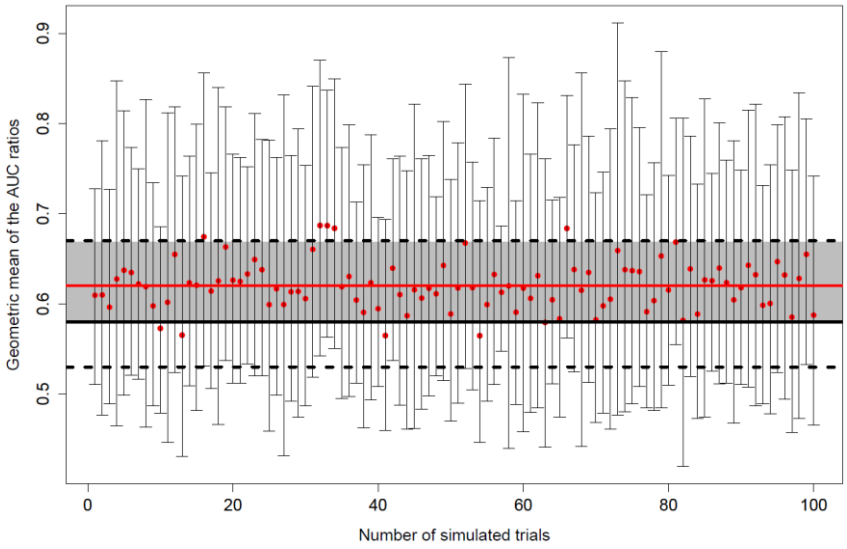

FIGURE 1: DDI CLINICAL TRIAL SIMULATION OF TRAMADOL AND RIFAMPICIN TO ASSESS THE CONTRIBUTION OF CYP2B6 AND CYP3A4. THE FIGURE DEPICTS THE RESULTS OF 100 TRIAL SIMULATIONS MIMICKING THE ORIGINAL TRIAL, WHEN CYP2B6 AND CYP3A4 CONTRIBUTIONS ARE ASSUMED TO BE 10 AND 42%, RESPECTIVELY. BLACK HORIZONTAL LINES REPRESENT THE *IN VIVO* OBSERVED RATIO OF AUC GEOMETRIC MEANS (SOLID) AND 90% CONFIDENCE LIMITS (DASHED). THE RED DOTS REPRESENT THE GEOMETRIC MEANS OF EACH TRIAL SIMULATION (AND ERROR BARS REPRESENT THE 90 CONFIDENCE INTERVAL). THE SOLID RED LINE REPRESENTS THE AVERAGE RATIO OF SIMULATED AUC GEOMETRIC MEANS. THE SOLID BLACK LINE IS IN THE 95% CONFIDENCE REGION (GREYED AREA) ONLY IF THE CYP2B6 CONTRIBUTION IS LESS THAN OR EQUAL TO 10%. DDI: DRUG-DRUG INTERACTION; AUC: AREA UNDER THE CURVE

4

5 DISCUSSION

Whenever pooled HLM activities are measured, the assumption is that every enzyme represents the population average activity. If this is not the case, the activity-adjustment factor (AAF) provides a way to correct for the difference between *in vitro* and *in vivo* activities. The AAF (equation 2 and *Appendix*) is an enzyme-specific factor, calculated from reference probe activity measurements *in vitro* and *in vivo* that allows appropriate scaling of a test drug's *in vitro* activity to the 'healthy volunteer' population level. The AAF for CYP3A4 in this study is 0.91 (Table 1) (1 represents no activity adjustment is needed). This implies that the CYP3A4 activity in the pooled HLM batch at hand, is nearly identical to that derived from the midazolam CLint, which was back-calculated from *in vivo* clearance values. Consequently, CYP3A4 activity measurements in this batch will be representative for the average population CYP3A4 activity. However, for CYP2D6, the AAF was computed at 1.97 (Table 1). This indicates that the CYP2D6 *in vitro* activity in this batch is about 2-fold below the typical 'healthy volunteer' population CYP2D6 activity. Calculation of an AAF thus accounts for any 'experimental' or 'batch-specific' activity difference between *in vitro* HLM and *in vivo* derived activity. The importance of using the AAF concept is illustrated by integrating it in the IVIVE of tramadol metabolism to its two primary metabolites O-desmethyl tramadol (ODT) and N-desmethyl tramadol (NDT). The metabolism parameters used in the IVIVE are displayed in Table A1 (*Appendix)*.

Although the retrograde-scaled approach is an attractive way to calculate CYP contributions based on *in vivo* data, it also depends on the quality of these *in vivo* data. The 10% involvement threshold for CYP2B6 in the retrograde model should be viewed as an approximate value for two reasons: (i) for CYP2B6, an AAF could not be calculated since CYP2B6 *in vitro* probe data were not available (see Table 2), and (ii) the design of the rifampicin-tramadol *in vivo* DDI study allowed only a partial differentiation of the CYP2B6 and CYP3A4 contributions. In essence, since for CYPD6 the different data elements were all available, the CYP2D6 approach could serve as proof of concept for the proposed methodology. The activity-adjusted CYP2D6 contribution turned out to be very similar to the one estimated from *in vivo* clearance data (RG approach), and shows a large improvement versus its contribution calculated in non-activity adjusted models (Table 2). This finding underscores the method's potential benefit.

6 CONCLUSION

Taken together, the AAF (i) provides compound-independent information about specific enzyme activities that should be incorporated whenever *in vitro* HLM activities are measured for a test drug, and (ii) allows to accurately calculate CYP contributions *in vivo*, even before clinical data of the test drug is available. In view of the increasing role of IVIVE-PBPK in drug development programs, it is important to determine the actual enzyme contributions in the hepatic clearance as early as possible. This way, clinical trial designs and clinically important drug-drug interactions may be better anticipated. In the current work, tramadol was used as a proof-of-concept compound, but more work is needed to extensively validate the proposed approach across a broader range of compounds.

4

7 REFERENCES

1. Johnson TN, Rostami-Hodjegan A. Resurgence in the use of physiologically based pharmacokinetic models in pediatric clinical pharmacology: parallel shift in incorporating the knowledge of biological elements and increased applicability to drug development and clinical practice. Pediatric Anesthesia. 2010;21(3):291-301.

2. Salem F, Johnson TN, Barter ZE, Leeder JS, Rostami-Hodjegan A. Age Related Changes in Fractional Elimination Pathways for Drugs: Assessing the Impact of Variable Ontogeny on Metabolic Drug-Drug Interactions. J Clin Pharmacol. 2013;53(8):857-65.

3. Donato MT, Lahoz A, Jimenez N, Perez G, Serralta A, Mir J, et al. Potential impact of steatosis on cytochrome P450 enzymes of human hepatocytes isolated from fatty liver grafts. Drug Metab Dispos. 2006;34(9):1556-62.

4. Rowland A, Knights KM, Mackenzie PI, Miners JO. The "albumin effect" and drug glucuronidation: bovine serum albumin and fatty acid-free human serum albumin enhance the glucuronidation of UDP-glucuronosyltransferase (UGT) 1A9 substrates but not UGT1A1 and UGT1A6 activities. Drug Metab Dispos. 2008;36(6):1056-62.

5. Chen Y, Liu L, Nguyen K, Fretland AJ. Utility of Intersystem Extrapolation Factors in Early Reaction Phenotyping and the Quantitative Extrapolation of Human Liver Microsomal Intrinsic Clearance Using Recombinant Cytochromes P450. Drug Metab Dispos. 2011;39(3):373-82.

6. Subrahmanyam V, Renwick AB, Walters DG, Young PJ, Price RJ, Tonelli AP, et al. Identification of cytochrome P-450 isoforms responsible for cis-tramadol metabolism in human liver microsomes. Drug Metab Dispos. 2001;29(8):1146-55.

7. Walsky RL, Obach RS. Validated assays for human cytochrome P450 activities. Drug Metab Dispos. 2004;32(6):647-60.

8. T'Jollyn H, Snoeys J, Colin P, Van Bocxlaer J, Annaert P, Cuyckens F, et al. Physiology-Based IVIVE Predictions of Tramadol from in Vitro Metabolism Data. Pharm Res. 2015;32(1):260-74.

9. Lu C, Li P, Gallegos R, Uttamsingh V, Xia CQ, Miwa GT, et al. Comparison of intrinsic clearance in liver microsomes and hepatocytes from rats and humans: evaluation of free fraction and uptake in hepatocytes. Drug Metab Dispos. 2006;34(9):1600-5.

10. Witherow LE, Houston JB. Sigmoidal kinetics of CYP3A substrates: an approach for scaling dextromethorphan metabolism in hepatic microsomes and isolated hepatocytes to predict in vivo clearance in rat. J Pharmacol Exp Ther. 1999;290(1):58-65.

11. De Bock L, Boussery K, Colin P, De Smet J, T'Jollyn H, Van Bocxlaer J. Development and validation of a fast and sensitive UPLC-MS/MS method for the quantification of six probe metabolites for the in vitro determination of cytochrome P450 activity. Talanta. 2012;89:209-16.

12. Yeo KR. Abundance of cytochromes P450 in human liver: a meta-analysis. Br J Clin Pharmacol. 2004;57(5):687-8.

13. Saarikoski T, Saari T, Hagelberg N, Neuvonen M, Neuvonen P, Scheinin M, et al. Rifampicin markedly decreases the exposure to oral and intravenous tramadol. Eur J Clin Pharmacol. 2013;69(6):1293-301.

14. Rekic D, Roshammar D, Mukonzo J, Ashton M. In silico prediction of efavirenz and rifampicin drug-drug interaction considering weight and CYP2B6 phenotype. Br J Clin Pharmacol. 2011;71(4):536-43.

15. Gertz M, Harrison A, Houston JB, Galetin A. Prediction of human intestinal first-pass metabolism of 25 CYP3A substrates from in vitro clearance and permeability data. Drug Metab Dispos. 2010;38(7):1147-58.

16. Ito T, Kato M, Chiba K, Okazaki O, Sugiyama Y. Estimation of the interindividual variability of cytochrome 2D6 activity from urinary metabolic ratios in the literature. Drug Metab Pharmacokinet. 2010;25(3):243-53.

17. Hallifax D, Houston JB. Saturable uptake of lipophilic amine drugs into isolated hepatocytes: Mechanisms and consequences for quantitative clearance prediction. Drug Metab Dispos. 2007;35(8):1325-32.

18. Pedersen RS, Damkier P, Brosen K. Enantioselective pharmacokinetics of tramadol in CYP2D6 extensive and poor metabolizers. Eur J Clin Pharmacol. 2006;62(7):513-21.

4

8 APPENDIX

TABLE A1: REPRESENTATION OF ALL CLINT AND ISEF VALUES THAT WERE USED PER HEPATIC CLEARANCE MODEL AS INPUT PARAMETERS FOR THE ENZYME KINETICS TAB IN THE SIMCYP® SIMULATOR.

Model / Reaction	HLM model $CLint_{HLM}$ (µL/min/mg)	HLMaa model $CLint_{aa,HLM}$ (µL/min/mg)	rhCYP model CLint [ISEF] (µL/min/pmol P450)	rhCYPaa model CLint [$ISEF_{aa}$] (µL/min/pmol P450)	RG model $CLint_{RG}$ (µL/min/pmol P450)
3A4-ODT	0.120	0.1092 (AAF_{3A4}= 0.91)	0.000 [0.23]	0.000 [0.21] (AAF_{3A4}= 0.91)	0.0154 (42% HepCL)
3A4-NDT	1.060	0.9646 (AAF_{3A4}= 0.91)	0.110 [0.23]	0.110 [0.21] (AAF_{3A4}= 0.91)	
2D6-ODT	0.640	1.261 (AAF_{2D6}= 1.97)	0.57 [0.45]	0.57 [0.89] (AAF_{2D6}= 1.97)	0.301 (48% HepCL)
2D6-NDT	0.080	0.158 (AAF_{2D6}= 1.97)	0.054 [0.45]	0.054 [0.89] (AAF_{2D6}= 1.97)	
2B6-ODT[1]	0.040	0.040 (AAF_{2B6}= 1)	0.018 [0.43]	0.018 [0.43] (AAF_{2B6}= 1)	0.0295 (10% HepCL)
2B6-NDT[1]	0.500	0.500 (AAF_{2B6}= 1)	0.200 [0.43]	0.200 [0.43] (AAF_{2B6}= 1)	

[1] The CYP2B6 ISEF was not measured in these experiments and so (i) the standard Simcyp® ISEF of 0.43 was used, and (ii) the AAF is considered to be 1= no activity adjustment.

Calculation of the AAF and ISEF for CYP3A4 and CYP2D6

CYP3A4 (Midazolam)

1. Calculation of total hepatic CLint from *in vivo* data [15]

$CLint_H$ (mL/min) = 440 mL/min/kg x 70 kg = 30800 mL/min

$CLint_H$ (µL/min/mg MP) = 30800 mL/min / 1718 g / 39.5 MPPGL= **454 µL/min/mg MP**

Via the Simcyp® midazolam compound file (V12.1, PK profiles, n=1000) it was calculated that CYP3A4 is involved for (only) 74% in the above midazolam $CLint_H$. Therefore:

$CLint_{u,invivo,3A4}$ (µL/min/mg MP) = 454 µL/min/mg MP x 0.74 = **336 µL/min/mg MP**

2. Calculation of the AAF for CYP3A4 in pooled HLM

$CLint_{u,invivo,3A4}$ = unbound CYP3A4 CLint calculated from *in vivo* data = 336 µL/min/mg MP

$CLint_{u,HLM,3A4}$ = Batch-specific unbound CLint calculated from HLM midazolam activity (369 µL/min/mg MP)

- $CLint_{HLM,3A4}$ = 358 µL/min/mg MP, determined experimentally, with conditions provided in the materials and methods section
- $Fumic_{MDZ}$ = 0.97 at 0.15 mg MP/mL. This value is derived from the $fumic_{MDZ}$ of 0.83 in the presence of 0.5 mg MP/mL [9] and the formula $fu_2 = [C_2/C_1*((1-fu_1)/fu_1) + 1]^{-1}$, which allows calculation of fumic for different protein concentrations

AAF = $CLint_{u,invivo,3A4}$ / $CLint_{u,HLM,3A4}$ = 336 / 369 = **0.91**

3. Calculation of the ISEF for CYP3A4

$CLint_{u,HLM,3A4}$ = Batch-specific unbound CLint calculated from *in vitro* HLM midazolam activity = 369 µL/min/mg MP

$CLint_{u,rh3A4}$ = Batch-specific unbound CLint calculated from rh3A4 midazolam activity = 11.53 µL/min/pmol rh3A4

$[CYP3A4]_{invivo}$ = CYP3A4 abundance *in vivo* = 137 pmol/mg MP [12]

ISEF = $CLint_{u,HLM,3A4}$ / ($CLint_{u,rh3A4}$ x $[CYP3A4]_{invivo}$) = **0.23**

CYP2D6 (Dextromethorphan)

1. **Calculation of CYP2D6 hepatic CLint from *in vivo* data [16]**

$CLint_{H,2D6}$ (µL/min/g liver) = 3900 µL/min/mL liver / 1.08 mL/g = **3611 µL/min/g liver**

$CLint_{H,2D6}$ (µL/min/mg MP) = 3611 µL/min/g liver / 39.5 MPPGL / 1.56 = **58.60 µL/min/mg MP**

Why division by 1.56?

Dextromethorphan behaves as a lipophilic weak base concerning its distribution at the hepatocellular level. Because the pH in hepatocytes is somewhat lower (pH=7.0 – 7.2) than in plasma (7.4), an ion trapping phenomenon can be observed resulting in higher concentrations of dextromethorphan in the cytosolic space of the hepatocyte than expected [17]. For dextromethorphan, a hepatic uptake factor of 1.56 is considered.

2. **Calculation of the AAF for CYP2D6 in pooled HLM**

$CLint_{u,invivo,2D6}$ = unbound CYP2D6 CLint calculated from *in vivo* data = 58.90 µL/min/mg MP

$CLint_{u,HLM,2D6}$ = Batch-specific unbound CLint calculated from HLM dextromethorphan activity (29.87 µL/min/mg MP)

- $CLint_{HLM,2D6}$ = 29.27 µL/min/mg MP, determined experimentally, with conditions provided in the materials and methods section

- $Fumic_{DEX}$ = 0.98 at 0.3 mg MP/mL. This value is derived from the $fumic_{DEX}$ of 0.96 in the presence of 0.5 mg MP/mL (Witherow & Houston, 1999 JPET) and the formula $fu_2 = [C_2/C_1*((1-fu_1)/fu_1) + 1]^{-1}$, which allows calculation of fumic for different protein concentrations

AAF = $CLint_{u,invivo,2D6}$ / $CLint_{u,HLM,2D6}$ = 58.90 / 29.87 = **1.97**

3. Calculation of the ISEF for CYP2D6

$CLint_{u,HLM,2D6}$ = Batch-specific unbound CLint calculated from HLM dextromethorphan activity = 29.87 µL/min/mg MP

$CLint_{u,rh2D6}$ = Batch-specific unbound CLint calculated from rh2D6 dextromethorphan activity = 4.56 µL/min/pmol rh2D6

$[CYP2D6]_{invivo}$ = CYP2D6 abundance *in vivo* = 8 pmol/mg MP [12]

ISEF = $CLint_{u,HLM,2D6}$ / ($CLint_{u,rh2D6}$ x $[CYP2D6]_{invivo}$) = **0.45**

4

CHAPTER 5

PHYSIOLOGICALLY-BASED PHARMACOKINETIC PREDICTIONS OF TRAMADOL EXPOSURE THROUGHOUT PEDIATRIC LIFE: AN ANALYSIS OF THE DIFFERENT CLEARANCE CONTRIBUTORS WITH EMPHASIS ON CYP2D6 MATURATION

This chapter is based on:

T'jollyn, Huybrecht; Snoeys, Jan; Vermeulen, An; Michelet, Robin; Cuyckens, Filip; Mannens, Geert; Van Peer, Achiel; Annaert, Pieter; Allegaert, Karel; Van Bocxlaer, Jan & Boussery, Koen. Physiologically Based Pharmacokinetic Predictions of Tramadol Exposure Throughout Pediatric Life: an Analysis of the Different Clearance Contributors with Emphasis on CYP2D6 Maturation. *AAPS J*. 2015 Nov; 17(6):1376-87

5

TABLE OF CONTENTS

5

1 ABSTRACT

Background & Objective

This paper focuses on the retrospective evaluation of PBPK techniques used to mechanistically predict clearance throughout pediatric life. The objective was to evaluate the bottom-up predictions of the clearance against top-down clearance predictions in pediatrics, with a focus on neonates and infants.

Methods

An intravenous tramadol retrograde PBPK model was set up in Simcyp® using adult clearance values, qualified for CYP2D6, CYP3A4, CYP2B6, and renal contributions. Subsequently, the model was evaluated for mechanistic prediction of total, CYP2D6-related, and renal clearance predictions in very early life. In 2 *in vitro* pediatric HLM batches (1 and 3 months), O-desmethyltramadol and N-desmethyltramadol formation rates were compared with CYP2D6 and CYP3A4 activity, respectively. Additionally, the clearance maturation of the PBPK model predictions was compared to two *in vivo* maturation models (Hill and exponential) based on plasma concentration data, and to clearance estimations from a WinNonlin® fit of plasma concentration and urinary excretion data.

Results

O-desmethyltramadol formation *in vitro* was mediated only by CYP2D6, while N-desmethyltramadol was mediated in part by CYP3A4. Concerning the bottom-up predictions, in early life maturation of renal and CYP2D6 clearance is captured well in the PBPK model predictions, although CYP2D6 clearance was underpredicted from 2 years of age. The total tramadol clearance is underpredicted over the complete lifespan. The most pronounced underprediction of total and CYP2D6-mediated clearance was observed in the age range of 2-13 years.

Conclusion

In conclusion, the PBPK technique showed to be a powerful mechanistic tool capable of predicting maturation of CYP2D6 and renal tramadol clearance in early infancy, although some underprediction occurs between 2-13 years for total and CYP2D6-mediated tramadol clearance.

5

2 INTRODUCTION

The present study focuses on the mechanistic prediction of tramadol clearance over the pediatric lifespan, since this parameter drives the total exposure to the drug and is key in titrating to the right drug dosage. Physiologically-based pharmacokinetic (PBPK) modeling enables pediatric pharmacological research to proceed to the next level, by guiding dose finding studies and the formulation design for the different stages in pediatric life [1-4]. The stronghold of PBPK models is that they separate intrinsic from extrinsic patient factors i.e., drug-independent (system) factors versus drug-dependent factors and study design, so that a physiologically plausible generic human model structure can be applied for any drug under various study conditions [3, 5]. In addition, a PBPK model, which incorporates demographical, physiological, and biochemical data elements, can be adjusted depending on a specific subpopulation of interest in order to make mechanistic PK predictions. In pediatrics, these models account for the ontogeny of different enzymes, changing tissue volumes and composition, as well as blood flows to these organs [6]. At this time, research into the ontogeny of transporters [7, 8] lags behind that of hepatic enzymes.

Tramadol is a centrally acting analgesic drug mediating its effect through noradrenaline re-uptake inhibition, increased release of serotonin, and decreased re-uptake of serotonin in the spinal cord. Although in healthy volunteers tramadol is excreted unchanged in urine for about 25%, the greater part is metabolized [9]. Tramadol is oxidized to an active metabolite O-desmethyltramadol (ODT) via CYP2D6, having a μ-opioid activity 300 times that of the parent drug. Additionally, tramadol is inactivated to N-desmethyltramadol (NDT) by CYP3A4 and CYP2B6. Secondary metabolism involves further oxidation and phase 2 conjugative reactions [10]. In early life, however, these primary metabolic pathways mature differently, and as a consequence not only the absolute value of the clearance but also relative contributions of the different eliminating pathways may change over time. Therefore, tramadol serves as a model drug in our PBPK study to evaluate whether maturation of the clearance is adequately predicted over the pediatric lifespan. In order to make mechanistically sound pediatric tramadol exposure predictions, different elimination pathways in the tramadol clearance should first be validated in an adult PBPK model previous to predicting pediatric exposure [11]. In the application of this methodology these limitations/assumptions should be considered: (i) clearance pathways in children are the same as those observed in adults, (ii) enzyme kinetics of metabolic contributors are first order, (iii) clearance models are perfusion limited (well-stirred), and (i.v.) no transporters are involved for which ontogeny information is unknown. These assumptions should always be checked since they are key in the mechanistic prediction of pediatric PK from adult data. Violation of these assumptions may result in clearance under- or overprediction if the clearance pathways differ between children and adults [12], if enzyme processes become saturated or enzyme affinities decrease (e.g. due to the

presence of free fatty acids or bilirubin), and if liver/kidney perfusion is altered (e.g. in the case of cirrhosis). Neglecting important transporter involvements might substantially over- or underpredict the clearance, depending on the specific transport mechanism at hand [13]. In the case of tramadol, although no OCT1-transport is involved [14], a minor contribution of proton dependent efflux pumps could not be ruled out [15].

In this work, first, an adequate intravenous adult PBPK model was set up in the Simcyp Simulator that accurately describes the total adult clearance, as well as the different CYP contributions (CYP2D6, CYP2B6, CYP3A4), and the renal elimination part, composing this clearance. Second, system specific parameters were adjusted to represent the physiological and biochemical changes occurring during childhood. The mechanistic prediction of the formation clearance to ODT and NDT in pediatrics has to take into account (i) ontogenic profiles of the CYP isoforms 2D6, 3A4, and 2B6 [16], as well as changes in (ii) amount of microsomal proteins per gram of liver, (iii) liver size, (iv) liver blood flow, and (v) plasma protein binding [17, 18]. Third, on the one hand, CYP maturation functions for CYP2D6 [17] and CYP3A4 [18] were compared to experimentally determined human liver microsomal (HLM) activities of tramadol (together with the activity of CYP-specific probe substrates dextromethorphan (DEX for CYP2D6) and midazolam (MDZ for CYP3A4)) in two pediatric batches of 1 and 3 months of age. On the other hand, the pediatric PBPK *in vivo* clearance predictions were compared to popPK-derived maturation functions [19, 20].

5

3 MATERIALS AND METHODS

3.1 CHEMICALS AND REAGENTS

All chemicals and reagents used were of the highest available grade: Na_2HPO_4, KH_2PO_4, KCl, $MgCl_2$, NADP, HCl (Merck, Darmstadt, Germany), glucose-6-phosphate, glucose-6-phosphate dehydrogenase (Roche Diagnostics GmbH, Mannheim, Germany), tramadol, midazolam (MDZ), dextromethorphan (DEX), O-desmethyltramadol (ODT), N,O-didesmethyltramadol (NODT), 1-OH midazolam, dextrorphan, O-desmethyltramadol-D6, and deuterated 1-OH midazolam (TRC inc, Toronto, Canada), N-desmethyltramadol (NDT) (LGC GmbH, Luckenwalde, Germany), chlorpropamide (Sigma Aldrich, St. Louis, USA).

3.2 ADULT VS PEDIATRIC *IN VITRO* METABOLISM OF TRAMADOL AND PROBE SUBSTRATES MDZ AND DEX

3.2.1 TRAMADOL HLM INCUBATION CONDITIONS

One pooled adult batch and two pediatric human liver microsomal (HLM) batches (BD Biosciences, Woburn, USA) were used in this study, collected from children aged 1 (male, Caucasian, head trauma) and 3 months (male, Hispanic, anoxia), and stored at -80°C in an Ultra Freezer (New Brunswick scientific, Rotselaar, Belgium). Incubation mixtures (total volume 600 µL) consisted of 297 µL microsomal protein, 3 µL of a tramadol dissolved in MeOH, and 300 µL cofactor mix containing an NADPH-regenerating system consisting of 1 mg of glucose-6-phosphate, 0.50 units of glucose-6-phosphate dehydrogenase, 0.25 mg of NADP and 1 mg of $MgCl_2.6H_2O$ in 1 mL of 0.5 M Na,K-phosphate buffer pH 7.4. A preincubation with cofactor mix was done for 5 minutes in a shaking water bath at 37°C (100 oscillations/min) (Thermo, Waltham, USA). Incubations were started by adding 3 µL of a substrate solution, and stopped by transferring 100 µL aliquots into 96-well plates containing 10 µL ice-cold 4N HCl and 10 µL of internal standard (O-desmethyltramadol-D6, 6 ng/mL).

Linearity of tramadol metabolite formation was assessed as a function of time and protein concentration at the lowest *in vitro* substrate concentration in the adult HLM batch. The formation rate was linear up to 10 min and 1 mg protein/mL (data not shown). The enzyme kinetic parameters of tramadol in pediatric HLM were assessed by using a range of incubation concentrations (0.5, 1, 5, 20, 50, 100, 150, 250, 300 and 500 µM). For each substrate and protein concentration level, samples were incubated in duplicate or triplicate and boiled control incubates were run in parallel to correct for non-enzymatic degradation. 96-well plates were then stored at -20°C awaiting to be analyzed by UPLC-MS/MS.

3.2.2 MDZ AND DEX HLM INCUBATION CONDITIONS

MDZ/DEX incubation materials and methods were essentially the same as those for the tramadol metabolism assays. The incubation mixture consisted of 120 µL diluted microsomes, 100 µL cofactor mix for NADPH regeneration system, and 5 µL test compound. After a preincubation period of 5 min at 37°C and 100 oscillations/min, NADP was added to the preincubation mixture to a final volume of 250 µL to initiate the reaction. Midazolam was incubated at 0.2 µM and 0.05 mg protein/mL. The reaction was stopped after 10 min with 250 µL DMSO containing deuterated 1-OH midazolam as the internal standard (0.1 µg/mL). Dextromethorphan was incubated at 0.5 µM and 0.3 mg protein/mL. The reaction was stopped after 10 min with 250 µL DMSO containing chlorpropamide as the internal standard (0.22 µg/mL). Samples were centrifuged for 10 min at 1711g and the supernatans introduced to the UPLC-MS system. The intrinsic clearance was calculated in the Enzyme Kinetics module of Sigma Plot.

3.2.3 BIOANALYSIS

Tramadol's main metabolites O-desmethyltramadol (ODT, M1), N-desmethyltramadol (NDT, M2), and N,O-didesmethyltramadol (NODT, M5) were quantified by a sensitive UPLC-MS/MS method. A Nexera UHPLC system (Shimadzu, Kyoto, Japan) was coupled to an API 4000 QTRAP (AB Sciex, Toronto, Canada) equipped with a Turbo V^{TM} ion source in ESI+ mode. For the chromatographic separation, a gradient was run - with solvents A (0.025M ammonium acetate, pH 8.5) and B (acetonitrile:methanol 80:20, v/v) - from 5% to 50% B in 3 min, to 100% B in an immediate step gradient, held for 0.3 min, and back to 5% B, allowing 2 min re-equilibration, at a flow rate of 0.6 mL/min. The column was an Acquity UPLC BEH C18 (1.7µm) 50 x 2.1 mm column (Waters, Milford, USA), maintained at 60°C. More details about this method were published earlier by our group in T'jollyn et al., 2015 [16] and are described in Chapter 3, hence they will not be repeated here.

The MDZ metabolite, 1-OH midazolam, was analyzed using a Waters Acquity UPLC system coupled to a Thermo LTQ mass spectrometer (Thermo Fisher Scientific, San Jose, U.S.) in APCI +. The column was an Acquity UPLC BEH C18 (1.7µm) 50 x 2.1 mm held at 60°C with mobile phase constituents 0.1% HCOOH in ULC water and 0.1% HCOOH in CH_3CN in a linear gradient. Run time was 3 min and flow rate 0.6 mL/min. Mass transitions for 1-OH midazolam and deuterated 1-OH midazolam (internal standard) using a collision energy (CE) of 30 eV were 342>325, and 346>328, respectively. Calibration curves were always made in the same microsomal matrix as the incubates using at least 8 calibrator levels and 3 QC levels for the calibration curve. The DEX metabolite, dextrorphan, was analyzed using a Waters Acquity UPLC system coupled to a Micromass Quattro Ultima triple quadrupole, operating in ESI +. The column was an Acquity UPLC BEH C18 (1.7µm) 50 x 2.1 mm at 35°C with mobile phase constituents 0.1% HCOOH in ULC water and 0.1% HCOOH in CH_3CN in a linear gradient. Run time was 5.25 min and flow rate 0.4

mL/min. Mass transitions for dextrorphan and chlorpropamide using a CE of 28 and 25 eV were 258>157, and 277>275 [21], respectively.

3.2.4 Enzyme kinetic data analysis

Concentrations of metabolites in the incubation samples were corrected for protein concentration (mg microsomal protein/mL), reaction time (min), and initial substrate concentration (µM) in order to calculate the apparent *in vitro* clearance (CL_{app}) for every metabolite. For tramadol, CL_{app} was plotted vs. tramadol incubation concentration and a nonlinear model –with the model structure provided in equation 1- was fitted to the data, using R v3.1.1 [22]. Models were evaluated by visually inspecting residual plots for bias. In equation 1, CL_{app} is the apparent *in vitro* clearance, v_o is the initial rate of metabolite formation in the incubate, *[S]* is the tramadol concentration (µM), *Km is* the Michaelis-Menten constant (µM) and *Vmax* the maximum velocity. This equation allowed estimation of the parameters Km and Vmax, and hence the calculation of CLint. An unbound fraction in microsomes (fu_{mic}) of ~0.96 was estimated *in silico* using the prediction toolbox in Simcyp® v13 [23].

$$CL_{app} = \frac{v_o}{[S]} = \frac{Vmax}{Km + [S]}$$

EQUATION 1

3.3 Development of the adult tramadol PBPK model

An intravenous adult PBPK model was set up, using the retrograde calculator available in the Simcyp® Simulator (v13, Sheffield, UK), by extracting *in vivo* hepatic and renal clearance values from publications available in the scientific literature [24-28]. In this retrograde calculator, hepatic intrinsic clearances per CYP isoform are calculated, based on hepatic plasma clearance and apparent *in vivo* CYP contributions, using the well-stirred liver model [29, 30]. Table A1 with final numerical values for different parameters is provided in the supplementary data. Following approaches were used to define the contribution of CYP2D6, CYP2B6 and CYP3A4 in the adult hepatic clearance of tramadol.

3.3.1 CYP2D6 contribution

The CYP2D6 contribution in the tramadol hepatic clearance was assessed by comparing the hepatic clearance increase between poor and extensive metabolizers in observations and predictions. Observations were extracted from a study conducted by Pedersen et al. [31]. Patients from this study were genotyped as *1/*1 (EM; n=8) and *4/*4 (n=7) or *4/*6 (PM) (n=1). By taking into account the actual age range, administered dose, and proportion of males and females in the PBPK trial design, we mimicked the actual clinical trial in our predictions. Virtual populations are generated in the Simcyp®

Simulator by using a correlated Monte Carlo approach. For a more detailed description, we redirect the interest reader to Jamei et al, 2009[32].

3.3.2 CYP2B6-CYP3A4 CONTRIBUTION

Although CYP2B6 seems to be a minor contributor to the total clearance, the CYP2B6 contribution apart from the CYP3A4 involvement was assessed by performing a tramadol-rifampicin drug-drug interaction (DDI) simulation and by comparison of predicted with observed AUCs. Using information of the study population and design by Saarikoski, et al. [33], 100 virtual trials were simulated with 12 subjects each receiving six doses of 600 mg oral rifampicin (RIF) every 24h were simulated. Twelve hours after the last rifampicin dose, 50 mg tramadol was administered and the change in AUC reported. Subjects ranged from 18 to 30 years of age and the female proportion was set to 0.42. Drug-specific parameters for rifampicin (elimination and induction effects on CYP2B6 and CYP3A4), described elsewhere [34], were used in this simulation. While keeping the CYP2D6 contribution in the tramadol adult PBPK model fixed, the CYP2B6 contribution was increased from 0 to 30% while the CYP3A4 contribution was (in parallel) decreased from 52 to 22%. The sum of the contributions of CYP2D6 and CYP2B6-3A4 always added up to 100% of the hepatic intrinsic clearance. Results for the 100 simulated trials were expressed as the geometric mean ratio of the $AUC_{control}/AUC_{induced}$ and were compared to the observed geometric mean ratio from the actual *in vivo* DDI study [33].

3.4 PREDICTION OF PEDIATRIC CLEARANCE WITH THE DEVELOPED TRAMADOL PBPK MODEL

The developed PBPK model was used to predict the clearance (total, CYP2D6, and renal component) over the pediatric lifespan, using the pediatric module of the Simcyp® Simulator. This module contains ontogeny information for the different CYP enzymes considered in this work (CYP2D6 and CY2B6 ontogeny functions are described by Johnson et al. in [17], whereas CYP3A4 ontogeny information is described by Salem et al. in [35]). Additionally, the changes in tissue volumes (i.e. liver, kidney), tissue composition (lipids vs. water content), and blood flows (i.e. Q_H, GFR), also described in [17], all vary as a function of age and determine the extent of the clearance in a specific pediatric subject.

3.5 MODEL EVALUATION

On the *in vitro* level, theoretical CYP maturation functions for CYP2D6 [17] and CYP3A4 [18] were compared to experimentally determined human liver microsomal (HLM) activities of tramadol (together with the activity of CYP-specific probe substrates dextromethorphan (DEX for CYP2D6) and midazolam (MDZ for CYP3A4)) in two pediatric batches of 1 and 3 months of age. On the *in vivo* level, pediatric PBPK model predictions (from a full term 40 weeks PMA onwards) were visually compared to *in vivo* clearance

maturation models, in terms of total, CYP2D6, and renal tramadol clearance, published in literature and described in more detail in the previous section “Available pediatric *in vivo* reference data”.

3.6 AVAILABLE PEDIATRIC *IN VIVO* REFERENCE DATA

Clearance maturation parameter estimates were collected from publications in the scientific literature [19, 20]. The overall maturation function (maturation + size function) was applied to predict individual clearance values for extensive CYP2D6 metabolizers only, given the subjects’ age (post-menstrual age; PMA) and weight (kg). Besides, the raw clinical data of a subset of 57 neonates and young infants, used for estimating total, CYP2D6 and renal clearance parameters, were available.

3.6.1 EXPONENTIAL MATURATION FUNCTION

The first published maturation function for total and CYP2D6 mediated tramadol clearance originates from a publication by Allegaert et al.[20]. This resulting maturation curve for the total clearance is obtained by summation of ‘CYP2D6’ and ‘non-CYP2D6’ clearance maturation, both taking on following form:

$$CL_i = CL_{std} * Fsize * \exp\{SLPCL * (PMA - 40)\}$$

EQUATION 2

in which *CLstd* is the standardized clearance, *Fsize* is the factor taking into account the size effect (WTi/WTstd)**0.75, *SLPCL* (slope of clearance) is the exponent of the maturation function centered around a term age of 40 weeks PMA. Numerical values for these parameters are provided in Table A2 in the *Appendix*.

3.6.2 HILL MATURATION FUNCTION

The second maturation function was derived from a pooled popPK analysis [19] in pediatric and adult subjects in which the maturation of ‘CYP2D6’ and ‘non-CYP2D6’ tramadol clearance was described by a Hill function, as follows:

$$CL_i = CL_{std} * Fsize * \frac{1}{1 + \frac{PMA}{TM50}^{-Hill}}$$

EQUATION 3

in which *TM50* is the age (PMA) at 50% of maturation, and *Hill* is the Hill coefficient describing the steepness of the maturation function. Numerical values for these parameters are provided in Table A2 in the *Appendix*. Both modelling attempts assume a 2-compartmental, linear disposition model for tramadol with 1st order elimination, consisting of different clearance pathways, based on plasma observations of parent tramadol and ODT metabolite. The major difference between these 2 models lies in how the PK of the metabolite is described. In the first model, the metabolite volume is fixed to 224 L/70kg and metabolite clearance is estimated to exponentially increase with PMA [20]. In the second model, the metabolite volume is estimated by applying allometric principles to an observed metabolite volume in dogs. Metabolite clearance is fixed by a Hill function assuming a maturation of the glomerular filtration rate [19].

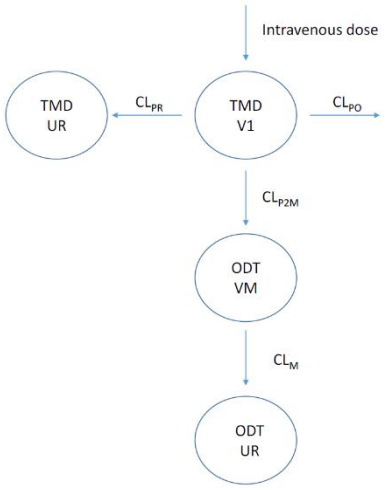

FIGURE 1: A ONE-COMPARTMENT LINEAR DISPOSITION MODEL WAS USED TO FIT THE PARENT DRUG. AN ADDITIONAL COMPARTMENT FOR THE ODT METABOLITE WAS LINKED TO THE CENTRAL COMPARTMENT BY ITS FORMATION CLEARANCE (CL_{P2M}). URINARY EXCRETION OF TRAMADOL (CL_{PR}) WAS ESTIMATED BASED ON THE TOTAL AMOUNT OF TRAMADOL FOUND IN URINE (UR). ODT MOIETY-RELATED CLEARANCE (CL_M) AND VOLUME (V_M) WERE ESTIMATED BASED ON THE ODT PLASMA CONCENTRATIONS AND TOTAL ODT AMOUNT FOUND IN URINE (UR); CL_{PO} OTHER CLEARANCE PARENT

3.6.3 WinNonlin® fitting of subjects with rich sampling

In addition to the previously described popPK models, which are solely based on plasma observations, we performed a one-by-one fitting procedure in WinNonlin®, taking into account not only plasma observations but also urinary excretion data of parent and metabolite [36]. These were available for 9 out of 57 neonates and young infants from the original dataset, which were richly sampled. The compartmental model depicted in Figure 1 was used to estimate the different clearance parameters. Pharmacokinetic analysis for the one-by-one fitting was performed by WinNonlin® Professional version 5.2.1. (Pharsight, St-Louis, MI, USA). Plasma and urinary concentrations of parent and metabolite were simultaneously modeled, applying a user-written differential equation model. Both plasma and urine

concentrations were modeled using the 1/Y weight, and the Gauss-Newton (Levenberg and Hartley) algorithm with 50 iterations. A 1-compartment model for tramadol was retained on the basis of visual inspection of the fitted plasma concentration-time profiles and standard errors of the estimated PK parameters. Tramadol was cleared by renal excretion (CL_{PR}), CYP2D6 clearance (CL_{P2M}), and other clearance routes (CL_{PO}). For the CYP2D6 metabolite, ODT, a 1-compartment model was used with formation clearance (CL_{P2M}), ODT moiety-related clearance (CL_M) and volume (V_M). The metabolite clearance (CLM) is a hybrid clearance parameter describing the total mass outflux of ODT, since ODT concentrations measured in urine are the sum of unchanged as well as conjugated ODT [36].

4 RESULTS

4.1 QUALIFICATION OF TRAMADOL ADULT PBPK MODEL

By scaling back intravenous tramadol *in vivo* adult clearance data, the tramadol adult PBPK model is provided with information on the CYP2D6 involvement by comparing hepatic clearances between different CYP2D6 metabolizer statuses [31], and the CYP2B6-CYP3A4 involvement by comparing AUC ratios after induction of tramadol metabolism by rifampicin [33] (Table 1). CYP2D6 was calculated to be involved for 48% in the hepatic clearance, based on an *in vivo* observed 1.74-fold hepatic clearance increase from CYP2D6 poor metabolizer (PM, no remaining CYP2D6 activity) to extensive metabolizers (EM). The DDI clinical trial simulation of tramadol and rifampicin was used to calculate the relative CYP2B6-3A4 involvement. The observed geometric mean AUC ratio (induced/control) fell within the 90% confidence interval around the predicted geometric mean AUC ratio, based on 100 virtual trials mimicking the actual *in vivo* trial (Figure 2), only if the CYP2B6 contribution in the hepatic intrinsic clearance was less than 10% and the CYP3A4 contribution not below 42%. Therefore, the percentage CYP2B6 involvement in hepatic tramadol metabolism was estimated to be not more than 10%. As a consequence, the CYP3A4 contribution was estimated to constitute between 42 and 52% of tramadol hepatic metabolism (Table 1).

TABLE 1: CRITERIA BY WHICH CYP CONTRIBUTIONS IN THE RETROGRADE MODEL ARE ASSESSED. CYP2D6 INVOLVEMENT WAS ESTIMATED BY COMPARING HEPATIC CLEARANCE FOLD INCREASE FROM PM TO EM BETWEEN PREDICTIONS AND *IN VIVO*. CYP2B6-CYP3A4 INVOLVEMENT WAS ESTIMATED BY COMPARING $AUC_{INDUCED}/AUC_{CONTROL}$ RATIOS BETWEEN PREDICTIONS AND OBSERVATIONS.

PM/EM= POOR OR EXTENSIVE METABOLIZER; RG= RETROGRADE; DDI= DRUG-DRUG INTERACTION

The retrograde model for CYP involvement in tramadol metabolism				
	criterion	*in vivo observation*	*RG PBPK model prediction*	*% involvement in Hep CL*
CYP2D6	Hepatic CL fold increase from PM to EM	1.74 [a]	1.73	48% CYP2D6
CYP2B6 ***CYP3A4***	$AUC_{Ind}/AUC_{control}$ in Rifampicin-Tramadol DDI clinical trial simulation	0.58 [b]	0.61->0.62	0->10% CYP2B6 52->42% CYP3A4

[a] [31]; [b] [33]

5

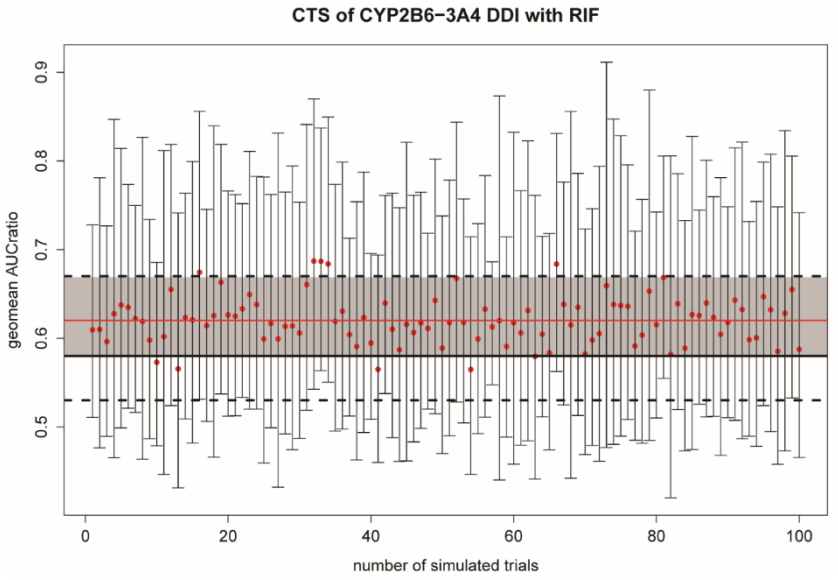

FIGURE 2: DDI CLINICAL TRIAL SIMULATION OF TRAMADOL AND RIFAMPICIN TO ASSESS THE CYP2B6-3A4 CONTRIBUTION. THE FIGURE DEPICTS THE RESULTS OF 100 TRIAL SIMULATIONS MIMICKING THE ORIGINAL TRIAL, WHEN CYP2B6-3A4 CONTRIBUTIONS ARE ASSUMED TO BE 10-42%, RESPECTIVELY. BLACK HORIZONTAL LINES REPRESENT THE *IN VIVO* OBSERVED RATIO OF AUC GEO MEANS (SOLID) AND 90% CONFIDENCE LIMITS (DASHED). THE SOLID RED LINE REPRESENTS THE AVERAGE RATIO OF SIMULATED AUC GEO MEANS. SINCE THE SOLID BLACK LINE STILL IS IN THE 90% CONFIDENCE REGION (GREYED AREA) OF THE SIMULATED RATIO, WE ASSUME THAT CYP2B6 CONTRIBUTION SHOULD BE BETWEEN 0 AND 10%.

4.2 ADULT VS PEDIATRIC *IN VITRO* METABOLISM OF TRAMADOL AND PROBE SUBSTRATES MDZ AND DEX

The *in vitro* metabolism of tramadol to its 2 primary metabolites (ODT and NDT) is displayed for pediatric HLM batches of 1 and 3 months of age in figures S1 and S2, respectively, provided in the *Appendix*. *In vitro* clearance values were modelled versus the tramadol incubation concentration. Additionally, fractional activities were measured in both pediatric HLM batches versus the adult HLM pool for tramadol's primary metabolites, as well as for the probe substrates dextromethorphan (DEX) and midazolam (MDZ), providing information about the activity of CYP2D6 and CYP3A4 in these batches, respectively. Fractional activities for either ODT/NDT, DEX, or MDZ (Table 2) were calculated as the ratio of their intrinsic clearances, i.e. $CLint_{pedHLM}/CLint_{adultHLM}$.

TABLE 2: FRACTIONAL ACTIVITIES OF PEDIATRIC TRAMADOL METABOLISM (RELATIVE TO ADULT ACTIVITY) FOR THE FORMATION OF ODT AND NDT ARE PROVIDED, TOGETHER WITH THOSE FOR THE PROBE SUBSTRATES DEX AND MDZ REPRESENTATIVE OF CYP2D6 AND CYP3A4 ACTIVITY, RESPECTIVELY.

	Fractional activity of tramadol to ODT / NDT	Fractional activity of DEX	Fractional activity of MDZ
1 month	1.61 / 0.21	1.59	0.25
3 months	1.91 / 0.14	1.71	0.05

The lines in Figure 3, panel A display the 'assumed' or 'theoretical' maturation of CYP2D6 [17] and CYP3A4 [18] on the per mg microsomal protein level, expressed as fractional activity relative to adult up to 1 year of age, whereas the points display *in vitro* measured fractional activities for the two pediatric batches, which are also displayed in Table 2. These values represent measured fractional activities of the pediatric intrinsic clearance relative to the measured adult intrinsic clearance for tramadol, midazolam (MDZ), and dextromethorphan (DEX). MDZ and DEX were included as probe substrates in the *in vitro* HLM batches in order to correct for batch-specific activities of CYP3A4 and CYP2D6, respectively. Fractional activity of ODT formation in the pediatric batches is 1.6 and 1.9-fold higher than in the pooled adult HLM batch, for 1 month and 3 months of age, respectively. This is highly analogous to the fractional activity of DEX for the 2 pediatric batches, being 1.6- and 1.7-fold higher (Table 2). Correction of the measured batch-specific fractional activities for ODT and NDT formation with the theoretical fractional activities of DEX and MDZ, denoted by equation 4, can be found in Figure 3, panel B. Because the corrected fractional activity of ODT formation for both batches ("corrODT 1M" and "corrODT 3M") strictly follows the maturation profile of CYP2D6, ODT formation is highly correlated with CYP2D6 maturation.

$$corrODT = \frac{fractODTi}{d(fractDEX_i - theorDEX_i)}$$

EQUATION 4

in which *corrODT* is the fractional activity of ODT formation corrected by the batch-specific fractional activity of DEX at a given age *i*, *fractODT* is the fractional activity of ODT formation for a given age *i*, *d(fractDEX-theorDEX)* is the distance from the measured fractional activity of DEX to the theoretical maturation of DEX at a given age *i* (i.e.1 and 3 months). (analogous for NDT)

Tramadol's NDT formation was not well correlated with MDZ metabolism, as the NDT formation corrected by the batch-specific CYP3A4 activity for the 3 months batch is not following the maturation profile in Figure 3, panel B.

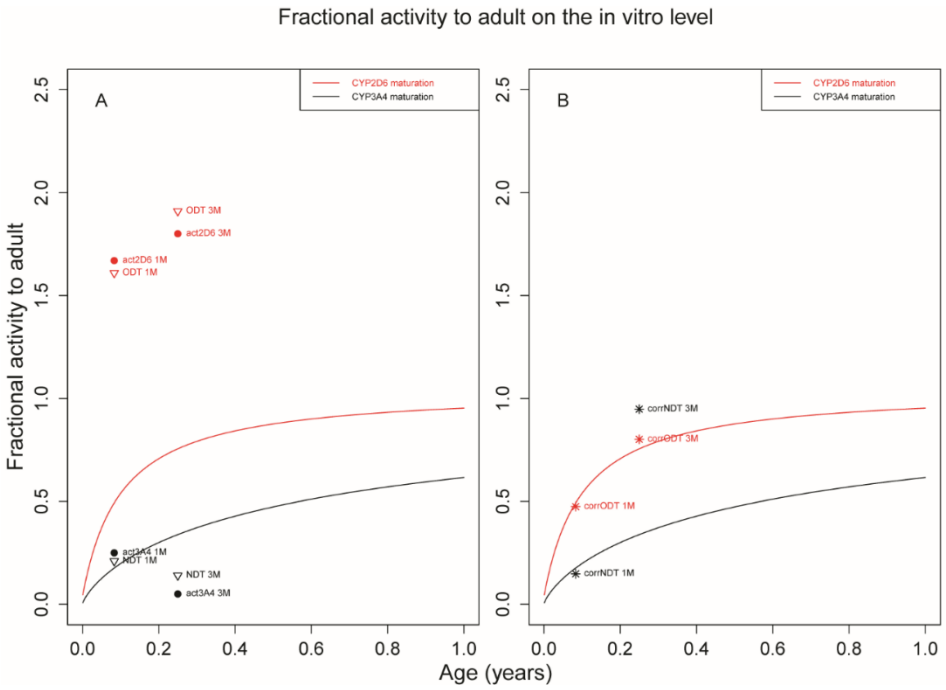

FIGURE 3: THEORETICAL MATURATION OF CYP2D6 (17) (RED LINE) AND CYP3A4 (18) (BLACK LINE) EXPRESSED AS FRACTIONAL ACTIVITY VS. AGE. IN THE LEFT PLOT ODT/NDT ACTIVITY (SOLID DOTS) FOR 2 PEDIATRIC HLM BATCHES (1 AND 3 MONTHS) ARE DEPICTED TOGETHER WITH THE ACTIVITIY OF PROBES (OPEN TRIANGLES) DEX (ACT2D6) AND MDZ (ACT3A4). IN THE RIGHT PLOT, THE RATIO OF EACH CORRESPONDING PAIR IS TAKEN AS DESCRIBED IN THE BODY TEXT AND INDICATED AS CORRODT AND CORRNDT. ODT FORMATION FOLLOWS THE CYP2D6 MATURATION PROFILE, WHILE NDT FORMATION DOES NOT FOLLOW THE CYP3A4 MATURATION PROFILE.

4.3 COMPARISON OF PEDIATRIC PBPK PREDICTIONS WITH PEDIATRIC *IN VIVO* REFERENCE DATA

Pediatric PBPK predictions of total tramadol clearances were compared to tramadol clearances derived using 2 published maturation models (exponential and Hill-type), as well as from a WinNonlin® fit incorporating urine observations. Figure 4 displays the total tramadol clearance as a function of PMA (left) and body weight (right). The Hill and exponential model are depicted by a solid black and red line, respectively, while the WinNonlin® fit is illustrated as light brown points together with their smoother function. Dark blue points are the mechanistic pediatric PBPK predictions of the total tramadol clearance. An underprediction of the PBPK predicted total tramadol clearance is apparent from both plots (i.e. as a function of PMA or weight) when comparing with any of the *in vivo* maturation models.

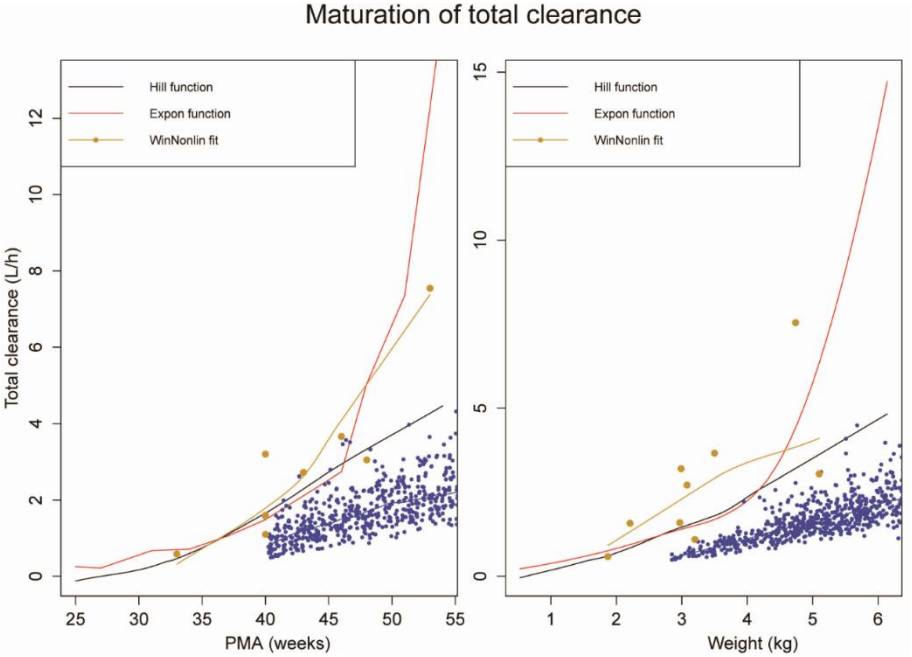

FIGURE 4: MATURATION OF TOTAL TRAMADOL CLEARANCE AS A FUNCTION OF PMA (LEFT) AND BODY WEIGHT (RIGHT). PBPK PREDICTIONS, REPRESENTED AS BLUE DOTS, ARE COMPARED TO *IN VIVO* MATURATION FUNCTIONS: HILL MODEL [19] (BLACK), EXPONENTIAL MODEL [20] (RED), AND WINNONLIN FITS (LIGHT BROWN).

Figure 5 displays the maturation of tramadol clearance mediated by CYP2D6 as a function of PMA (left) and bodyweight (right). Noticeable from these plots is that PBPK predictions of tramadol CYP2D6 clearance are in line with the Hill model (black line) and the WinNonlin® fits, but not with the exponential maturation model.

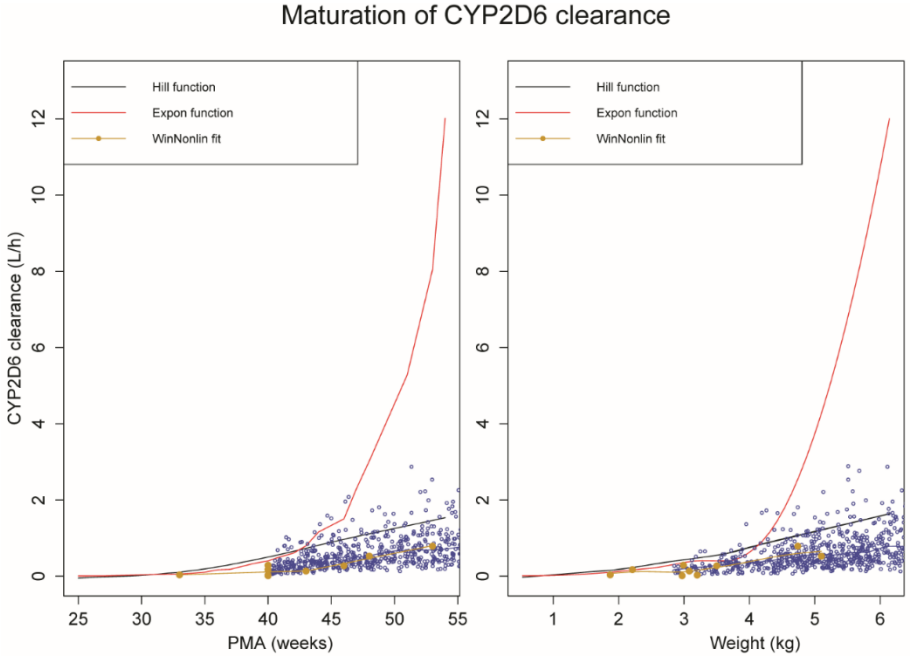

FIGURE 5: MATURATION OF CYP2D6 TRAMADOL CLEARANCE AS A FUNCTION OF PMA (LEFT) AND BODY WEIGHT (RIGHT). PBPK PREDICTIONS, REPRESENTED AS BLUE DOTS, ARE COMPARED TO *IN VIVO* MATURATION FUNCTIONS: HILL MODEL (19) (BLACK), EXPONENTIAL MODEL (20) (RED), AND WINNONLIN FITS (LIGHT BROWN).

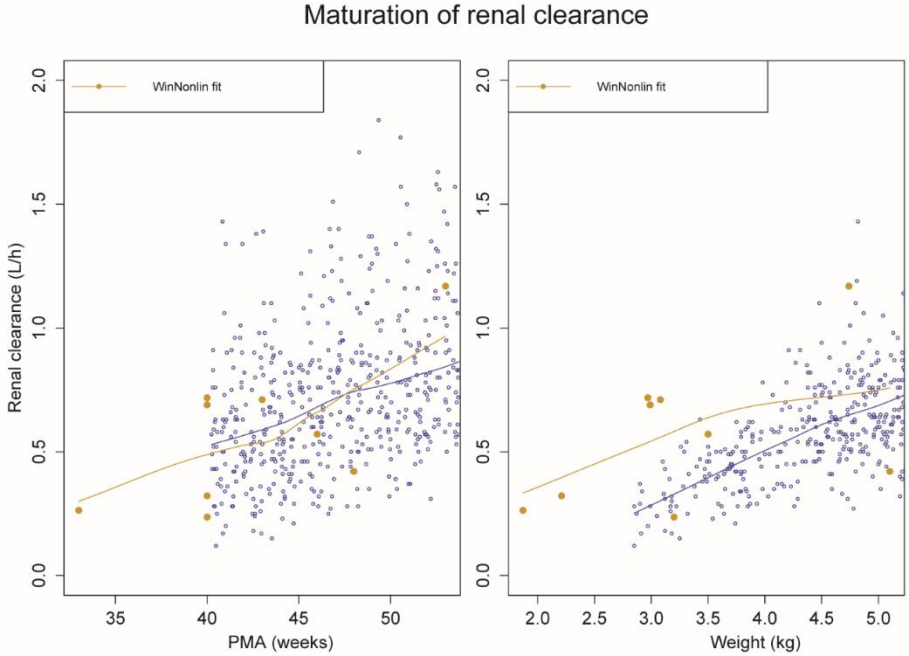

FIGURE 6: MATURATION OF RENAL TRAMADOL CLEARANCE AS A FUNCTION OF PMA (LEFT) AND BODY WEIGHT (RIGHT). PBPK PREDICTIONS, REPRESENTED AS BLUE DOTS, ARE COMPARED TO WINNONLIN FITS (LIGHT BROWN).

Figure 6 depicts the maturation of renal clearance (as a function of PMA and bodyweight) and enables comparison of PBPK predicted renal clearance and *in vivo* observed renal clearance. *In vivo* estimates for the renal clearance of unchanged tramadol are only available from the WinNonlin® fits because only in this modeling approach, urinary data was considered. PBPK predicted renal clearance is very analogous to the *in vivo* estimates.

Finally, figures 7 and 8 display the complete age span from 40 to 1300 weeks PMA (25 years) for the total and CYP2D6 clearance maturation, comparing PBPK predictions (blue dots) and Hill function predictions (red dots). Tramadol clearance is underpredicted over the complete pediatric life span. CYP2D6 clearance predictions are in line with *in vivo* observations in very early life (40-53 weeks PMA, Figure 8), but start to deviate from the *in vivo* maturation trend from 53 weeks PMA (1 year) onwards until 700 weeks PMA (13 years). For adults, predictions are again in line with *in vivo*.

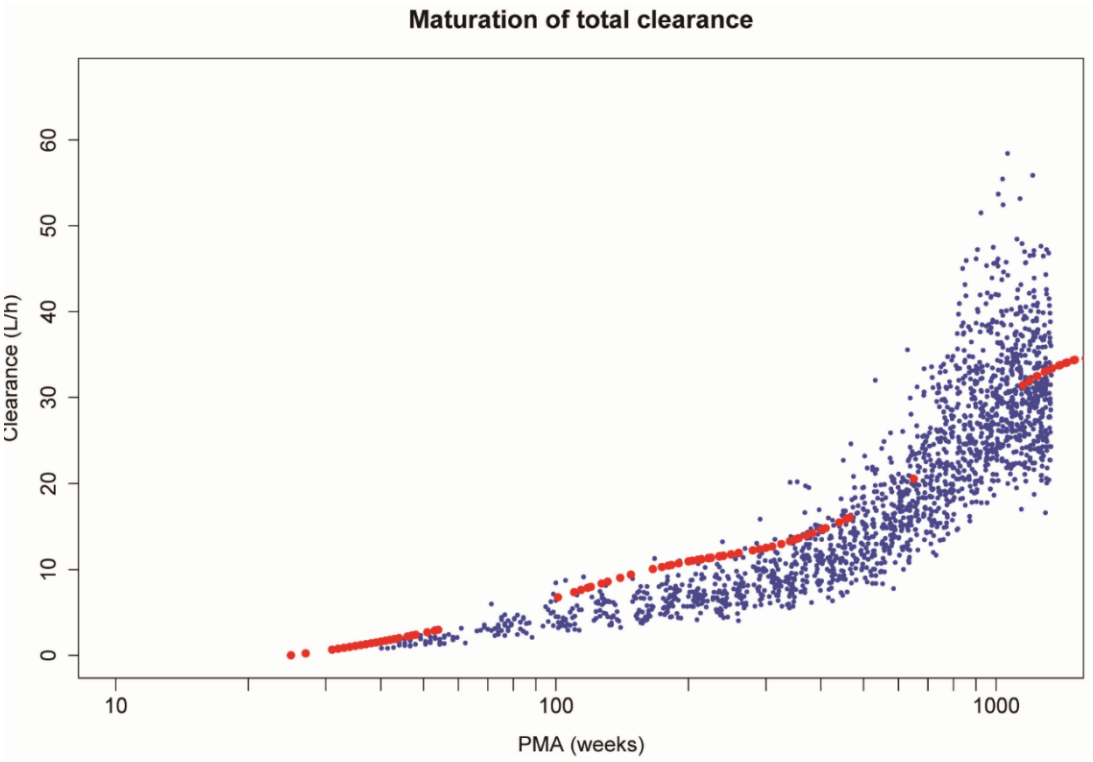

FIGURE 7: MATURATION OF TOTAL TRAMADOL CLEARANCE AS A FUNCTION OF PMA. COMPARING THE PBPK PREDICTIONS (BLUE DOTS) TO THE *IN VIVO* HILL MATURATION FUNCTION (RED DOTS) REVEALS THAT THE LARGEST UNDERPREDICTION IN TOTAL CLEARANCE IS MANIFESTED BETWEEN 2-13 YEARS (100-650 WEEKS) OF AGE

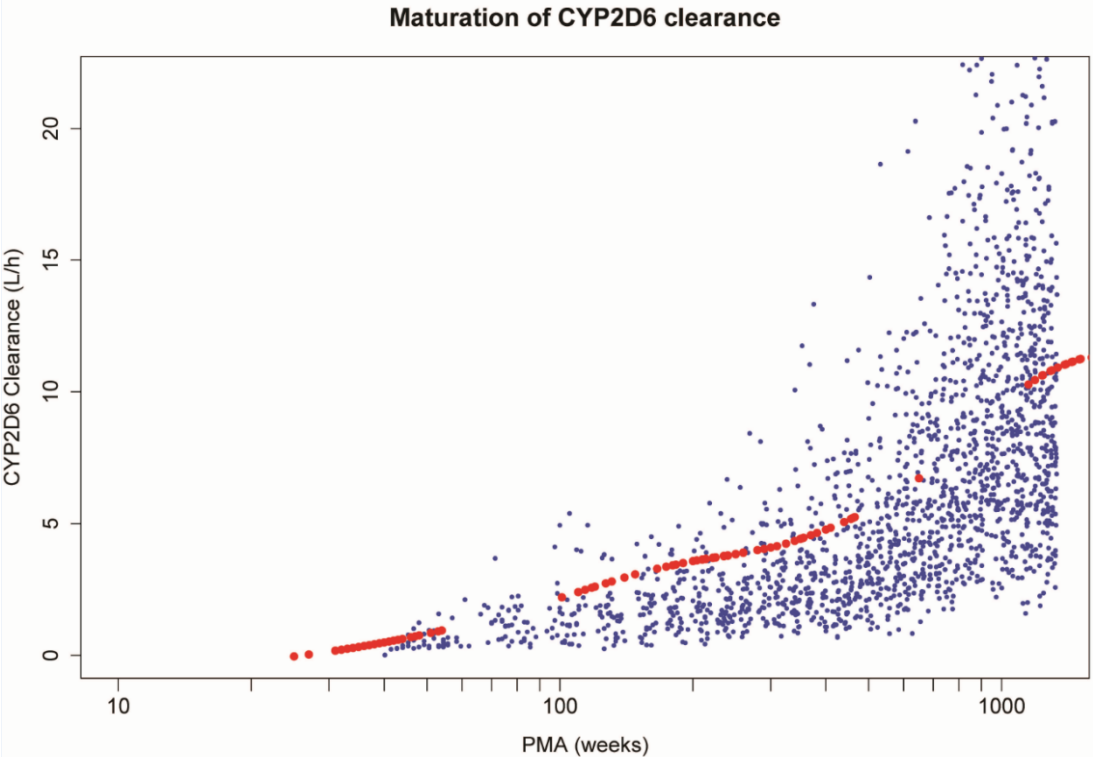

FIGURE 8: MATURATION OF CYP2D6 TRAMADOL CLEARANCE AS A FUNCTION OF PMA. COMPARING THE PBPK PREDICTIONS (BLUE DOTS) TO THE *IN VIVO* HILL MATURATION FUNCTION (RED DOTS) REVEALS THAT THE LARGEST UNDERPREDICTION IN CYP2D6 CLEARANCE IS MANIFESTED BETWEEN 2-13 YEARS (100-650 WEEKS) OF AGE

5

5 DISCUSSION

The first step in building a pediatric PBPK model is to develop an accurate, robust adult PBPK model. Although our group already demonstrated that PBPK models of tramadol could be built up from actual HLM or rhCYP *in vitro* enzyme kinetic data [16], we choose to use a PBPK modelling approach that was built from *in vivo* clearance values, to be able to predict pediatric PK, since it is the most accurate model for describing adult tramadol PK in healthy volunteers. In this approach, intrinsic clearance values are calculated from *in vivo* clearance values from healthy adult volunteers, using a well-stirred model, to obtain a PBPK model that accurately predicts the *in vivo* clearance. In addition, specific CYP enzyme contributions can be incorporated in this adult PBPK model, which is described in the "materials and methods" section. Pediatric predictions derived from this adult PBPK model are mechanistic because all relevant pathways observed in adults are used for predicting the PK in pediatrics, based on knowledge of functionality maturation in different tissues (e.g. liver eliminating capacity, renal filtration rate, etc.). Although in the adult PBPK model a CYP2D6, a CYP2B6-CYP3A4, and a renal component were implemented, we only focused on prediction of the total, CYP2D6 and renal clearance component for the pediatric populations, since *in vivo* reference data were available for these pathways. After having studied the adult *in vitro* metabolism in HLM, we assessed whether formation of the primary metabolites O-desmethyltramadol (ODT) and N-desmethyltramadol (NDT) in pediatric HLM is governed by the same enzymes as in adult HLM. The result of this experiment would indicate if our approach of applying known maturation functions [17, 35] of the responsible CYP enzymes in adults to predict the pediatric clearance, is valid. Therefore, in order to assess the fractional activity of ODT and NDT formation relative to adult HLM, pooled adult HLM were incubated with tramadol, as well as probe substrates DEX (CYP2D6) and MDZ (CYP3A4) in pediatric and adult HLM. Fractional activity is calculated by taking the ratio of the activity observed in pediatric HLM and the activity observed in pooled adult HLM, as described in the materials section. High fractional activities were found for ODT (1.6- and 1.9-fold,Table 2) which can be explained by the fact that we have observed a relatively low CYP2D6 activity in the pooled adult HLM batch (data not shown). Because we also measured CYP2D6 fractional activity for the probe substrate (Table 2), we were able to calculate the difference between the measured CYP2D6 (DEX) fractional activity and the theoretical (based on *in vitro* ontogeny) CYP2D6 activity. This difference illustrates to what extent the measured CYP2D6 activity deviates from what one would expect for a given age. Correction of the measured ODT fractional activity with the previously calculated difference, which yields "corrODT 1M" and "corrODT 3M" in Figure 3 panel B, confirms us that ODT formation in pediatrics, just as in adults, is CYP2D6-mediated. Applying an analogous correction to NDT formation with measured MDZ activity yields predictions in Figure 3, panel B that are not in line with the CYP3A4 activity at all. A possible explanation is that CYP3A4 is not the only CYP enzyme contributing

to the formation of NDT, also confirmed by other reports [16, 37]. This comparison at the *in vitro* level enabled us to validate the assumption that in adult as well as in early life, CYP2D6 is the major isoform contributing to the metabolism of tramadol to O-desmethyltramadol, making this metabolite a valid probe to study CYP2D6 maturation. Nevertheless, it would be valuable to test more pediatric batches in addition to the pediatric batches described in this study in order to compare/validate the ontogeny functions for the enzymes of interest over a broader age range. In addition, since the ontogeny data for different CYP isoforms are available, the extent of pediatric *in vitro* metabolism can be predicted, extrapolating from adult *in vitro* metabolism data. This approach can serve as guidance for interpreting pediatric metabolism studies, e.g. a significant elevation of an assumed 3A4 metabolite in combination with an anticipated low 3A4 activity, may e.g. indicate CYP3A7 involvement, if substrate overlap is expected.

Pediatric PBPK predictions of tramadol were performed with the pediatric module of the Simcyp® Simulator, which was first used for the setup of an adult PBPK model. At the *in vivo* level, the maturation of total tramadol clearance could be compared between PBPK predicted and *in vivo* observed data sets (Figure 4). The clearance as a function of weight or PMA by the PBPK model is underpredicted compared to the *in vivo* maturation profiles. As has been described above, the clearance prediction for this PBPK model is based on 3 hepatic components (CYP2D6, CYP3A4, and CYP2B6) and one renal component (GFR). Possible explanations for an underprediction are (i) incorrect maturation function for either of the implemented CYP enzymes, (ii) other metabolic pathways contributing to tramadol's metabolism in pediatric life (FMO, CYP3A7) [12, 38] or (iii) neglecting other minor pathways in tramadol metabolism [10]. Therefore, the total clearance of tramadol was decomposed in its constituents and compared to *in vivo* observations, when possible. To this end, (i) since we had strong *in vitro* proof that ODT is a good CYP2D6 activity probe, we compared the predicted vs. *in vivo* observed tramadol CYP2D6 clearance increase, documented in Figure 5; and (ii) we compared the tramadol renal clearance increase versus *in vivo* maturation, illustrated in Figure 6. Concerning the renal clearance maturation, we could only compare our PBPK predictions to the WinNonlin® fits (light brown) since this was the only *in vivo* model that incorporated urinary data for estimation of the clearance parameters. The comparison of the renal clearance, plotted as a function of PMA, between PBPK and WinNonlin® fits yielded good agreement, while the comparison as a function of WT was less good but still acceptable. As for the CYP2D6 clearance maturation, PBPK predictions are in close agreement with the Hill maturation model (black) and the WinNonlin® fits (light brown), but not with the exponential maturation model (red). So which *in vivo* model is the best representation of the CYP2D6 clearance increase? Both the exponential and the Hill model are population PK models built on plasma observations for parent and ODT metabolite, and share an allometric relationship in their covariate structure, but the age models are respectively exponential

and Hill-type. Furthermore, the exponential model is based on plasma observations for 57 neonates and young infants, using a fixed metabolite volume of 224 L/70kg whereas the Hill model incorporates plasma observations from 295 subjects from early to adult life and estimates a metabolite volume based allometric principles from dogs. Because in neither model urinary data was included, we performed a WinNonlin® fitting procedure including urinary data of parent and metabolite. This allowed estimation of the ODT moiety-related volume and its associated clearance value, as well as volume and clearance of tramadol. Although the WinNonlin® parameter estimates are few in number, they agree with the Hill function as descriptor for maturation in CYP2D6 clearance. We believe that the Hill model is the better representation of clearance maturation in pediatrics because this maturation function is physiologically more plausible, since the 'developmental' processes of cells tend to reach their end state at a certain point in childhood, while 'growth' processes take over the increasing elimination capacity of such organs. As the Hill model is also based on the larger data set, we choose the Hill model as a more correct *in vivo* model to compare the PBPK predictions against. It turns out that the CYP2D6 clearance maturation from PBPK aligns much better with our WinNonlin® fits and the Hill model than with the exponential model. Finally, the maturation from birth to adult life is presented for total and CYP2D6 tramadol clearance in figures 7 and 8, respectively. The maturation increase for the total and the CYP2D6 clearance seem to agree with the *in vivo* model in very early life, with CYP2D6 absolute clearance values that are also in line with *in vivo* observed values. However, until the age of 13 (700 weeks PMA), both predicted clearance parameters display a relatively constant underprediction, which disappears again in adulthood. It might be that in children the maturation of liver size as a function of bodyweight is underestimated, since demographic parameters in Simcyp® are mainly based on UK growth charts (personal communication). We acknowledge that choosing the ages where clearances deviate significantly from predictions can be subject to discussion, which again highlights the need for developing adequate evaluation techniques in PBPK.

6 CONCLUSION

In conclusion, PBPK modelling and simulation techniques allow a mechanistic prediction of maturation of CYP2D6-mediated and renal tramadol clearance in very early life. Some underprediction occurred between 2-13 years for total and CYP2D6 tramadol clearance. Care has to be taken when selecting *in vivo* maturation models as a reference, since these 'top-down' models also rely on assumptions made.

5

7 REFERENCES

1. Maharaj AR, Barrett JS, Edginton AN. A Workflow Example of PBPK Modeling to Support Pediatric Research and Development: Case Study with Lorazepam. AAPS J. 2013;15(2):455-64.

2. Manolis E, Osman TE, Herold R, Koenig F, Tomasi P, Vamvakas S, et al. Role of modeling and simulation in pediatric investigation plans. Paediatr Anaesth. 2011;21(3):214-21.

3. Zhao P, Zhang L, Grillo JA, Liu Q, Bullock JM, Moon YJ, et al. Applications of physiologically based pharmacokinetic (PBPK) modeling and simulation during regulatory review. Clin Pharmacol Ther. 2011;89(2):259-67.

4. Bellanti F, Della Pasqua O. Modelling and simulation as research tools in paediatric drug development. Eur J Clin Pharmacol. 2011;67 Suppl 1:75-86.

5. Jamei M, Dickinson GL, Rostami-Hodjegan A. A framework for assessing inter-individual variability in pharmacokinetics using virtual human populations and integrating general knowledge of physical chemistry, biology, anatomy, physiology and genetics: A tale of 'bottom-up' vs 'top-down' recognition of covariates. Drug Metab Pharmacokinet. 2009;24(1):53-75.

6. Johnson TN, Rostami-Hodjegan A. Resurgence in the use of physiologically based pharmacokinetic models in pediatric clinical pharmacology: parallel shift in incorporating the knowledge of biological elements and increased applicability to drug development and clinical practice. Paediatr Anaesth. 2010;21(3):291-301.

7. Mooij MG, Schwarz UI, de Koning BA, Leeder JS, Gaedigk R, Samsom JN, et al. Ontogeny of human hepatic and intestinal transporter gene expression during childhood: age matters. Drug Metab Dispos. 2014;42(8):1268-74.

8. Sweet DH, Bush KT, Nigam SK. The organic anion transporter family: from physiology to ontogeny and the clinic. Am J Physiol Renal Physiol. 2001;281(2):F197-205.

9. Grond S. Clinical pharmacology of tramadol. Clin Pharmacokinet. 2004;43(13):879-923.

10. Wu WN, Mckown LA, Liao S. Metabolism of the analgesic drug ULTRAM (R) (tramadol hydrochloride) in humans: API-MS and MS/MS characterization of metabolites. Xenobiotica. 2002;32(5):411-25.

11. Leong R, Vieira ML, Zhao P, Mulugeta Y, Lee CS, Huang SM, et al. Regulatory experience with physiologically based pharmacokinetic modeling for pediatric drug trials. Clin Pharmacol Ther. 2012;91(5):926-31.

12. Yanni SB, Annaert PP, Augustijns P, Ibrahim JG, Benjamin DK, Thakker DR. In Vitro Hepatic Metabolism Explains Higher Clearance of Voriconazole in Children versus Adults: Role of CYP2C19 and Flavin-Containing Monooxygenase 3. Drug Metab Dispos. 2010;38(1):25-31.

13. Shitara Y, Horie T, Sugiyama Y. Transporters as a determinant of drug clearance and tissue distribution. Eur J Pharm Sci. 2006;27(5):425-46.

14. Tzvetkov MV, Saadatmand AR, Lotsch J, Tegeder I, Stingl JC, Brockmoller J. Genetically Polymorphic OCT1: Another Piece in the Puzzle of the Variable Pharmacokinetics and Pharmacodynamics of the Opioidergic Drug Tramadol. Clin Pharmacol Ther. 2011;90(1):143-50.

15. Kanaan M, Daali Y, Dayer P, Desmeules J. Uptake/Efflux Transport of Tramadol Enantiomers and O-Desmethyl-Tramadol: Focus on P-Glycoprotein. Basic Clin Pharmacol Toxicol. 2009;105(3):199-206.

16. T'Jollyn H, Snoeys J, Colin P, Van Bocxlaer J, Annaert P, Cuyckens F, et al. Physiology-Based IVIVE Predictions of Tramadol from in Vitro Metabolism Data. Pharm Res. 2015;32(1):260-74.

17. Johnson TN, Rostami-Hodjegan A, Tucker GT. Prediction of the Clearance of Eleven Drugs and Associated Variability in Neonates, Infants and Children. Clin Pharmacokinet. 2006;45(9):931-56.

18. Salem F, Johnson TN, Barter ZE, Leeder JS, Rostami-Hodjegan A. Age related changes in fractional elimination pathways for drugs: assessing the impact of variable ontogeny on metabolic drug-drug interactions. J Clin Pharmacol. 2013;53(8):857-65.

19. Allegaert K, Holford N, Anderson BJ, Holford S, Stuber F, Rochette A, et al. Tramadol and o-desmethyl tramadol clearance maturation and disposition in humans: a pooled pharmacokinetic study. Clin Pharmacokinet. 2015;54(2):167-78.

20. Allegaert K, van den Anker J, de Hoon J, van Schaik R, Debeer A, Tibboel D, et al. Covariates of tramadol disposition in the first months of life. Br J Anaesth. 2008;100(4):525-32.

21. De Bock L, Boussery K, Colin P, De Smet J, T'Jollyn H, Van Bocxlaer J. Development and validation of a fast and sensitive UPLC-MS/MS method for the quantification of six probe metabolites for the in vitro determination of cytochrome P450 activity. Talanta. 2012;89:209-16.

22. Team RC. R: A Language and Environment for Statistical Computing. R Foundation for Statistical Computing, Vienna, Austria. 2013.

23. Turner DB, Yeo KR, Tucker GT, Rostami-Hodjegan A. Prediction of nonspecific hepatic microsomal binding from readily available physicochemical properties. Drug Metab Rev. 2006;38:162-.

24. Garcia-Quetglas E, Azanza JR, Cardenas E, Sadaba B, Campanero MA. Stereoselective pharmacokinetic analysis of tramadol and its main phase I metabolites in healthy subjects after intravenous and oral administration of racemic tramadol. Biopharm Drug Dispos. 2007;28(1):19-33.

25. Lintz W, Barth H, Becker R, Frankus E, Schmidt-Bothelt E. Pharmacokinetics of tramadol and bioavailability of enteral tramadol formulations - 2nd communication: Drops with ethanol. Arzneimittel-Forschung. 1998;48(5):436-45.

26. Lintz W, Barth H, Osterloh G, Schmidt-Bothelt E. Pharmacokinetics of tramadol and bioavailability of enteral tramadol formulations - 3rd communication: Suppositories. Arzneimittel-Forschung. 1998;48(9):889-99.

27. Lintz W, Becker R, Gerloff J, Terlinden R. Pharmacokinetics of tramadol and bioavailability of enteral tramadol formulations - 4th Communication: Drops (without ethanol). Arzneimittel-Forschung. 2000;50(2):99-108.

28. Lintz W, Erlacin S, Frankus E, Uragg H. Metabolismus von tramadol bei mensch und tier. Arzneimittel-Forschung. 1981;31(11):1932.

29. Bjorkman S. Prediction of drug disposition in infants and children by means of physiologically based pharmacokinetic (PBPK) modelling: theophylline and midazolam as model drugs. Br J Clin Pharmacol. 2005;59(6):691-704.

30. Jamei M, Bajot F, Neuhoff S, Barter Z, Yang J, Rostami-Hodjegan A, et al. A mechanistic framework for in vitro-in vivo extrapolation of liver membrane transporters: prediction of drug-drug interaction between rosuvastatin and cyclosporine. Clin Pharmacokinet. 2014;53(1):73-87.

31. Pedersen RS, Damkier P, Brosen K. Enantioselective pharmacokinetics of tramadol in CYP2D6 extensive and poor metabolizers. Eur J Clin Pharmacol. 2006;62(7):513-21.

32. Jamei M, Marciniak S, Feng K, Barnett A, Tucker G, Rostami-Hodjegan A. The Simcyp Population-based ADME Simulator. Expert Opin Drug Metab Toxicol. 2009;5(2):211-23.

33. Saarikoski T, Saari TI, Hagelberg NM, Neuvonen M, Neuvonen PJ, Scheinin M, et al. Rifampicin markedly decreases the exposure to oral and intravenous tramadol. Eur J Clin Pharmacol. 2013;69(6):1293-301.

34. Rekic D, Roshammar D, Mukonzo J, Ashton M. In silico prediction of efavirenz and rifampicin drug-drug interaction considering weight and CYP2B6 phenotype. Br J Clin Pharmacol. 2011;71(4):536-43.

35. Salem F, Johnson TN, Abduljalil K, Tucker GT, Rostami-Hodjegan A. A re-evaluation and validation of ontogeny functions for cytochrome P450 1A2 and 3A4 based on in vivo data. Clin Pharmacokinet. 2014;53(7):625-36.

36. Allegaert K, Van Den Anker J, Verbesselt R, de Hoon J, Vanhole C, Tibboel D, et al. O-demethylation of tramadol in the first months of life. Eur J Clin Pharm. 2005;61(11):837-42.

37. Subrahmanyam V, Renwick AB, Walters DG, Young PJ, Price RJ, Tonelli AP, et al. Identification of Cytochrome P-450 Isoforms Responsible for cis-Tramadol Metabolism in Human Liver Microsomes. Drug Metab Dispos. 2001;29(8):1146-55.

38. Ince I, Knibbe CA, Danhof M, de Wildt SN. Developmental changes in the expression and function of cytochrome P450 3A isoforms: evidence from in vitro and in vivo investigations. Clin Pharmacokinet. 2013;52(5):333-45.

5

8 APPENDIX

Tables

TABLE A1: OVERVIEW OF DRUG-SPECIFIC PBPK INPUT USED FOR PEDIATRIC PREDICTIONS

Physchem data		
	Molecular weight	263.38
	Log Po:w	1.35
	Pka monoprotic base	9.41
	B:P	1.09
	Fup	0.8 (user input)
Elimination (liver)		
	CLint CYP2D6	0.301139 µL/min/pmol 2D6
	CLint CYP2B6	0.02949 µL/min/pmol 2B6
	CLint CYP3A4	0.01538 µL/min/pmol 3A4
	Hepatic uptake	1.58 [a]
Elimination (kidney)		6.6 L/h

[a] readers are referred to Chapter 3 for more information on this value

TABLE A2: OVERVIEW OF THE NUMERIC VALUES FOR THE DIFFERENT POPPK DERIVED MATURATION FUNCTIONS

	Parameter	Exponential model Allegaert et al, 2008 [20]	Hill model Allegaert et al, 2015 [19]
CYP2D6	CLstd (L/h/70kg)	4.11	10.5
	SLPCL (weeks PMA $^{-1}$)	0.207	
	TM50 (weeks PMA)		40.3
	Hill coef		9.09
Non-CYP2D6	CLstd (L/h/70kg)	11.6	21.6
	SLPCL (weeks PMA $^{-1}$)	0.0275	
	TM50 (weeks PMA)		39.0
	Hill coef		6.76

CLstd: the estimated population clearance, standardized to a 70 kg person using an allometric model, SLPCL: slope parameter estimating magnitude of clearance increase with PMA, TM50: PMA at which clearance is 50 % of the mature value, Hill coef: Hill coefficient, which determines the steepness of the maturation curve

Figures

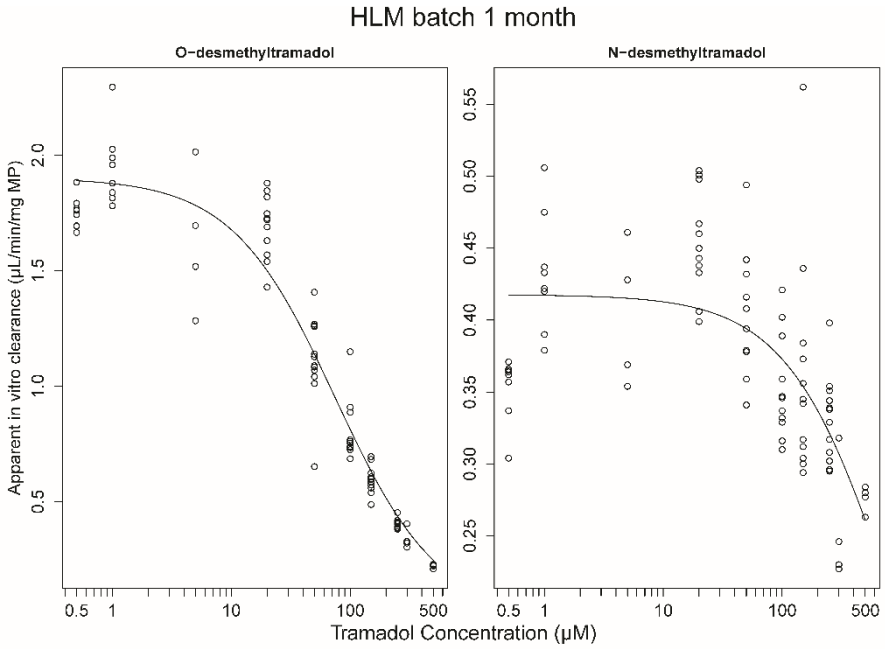

FIGURE A1: *IN VITRO* CLEARANCE FROM TRAMADOL TO ODT (LEFT) AND NDT (RIGHT) VS. SUBSTRATE CONCENTRATION FOR A PEDIATRIC BATCH AGED 1 MONTH

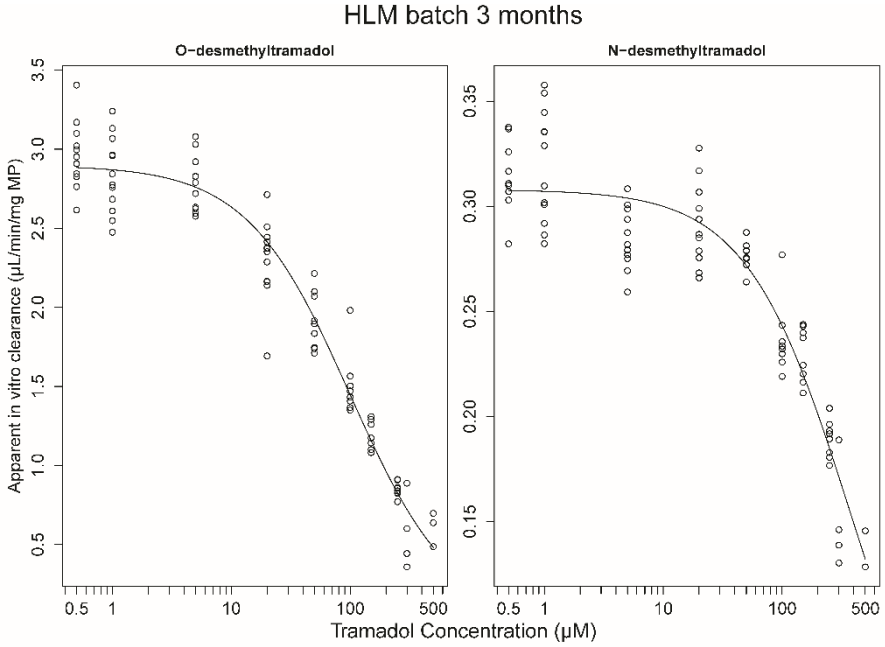

FIGURE A2: *IN VITRO* CLEARANCE FROM TRAMADOL TO ODT (LEFT) AND NDT (RIGHT) VS. SUBSTRATE CONCENTRATION FOR A PEDIATRIC BATCH AGED 3 MONTHS

5

CHAPTER 6

PBPK AND ITS VIRTUAL POPULATIONS: THE IMPACT OF PHYSIOLOGY ON PEDIATRIC PHARMACOKINETIC PREDICTIONS OF TRAMADOL

This chapter is based on:

PBPK and its virtual populations: the impact of physiology on pediatric pharmacokinetic predictions of tramadol. *Under review*.

6

TABLE OF CONTENTS

6

1 ABSTRACT

Background & Objective

In pediatric PBPK models, age-related changes in the body (system) are known to occur: tissue volumes, tissue blood flow rates, tissue composition, as well as renal and enzymatic function need to be adapted. Given the sparsity of and the variability associated with relevant physiological parameters, the implementation of these adaptations may be different across the available PBPK software tools. In this work, three commercially available PBPK softwares (PK-Sim®, Simcyp®, Gastroplus®) were investigated regarding their differences in system-related information, possibly affecting clearance prediction.

Methods

To this end, tramadol was used as model compound. Each adult PBPK clearance model was calibrated to the tramadol adult clearance prediction obtained from a published pooled popPK model. The resulting PBPK (retrograde) clearance models were qualified in terms of total, CYP2D6, and renal clearance. Tramadol pediatric clearance predictions were compared between the different PBPK (bottom-up) models and the popPK (top-down) model in the lifespan range from neonates to adolescents. Fold prediction errors were used to evaluate the results.

Results

Marked differences in liver maturation between PBPK models were observed. In the neonatal age category, the median fold error on the total clearance was 0.79, 0.34, and 0.69 for PK-Sim, Simcyp, and Gastroplus, respectively. For the CYP2D6 clearance, the median fold errors were 1.00, 0.35, and 0.47 for PK-Sim, Simcyp, and Gastroplus, respectively. Interestingly, in the case of CYP2D6, the PBPK model with the shortest maturation half-life (PK-Sim) agreed best with the *in vivo* CYP2D6 maturation model. Obviously, the differences in physiological data to leverage system-related parameters, leads to marked differences in hepatic clearance prediction in early life between the various PBPK softwares tested.

Conclusion

Consensus on the most suited pediatric data to use should harmonize and optimize pediatric clearance predictions. Moreover, the combination of bottom-up and top-down approaches, using a convenient probe substrate, has the potential to update system-related parameters in order to better represent pediatric physiology. Continued research using a broader range of compounds could strengthen these findings.

2 INTRODUCTION

Physiologically-based pharmacokinetic modelling and simulation (PBPK-M&S) is a relatively old concept [1], but received renewed interest recently. It holds potential in support of pediatric drug development and pharmacotherapy, both considered to be at the forefront of clinical pharmacology. 'Bottom-up' PBPK-M&S methods make an *a priori* distinction between the system (i.e. the human body) and the drug properties (e.g. molecular descriptors, physicochemical and permeability parameters, metabolic intrinsic clearance (CLint)). PBPK models may be used to predict the *in vivo* clearance and drug distribution in relevant subpopulations. Based on a mechanistic understanding of the drug disposition in healthy adult subjects, qualified PBPK models may be used to mechanistically predict pediatric pharmacokinetics (PK) [2, 3].

Drug clearance in PBPK may be predicted using the metabolic parameters Km, Vmax or CLint. In the bottom-up modelling process, the CLint is used to reflect the intrinsic capacity of the liver to metabolize a given drug. This drug-specific CLint may represent a 'lumped' total liver CLint, but may also be assigned to different contributing enzymes. Besides, it may either be derived from *in vitro* metabolism assays or from *in vivo* phenotypic data. In the latter case, the *in vivo* observed clearance for a test drug is back-calculated to the CLint at the enzyme level (retrograde clearance model) [3, 4]. Such a retrograde clearance model has the ability to simulate the drug's PK in any given population for which the system's data are available. This retrograde model has the advantage that it accurately incorporates the relevant routes of *in vivo* drug clearance in a mechanistic way. A disadvantage is that for drugs with many complex processes involved in their drug disposition, the setup of this retrograde model may become challenging.

Key in this approach is furnishing the system's data, relevant for the population under study. The collection of the correct physiological information that captures relevant differences compared to healthy volunteers, may be very challenging e.g. in pediatrics, renally impaired and cirrhotic patients. In very young children (<2 years of age), age-related physiological changes occur in tissue volumes, tissue blood flow rates, tissue composition, as well as in renal and enzymatic function [5]. To date, several groups have collected information on tissue volumes, tissue composition, and blood flows [6-9], as well as changes in enzyme activity [10, 11] as a function of age, bodyweight, height, or their composite parameters (BSA, BMI). In addition, anthropometric data, e.g. the NHANES III study [12] and/or national census initiatives, provide information on the variability of these metrics in the population. Integrating this information in a PBPK M&S platform allows to create physiologically relevant virtual subjects, constituting a realistic 'virtual' population. Commercially available PBPK platforms (PK-Sim®, Simcyp®, Gastroplus®) have integrated this information in order to create virtual pediatric subjects [3, 13].

However, given the sparsity of and the variability associated with relevant physiological parameters, virtual pediatric subjects created by different available PBPK software tools may differ. Possible differences in liver blood flow, plasma protein binding, liver size, mg protein per gram of liver (MPPGL), and ontogeny of drug metabolizing enzymes may influence the prediction of hepatic clearance. The maturation of the glomerular filtration rate (GFR) has been studied quite extensively [14-17], but the question remains which of these maturation models is used to describe the GFR development *in silico* in the different softwares, and how this impacts the simulation results.

Obtaining an accurate prediction of clearance is a prerequisite for a successful dose extrapolation towards pediatric subjects. Hence, this study addresses the impact of possible differences in physiological information as present in commercial softwares on the prediction of the hepatic and renal clearance in kids. To this end, tramadol is used as model compound. Tramadol is a centrally acting analgesic drug with weak opioid activity, broadly studied in different pediatric age groups and adults [18-28]. Multiple relevant CYP enzymes (CYP2D6, CYP3A4, CYP2B6) are involved in its metabolism [29]. Not until recently, a pooled population pharmacokinetic analysis was published, describing the maturation of the total and CYP2D6 clearance over the complete pediatric lifespan to adulthood [30]. The 'top-down' estimated maturation functions from this published work were quantitatively compared to the PBPK-predicted, physiology-driven clearances across age groups. For each software package separately, first, an adult clearance model was constructed and qualified. Second, pediatric predictions were performed for different age groups. Finally, maturation in pediatric clearance was compared between predictions and observations.

3 METHODS

3.1 PBPK MODELLING SOFTWARE AND SETUP OF THE TRAMADOL ADULT PBPK MODEL

In order to develop a whole-body PBPK model, three specialized software tools were used. Simcyp® (v14.1, Certara, Inc., NJ, USA), PK-Sim® (v6.2, Bayer Technology Services, Leverkusen, Germany), and Gastroplus® (v9.0, SimulationsPlus (Cognigen), California, USA) were used for mechanistic prediction of adult and pediatric drug disposition. These tools provide the necessary building blocks to construct a user-defined PBPK model. Specific details pertaining to the different software tools can be found in scientific literature [3, 31, 32].

A specific workflow was followed to mechanistically implement the adult tramadol clearance for each software package and is clarified in the following steps. First, clearance and distribution parameters after intravenous administration of tramadol in healthy adult subjects were gathered from literature. In a pooled population pharmacokinetic analysis by Allegaert et al. [30], the standardized total clearance, CYP2D6 clearance and volume of distribution were estimated. They are presented in Table 2, column 'Reference'. In addition, the individual CYP contributions were determined from *in vivo* data. The CYP2D6 contribution was calculated as the ratio of CL_{2D6}/CL_{TOT} in the pooled popPK model and represented 43% of the hepatic clearance. The CYP2B6 contribution was determined before as 10% of the hepatic clearance, see Chapter 5. The remaining CYP3A4 contribution is 47%. Second, for each PBPK software separately, a distinct so-called 'retrograde' clearance model was constructed. The total clearance was mechanistically integrated as the sum of the hepatic metabolism by CYP2D6, CYP3A4 and CYP2B6,and the renal excretion. The contributions for these pathways in the PBPK clearance module were set to represent their *in vivo* contributions using *in vivo* derived phenotypic information (the 'retrograde' clearance model). In short, the hepatic clearance was back-calculated - using the well-stirred liver model - to the hepatic intrinsic clearance ($CLint_H$), using the fraction unbound in blood (fu_b) and the hepatic blood flow. CYP-enzyme specific intrinsic clearances ($CLint_{CYP}$) were obtained from $CLint_H$ using the *in vitro*-to-*in vivo* (IVIVE) scalars liver weight, microsomal protein per gram liver (MPPGL), and enzyme abundances. The parameters used for this retrograde back-calculation are provided in Table 1, under 'Parameters used for retrograde calculation', and include the hepatic blood flow, fu_b, liver weight, individual CYP contributions in the hepatic clearance, and the CYP enzymes' liver concentrations. Except for the CYP contributions, all other parameters were different for every software package and were collected as follows. For PK-Sim® and Simcyp®, an adult virtual population (Caucasian, n=1000, range 25-45 years, 50% females) was created from which these parameters are calculated as the medians. For Gastroplus® these values were collected from the graphical user interface, without creating a virtual population (see discussion for further details). Obviously, the intrinsic clearances for

CYP2D6, CYP3A4, and CYP2B6 are different per software package and are provided in Table 1 (section 'PBPK Input Parameters'). Third, all the drug-related (physicochemical and elimination) input parameters used for the bottom-up prediction of the clearance in every software package are presented in Table 1 (section 'PBPK Input Parameters'). The adult PBPK model development was performed using the CYP2D6 'extensive' metabolizer (EM, UM) genotype, since a PM has no CYP2D6 activity, due to two null-alleles leading to absence of functional CYP2D6 protein [33].

The tissue distribution of tramadol was governed by the tissue-to-plasma (Kp) ratios predicted using the Rodgers and Rowland models for basic amines [34]. The B:P ratio was adjusted per software (as indicated in Table 1), as needed, in order to provide reliable *in silico* estimates of the *in vivo* volume of distribution.

The PBPK models, set up in the different software packages, were qualified for adults, based on their prediction of the total, renal, and CYP2D6 clearance. For PK-Sim® and Simcyp®, a virtual adult population was created (Caucasian, n=1000, range 25-45 years, 50% females) to qualify the retrograde PBPK model. The median of the predicted total, renal, and CYP2D6 clearance and volume of distribution are provided in Table 2. For Gastroplus®, the typical American individual of 86.27 kg was chosen for qualification of the retrograde PBPK model, and no population variability was incorporated in the predictions (see discussion). The predicted total, renal, and CYP2D6 clearance and volume of distribution are provided in Table 2. Clearance values were individually calculated from the predicted plasma concentration-time curves as dose/AUC. The different clearance values for CYP2D6, CYP3A4 and CYP2B6 were calculated by multiplying the total clearance value with the respective CYP contributions (calculated as fraction of the total dose) per virtual individual.

3.2 PREDICTION OF PEDIATRIC CLEARANCE

Different PBPK software packages were instructed to predict pediatric pharmacokinetics in specified age groups, as defined below:

- Neonate (40 – 44 weeks PMA)
- Infant (44 weeks PMA – 2 yrs PNA)
- Young Child (2 – 6 yrs)
- Child (6 – 12 yrs)
- Adolescent (12 – 18 yrs)
- Young Adult (18 – 25 yrs)
- Adult (25 – 45 yrs)

TABLE 1: A REPRESENTATION OF THE PARAMETERS USED FOR RETROGRADE CALCULATION PER SOFTWARE TOOL, AND THE PBPK INPUT PARAMETERS THAT WERE USED AS INPUT FOR THE PBPK MODEL

Parameter	PK-Sim	Simcyp	Gastroplus
Parameters used for retrograde calculation			
Back-calculation from CL_H to $CLint_H$			
Hepatic blood flow (L/h)	99.15	84.92	91.02
fu_b	0.73	0.73	0.73
Back-calculation from $CLint_H$ to $CLint_{CYP}$			
Liver Weight	2.07 kg	1.58 kg	1.77 kg
Individual CYP contribution in the hepatic clearance	CYP2D6 43% - CYP3A4 47% - CYP2B6 10%		
CYP2D6 liver concentration	0.42 nmol/g	0.26 nmol/g	0.30 nmol/g
CYP3A4 liver concentration	4.36 nmol/g	4.87 nmol/g	4.22 nmol/g
CYP2B6 liver concentration	1.86 nmol/g	0.37 nmol/g	0.43 nmol/g
PBPK Input Parameters			
Molecular weight (Da)	263.4	263.4	263.4
logP	1.35	1.35	1.35
fu_p	0.8	0.8	0.8
Compound type (pKa)	Base (9.41)	Base (9.41)	Base (9.41)
B:P	1.07	1.09	1.075
$CLint_{CYP2D6}$ (µL/min/pmol)	0.337	0.739	35.72/100[a]
$CLint_{CYP3A4}$ (µL/min/pmol)	0.0341	0.0472	2.81/100 [a]
$CLint_{CYP2B6}$ (µL/min/pmol)	0.0201	0.0809	6.04/100 [a]
CL_r (L/h/70kg)	6.62	7.11	6.36

[a] Vmax/Km; CLint values could only be provided as Vmax (pmol/min/pmol CYP) and Km (µM) values
CL_H: hepatic clearance, $CLint_H$: hepatic intrinsic clearance, $CLint_{CYP}$: CYP-specific intrinsic clearance, fu_b: fraction unbound in blood; fu_p: fraction unbound in plasma, B:P: blood-to-plasma ratio, CL_r: renal clearance

In the next step, the different clearance models were used to mechanistically predict the changes in clearance as a function of age. The system's information contained in the different PBPK software packages was used for pediatric predictions. In PK-Sim® and Simcyp®, 1000 virtual subjects were created per age group. For Gastroplus®, 1 virtual subject (representing the typical or population average subject)

was created for the following age periods: 41-50 weeks PMA (1 subject per week); 52-62 weeks PMA (1 subject every 2 weeks); 64-88 weeks PMA (1 subject every 4 weeks); 1-25 years of age (1 subject every year). These exact virtual subjects (for each PBPK software) were used as input (in fact their covariates bodyweight and PMA) to the structural model from the popPK analysis by Allegaert. This way, every virtual subject was linked to a PBPK-predicted clearance and a popPK-predicted clearance. The difference between the PBPK-predicted and the popPK-predicted clearances was expressed as fold prediction difference. The median of the fold prediction differences was calculated per age group and per software (Table 3). In addition, the evolution of the median fold prediction differences over the pediatric age range was assessed visually per software package (Figure 2). This complete workflow was iterated for total, CYP2D6, and renal tramadol clearance.

3.2.1 PK-Sim

The information used for building virtual populations in PK-Sim®, is based on the NHANES III study [12] and Annals of the ICRP [7]. NHANES III mainly provides anthropometric data, while the ICRP study focuses on mean organ weights and blood flows. Organ densities are all assumed to be 1 g/mL. Virtual populations are created within PK-Sim® using the algorithm "PK-Pop". The paper by Willmann et al. [13] elaborates on how virtual subjects are set up to represent a physiologically plausible population. This is the only software tool of the three that For the population simulations, the Healthy Male Caucasian was selected. In the hepatic clearance prediction, CYP2D6 (10.5 pmol/mg microsomal protein, MP), CYP3A4 (109 pmol/mg MP), and CYP2B6 (46.5 pmol/mg MP) enzyme abundances in the software were based on Rodrigues et al. [35] (Table 1). The MPPGL is considered to be 40 mg/g liver, independent of age. CYP2D6 ontogeny is based on published literature studies [36, 37] and is graphically represented in the *Appendix*. CYP3A4 ontogeny information is described in [10, 11]. Since no ontogeny function is currently present for CYP2B6, functional CYP2B6 activity data were digitized from Pearce et al. [38] using Web PlotDigitizer v3.8. The ontogeny model best describing CYP2B6 maturation was a power function, provided in *Appendix*. The geometric standard deviation was assumed to be 1.7. Liver blood flow (QH) is defined as the sum of portal and arterial liver blood flow. In pediatrics, QH follows the changes in cardiac output [7], although the percent of the cardiac output perfusing the liver remains the same as in adults. The adult renal clearance was defined in the PBPK model structure as an arbitrary fraction (1.43) of the GFR. The renal clearance is predicted in an age-dependent manner by taking the changes in GFR maturation into account (Hayton equation, based on age) [10].

3.2.2 Simcyp

Virtual populations in Simcyp® are built from the NHANES database, UK census data, and meta-analyses of numerous literature studies. First, individuals are selected by age, then linked to height, weight and

BSA. These anthropometrics are then used for an age-dependent prediction of different organ weights and volumes, e.g. cardiac output is related to age, while liver volume is related to BSA [11, 39]. Q_H is maintained as a fixed fraction of the cardiac output over the complete human lifespan [7]. Stochastic variation is applied using a correlated Monte-Carlo method. In this study, the North Caucasian Healthy Volunteer population was chosen for the adult simulations and the Pediatric population for pediatric simulations. The evolution of hepatic enzyme ontogeny and values for enzyme abundances are published in the literature for the CYP enzymes CYP3A4, CYP2D6, and CYP2B6 [11, 40, 41]. Furthermore, given the polymorphic nature of CYP2D6 and CYP2B6, the following abundances are used: CYP2D6 PM 0, EM 8, and UM 16 pmol/mg MP; CYP2B6 PM 6 and EM 17 pmol/mg MP. MPPGL varies with age, as published by Barter et al. [42]. Renal clearance was defined in the PBPK model as a fixed clearance estimate. Developmental variation was applied by the multiplication with a 'renal function' value, which is calculated using the pediatric GFR function (based on BSA) relative to adult [11]. Demographic information pertaining to percentages of CYP phenotypes in the population was kept constant throughout the simulations. Specifically for CYP2D6, this implies 8.2% poor – 5.3% ultrarapid – 86.5% extensive metabolizers, and for CYP2B6 11% poor – 89% extensive metabolizers.

3.2.3 GASTROPLUS

In Gastroplus®, age-related anthropometric data are derived from the NHANES study as well. In the Gastroplus® manual, the method for generating organ physiology values is described and involves calculating BMI and fat-free mass from weight, height, and bioimpedance. Then, constant perfusion rates per mL tissue are set [9] and blood volumes are calculated [6]. For each tissue, the weight, volume, density, and perfusion are calculated. In addition, the Gastroplus® manual also provides the results from an exhaustive literature search concerning changes in pediatric physiology over time, from preterm to adult. Subsections concern body and tissue sizes, blood parameters, and tissue compositions. Hepatic enzyme abundances that were as follows: for CYP2D6, 8 pmol/mg MP, for CYP3A4, 111 pmol/mg MP, and for CYP2B6, 11 pmol/mg MP. Ontogeny profiles implemented are the ones from Johnson et al. [11]. The renal clearance was implemented in the PBPK model structure as a fraction of the renal blood flow. Since renal blood flow varies over age, so will the renal clearance. Since tramadol renal clearance could not be implemented as arbitrary fraction of the GFR, using the renal blood flow turned out to be the second best option. In the Gastroplus® simulations, no variability was incorporated and only for selected ages the typical individual was used to predict pediatric clearance. It is however possible to perform populations simulations, but variability is considered stochastic noise instead of originating from correlated covariates, and the end-user is only able to extract plasma concentration-time profiles, without parameters related to a drug's fate (e.g. metabolic activity of CYP enzymes).

6

4 RESULTS

4.1 QUALIFICATION OF THE ADULT PBPK MODEL

The tramadol adult retrograde PBPK model that was constructed in different software packages (Simcyp®, PK-Sim®, Gastroplus®) was calibrated to the pooled population PK (popPK) model from Allegaert et al. [30] in terms of the PK parameters clearance (total, CYP2D6, and renal) and volume of distribution. Table 2 presents the agreement between predicted and observed adult PK parameters. Given the difference in median bodyweight between the different virtual populations, clearance values were standardized to 70kg. In addition, the predicted CYP enzyme contributions in the hepatic clearance (f_{2D6}, f_{3A4}, and f_{2B6} in Table 2) agree well with *in vivo* reference fractions (0.43, 0.47, and 0.1, respectively), used to build the retrograde clearance model. Since for PK-Sim® and Simcyp®, population simulations were used in qualifying their adult clearance model, simulated 5th (Q5) and 95th (Q95) percentiles are displayed for their CYP enzyme contributions. Except for CYP2B6, the Q5 - Q95 ranges for the enzyme contributions are similar between Simcyp® and PK-Sim®. Since the pooled popPK model does not provide an estimate for the renal clearance, it was extracted from an internal Grünenthal Research Report and was scaled in the PBPK models using GFR or kidney blood flow (see methods). Only Simcyp® predicts this value to be 1.13-fold higher, due to a built-in algorithm for renal clearance.

TABLE 2: OVERVIEW OF THE REFERENCE PK PARAMETERS (AS EXTRACTED FROM THE POPPK MODEL) AND PBPK-PREDICTED PARAMETERS FOR THE ADULT POPULATION. CONSISTENCY BETWEEN THESE PARAMETERS QUALIFIES THE PBPK CLEARANCE MODEL

	Reference	PK-Sim	Simcyp	Gastroplus
		PK parameters		
V_{ss} *(L/kg)*	2.63[a]	2.62	2.64	2.63
$CL_{tot,EM}$ *(L/h/70kg)*	32.13[a]	32.82	33.73	31.86
$CL_{2D6,EM}$ *(L/h/70kg)*	10.70[a]	10.85	10.57	10.75
CL_r *(L/h/70kg)*	6.60[b]	6.62	7.11	6.36
Median BW	70.00	67.00	74.00	86.27
		Fractions of hepatic clearance Q50 (Q5-Q95)		
f_{2D6}	0.43	0.430 (0.146-0.751)	0.423 (0.182-0.689)	0.429
f_{3A4}	0.47	0.440 (0.192-0.704)	0.476 (0.234-0.732)	0.468
f_{2B6}	0.10	0.108 (0.0305-0.264)	0.0637 (0.00765-0.288)	0.101

[a] [30]; [b] Internal Research Report Grünenthal GmbH

4.2 PEDIATRIC PREDICTIONS

4.2.1 TOP-DOWN VS. BOTTOM-UP CLEARANCE PREDICTIONS

The predicted increase in total, CYP2D6 and renal clearance as a function of age in actual pediatric subjects is depicted in Figure 1. The total and CYP2D6 clearance maturation (for extensive metabolizers) was extracted from the popPK model by Allegaert et al. [30]. Individual predictions based on the actual subjects's age and weight are displayed as dots. The observations of renal clearance (displayed with a smoother function) were obtained via a one-by-one fitting procedure in WinNonlin® for a subset of the neonates/infants enrolled in the Allegaert study. This procedure is described in more detail in Chapter 5. This analysis focuses on total, CYP2D6, and renal clearance only, because the popPK model by Allegaert provides estimates for just total and CYP2D6 clearance, while the renal clearances are derived from the WinNonlin® model (see above).

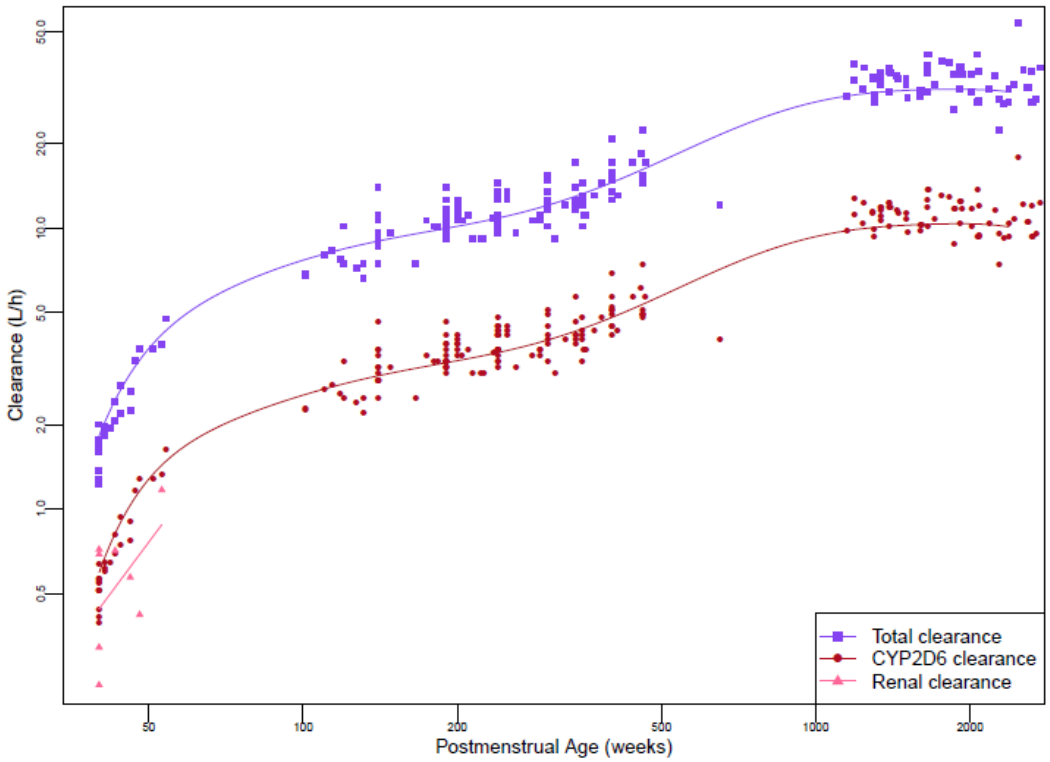

FIGURE 1: MATURATION OF THE TOTAL, CYP2D6 AND (EARLY) RENAL TRAMADOL CLEARANCE AS PREDICTED BY THE POPPK MODEL. DOTS FOR TOTAL AND CYP2D6 CLEARANCE REPRESENT THE POPULATION PREDICTIONS (BODYWEIGHT AND PMA) FROM ACTUAL INDIVIDUALS IN THE CLINICAL TRIALS, AND THE LINES THE BEST FIT CURVE THROUGH THESE DATA. DOTS FOR THE RENAL CLEARANCE REPRESENT THE ESTIMATED CLEARANCES FOR THESE SUBJECT BY WINNONLIN

As indicated in the methods section, in PK-Sim® and Simcyp®, 1000 virtual subjects were created per age group, while for Gastroplus® 1 typical population representative was created at selected ages. Each virtual subject, originating from a given PBPK software, was used as input for both the PBPK, as well as

the popPK clearance model. Therefore, every virtual subject was linked to a PBPK-predicted clearance and a popPK-predicted clearance. Figure 2 provides a smoothed image of the evolution of the median fold prediction differences between PBPK and popPK over the pediatric age range, for tramadol total, CYP2D6 and renal clearance (the latter only accounting for the first 12 weeks of life). Table 3 provides the actual numbers, stratified per age group. PK-Sim® and Gastroplus® predict the total clearance within 2-fold, while Simcyp® underpredicts the total clearance in the first 30 weeks of life. Only from 2 years of age onwards, 95% of the total clearance predictions fall within 2-fold of the observed maturation profile. CYP2D6 clearance is predicted within 2 fold (even within 20%) of the *in vivo* maturation by PK-Sim®. Simcyp® and Gastroplus® underpredict the CYP2D6 clearance below the 2-fold boundary up to 55 weeks and 43 weeks PMA, respectively. Concerning the renal clearance, both Simcyp® and PK-Sim® are within the 2-fold boundary. The Gastroplus® renal clearance is acceptable from 44 weeks PMA onwards.

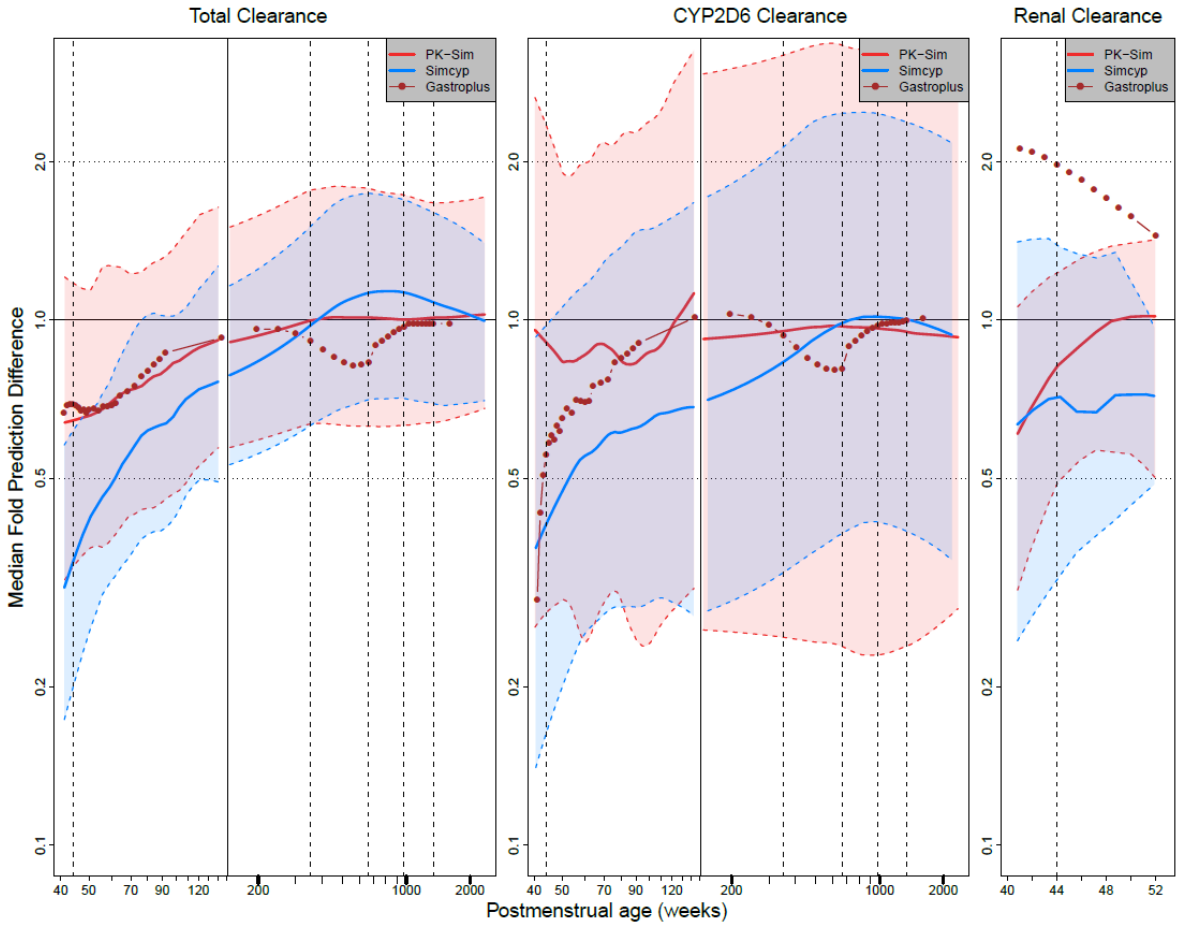

FIGURE 2: MEDIAN FOLD PREDICTION DIFFERENCE OF 3 DIFFERENT PBPK SOFTWARE PLATFORMS (PK-SIM, SIMCYP, AND GASTROPLUS), COMPARED TO POPPK PREDICTIONS WITH THE SAME VIRTUAL SUBJECTS FOR THE TOTAL, CYP2D6, AND RENAL CLEARANCE.

TABLE 3: TABLE WITH MEDIAN FOLD ERRORS PER AGE CATEGORY AND PER SOFTWARE FOR CL_{TOT} AND CL_{2D6}

	Neonate	Infant	Young Child	Child	Adolescent	Young Adult	Adult
				PK-Sim			
CL_{TOT}	0.79	0.82	1.02	1.07	1.03	1.01	1.03
CL_{2D6}	1.00	0.94	1.06	1.08	1.05	0.99	1.03
				Simcyp			
CL_{TOT}	0.34	0.65	0.84	1.08	1.16	1.12	1.04
CL_{2D6}	0.35	0.63	0.76	0.94	1.08	1.05	1.01
				Gastroplus			
CL_{TOT}	0.69	0.70	0.95	0.83	0.94	0.98	0.99
CL_{2D6}	0.47	0.71	1.00	0.82	0.94	0.99	1.01

In order to provide the full picture, all clearance contributors are depicted in Figure 3. Although there is no *in vivo* maturation function available to compare with the CYP3A4 and CYP2B6 predicted clearances, it remains interesting to note the differences between softwares.

The total tramadol clearance consists of 4 different elimination routes, 3 hepatic and 1 renal. From these 4 elimination routes, only the CYP3A4 maturation is consistent between the 3 software packages. The maturation of CYP2D6 is fastest in PK-Sim®, followed by Gastroplus®, and Simcyp®. Whereas CYP2B6 has a very pronounced ontogeny profile in Gastroplus®, both in Simcyp® and PK-Sim® its activity is already relatively high at birth. Renal clearance in PK-Sim® and Simcyp® initially is the same, but increases faster in PK-Sim®. Renal clearance in Gastroplus® even decreases in the first 2 years of life, starting off from an initial higher clearance.

4.2.2 Effect of pediatric physiology on the bottom-up clearance prediction

Parameters that determine the prediction of hepatic clearance are the hepatic blood flow, fraction unbound in blood, liver weight, and enzyme abundances of the different enzymes involved. Figure 4 illustrates the evolution of these parameters in the first 2 years of life, whereas Figure 5 displays the development of these parameters from 2 year onwards. Figure 4 shows that minor differences exist between the different virtual populations, created per software, in terms of bodyweight and hepatic blood flow versus PMA. On the other hand, liver weight is consistently higher for PK-Sim®, and fraction unbound is slightly higher in the first few weeks for the Gastroplus® population. The CYP3A4 abundance is in good agreement across the different virtual populations, though CYP2D6 and CYP2B6 ontogenic differences are observed. CYP2D6 abundance rapidly reaches mature levels in the PK-Sim® population,

followed by Gastroplus® and then Simcyp®, which both show a pronounced maturation profile. CYP2B6 abundance is again highest for the PK-Sim® population, followed by Simcyp®, with both starting off with relatively high levels at birth. The Gastroplus® virtual population displays a distinctive CYP2B6 maturation profile.

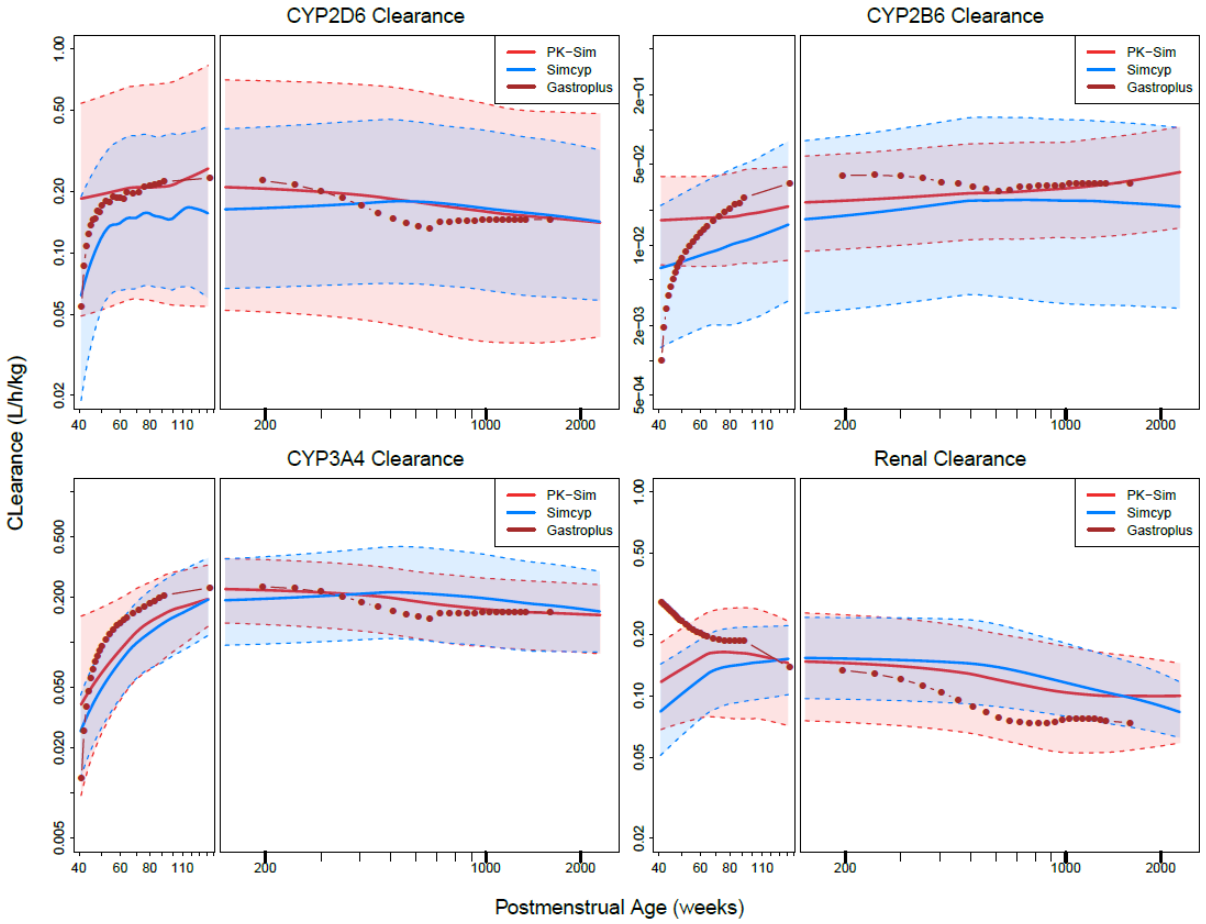

FIGURE 3: CYP2D6, CYP2B6, CYP3A4 AND RENAL CLEARANCE AS A FUNCTION OF PMA FROM BIRTH TO ADULTHOOD. THESE 4 ELIMINATION ROUTES MAKE UP THE TOTAL TRAMADOL CLEARANCE. THE ONLY CLEARANCE SHOWING CONSISTENCY IN MATURATION OVER THE 3 SOFTWARE TOOLS, IS THE CYP3A4 MATURATION.

Figure 5 shows that there is still an important increase in bodyweight, hepatic blood flow, and liver weight with PMA beyond 2 years of age, while the unbound fraction in blood and the different CYP abundances (on a pmol/g liver basis) remain relatively constant. The exception is CYP2B6, and we will further elaborate on this in the discussion.

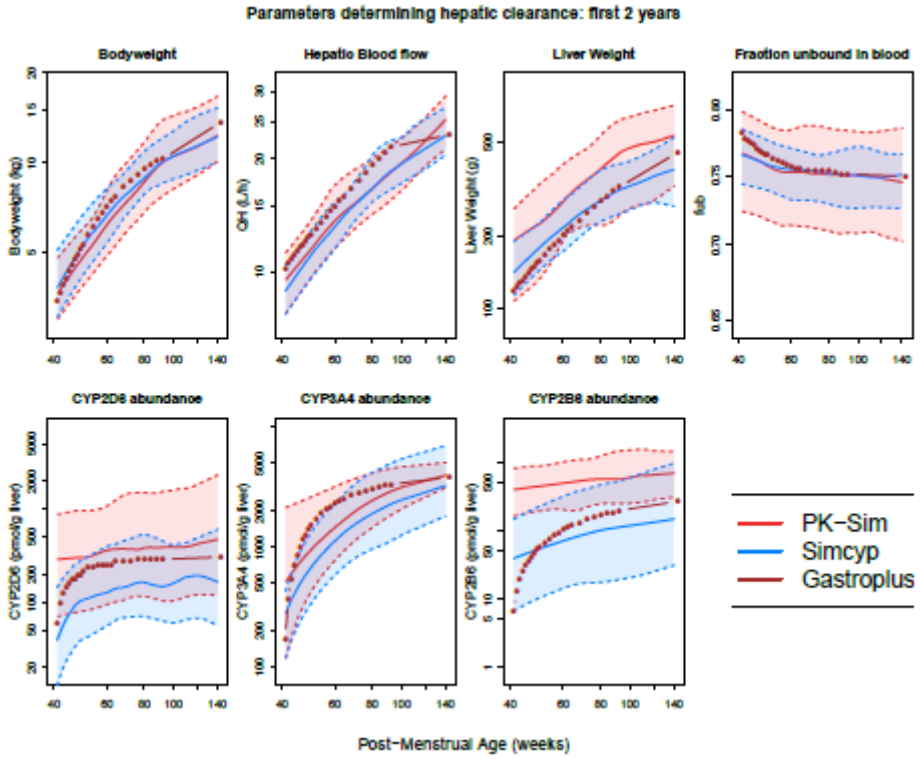

FIGURE 4: ILLUSTRATION OF THE BODYWEIGHT AND THE UNDERLYING PARAMETERS THAT DETERMINE MATURATION OF HEPATIC CLEARANCE AS A FUNCTION OF PMA IN THE FIRST 2 YEARS OF LIFE. MEDIAN ABUNDANCE OF THE CYP2D6, CYP3A4, AND CYP2B6 ENZYMES IS VARIABLE BETWEEN THE SOFTWARE TOOLS. DIFFERENCES IN HEPATIC BLOOD FLOW AND LIVER WEIGHT ARE PRESENT AS WELL, ALTHOUGH THE MATURATION TREND IS SIMILAR.

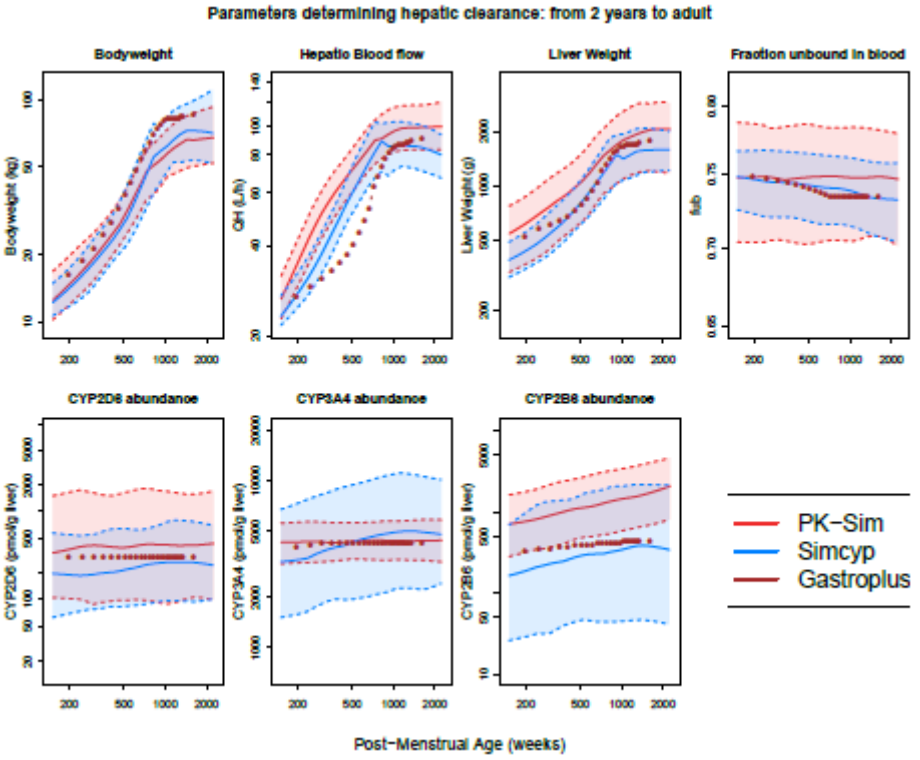

FIGURE 5: ILLUSTRATION OF THE BODYWEIGHT AND THE UNDERLYING PARAMETERS THAT DETERMINE MATURATION OF HEPATIC CLEARANCE AS A FUNCTION OF PMA FROM 2 YEARS TO ADULTHOOD. STILL DIFFERENCES ARE OBSERVED IN MATURATION FOR CYP3A4 AND CYP2B6, WHILE CYP2D6 SEEMS TO HAVE STABILIZED. AN IMPORTANT DIFFERENCE IN HEPATIC BLOOD FLOW IS OBSERVED IN GASTROPLUS AS, COMPARED TO THE OTHER MODELS.

6

5 DISCUSSION

The three most extensive and broadly applied PBPK M&S software tools (PK-Sim®, Simcyp®, Gastroplus®) were evaluated at the level of their system's properties for predicting changes in pediatric PK. To this end, a retrograde clearance model for tramadol was created for each software tool. Using the physiological information, contained in each software package (Table 1, 'Parameters used for retrograde calculation'), an intrinsic clearance at the level of the contributing CYP enzyme was calculated with the well-stirred liver model (Table 1, 'PBPK Input Parameters'). *In vivo* information about the tramadol total and CYP2D6 clearance was available from Allegaert et al [30]. 43% of the hepatic clearance could be attributed to CYP2D6. Based on a previous study [43], described in Chapter 5, the remaining 57% was subdivided into 47% CYP3A4 and 10% CYP2B6. Since the popPK model did not provide an estimate for the adult renal clearance, it was extracted from an internal Grünenthal Research Report and was scaled down using GFR maturation for Simcyp® and PK-Sim®, and kidney blood flow for Gastroplus®. As is described in the methods section and presented in the results section, each retrograde clearance model for each PBPK software was qualified for the adult predictions in terms of total, CYP2D6, and renal tramadol clearance (Table 2).

After qualification of the adult clearance models, 7 different age groups were defined for the pediatric predictions (see methods section). In PK-Sim® and Simcyp®, the clearance for every pediatric age group was predicted using a virtual population of 1000 subjects from that age category. In Gastroplus®, instead of virtual populations, a virtual population representative, i.e. the typical individual, was used for the predictions. Next, the total and CYP2D6 tramadol clearance predictions were compared to the estimated maturation profiles from a pooled popPK study by Allegaert et al. [30], depicted in Figure 1. The comparison of the *in vivo* and *in silico* maturation profiles of total and CYP2D6 clearance was first evaluated per age group and is illustrated, per software, in the *Appendix*. When comparing the total, CYP2D6 and renal tramadol clearance over the complete lifespan, specific attention was given to the developments in the first 2 years of age. What drives the difference between these clearance predictions? First of all, there is a difference in the ontogeny function for CYP2D6 at the level of the CYP2D6 fractional activity to adult. The equations describing this ontogeny are identical in Simcyp® and Gastroplus® and were previously described by Johnson et al. [11]. The ontogeny function for CYP2D6 within PK-Sim® assumes that maturation takes places *in utero* and is graphically represented in the *Appendix* in Figure A1. As a consequence, the CYP2D6 clearance does not have the typical maturation shape for term neonates. Second, the notably longer maturation half-life for Simcyp® CYP2D6 clearance originates from the MPPGL maturation model, not present in the two other PBPK packages. Based on these findings, tramadol CYP2D6 clearance maturation seems best described assuming an progressively matured CYP2D6 enzyme activity at birth (without MPGGL maturation). Very recently, this finding is

independently confirmed by another group using propafenone as an *in vivo* probe for CYP2D6 activity [44]. The CYP3A4 clearance is in good agreement between the different software packages. There is of course a lot of data available for CYP3A4, making it a well characterized CYP enzyme. Maturation occurs later compared to CYP2D6, with adult CYP3A4 activity present around 2 years of age. The maturation differences in CYP2B6 clearance between the softwares cannot be solely attributed to the underlying physiological information. CYP2B6 ontogeny is implemented in Gastroplus® and Simcyp® as described in [11]. Since PK-Sim® does not provide, at this time, an ontogeny function for CYP2B6, it was user-provided. As described in the methods section, for PK-Sim®, the CYP2B6 maturation function was fitted as an exponential function to the dataset from [38]. Next, it was integrated into PK-Sim® with the associated variability from the dataset (geometric standard deviation of 1.7), an analogous procedure as for other enzyme ontogeny functions. However, this geometric standard deviation was initially estimated as 5.12, given the huge variability in the dataset. It was reduced to 1.7 for the predictions since higher values provided technical issues in qualifying the adult retrograde model. These issues associated with a high CYP2B6 variability were also visible from the Simcyp® adult model results – for Simcyp®, the variability was not changed since here it is assumed to result from an underlying CYP2B6 polymorphism . The $CLint_{2B6}$, which *in vivo* represents 10% of the total hepatic CLint, is calculated to contribute only 6% (median) to the predicted hepatic clearance with an associated broad 90% prediction interval (Table 2). As confirmation, the predicted CYP2B6 contribution aligns again with *in vivo* if the highly-skewed variability is progressively reduced in the predictions (data not shown). Furthermore, although the ontogeny function for CYP2B6 is the same in Simcyp® and Gastroplus®, again the high variability masks this maturation trend in the CYP2B6 clearance prediction of Simcyp® (Figure 3). Renal clearance prediction is in line with *in vivo* observations, except for the first 4 weeks of age in the Gastroplus® software (Figure 2). This difference is further illustrated in Figure 3. The maturation in GFR accounts for the changing elimination capacity of the kidneys over time. Since in Gastroplus®, the renal clearance could not be described as an arbitrary fraction of GFR, we chose a fraction of the kidney blood flow as surrogate. The renal clearance is initially high and decreases in Gastroplus®, whereas it more slowly matures in PK-Sim® and Simcyp®. The reason for the overprediction in Gastroplus® might be that the filtration capacity depends on more than just blood flow (e.g. also on the vascular resistance [10]). Therefore, GFR is the better predictor for maturation of the renal elimination function. We should however be cautious with interpreting the data for tramadol renal clearance since this maturation function i) is based on only 9 subjects, and ii) was not estimated as part of the population PK model.

Because of the strict *a priori* distinction of drug- and system-specific information, PBPK M&S allows to investigate critical processes underlying drug disposition beyond compound-specific pharmacokinetic properties. The underlying physiological information that determines the hepatic extraction of tramadol,

is provided for the first 2 years of life (Figure 4) and beyond (Figure 5). The different clearances, as subdivided in Figure 3, are the resultant of CYP ontogeny, liver weight, and to a minor extent fraction unbound in blood and hepatic blood flow. Note the high correlation between the CYP abundance profiles and the maturation of the different clearance pathways, indicating a typical behavior for low extraction compounds. Notably, although the unbound fraction in blood is an important parameter for low hepatic extraction compounds, tramadol displays low plasma protein binding (fup= 80%). Therefore, a change in plasma protein binding will hardly affect the unbound fraction.

The concentrations that drive drug ADME *in vivo* are unbound drug concentrations. Moreover, in order to correctly capture hepatic clearance, an accurate prediction of the unbound intracellular hepatocyte concentration is required. Each evaluated software package has its own philosophy on how to handle the prediction of these hepatocyte unbound drug concentrations. The default model in Simcyp® and Gastroplus® is a hepatic well-stirred liver model, which is perfusion rate-limited. Unbound, unionized drug concentrations instantaneously cross the hepatocyte membrane, so that they are the same in hepatocytes and plasma. In Simcyp®, it is this concentration that drives metabolism. In Gastroplus®, unbound (ionized + unionized) concentrations, as calculated by the Rodgers and Rowland equations, drive metabolism, independent of the distribution model chosen. The consequence is that, by default, ionization has an important effect on drug elimination in Gastroplus®, but not in Simcyp®. The modeler should be aware of this difference when scaling up *in vitro* data to *in vivo* (IVIVE). In PK-Sim®, the kinetics of drugs distributing to tissues are handled by P*SA (P= permeability, SA= surface area of the tissue), while the extent of tissue distribution of drugs is defined by the tissue-to-plasma partition coefficient. In this philosophy, there is no arbitrary division between perfusion or permeability limitations. Depending on which step is fastest, P*SA or blood flow, permeability or perfusion-limited behavior will occur *in silico*. Although the methods for calculation of the permeability parameters are described in [45], they are usually unknown and rarely accessible directly.

Virtual populations of individuals created in the different software packages are different. Not necessarily at the anthropometric level (NHANES), but in the physiology that is used to build the underlying structure of the virtual system. The reason for this lies in the implementation of different literature sources and datasets (see methods section). The effect is most visible in the younger pediatric ages where data are often highly variable and sparse. Furthermore, the concentration of CYP enzymes in liver samples that determine *in vivo* abundancies, still is obtained using semi-quantitative techniques (e.g. Western blots). This also results in uncertainty about which CYP concentrations to use in the IVIVE (Table 1, enzyme liver concentrations). Some groups have already started quantitative LC-MSMS analyses in order to measure *in vivo* concentrations of proteins [46, 47]. In addition, concerning the

PBPK distribution model, accurate and precise measurement of cardiac output and blood flows to the different tissues is difficult to achieve, let alone defining the relative changes that occur in pediatric life.

In conclusion, all PBPK software tools were able to predict the total and CYP2D6-related clearance maturation within 2-fold of the observed maturation profile, between 2 years of age and adulthood. In neonates and infants, clearance prediction was not always within 2-fold for every software and varied largely between the packages. Interestingly, the PBPK tool with the shortest CYP2D6 maturation half-life (PK-Sim®), provided the best prediction of *in vivo* CYP2D6 clearance maturation. Very recently, this finding was confirmed by another group, which derived an *in vivo* ontogeny function from *in vivo* propafenone data [44]. Although two independent research groups reaching the same conclusion with different approaches, strengthens this result, investigating more compounds would still be needed to further validate our findings. All physiological information required to build virtual subjects is publically available. However, there still is a significant difference in the data sources that are used per software package, leading to marked differences in predicted PK parameters. Consensus on the selection of the best pediatric data to use, should help to harmonize and optimize pediatric clearance predictions.

6

6 REFERENCES

1. Teorell T. Kinetics of distribution of substances administered to the body. I. The extravascular modes of administration. Arch Int Pharmacodyn Ther. 1937(57):202-5.

2. Barrett JS, Della Casa Alberighi O, Laer S, Meibohm B. Physiologically based pharmacokinetic (PBPK) modeling in children. Clin Pharmacol Ther. 2012;92(1):40-9.

3. Jamei M, Marciniak S, Feng K, Barnett A, Tucker G, Rostami-Hodjegan A. The Simcyp Population-based ADME Simulator. Expert Opinion on Drug Metabolism & Toxicology. 2009;5(2):211-23.

4. Johnson TN, Rostami-Hodjegan A. Resurgence in the use of physiologically based pharmacokinetic models in pediatric clinical pharmacology: parallel shift in incorporating the knowledge of biological elements and increased applicability to drug development and clinical practice. Paediatr Anaesth. 2010;21(3):291-301.

5. Bouzom F, Walther B. Pharmacokinetic predictions in children by using the physiologically based pharmacokinetic modelling. Fundam Clin Pharmacol. 2008;22(6):579-87.

6. Haddad S, Restieri C, Krishnan K. Characterization of age-related changes in body weight and organ weights from birth to adolescence in humans. J Toxicol Environ Health A. 2001;64(6):453-64.

7. ICRP. Basic anatomical and physiological data for use in radiological protection: reference values. A report of age- and gender-related differences in the anatomical and physiological characteristics of reference individuals. ICRP Publication 89. Ann ICRP. 2002;32(3-4):5-265.

8. Johnson TN, Tucker GT, Tanner MS, Rostami-Hodjegan A. Changes in liver volume from birth to adulthood: a meta-analysis. Liver Transpl. 2005;11(12):1481-93.

9. Price K, Haddad S, Krishnan K. Physiological modeling of age-specific changes in the pharmacokinetics of organic chemicals in children. J Toxicol Environ Health A. 2003;66(5):417-33.

10. Edginton AN, Schmitt W, Voith B, Willmann S. A mechanistic approach for the scaling of clearance in children. Clin Pharmacokinet. 2006;45(7):683-704.

11. Johnson TN, Rostami-Hodjegan A, Tucker GT. Prediction of the clearance of eleven drugs and associated variability in neonates, infants and children. Clin Pharmacokinet. 2006;45(9):931-56.

12. Third National Health and Nutrition Examination Survey (NHANES III). In: National Center for Health Statistics Hyattsville MU, editor.; 1997.

13. Willmann S, Hohn K, Edginton A, Sevestre M, Solodenko J, Weiss W, et al. Development of a physiology-based whole-body population model for assessing the influence of individual variability on the pharmacokinetics of drugs. J Pharmacokinet Pharmacodyn. 2007;34(3):401-31.

14. Rhodin MM, Anderson BJ, Peters AM, Coulthard MG, Wilkins B, Cole M, et al. Human renal function maturation: a quantitative description using weight and postmenstrual age. Pediatr Nephrol. 2009;24(1):67-76.

15. Schwartz GJ, Feld LG, Langford DJ. A simple estimate of glomerular filtration rate in full-term infants during the first year of life. J Pediatr. 1984;104(6):849-54.

16. Schwartz GJ, Haycock GB, Edelmann CM, Jr., Spitzer A. A simple estimate of glomerular filtration rate in children derived from body length and plasma creatinine. Pediatrics. 1976;58(2):259-63.

17. Traub SL, Johnson CE. Comparison of methods of estimating creatinine clearance in children. Am J Hosp Pharm. 1980;37(2):195-201.

18. Murthy BV, Pandya KS, Booker PD, Murray A, Lintz W, Terlinden R. Pharmacokinetics of tramadol in children after i.v. or caudal epidural administration. Br J Anaesth. 2000;84(3):346-9.

19. Garrido MJ, Habre W, Rombout F, Troconiz IF. Population pharmacokinetic/pharmacodynamic modelling of the analgesic effects of tramadol in pediatrics. Pharm Res. 2006;23(9):2014-23.

20. Bressolle F, Rochette A, Khier S, Dadure C, Ouaki J, Capdevila X. Population pharmacokinetics of the two enantiomers of tramadol and O-demethyl tramadol after surgery in children. Br J Anaesth. 2009;102(3):390-9.

21. Lintz W, Barth H, Becker R, Frankus E, Schmidt-Bothelt E. Pharmacokinetics of tramadol and bioavailability of enteral tramadol formulations - 2nd communication: Drops with ethanol. Arzneimittel-Forschung. 1998;48(5):436-45.

22. Lintz W, Barth H, Osterloh G, Schmidt-Bothelt E. Pharmacokinetics of tramadol and bioavailability of enteral tramadol formulations - 3rd communication: Suppositories. Arzneimittel-Forschung. 1998;48(9):889-99.

23. Lintz W, Becker R, Gerloff J, Terlinden R. Pharmacokinetics of tramadol and bioavailability of enteral tramadol formulations - 4th Communication: Drops (without ethanol). Arzneimittel-Forschung. 2000;50(2):99-108.

24. Lintz W, Erlacin S, Frankus E, Uragg H. Metabolismus von tramadol bei mensch und tier. Arzneimittel-Forschung. 1981;31(11):1932.

25. Allegaert K, van den Anker JN, de Hoon JN, van Schaik RH, Debeer A, Tibboel D, et al. Covariates of tramadol disposition in the first months of life. Br J Anaesth. 2008;100(4):525-32.

26. Allegaert K, Anderson BJ, Verbesselt R, Debeer A, de Hoon J, Devlieger H, et al. Tramadol disposition in the very young: an attempt to assess in vivo cytochrome P-450 2D6 activity. Br J Anaesth. 2005;95(2):231-9.

27. Pedersen RS, Damkier P, Brosen K. Enantioselective pharmacokinetics of tramadol in CYP2D6 extensive and poor metabolizers. Eur J Clin Pharmacol. 2006;62(7):513-21.

28. Stamer UM, Musshoff F, Kobilay M, Madea B, Hoeft A, Stuber F. Concentrations of Tramadol and O-desmethyltramadol Enantiomers in Different CYP2D6 Genotypes. Clin Pharmacol Ther. 2007;82(1):41-7.

29. Grond S, Sablotzki A. Clinical pharmacology of tramadol. Clin Pharmacokinet. 2004;43(13):879-923.

30. Allegaert K, Holford N, Anderson BJ, Holford S, Stuber F, Rochette A, et al. Tramadol and o-desmethyl tramadol clearance maturation and disposition in humans: a pooled pharmacokinetic study. Clin Pharmacokinet. 2015;54(2):167-78.

31. Dickins M, van de Waterbeemd H. Simulation models for drug disposition and drug interactions. Drug Discovery Today: BIOSILICO. 2004;2(1):38-45.

32. Willmann S, Lippert J, Sevestre M, Solodenko J, Fois F, Schmitt W. PK-Sim®: a physiologically based pharmacokinetic 'whole-body' model. BIOSILICO. 2003;1(4):121-4.

33. Zanger UM, Fischer J, Raimundo S, Stuven T, Evert BO, Schwab M, et al. Comprehensive analysis of the genetic factors determining expression and function of hepatic CYP2D6. Pharmacogenetics. 2001;11(7):573-85.

34. Rodgers T, Leahy D, Rowland M. Physiologically based pharmacokinetic modeling 1: Predicting the tissue distribution of moderate-to-strong bases. J Pharm Sci. 2005;94(6):1259-76.

35. Rodrigues AD. Integrated cytochrome P450 reaction phenotyping: attempting to bridge the gap between cDNA-expressed cytochromes P450 and native human liver microsomes. Biochem Pharmacol. 1999;57(5):465-80.

36. Stevens JC, Marsh SA, Zaya MJ, Regina KJ, Divakaran K, Le M, et al. Developmental changes in human liver CYP2D6 expression. Drug Metab Dispos. 2008;36(8):1587-93.

37. Treluyer JM, Jacqz-Aigrain E, Alvarez F, Cresteil T. Expression of CYP2D6 in developing human liver. Eur J Biochem. 1991;202(2):583-8.

38. Pearce RE, Gaedigk R, Twist GP, Dai H, Riffel AK, Leeder JS, et al. Developmental Expression of CYP2B6: A Comprehensive Analysis of mRNA Expression, Protein Content and Bupropion Hydroxylase Activity and the Impact of Genetic Variation. Drug Metab Dispos. 2016;44(7):948-58.

39. Rostami-Hodjegan A, Tucker GT. Simulation and prediction of in vivo drug metabolism in human populations from in vitro data. Nat Rev Drug Discov. 2007;6(2):140-8.

40. Salem F, Johnson TN, Abduljalil K, Tucker GT, Rostami-Hodjegan A. A re-evaluation and validation of ontogeny functions for cytochrome P450 1A2 and 3A4 based on in vivo data. Clin Pharmacokinet. 2014;53(7):625-36.

41. Yeo KR. Abundance of cytochromes P450 in human liver: a meta-analysis. Br J Clin Pharmacol. 2004;57(5):687-8.

42. Barter ZE, Chowdry JE, Harlow JR, Snawder JE, Lipscomb JC, Rostami-Hodjegan A. Covariation of human microsomal protein per gram of liver with age: absence of influence of operator and sample storage may justify interlaboratory data pooling. Drug Metab Dispos. 2008;36(12):2405-9.

43. T'Jollyn H, Snoeys J, Vermeulen A, Michelet R, Cuyckens F, Mannens G, et al. Physiologically Based Pharmacokinetic Predictions of Tramadol Exposure Throughout Pediatric Life: an Analysis of the Different Clearance Contributors with Emphasis on CYP2D6 Maturation. AAPS J. 2015;17(6):1376-87.

44. Upreti VV, Wahlstrom JL. Meta-analysis of hepatic cytochrome P450 ontogeny to underwrite the prediction of pediatric pharmacokinetics using physiologically based pharmacokinetic modeling. J Clin Pharmacol. 2016;56(3):266-83.

45. Kawai R, Lemaire M, Steimer J-L, Bruelisauer A, Niederberger W, Rowland M. Physiologically based pharmacokinetic study on a cyclosporin derivative, SDZ IMM 125. J Pharmacokinet Biopharm. 1994;22(5):327-65.

46. Russell MR, Achour B, McKenzie EA, Lopez R, Harwood MD, Rostami-Hodjegan A, et al. Alternative fusion protein strategies to express recalcitrant QconCAT proteins for quantitative proteomics of human drug metabolizing enzymes and transporters. J Proteome Res. 2013;12(12):5934-42.

47. Prasad B, Gaedigk A, Vrana M, Gaedigk R, Leeder JS, Salphati L, et al. Ontogeny of hepatic drug transporters as quantified by LC-MS/MS proteomics. Clin Pharmacol Ther. 2016;AOP.

7 APPENDIX

7.1 PK-SIM ONTOGENY FUNCTIONS FOR

7.1.1 CYP2D6

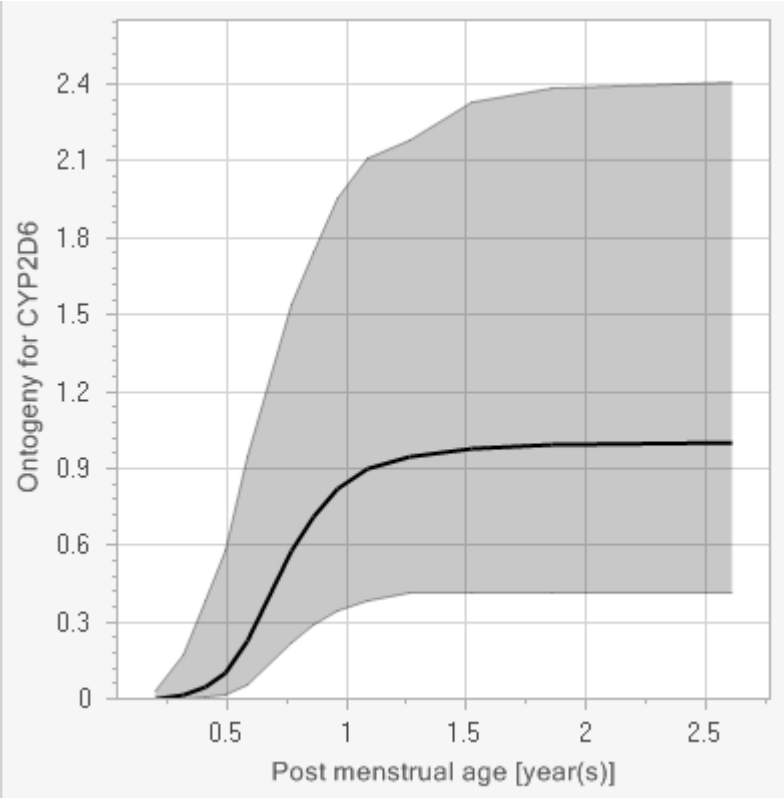

Figure A1: Ontogeny function for CYP2D6 in PK-Sim® versus PMA in years. The maturation half-life for CYP2D6 is much faster than estimated by Johnson et al, 2006. At term age, a newborn is 40 weeks or 0.77 years PMA, coinciding with a CYP2D6 fractional activity of about 70% relative to adult.

7.1.2 CYP2B6 (EXTRACTED FROM CURRENT LITERATURE)

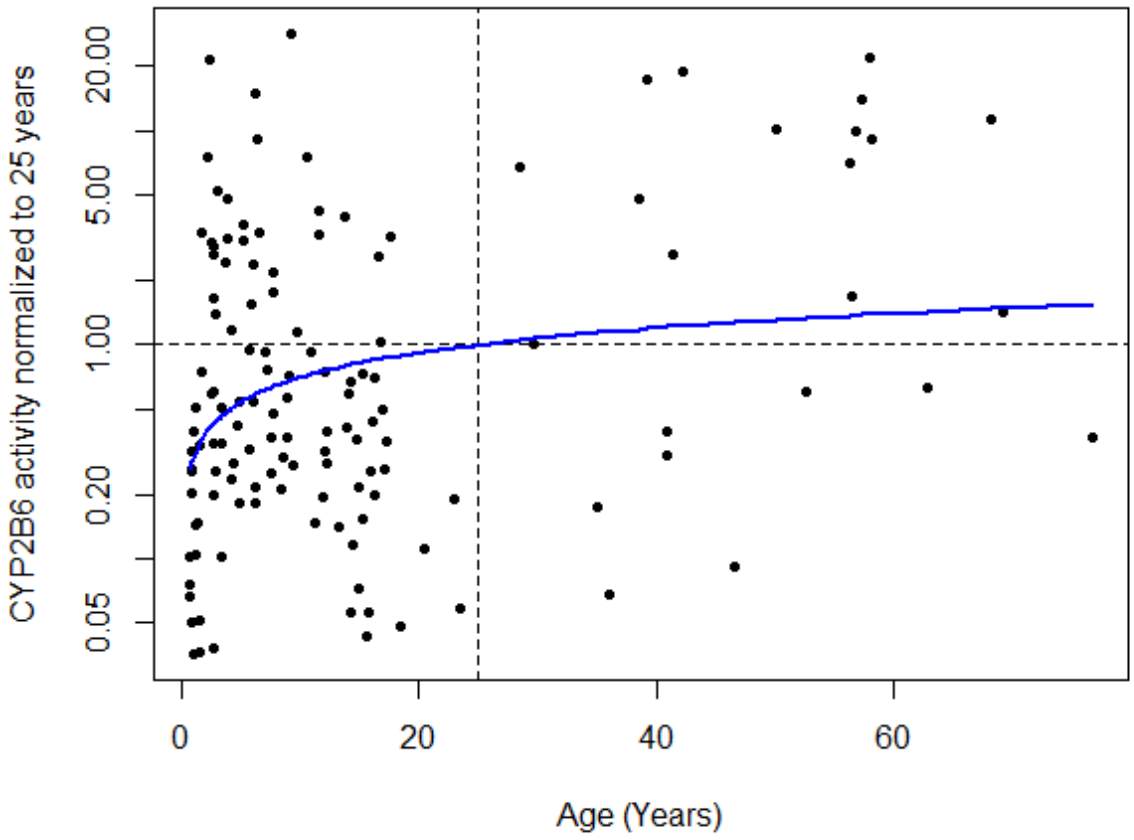

Figure A2: CYP2B6 activity data from Pearce et al., 2016 were digitized and were modeled in order to extract an ontogeny model for CYP2B6 in PK-Sim®. Next, the data were normalized to the activity at 25 years to obtain a relative activity value to adults.

7.2 PEDIATRIC PBPK PREDICTIONS PER AGE CATEGORY AND PER SOFTWARE

7.2.1 PK-SIM

7.2.1.1 TOTAL CLEARANCE

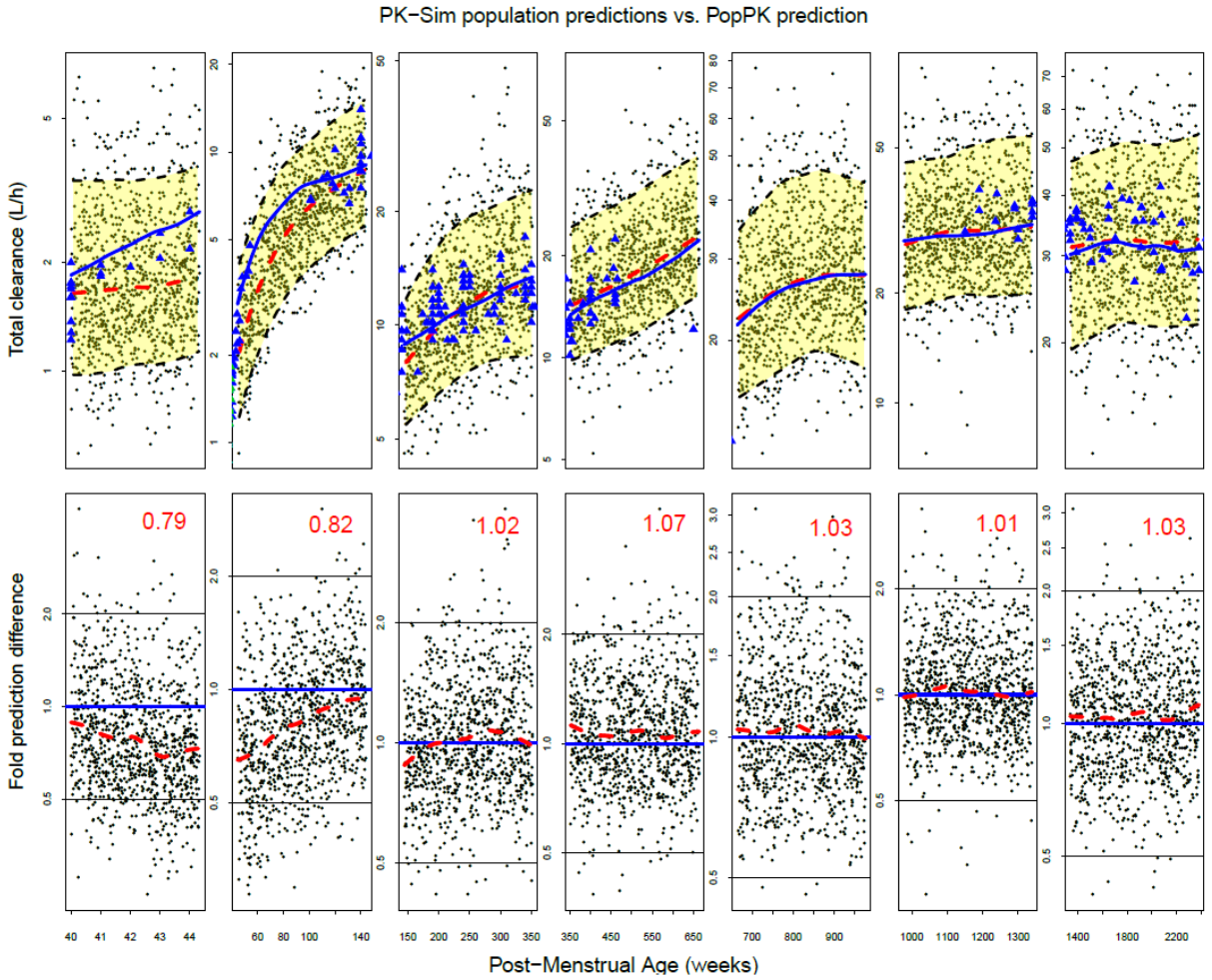

7.2.1.2 CYP2D6 CLEARANCE

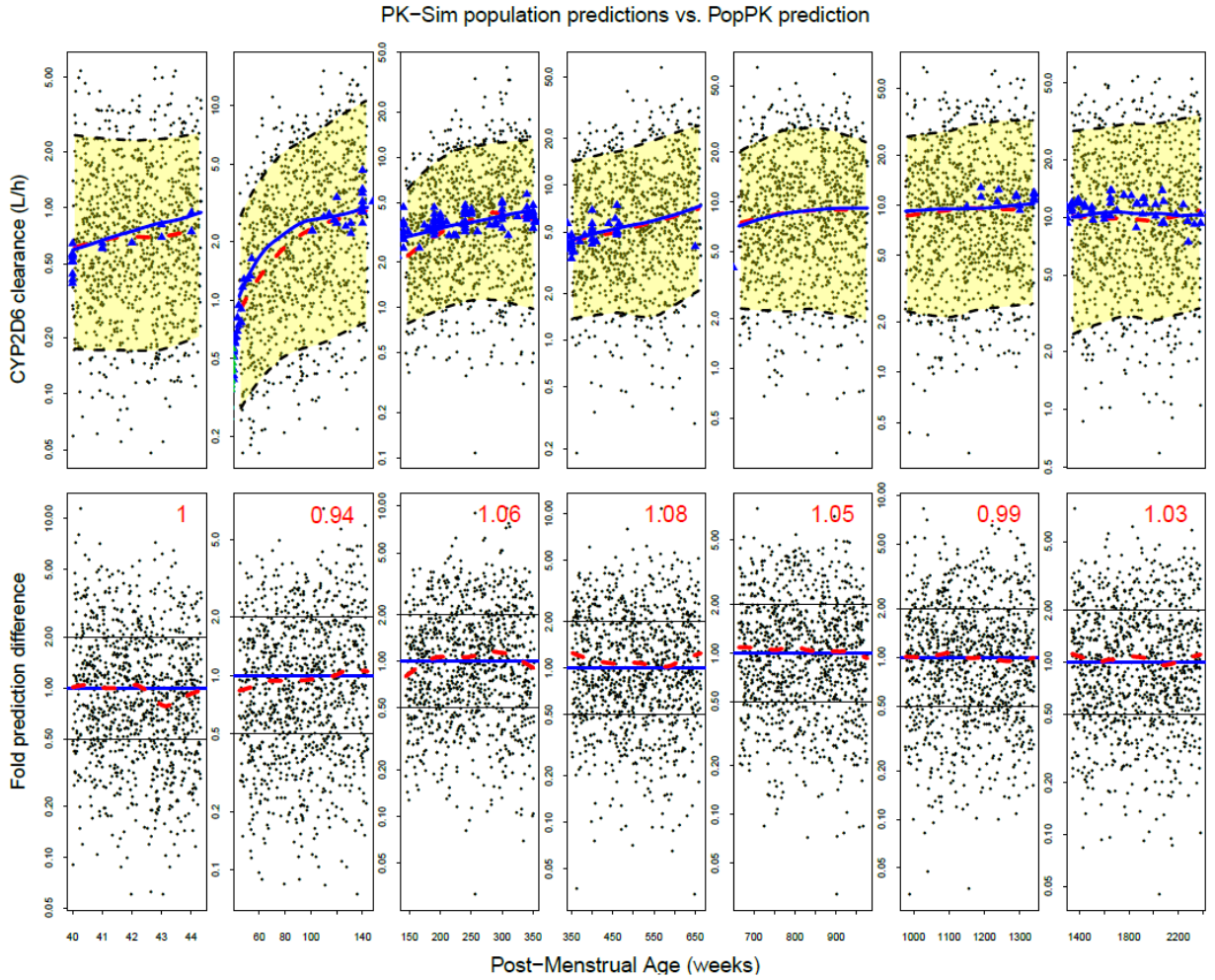

7.2.2 SIMCYP

7.2.2.1 TOTAL CLEARANCE

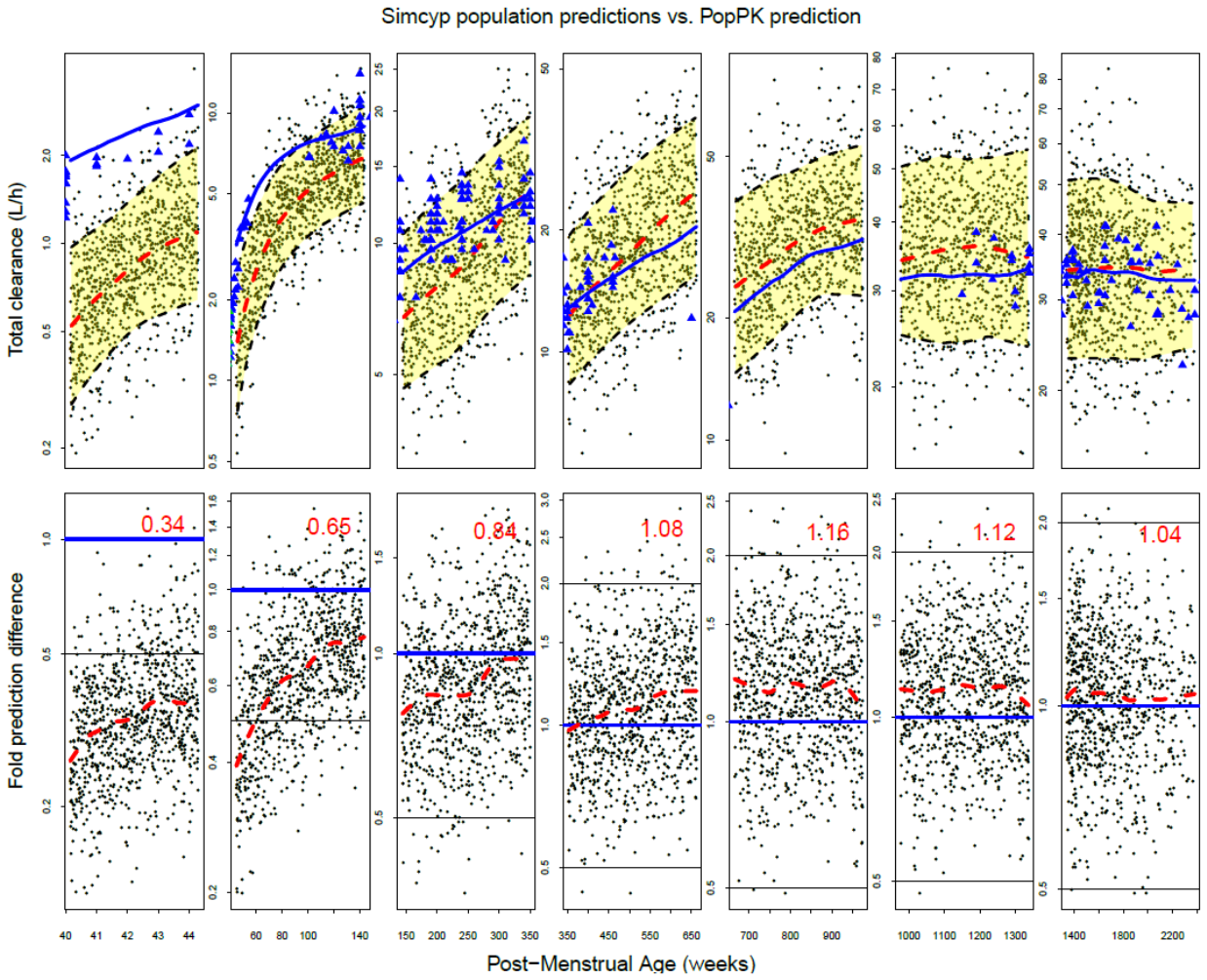

7.2.2.2 CYP2D6 CLEARANCE

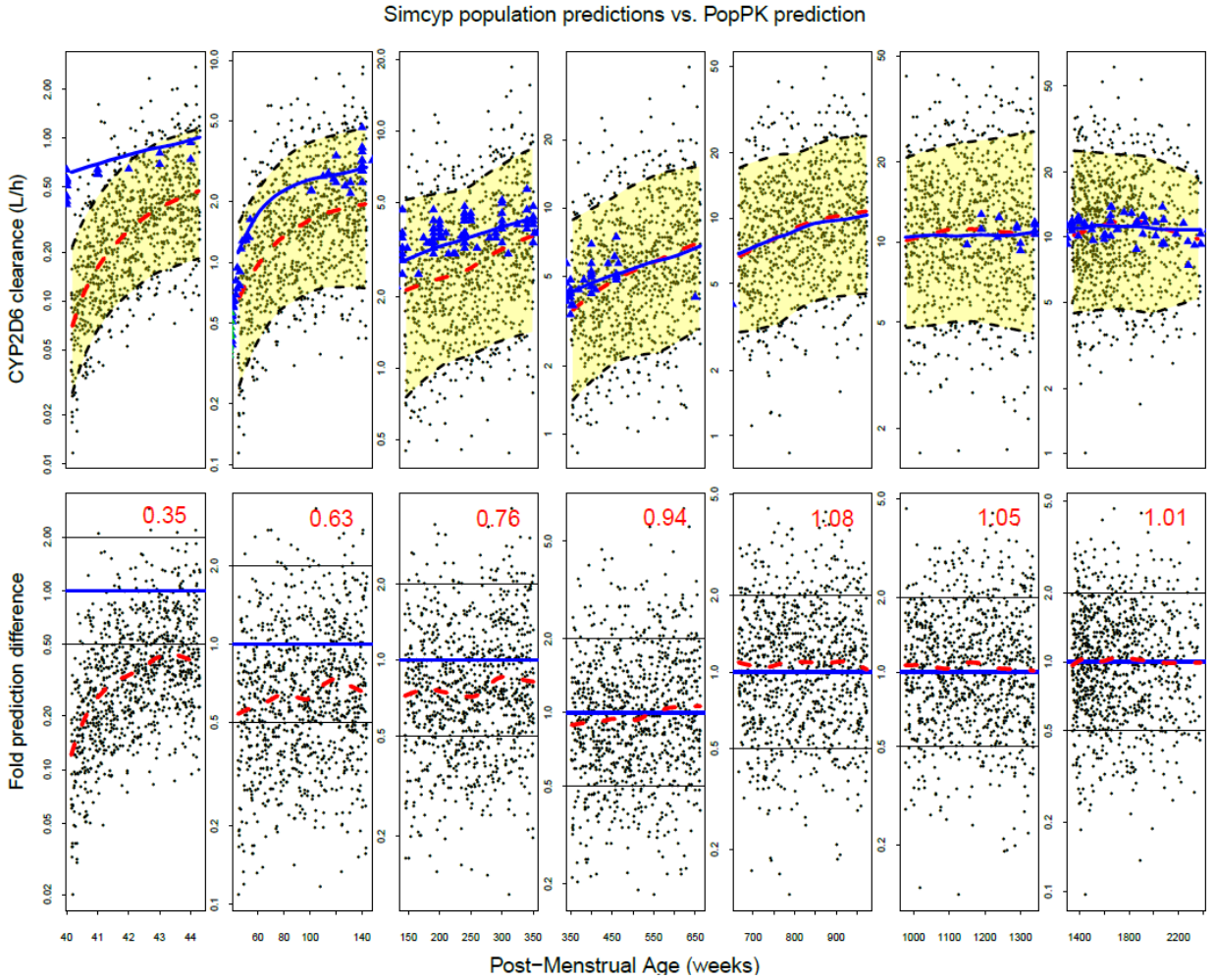

7.2.3 GASTROPLUS

7.2.3.1 TOTAL CLEARANCE

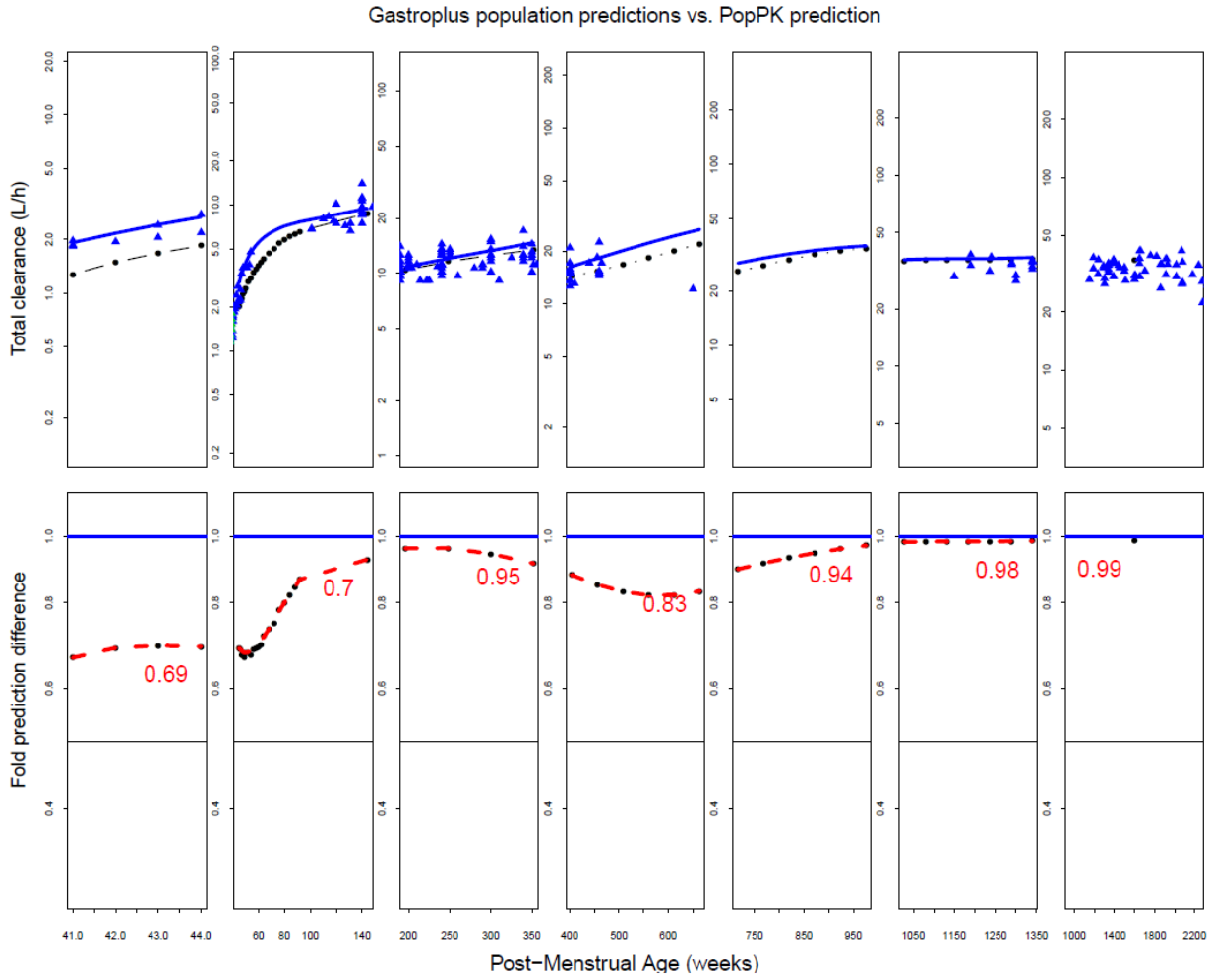

7.2.3.2 CYP2D6 CLEARANCE

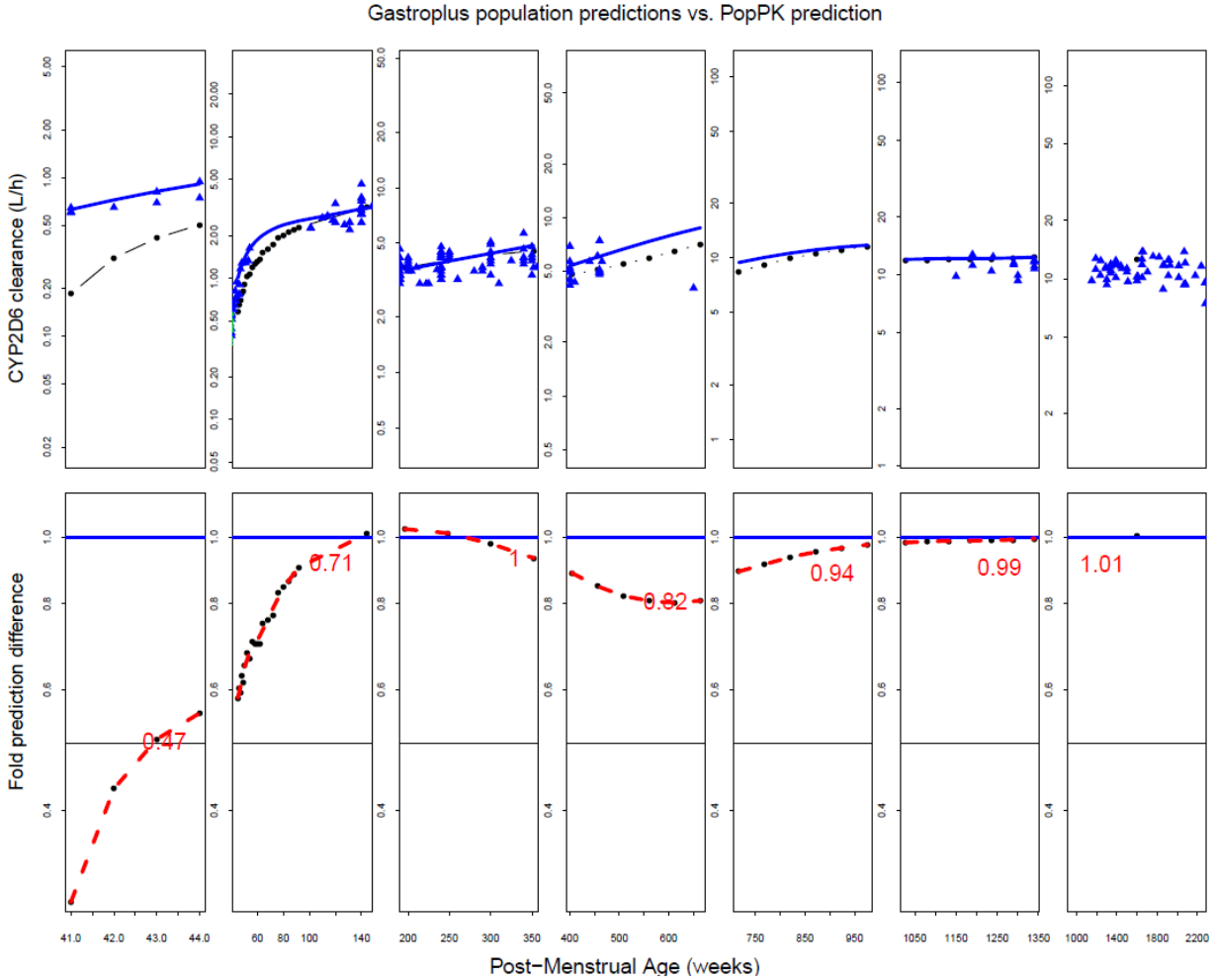

CHAPTER 7

GENERAL DISCUSSION AND CONCLUSION

7

TABLE OF CONTENTS

7

1 INTRODUCTION

Children represent a vulnerable population for drug treatment, and it is important to get the dose right in order to ensure optimal treatment effects while at the same time avoiding side effects/toxicity. Both in pediatric drug development as well as in off-label drug use, the pediatric drug dose may be extrapolated from adults by scaling the pharmacokinetic (PK) parameters [1]. Generally, scaling of PK parameters is done according to allometric principles using body weight or body surface area, either linearly (for volumes) or exponentially (for clearances) [2]. However, especially in the first few years of life, the biochemical and physiological properties in children are changing non-linearly with bodyweight or body surface area. Recent analyses have pointed out that these methods are not suited to extrapolate the adult dose over the entire pediatric age range and that these scaling methods should be used with caution [3]. The optimal way to predict pharmacokinetic changes over the complete pediatric age range, and by extension over the human life span from pediatrics to geriatrics, is by integrating the biochemical and physiological changes occurring in each stage of life *a priori* in the predictions. This may be achieved by developing and verifying pediatric physiologically-based pharmacokinetic (PBPK) models. PBPK models do combine pediatric physiological information with drug-specific information in a mechanistic way, in order to predict the exposure to xenobiotics in neonates, infants, and children.

Although many successful pediatric PBPK applications exist, limitations in and inconsistencies between *in silico* predictions and *in vivo* observations do sometimes emerge [4]. In order to identify and address current methodological and/or data information gaps, the general aim of the work described in this thesis was to perform an in-depth **evaluation of the PBPK approach for a reliable bottom-up clearance prediction of the model compound tramadol in pediatric life**. More specifically, we sought **to identify the underlying reasons for inaccuracies in the predictions** and offer alternative approaches to improve these.

Tramadol was chosen as model compound in order to compare the clearance maturation in children, calculated by applying a bottom-up PBPK approach, with the one obtained using a top-down approach on *in vivo* data. If a PBPK bottom-up approach is applied in in a pediatric context, a specific workflow is required [5], which is in line with the different objectives of the current work. As a **first** step in the development of a pediatric bottom-up clearance model for tramadol, an adult clearance model has to be constructed. This clearance model mechanistically represents the different elimination pathways of tramadol in adults. Therefore, *in vitro* metabolism experiments were conducted and the relative importance of each individual liver enzyme in the hepatic clearance was assessed. By verifying the bottom-up clearance predictions against observed adult *in vivo* data, the adult clearance model is said to be 'qualified'. For this specific application, the model was qualified in terms of absolute total clearance prediction, as well as the CYP2D6 and renal contributions to it (Objectives 1 & 2). **Second**, this

qualified clearance model was used for predicting maturation in the clearance over the pediatric age range. In essence, the drug-related data are retained from the qualified adult model, but the physiological data now represents a pediatric population *in silico*. Changes in this physiological data, relative to the adult, include ontogeny of enzymes/transporters, altered tissue composition, tissue volumes and blood flows. Finally, these pediatric (bottom-up) clearance predictions were compared to a (top-down) derived clearance maturation function using *in vivo* observed pediatric data. For the latter goal, the total, CYP2D6 and renal tramadol clearance were investigated (Objectives 3 & 4).

7

2 BOTTOM-UP INVESTIGATION OF TRAMADOL ADULT CLEARANCE

2.1 *IN VITRO* METABOLISM INVESTIGATION

In the bottom-up investigation of tramadol clearance, it is absolutely key to obtain a quantitatively solid understanding of the different enzymatic and other pathways contributing to the clearance. Tramadol *in vivo* adult clearance can be subdivided in a renal component (ca. 25%) and hepatic metabolism (75%). In order to characterize this hepatic metabolism, *in vitro* metabolism assays with tramadol were performed in human liver microsomes (HLM) and human recombinant enzyme systems (rhCYP). Results from this analysis are described in Chapter 3. First, the *in vitro* kinetic parameters (Km, Vmax, CLint) describing the formation of the metabolites O-desmethyltramadol (ODT) and N-desmethyltramadol (NDT) were estimated using non-linear regression analysis. The formation rate of NDT (CLint = 1.63 µL/min/mg microsomal protein, MP) seemed to be twice as fast as the formation rate of ODT (CLint = 0.80 µL/min/mg MP), while the Km-value for ODT (57.5 µM) was 4 times lower than that for NDT (242 µM). Although the Km-values could be estimated *in vitro*, the *in vivo* plasma concentrations (max 5 µM after a 100mg i.v. bolus dose) never come close to saturating any of the two metabolizing routes. Hence, the hepatic clearance of tramadol was considered linear and CLint values were used for the bottom-up predictions of the hepatic clearance.

In order to quantify the efficiency with which the substrate is metabolized or its metabolites are formed over an array of substrate concentrations, typically Km and Vmax parameters are determined. As theory states, metabolic efficiency declines with higher substrate concentrations and reaches a plateau value at Vmax. Although this illustration of theory is correct, unintentionally it implies a specific experimental design, i.e. incubation of high substrate concentrations to locate the Vmax. From a physiological angle, there are some points of criticism to make on this approach. In most cases, the drug concentrations interacting with phase I/II enzymes *in vivo*, are below the Km-value [6]. In addition, when incubating poorly soluble compounds *in vitro*, the Vmax at high substrate concentrations might be a combination of enzyme as well as solubility saturation. Therefore, a better approach to obtain reliable *in vitro* metabolism parameters, is to fit a model to the metabolism data, which is a re-arrangement of the Michaelis-Menten equation allows estimation of the parameters intrinsic clearance (CLint) and Km. When applying this alternative approach, the apparent *in vitro* clearance is expected to reach a plateau at the CLint-value for low substrate concentrations instead. An additional advantage is that confidence intervals on the CLint value can be directly estimated from the model. The availability of this confidence interval then allows to implement uncertainty in the prediction of the hepatic clearance. It was this modelling approach that was applied to estimate the CLint and Km values from the HLM and rhCYP metabolism assay data.

In addition, the individual liver enzyme contribution in the formation of the two tramadol metabolites was determined (phenotyping experiment). In the HLM assay, chemical inhibition was used to inhibit specific CYP enzymes, whereas the rhCYP assay can be considered a phenotyping experiment in itself, since only one specific CYP enzyme is expressed. From the chemical inhibition assay, it was concluded that formation of ODT was mainly mediated by CYP2D6 (80%), while NDT formation was mediated in part by CYP3A4 (65%) and in part by CYP2B6 (30%). In the rhCYP assay, the CLint/Km values were determined for the different CYP enzymes involved (CYP2D6, CYP2B6, CYP3A4). Moreover, Inter-System Extrapolation Factors (ISEF) were used to correct for the activity difference between the genetically engineered rhCYP systems and the *ex vivo* prepared HLM [7]. This way, the activity measured in 'artificial' rhCYP assays may be translated to the HLM system, which is assumed to be more representative for the *in vivo* situation. ISEF values were specifically calculated for this experiment. Midazolam and dextromethorphan were incubated alongside tramadol in both *in vitro* assays as probe substrates for CYP3A4 and CYP2D6, respectively. The calculated ISEF value for CYP3A4 was 0.23 and for CYP2D6 0.45. This implies that the activity of CYP3A4 and CYP2D6 is respectively 4.3- and 2.2- times higher in the rhCYP compared to the HLM assay and should be corrected (with the ISEF) to make the data of both assays comparable. We did not include a study-specific CYP2B6 probe in the experiments, because a CYP2B6 probe with adequate *in vivo* data and a straightforward IVIVE was not available at that time. In addition, CYP2B6 was considered a minor contributor to the hepatic clearance of tramadol. Thus, the standard Simcyp® ISEF of 0.43 was used instead.

In vitro phenotyping experiments identify the enzymes involved in a compound's metabolism. On the one hand, the design of a CYP phenotyping experiment in HLM systems implies co-incubation of substrate drug and a chemical inhibitor of a specific CYP-enzyme. These so-called chemical inhibition assays use an *ex vivo* liver matrix, expressing a whole arsenal of enzymes. A major drawback of this approach is selectivity issues, since chemical inhibitors tend to not only inhibit just one CYP enzyme. Although this can be circumvented by using monoclonal antibodies against CYP isoforms, this would heavily increase the cost of such an experiment. Chemical inhibitors for specific enzymes should be incubated at an optimal concentration, high enough to substantially block the enzyme, but not too high to avoid inhibiting more than the enzyme of interest [8]. On the other hand, CYP phenotyping in rhCYP systems studies the interaction between the substrate drug and one specific CYP enzyme in a genetically engineered *in vitro* system, assuring selectivity for only one enzyme. Metabolic activities of recombinant CYP enzymes are often overemphasized, compared to HLM. Although Inter-system extrapolation factors (ISEF), relative activity factors (RAF) or relative expression factors (REF) may be used to correct for this difference, Chen et al., 2011 [9] discussed the inferiority of CYP abundance factors (such as REF) in *in vitro*-to-*in vivo* extrapolation (IVIVE), and the difficulty of using RAF due to variability of CYP abundance

between the HLM and rhCYP systems. This makes the ISEF the correction factor of choice for recombinant enzyme systems, which is the approach we applied in our work.

2.2 MECHANISTIC *IN VITRO*-TO-*IN VIVO* EXTRAPOLATION

Mechanistic IVIVE is a technique used to predict the organ (liver) clearance based on data obtained from (sub)cellular *in vitro* metabolism assays. Drug-specific factors Km, Vmax, and CLint are combined with physiological information in order to mechanistically scale the *in vitro* metabolism parameters to a hepatic *in vivo* clearance. Since the physiological information, used for this purpose, is fully integrated in the PBPK-M&S platform Simcyp®, the latter was used for the IVIVE. IVIVE clearance models were constructed by supplying the *in vitro* metabolism data from the two assays (HLM and rhCYP), described in the previous section. In addition, a retrograde clearance model was set up that uses *in vivo* phenotypic information to derive contributions for different elimination pathways. In this retrograde clearance model, the CYP2D6 contribution was calculated from the difference in tramadol hepatic clearance between CYP2D6 poor and extensive metabolizers. Besides, the CYP2B6 contribution was determined using a clinical trial simulation approach mimicking a tramadol drug-drug interaction study with co-administration of rifampicin to induce the CYP2B6 activity. Details on the construction of the IVIVE and retrograde clearance models are presented in Chapter 3.

In the initial bottom-up extrapolation from *in vitro* to *in vivo*, the 2 IVIVE clearance models (from HLM and rhCYP data) underpredicted the absolute clearance value more than 2-fold and the CYP enzyme contributions were not in line with *in vivo* CYP contributions. Two underlying issues, creating this apparent mismatch, were identified. First, concerning the underprediction of the hepatic clearance, papers by Berezhkovskiy [10] and Hallifax [11] suggested an intracellular accumulation for basic amines (such as tramadol) in hepatocytes due to the pH difference across the hepatocyte membrane. However, in scientific literature, there is still debate whether the value of the cytosolic pH is 7.0 or rather 7.2. Depending on the pH difference across the membrane and taking into account tramadol's pKa (9.41), an intracellular accumulation of 2.5- or 1.58-fold is expected for intracellular pH-values of 7.0 and 7.2, respectively. Since the sensitivity analysis in Chapter 3 pointed out that the hepatic accumulation factor greatly influences the prediction of the hepatic clearance, it was decided to use a factor of 1.58 in the simulations, since it is the more conservative and thus 'safer' option for the prediction of the clearance. Second, in order to investigate the disagreement in CYP contributions between *in vitro* and *in vivo*, a separate study was set up (Chapter 4). In this study, probe substrates midazolam (CYP3A4) and dextromethorphan (CYP2D6) were used to determine the batch-specific enzyme activity in pooled HLM, used for the tramadol experiments. The measured batch-specific CYP2D6 and CYP3A4 enzyme activities in HLM were compared to the enzyme activity, typically expected for a representative healthy volunteer.

This typically expected activity was calculated from *in vivo* data, using a retrograde modelling approach. The results indicate that while CYP3A4 activity was well contained *in vitro* and only deviated 10% from the expected population activity value, measured CYP2D6 HLM activity appeared to have decreased by 2-fold. In other words, when translating these findings to predict tramadol's *in vivo* metabolism, the CYP2D6 contribution should have been higher than initially estimated. Although pooled HLM (n=50) were used for the experiments, the CYP2D6 batch-specific enzyme activity did not represent the average population activity. The lot-to-lot variability was determined by the supplier as a function of the number of donors, using Monte Carlo analysis [12]. From this analysis, it was apparent that the coefficient of variation was only around 10% for 50 donors. However, Foti et al. [13] also observed a reduction in CYP2D6 activity in human liver microsomes. They concluded that the CYP2D6 enzyme appears to be less stable than the other CYP enzymes *in vitro*. Therefore, in order to monitor the CYP2D6 activity in the HLM experiments, Chapter 4 suggests to incubate a CYP2D6 probe alongside the test substrate tramadol. From this probe substrate activity data, an activity-adjustment factor (AAF) can be calculated, which corrects for any difference in measured and expected HLM activity. In this specific study, the calculation of AAF for midazolam and dextromethorphan involved a retrograde well-stirred and a parallel tube approach, respectively. Although this may give the impression that model selection is very arbitrary and the best model is picked to fit our purpose, it is not. The back-calculation of the *in vivo* CLint is more sensitive to the model selection for dextromethorphan (60% difference in *in vivo* CLint), compared to midazolam (13% difference in *in vivo* CLint). The reason is that the part of the blood clearance that is due to the CYP isoform these probes represent, is 71 L/h for dextromethorphan (by CYP2D6) and 22 L/h for midazolam (by CYP3A4). It is obvious that dextromethorphan's CYP2D6 clearance is approaching the limiting value of 90 L/h for hepatic blood flow. Therefore, dextromethorphan IVIVE will, as theory states, be better represented by the parallel tube model. In addition, the article that was used to derive the dextromethorphan *in vivo* CLint in Chapter 4, also favored the parallel tube approach and argued its feasibility. As a general approach, we propose to include reference probe substrates, indicative of the activity of the major enzymes involved in the metabolism of the test drug any time *in vitro* metabolism assays are initiated for a given test drug. Probe substrates specific for the different CYP enzymes can be looked up in the paper of Walsky & Obach [14]. A weakness of the study described in Chapter 4 was that only one compound was considered to assess the potential value of the use of AAF, and that data on more compounds in addition to tramadol need to be generated to further strengthen this finding.

The liver model that was used in these IVIVE predictions, was the well-stirred liver model. Other models that describe liver extraction are the parallel tube and dispersion model. Latter models typically provide an important advantage over the well-stirred liver model for high clearance compounds. For a low clearance compound, such as tramadol, the choice for the mathematically simpler well-stirred liver

model seems appropriate. It needs mentioning however, that upon applying the parallel tube model to tramadol *in vitro* data, the clearance increased approximately 20%. Although this higher clearance is closer to the observed adult clearance value, still the well-stirred model was preferred over the parallel tube model. It is the only liver model that could be used in the PBPK software tools as time-dependent model. The parallel tube and dispersion models can (for now) only be used as static liver models, independent of time. Additionally, this finding does not invalidate our pediatric predictions (in which the well-stirred liver model was used), since the retrograde model that is *in vivo*-calibrated, was used to this end.

The retrograde clearance model has been an essential aspect in the IVIVE model building process and in the mechanistic understanding of the different tramadol clearance contributors. Since it is constructed using *in vivo* phenotypic information, a retrograde model combines the mechanistic nature of a bottom-up model, with the prediction accuracy of a top-down model. Hence, it may serve as a reference, concerning hepatic clearance prediction and CYP enzyme involvement, to other tramadol IVIVE models, built up from *in vitro* metabolism data. Although such retrograde models provide attractive features, they display limitations as well. The assumptions that underlie a correct use of these retrograde models can be summarized as: i) the liver is perfusion rate-limited and behaves as a well-stirred or parallel-tubed compartment, ii) the investigated compound's hepatic clearance is linear, iii) composed of only a few major metabolic pathways, and iv) preferably dominates the total clearance. In line with the objectives of our work, the most adequate tramadol adult clearance model should be able to accurately capture tramadol total clearance, as well as CYP2D6 and renal contributions. The retrograde clearance model is created by mechanistically incorporating the *in vivo* observed renal and hepatic clearance with relevant enzyme contributions. Therefore, it will always accurately represent the total clearance with the appropriate renal and hepatic contribution. Additionally, the CYP2D6 contribution is also adequately built in into the model, as is indicated in Table 1, Chapter 5. Eventually, the tramadol retrograde model, backed-up by a body of *in vitro* metabolism evidence (as described above), was deemed fit and qualified for the bottom-up prediction of tramadol's pediatric total, CYP2D6, and renal clearance.

3 BOTTOM-UP PREDICTION OF TRAMADOL PEDIATRIC CLEARANCE

Using the retrograde model defined in Simcyp® as described above, the clearance was predicted bottom-up across the pediatric age range. Chapter 5 describes the comparison of these predicted clearances with the observed *in vivo* clearances. The *in vivo* reference data were derived from 2 published top-down (NONMEM) population PK models, and 1 WinNonlin® modelling effort with individually fitted clearance values. The data set for this WinNonlin® modelling analysis consisted of only richly sampled subjects with available plasma and urine data from the original NONMEM data set. The population PK models provided estimates for the maturation of total and CYP2D6 clearance, while the WinNonlin® fits added renal clearance estimates for the richly sampled subjects.

The two available (NONMEM) population PK models that should serve as a reference to compare the bottom-up predictions with, differed tremendously in the estimated total and CYP2D6 tramadol clearance maturation. Figures 4 and 5 in Chapter 5 illustrate this statement. From these two top-down models, the Hill-type model was chosen as the relevant maturation model, as it adequately described tramadol clearance maturation *in vivo*. This is because the Hill-type model: i) is per se physiologically more plausible than an exponential model; ii) was modelled using a pooled, extended dataset from neonates to adults; and iii) produced similar estimates for CYP2D6 clearance as the WinNonlin® fits. Although in very early life, an exponential function is an acceptable approximation of a Hill-function to describe maturation, caution is always advised when analyzing sparse data in a population PK analysis. This is certainly true in situations where identifiability issues for some estimated parameters, i.e. CYP2D6 clearance in the current population model, are present.

By visually comparing the Simcyp® bottom-up predicted clearance values to the *in vivo* Hill maturation model, the bottom-up approach seemed to capture the overall maturation trend well. However, a general underprediction was apparent in the total and CYP2D6 clearance maturation, but not in the renal clearance. This is illustrated in Chapter 5 for neonates/infants (Figures 4-6) and for the complete pediatric lifespan from birth to adulthood (Figures 7-8). Although reasons for the underprediction of the total tramadol clearance may be sought in alternative metabolic routes, this is unlikely to be the real explanation since the CYP2D6 clearance maturation suffers from a similar underprediction. Therefore, in Chapter 5, reasons for the underprediction were attributed to a difference in physiology (e.g. liver size) between the real and virtual pediatric subjects, both affecting predicted total and CYP2D6 clearance in a similar way. In order to challenge this theory, in Chapter 6, two other commercially available PBPK software packages (PK-Sim® and Gastroplus®) were evaluated in addition to Simcyp®. Prediction differences among the total and CYP2D6 clearance maturation - if observed - would only be

the result of differences in physiological information, included in these softwares, if for the rest similar assumptions were used to build the models.

The workflow implemented for the pediatric bottom-up clearance prediction in PK-Sim® and Gastroplus®, was analogous to the one described for Simcyp®. In short, physiological information contained in each software package was used to construct a software-specific retrograde model. The *in vivo* clearance values that were used to calibrate the retrograde models were extracted from the tramadol pooled popPK publication [15]. This way, similar tramadol retrograde models were obtained for the adult population and were qualified for total, CYP2D6 and renal clearance (see Chapter 6, Table 2). The choice of the PBPK software package has a significant impact on the predicted maturation of total, CYP2D6 and renal clearance (Chapter 6, Figure 2). As is derived from the Figures 4 and 5 in that chapter, each software tool has its own physiological database from which information is extracted in order to generate the virtual subjects. Since the retrograde models were constructed with physiological information specific to each software tool, differences in the predicted pediatric clearances would only appear if the relative maturation functions (in e.g. blood flows, organ size, enzyme ontogeny) differed between softwares. The renal clearance is similar between PK-Sim® and Simcyp®, but initially starts off higher in Gastroplus® and then declines. However, this comparison may not be completely fair, since for Gastroplus®, only the kidney blood flow was assumed to drive the maturation of the renal clearance, while GFR controlled the maturation in the other two softwares. The parameter mostly affecting tramadol clearance prediction in early life, is the ontogeny of CYP enzymes (expressed as pmol CYP/g liver tissue). While the ontogeny for CYP3A4 seems very similar for the different packages, this is not the case for CYP2D6 and CYP2B6. Ontogeny information on CYP2D6, a major contributor to the total clearance of tramadol, is quite different between virtual populations, generated by the different softwares. Whereas PK-Sim® assumes a mature CYP2D6 activity at term age, Simcyp® and PK-Sim® display a pronounced ontogeny function over the first 20 weeks of life. In addition, Simcyp® implemented maturation at the scalar 'microsomal protein per gram liver' (or MPPGL) as well, further slowing down the maturation of CYP enzymes. Clearly, this difference in physiological information explains the prediction bias for tramadol total and CYP2D6 clearance maturation. To come back to the initial underprediction issue raised in the previous paragraph, it is not the liver size, but rather the CYP2D6 ontogeny and MPPGL maturation that take too long, causing Simcyp® to underpredict the total and CYP2D6 clearance observed in Chapter 5. In addition, the conclusions from Chapter 5 & 6 relating to the maturation of CYP2D6 activity in Simcyp® seem to contradict, with CYP2D6 clearance in early life being well captured in Chapter 5 and not well-captured in Chapter 6. In Chapter 5, different publications were used to extract reference adult and pediatric data and an overlay of bottom-up and top-down clearance maturation was used to judge the PBPK model. In Chapter 6 a much cleaner approach was

adopted by calibrating the PBPK models to the adult part of the pooled popPK model, so that any discrepancy between PBPK and popPK predicted pediatric clearances was only due to the maturation function. In addition, the same virtual subjects were used to predict the clearance in the PBPK and the popPK models, making a one-on-one comparison feasible allowing to calculate a prediction error per subject. Interestingly, PK-Sim® that assumed the shortest maturation half-life for CYP2D6, provided the best predictions compared to *in vivo*. This finding suggests that CYP2D6 activity should be almost fully mature at birth. This was independently confirmed by another group, using *in vivo* derived ontogeny functions from propafenone [16]. This statement may lead to the belief that ontogeny functions are more accurate when they are based on *in vivo* data instead of *in vitro* data. The question is whether this observation is only valid for CYP2D6 or if this is part of a generalizable concept for most/all liver enzymes. It might be that for CYP2D6 alone *in vitro* activity data is inappropriate, given its specific stability issues *in vitro* (see Chapter 4). To check this, a similar analysis should be conducted for multiple enzymes, based on multiple model compounds to confirm this finding. However, in our opinion, there are 2 sides to the story. *In vivo*-derived maturation functions are appropriate to predict the *in vivo* situation per se. The downside is that they may be confounded by many other physiological factors, whilst the *in vitro*-derived ontogeny functions present a 'cleaner' approach. This is because in the latter situation confounding is physically eliminated by resecting relevant liver tissue and measuring subcellular activities ex vivo. So why would *in vitro*-derived functions be inappropriate? The answer is to be found in the variability associated with these ex vivo measurements and the way the ex vivo matrix is resected and prepared. Illustrative of this fact, are the source data for CYP2D6 maturation, which are different for Simcyp/Gastroplus [17, 18] compared to PK-Sim [17, 19]. This means that while in theory the *in vitro*-derived functions are much cleaner, apparently the variability on the *in vitro* activity data is that high that it results in different CYP2D6 maturation functions for different software tools. This indicates that there is a high need for standardization in the way hepatic microsomes are prepared and consensus needs to be achieved about the activity data to be used for appropriate maturation functions. Again, this should be confirmed for other enzymes as well.

At this time, hepatic and kidney transporters [20] are not accounted for in the tramadol popPK model (neither in the current PBPK models), but their influence cannot be completely ruled out on the estimation of the CYP2D6 clearance maturation in the popPK approach. We believe however, that this popPK analysis still provides a much 'cleaner' vision on CYP2D6 maturation, compared to using parent/metabolite urinary ratios. Furthermore, tramadol total clearance was best described by PK-Sim®, although a minimal bias still persisted (be it within the 2-fold boundary). Thus it might still be possible that another enzyme, contributing relatively more in early life and disappearing with aging, may still be involved (e.g. CYP3A7, FMO1) [21].

7

The general aim of this PhD dissertation was to evaluate bottom-up predictions of the hepatic clearance and identify the gaps leading to prediction inaccuracies in the bottom-up predicted (*in silico*) compared to the top-down estimated (*in vivo*) clearances. Identification of these gaps should lead to an increased understanding and subsequently implement the missing or suboptimal elements in the PBPK model structure. Since PBPK M&S makes the *a priori* distinction between the system's and the drug's properties, mechanistic model development with a well-chosen probe substrate offers a way to look beyond the drug's specific properties. Its PK is representative for some part of the underlying system that is under investigation. *In casu*, all elements to study the maturation of CYP2D6 were in place: i) tramadol's hepatic extraction is about 25% (low hepatic extraction), making it sensitive to differences in enzyme abundance; ii) CYP2D6 is a major contributor to tramadol's metabolism; and iii) *in vivo* maturation functions of total and CYP2D6 clearance were available from a pooled popPK analysis. This way, tramadol provided us, via its metabolism, a means to study the ontogeny of the CYP2D6 enzyme, rather than just focusing on the disposition of tramadol.

To conclude, the investigation of tramadol's *in vitro* metabolism in HLM and rhCYP systems, yielded pro's and con's to both systems in providing enzyme contributions to the hepatic clearance. Furthermore, these contributions were scaled up from *in vitro* (HLM and rhCYP) to *in vivo*, the so-called *in vitro*-to-*in vivo* extrapolation (IVIVE). An important observation in this context was that, although pooled HLM were used for the experiments, the *in vitro* activity of the CYP2D6 enzyme did not represent the typical population *in vitro* value. Calculation of an AAF by specific probe substrates, i.e. dextromethorphan for CYP2D6, appears to resolve this *in vitro* inaccuracy, but needs to be confirmed with additional compounds. The construction of a retrograde tramadol clearance model (initially performed in Simcyp®), in parallel to the IVIVE clearance models, provided an invaluable feedback system to iteratively check assumptions and identify mechanisms involved in tramadol elimination. Eventually, this tramadol retrograde model, certified by the body of collected *in vitro* metabolism data, was qualified in terms of total, CYP2D6, and renal tramadol clearance in order to initiate pediatric bottom-up clearance predictions. Next, the most relevant, commercially available PBPK modeling and simulation softwares (PK-Sim®, Simcyp®, Gastroplus®) were implemented with the tramadol retrograde model for prediction of the pediatric clearance. These software tools seemed hugely versatile platforms enabling modelers to construct complex generic whole-body PBPK models, using a spectrum of pre-defined building blocks to approximate any clinical scenario *in silico*. Although 3 similar variants of the same retrograde clearance model for tramadol were constructed in the 3 software tools, comparison of the bottom-up clearance predictions with the top-down estimation of the clearance, revealed marked differences. The origin of this discrepancy could be traced back to the level of the

biological/physiological data underlying the clearance predictions in every tool. Apparently, uncertainty surrounded the ontogeny function of the CYP2D6 enzyme in children, under 2 years of age. Interestingly, the PBPK model with the shortest maturation half-life for CYP2D6 (PK-Sim®), correctly predicted CYP2D6 maturation in tramadol clearance in early life, as well as over the complete pediatric age range. This research, combining bottom-up and top-down modelling methodologies, showed potential to identify and fill knowledge gaps in the developing pediatric physiological information, thereby increasing the confidence with which doses are predicted for pediatrics

7

4 REFERENCES

1. Dunne J, Rodriguez WJ, Murphy MD, Beasley BN, Burckart GJ, Filie JD, et al. Extrapolation of adult data and other data in pediatric drug-development programs. Pediatrics. 2011;128(5):e1242-9.

2. Anderson BJ, Holford NH. Mechanism-based concepts of size and maturity in pharmacokinetics. Annu Rev Pharmacol Toxicol. 2008;48:303-32.

3. Johnson TN. The problems in scaling adult drug doses to children. Arch Dis Child. 2008;93(3):207-11.

4. Barrett JS, Della Casa Alberighi O, Laer S, Meibohm B. Physiologically based pharmacokinetic (PBPK) modeling in children. Clin Pharmacol Ther. 2012;92(1):40-9.

5. Leong R, Vieira ML, Zhao P, Mulugeta Y, Lee CS, Huang SM, et al. Regulatory experience with physiologically based pharmacokinetic modeling for pediatric drug trials. Clin Pharmacol Ther. 2012;91(5):926-31.

6. Cornish-Bowden A. Fundamentals of Enzyme Kinetics. 3rd ed. London: Portland Press; 2004.

7. Proctor NJ, Tucker GT, Rostami-Hodjegan A. Predicting drug clearance from recombinantly expressed CYPs: intersystem extrapolation factors. Xenobiotica. 2004;34(2):151-78.

8. Nirogi R, Palacharla RC, Uthukam V, Manoharan A, Srikakolapu SR, Kalaikadhiban I, et al. Chemical inhibitors of CYP450 enzymes in liver microsomes: combining selectivity and unbound fractions to guide selection of appropriate concentration in phenotyping assays. Xenobiotica. 2015;45(2):95-106.

9. Chen Y, Liu L, Nguyen K, Fretland AJ. Utility of intersystem extrapolation factors in early reaction phenotyping and the quantitative extrapolation of human liver microsomal intrinsic clearance using recombinant cytochromes P450. Drug Metab Dispos. 2011;39(3):373-82.

10. Berezhkovskiy LM, Liu N, Halladay JS. Consistency of the novel equations for determination of hepatic clearance and drug time course in liver that account for the difference in drug ionization in extracellular and intracellular tissue water. J Pharm Sci. 2012;101(2):516-8.

11. Hallifax D, Houston JB. Saturable uptake of lipophilic amine drugs into isolated hepatocytes: Mechanisms and consequences for quantitative clearance prediction. Drug Metab Dispos. 2007;35(8):1325-32.

12. Crespi CF, E; Patten, C. Optimizing Donor Number for Consistent Pooled Human Liver Microsomes (Application Note 465). 2006 [cited; Available from: https://www.corning.com/media/worldwide/cls/documents/an_DL_GT_070_Optimizing_Donor_Number_for_Consistent_Pooled_Human_Liver_Microsomes.pdf

13. Foti RS, Fisher MB. Impact of incubation conditions on bufuralol human clearance predictions: enzyme lability and nonspecific binding. Drug Metab Dispos. 2004;32(3):295-304.

14. Walsky RL, Obach RS. Validated assays for human cytochrome P450 activities. Drug Metab Dispos. 2004;32(6):647-60.

15. Allegaert K, Holford N, Anderson BJ, Holford S, Stuber F, Rochette A, et al. Tramadol and o-desmethyl tramadol clearance maturation and disposition in humans: a pooled pharmacokinetic study. Clin Pharmacokinet. 2015;54(2):167-78.

16. Upreti VV, Wahlstrom JL. Meta-analysis of hepatic cytochrome P450 ontogeny to underwrite the prediction of pediatric pharmacokinetics using physiologically based pharmacokinetic modeling. J Clin Pharmacol. 2016;56(3):266-83.

17. Treluyer JM, Jacqz-Aigrain E, Alvarez F, Cresteil T. Expression of CYP2D6 in developing human liver. Eur J Biochem. 1991;202(2):583-8.

18. Johnson TN, Rostami-Hodjegan A, Tucker GT. Prediction of the clearance of eleven drugs and associated variability in neonates, infants and children. Clin Pharmacokinet. 2006;45(9):931-56.

19. Stevens JC, Marsh SA, Zaya MJ, Regina KJ, Divakaran K, Le M, et al. Developmental changes in human liver CYP2D6 expression. Drug Metab Dispos. 2008;36(8):1587-93.

20. Tzvetkov MV, Saadatmand AR, Lotsch J, Tegeder I, Stingl JC, Brockmoller J. Genetically Polymorphic OCT1: Another Piece in the Puzzle of the Variable Pharmacokinetics and Pharmacodynamics of the Opioidergic Drug Tramadol. Clin Pharmacol Ther. 2011;90(1):143-50.

21. de Wildt SN. Profound changes in drug metabolism enzymes and possible effects on drug therapy in neonates and children. Expert Opin Drug Metab Toxicol. 2011;7(8):935-48.

7

CHAPTER 8

BROADER INTERNATIONAL CONTEXT, RELEVANCE, AND FUTURE PERSPECTIVES

8

TABLE OF CONTENTS

8

1 BROADER INTERNATIONAL CONTEXT & RELEVANCE

1.1 FINDING THE RIGHT DOSE FOR CHILDREN

Over the years, different approaches have been applied in order to derive an appropriate dose of a drug for children, starting from the dose administered to adults. Different options are available to calculate the pediatric dose for first-in-pediatric trials as well as in clinical practice. A set of rules, defined in many pharmacological textbooks are applied clinically, which use some covariates (body surface area, body weight, age) to scale the adult drug dose to the pediatric one, e.g. Clark's, Young's, Webster's, Fried's, Shirkey's, Salisbury rules. These rules are arbitrary, typically using linear scaling of some covariate to derive the child's dose (BSA or bodyweight). An internal FDA study of 2012 pointed out that any of these rules is not suitable to calculate an appropriate drug dose for every age group. Above 3 months of age the Shirkey, Webster, Clark and Salisbury rules provided the best results with 60% of children meeting an acceptable dose prediction. Below 3 months of age, Clark's and Salisbury's rules predicted an acceptable dose for 45% of pediatric patients, while the other methods landed at 5%. Therefore these methods were deemed unreliable [1]. The reason is that the correlation between dose and some covariate over the full pediatric age range is non-linear. It is well known that in selected cases, e.g. carbamazepine, children even need higher weight-adjusted doses than adults. Hence, in a linear scaling technique (i.e. only correcting for body weight with a fixed allometric exponent of 1, see below) involving some easily obtainable covariate, these scenarios are unanticipated [2]. In order to provide a solution, some authors have suggested to calculate the pediatric dose using a single fixed (based on allometric theory) or an estimated (from the data) allometric exponent. The theoretical concept is that this exponent correlates the dose to metabolic function. This method already provided better results than the empirical dosing rules, but still underperforms in early life. The rationale for dose adjustment in pediatric indications should be driven by differences in pharmacokinetics, pharmacodynamics, disease or a combination of these factors [2, 3]. When the clearance mechanisms are immature or impaired, any empirical scaling method is prone to inaccuracies if not specifically corrected for. Indeed, approaches providing superior predictive power incorporated different estimated exponents varying with weight or age, or involved interspecies scaling using adult rat, dog and human clearance values [1, 4]. The only solution to transcend empiricism in pediatric dose scaling is by implementing physiologically-based modelling, either in the form of bottom-up [5-7] or top-down [8-10] models. Moreover, it is currently recognized that pediatric doses should be derived based on actual acquired (clinical) data using a combination of bottom-up and top-down methods. The bottom-up approach allows to 'explore' and anticipate *in vivo* changes in pediatric dose safety/efficacy/toxicity by combining known physiological and genetic information with *in vitro* data. In the top-down approach, clinical

studies are set up to 'confirm' appropriate dosing regimens with acceptable safety/efficacy profiles and explain the observed *in vivo* variability [11]. Furthermore, given the future direction of the pharmacological area to a more personalized medicine approach, an apt combination of 'bottom-up' and 'top-down' techniques is the only way forward in terms of understanding and treating pediatric disease by providing the right dose at the right time.

As Cella et al. [2] state, efforts in two distinct areas of pediatric pharmacology research are needed. The first is to re-examine dose recommendations for older drugs, frequently used off-label in pediatric clinical practice. The collected pharmacokinetic, safety and efficacy data in adults and various pediatric age groups, may be implemented in a model-based approach to rethink dosing algorithms in the clinic, based on the totality of available data . The second area is the early drug development phase in which no data in children are readily available. Typically, PBPK models are used as a model-based bridging tool (from preclinical and adult clinical data) to calculate primary PK parameters and predict pediatric doses [2]. Although PBPK models are increasingly applied in early development, they are only as good as the scientific knowledge base used to construct them. Still today, knowledge gaps remain in some of the system's parameters, including the frequency, and functional activity of transporters, and of many metabolic enzymes beyond the CYPs, as well as the components of tissues influencing drug distribution, beyond the established ones consisting of lipids, phospholipids, and plasma proteins. In addition, some system's parameters, e.g. the ontogeny of CYP enzymes and transporters, or disease effects on CYP and transporter activity, are derived from *in vitro* or *ex vivo* tissues/tissue fractions and typically contain a certain level of uncertainty with respect to how representative they are for the *in vivo* situation. Improved confidence in (patho)physiological model parameter values may be gained by simultaneous modeling of the PK of several compounds, exposed to the same clinical conditions, e.g. neonatal immaturity, disease state, pregnancy, co-medication. In this situation, drugs can be used as *in vivo* probes to reflect and quantify the underlying properties of the system [12]. This PhD dissertation describes such efforts. Specifically, this work evaluates currently applied PBPK models by challenging their bottom-up prediction capabilities to a top-down model-based approach, using clinically collected pediatric PK data of the off-label used drug tramadol. Specifically, the bottom-up prediction of tramadol hepatic clearance was compared to the top-down estimated hepatic clearance in pediatric life, with a particular focus on CYP2D6 maturation in neonates and infants. This analysis showed that there is a substantial difference in the *in vitro* ontogeny information about CYP2D6 that is integrated in different PBPK software platforms (PK-Sim®, Simcyp®, Gastroplus®). By comparing bottom-up predicted with top-down estimated CYP2D6 clearance maturation, it was concluded that the true CYP2D6 activity should be already progressively matured at birth, which was independently confirmed by a recent publication from another group [13]. We acknowledge that uncertainty associated with *in vitro* derived enzyme

ontogeny can be decreased by deriving these ontogeny functions from *in vivo* data. Therefore, adequate probes allow to derive *in vivo* ontogeny functions of specific enzymes, in this case tramadol for CYP2D6. Furthermore, CYP2D6 is a relevant metabolic enzyme involved in the breakdown of many lipophilic, basic drugs, e.g. different antidepressants, antipsychotics, antiarrhythmics, antiemetics, ß-blockers and opioids [14]. Hence, since this work updated our current understanding of the system's parameter 'CYP2D6 ontogeny', it can be considered relevant for the bottom-up prediction of any CYP2D6-metabolized compound in pediatric drug research. Obviously, in order to increase the confidence related to CYP2D6 maturation, more compounds are needed that can confirm these findings. Moreover, although the workflow presented in this thesis provides an attractive and promising technique, the general approach still needs validation by expanding to more compounds, treated by (other) multiple enzymes/transporters.

1.2 Precision dosing and PBPK

> "Tonight, I'm launching a new Precision Medicine Initiative to bring us closer to curing diseases like cancer and diabetes — and to give all of us access to the personalized information we need to keep ourselves and our families healthier."
>
> — President Barack Obama, State of the Union Address, January 20, 2015

In his State of the Union Address, U.S. President Barrack Obama announced a research initiative that aims at taking precision medicine to a new level – the Precision Medicine Initiative (PMI). This program will leverage disease prevention and treatment strategies that account for individual variability in genetic make-up, environment, and lifestyle. Proteomics, metabolomics, genomics, and bioinformatics methods will all contribute to patient characterization and should lead to a better understanding of the mechanisms of disease. Ultimately, the knowledge gained from this PMI platform will inform clinical practice and support an optimal individual therapy. The immediate focus of the PMI lies in facing the long standing challenges in cancer research. In the longer term, the PMI wants to apply the precision medicine concept in order to generate knowledge applicable to the full range of health and disease [15, 16].

An integral part of precision medicine is the administration of a precise dose of medication to a specific individual to treat his/her disease, which is a critical step in the larger mission to deliver personalized healthcare. Modelling and simulation in drug research includes top-down (mixed-effects modelling) and bottom-up (physiologically-based modelling) techniques. Both modelling approaches have a proven

track record of rationalizing drug development and making it more efficient [17, 18]. However, they have yet to become a tool in 'point-of-care testing', a medical diagnostic technique at or near the point of care. At the PBPK side, work is in progress to create 'virtual twins'. A virtual twin is the *in silico* counterpart of a real patient that matches the patient's characteristics. These characteristics would include both intrinsic factors (age, weight, height, sex, race, and genetic information on, among others, metabolic enzymes and transporters) and extrinsic factors (environmental factors and co-medications). In this way, appropriate prior information, relevant for drug dosing, is incorporated to calculate the 'precise' dose for a given individual at the bedside. Because PBPK models have already implemented the mechanistic and structural framework to combine these intrinsic and extrinsic factors, this modelling technique is bound to profit from the large amounts of biochemical and physiological data that will become available during the PMI research program [7, 19]. Although the concepts put forward in this paragraph seem very promising and attractive, they still are in a premature stage. While scientists are developing ways to integrate these ideas (virtual twins, tool in point-of-care testing) into a modeling framework, and the necessary data are being collected, this work-in-progress is needed to preserve a role for PBPK in the precision dosing era.

1.3 PBPK AND THE LEARN-CONFIRM PARADIGM

In 1997, a commentary by Sheiner [20] illustrated that theory of alternating induction and deduction could be applied to drug development. The induction phase represents learning from experience, while deduction seeks to confirm from what has been learned. Applying this principle to drug development would make the whole process more adequate (better drugs) and efficient (sooner). In his vision, the application of modelling and simulation in clinical drug development stimulates the implementation of the 'learn-confirm' paradigm. In rational and more quantitative model-based drug development, these two elements (learn & confirm) reflect a proper balance that should be maintained throughout the development timeline. The better the 'learn' phase (science), the more efficient and appropriate the 'confirm' phases (phase 3 and drug approval). In this mindset, physiologically-based PK is perfectly positioned as it offers a way to integrate knowledge on a drug's properties, routinely collected during drug development, in all of its forms, in combination with our vast knowledge of the (human) biological system and how this determines PK and/or PD. In the preclinical stage, mainly *in silico/in vitro* drug data are collected. At this point, by differentiating system- and drug-related parameters, PBPK is already capable of predicting drug exposure *in vivo* in both animals and man. Different 'what-if' scenarios may be investigated and varying study designs explored. As the drug development program moves along, clinical *in vivo* data from healthy volunteers and patients are increasingly becoming available. A pivotal milestone in this process is to evaluate whether mechanistic preclinical (*in vitro* and animal) models accurately predict the acquired first-in-human *in vivo* data. This evaluation appraises the present

understanding (learning) of the drug's absorption and disposition, and of the biological system, and hence may or may not be confirmatory. Therefore, some authors suggested to expand the classical paradigm to 'predict-learn-confirm' [21, 22]. This is exactly why PBPK nowadays is considered to be an integral part of pediatric drug development. The mechanistic framework allows to gain insights into the drug's absorption & disposition and in pediatric physiology in one effort. Leong et al. [21] stated that the utility of PBPK models includes optimization of the pediatric study design, evaluation of clinically relevant covariate effects, and the attainment of insights related to the ontogeny of previously undocumented biological processes. As a consequence, even before one pediatric plasma sample for a new drug candidate is analyzed, different dosing regimens, clinical trial designs, and drug-drug interactions have already been explored *in silico*. This implies that the 'learning' in pediatric drug development has shifted from *post* to *pre* pediatric clinical trials, making them 'confirmatory' rather than 'exploratory'.

The real innovation of this technology is that at any point in the global drug development process, the PBPK model is iteratively updated to represent the state-of-art understanding of the new candidate's pharmacology. Even more than simply being a quantitative modelling and simulation tool, aimed at rationalizing drug development, PBPK ensures the continuous flow of data from preclinical to and within clinical phases of development. It becomes a platform by which scientists from different disciplines and backgrounds may communicate and leverage the existing knowledge of the drug as well as of the biological system.

Applied to this PhD dissertation, the 'predict-learn-confirm' concept was really tangible at two points in this project, in particular in the extrapolation of tramadol's *in vitro* enzymatic contributions to an *in vivo* hepatic clearance (IVIVE). First, freshly obtained tramadol intrinsic clearances (CLints) for each CYP enzyme from HLM, were scaled to the *in vivo* hepatic clearance. In this initial attempt, an underprediction of about 50% in the hepatic clearance was apparent ('predict'). An important shortcoming of *in vitro* HLM assays, lies in the fact that no cellular membrane is present and the metabolic enzymes are freely accessible. Basic lipophilic amines (such as tramadol), however, tend to accumulate in the intracellular environment, and are unable to do so in the HLM assay. The phenomenon in which basic drugs (or the other way around for acids) accumulate in more acidic (blood pH = 7.4 vs. intracellular pH = 7.2) environments, is called ion trapping ('learn'). A ratio of 1.58, representing the fold intracellular accumulation of tramadol, was implemented in the IVIVE and enhanced the prediction of the hepatic clearance ('confirm'). Although we had the intention to further confirm this behavior in *in vitro* hepatocyte cultures (with intact cell membranes), there was no guarantee that the same phenomenon would occur in the hepatocytes *in vitro* [23]. Therefore, given the uncertainty associated with this specific aspect of the *in vitro* model, we did not perform these

experiments. **Second**, in the comparison of CYP enzyme contributions between the HLM IVIVE clearance model (*in vitro*) and the retrograde clearance model (*in vivo*), the *in vitro* HLM contribution of CYP2D6 was underpredicted ('predict'). Subsequent incubations with dextromethorphan, a CYP2D6 probe, in that same HLM batch, yielded a similar underestimation of the CYP2D6 contribution ('learn'). To resolve this issue, an activity-adjustment factor (AAF) was calculated, based on the probe substrate data of dextromethorphan. Multiplication of the CYP2D6 activity with the AAF, corrected the inaccurate CYP2D6 contribution ('confirm'). Additional compounds need to be studied though, to confirm this finding.

1.4 DID PEDIATRIC REGULATIONS BY FDA & EMA DELIVER?

Since 2002 in the U.S. (FDA) and 2007 in Europe (EMA), a combination of incentives and requirements were put in place to ensure that medicines are regularly studied, developed and approved to meet the therapeutic needs of children. What has changed since then and, more importantly, did these initiatives deliver?

In the 5-year EMA progress report [24], the initiatives seemed to have had an impact on the number of pediatric clinical trials and pediatric subjects enrolled in such studies. By the end of 2012, 600 pediatric investigations were agreed upon by the Agency, of which 453 concerned medicines not yet authorized in the E.U.. The consequence is apparent in Figure 1. Now, for the first time, children below 23 months of age are enrolled in clinical trials, who were normally not included prior to 2008. In addition, the numbers of participating children in clinical trials in E.U. has increased vastly [24].

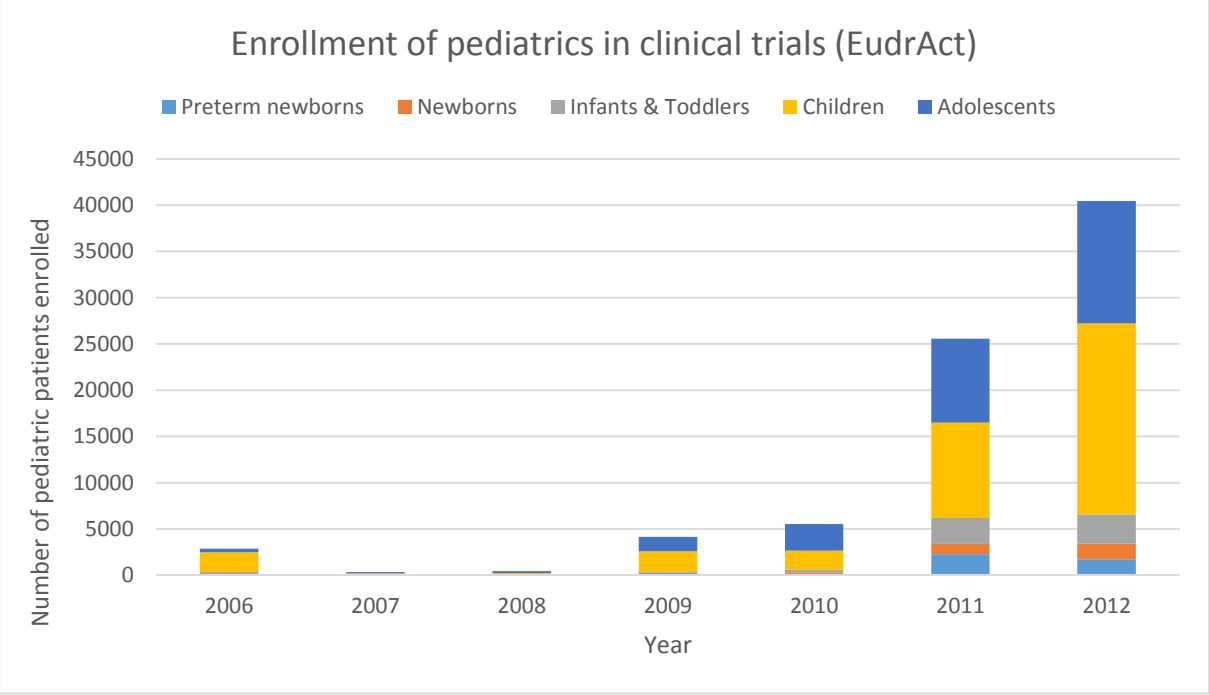

FIGURE 1: NUMBER OF PEDIATRIC PATIENTS ENROLLED IN CLINICAL TRAILS FROM 2006 TO 2012, BASED ON THE EMA PROGRESS REPORT

In the U.S., the enactment in 2012 of the U.S. Food and Drug Administration Safety and Innovation Act (FDASIA) updated the Pediatric Research Equity Act (PREA) and the Best Pharmaceuticals for Children Act (BPCA) and made them permanent. This has led to an enormous increase in the number of pediatric studies and permitted new pediatric labeling of more than 600 products, 149 of which occurred since the passage of FDASIA [25]. Moreover, a fundamental change in U.S. and E.U. company culture is apparent, since pediatric drug development is now accepted as an integral part of the overall drug development program [24, 25]. Although these reports indicate positive effects on the extent of pediatric drug research and the availability of drugs for children, a study by Corny et al. [26] questions the impact of regulatory measures at the clinical level. The objective of Corny's study was to compare unlicensed and off-label drug use in children, before and after governmental initiatives in E.U. and U.S. in 2007. In Europe, only a marginal decrease in unlicensed and off-label drug use prevalence was observed. In the U.S., there was not even a single report on studying pediatric unlicensed or off-label drug use after 2007. Obviously, there is a discrepancy between the efforts by industry to provide more and better drugs for children, and the clinical adoption of these new drug therapies (in E.U.). Reasons for this discrepancy may be that clinicians continue to use older drugs because they have more experience with these drugs in current day-to-day clinical practice. In addition, wide ranges of unlicensed and off-label drug use rates were observed. This is mainly due to differences in off-label and unlicensed use between institutions, as well as inconsistencies in the definition of 'unlicensed' and 'off-label' [26]. Although off-label and unlicensed drug use in children will never be completely ruled out, health care institutions should continue to collaborate in pediatric research networks (e.g. European Network of Paediatric Research (EMA), National Pediatric Research Network (FDA), SAFEPEDRUG and BPCRN (local initiatives)) with the main aim to harmonize the way in which pediatric drugs are applied in clinical practice. Provided that essential fundamental pediatric drug research is continued to increase our understanding of the processes that differ between adults and children, and that efforts remain to harmonize the research results and clinical implementation, only then, significant improvements will be made in a safer and more effective use of therapeutic agents in children.

2 FUTURE PERSPECTIVES

PBPK models are being increasingly used in drug research and development for the prediction of ADME in healthy volunteers and/or pediatrics. At this point, however, they are far from perfect. Our knowledge of their strengths and weaknesses increases, as their applications grow. The main challenge facing the further successful expansion of these models' application probably lies in the system-related parameters. With the growing understanding of physiological processes changing over a person's life time and with disease, and more specifically the way that system (body) elements interact with the drug, physiologically-based models are becoming increasingly complex. Hence, the amount and the level of detail needed in the systems-related parameters increases exponentially. Systems data, such as the abundance, activity, and ontogeny of non-CYP enzymes and transporters in various tissues, absorption-related data and how these are changing with age/disease status, are generally still lacking. Moreover, the quality and extent of biological data needed for predictions becomes even more challenging when applying PBPK for the mechanistic prediction of biologics or safety/efficacy assessments. The collection of this kind of data is typically difficult, therefore, initiatives bringing together industrial and academic partners that share in the burden as well as in the benefit of these research projects, may be set up in a pre-competitive manner [17, 18, 27]. In the meantime, a strategy to investigate the effect of a given diseased condition on drug disposition, may consist of altering the relevant (set of) physiological parameter(s) in the PBPK software to represent a diseased value, e.g. the influence of hypo-albuminaemia (decreased plasma albumin concentrations in the model) on drug elimination and distribution (manuscript accepted). In this manuscript, treatment of critically ill patients suffering from hypo-albuminemia, is suggested to benefit from increasing the dose/dosing frequency, based on albumin levels. However, PBPK simulations in virtual hypoalbuminemic patients predict that the dose should not be increased (and rather decreased in some situations). This manuscript illustrates that the full (patho)physiological knowledge of critical illness does not need to be fully clarified in order to help resolve selected issues in understanding some aspects of the drug's behavior in a particular disease. This example shows that PBPK models are hugely versatile and may be deployed in all areas of drug research. Given the *a priori* separation of drug and system data in a fully mechanistic framework, any population may be studied under any situation, as long as the detail in both data sets allows. Moreover, fully integrated sensitivity analyses may further indicate which parameters strongly influence the altered drug disposition in several conditions and lead to designing the necessary set of studies/experiments to decrease the uncertainty in some of the most influential assumptions .

The integration of pharmacokinetic and pharmacodynamic data in fully mechanistic PBPK-PD models, with associated variability, should come to fruition in the near future. By mapping drug-receptor interactions and their variation due to age/disease, etc., pharmacological responses may be predicted

and extrapolated to different populations. However, due to the increasing model complexity, PBPK-PD models should be rigorously evaluated and reported in a transparent and reproducible manner. In fact, as of July 29, 2016 the EMA has made their 'Guideline on the qualification and reporting of PBPK modelling and simulation' available for public consultation [28], stressing the importance of transparency in PBPK M&S. Underlying assumptions should always be specified so that identification of the relevant physiological processes is clearly defined [7, 18]. In particular for pediatrics, it is becoming more evident that, due to the increasing number of pediatric studies, adult safety profiles cannot be directly translated to children even when the disease processes are the same [7]. It is essential that future studies involve defining the pediatric PK-PD relationship to better assess safety and efficacy, if prospective clinical studies on PK-derived dosing recommendations suggest a different outcome between adults and children. Efforts should continue to define how one can optimally combine top-down and bottom-up approaches in order to increase our understanding of developmental pharmacology, by looking beyond compound-specific properties [10, 29]. A methodology that could prove really useful in this setup are microdose/microtracer studies, especially for drugs with complex metabolism and/or poor understanding of ontogeny. Microtracer studies involve the administration of radiolabeled drug together with a therapeutic dose of the drug via the same or another route, while in microdose studies, only the radiolabeled drug is given in a subtherapeutic dose. Recently, initiatives exposing infants to ^{14}C-paracetamol and ^{14}C-midazolam proved the feasibility of this approach. A perceived risk of adverse effects exists due to the administered radio-activity but it is unfounded [30].

Currently, there is a clear distinction between the typical 'bottom-up' and 'top-down' approaches. Quite recently, it has been suggested that combining both approaches in a so-called 'middle-out' approach could have beneficial value [31-33]. Bottom-up techniques have the great advantage of extrapolating outside the studied population and experimental conditions. The compromise is that they are defined by a complex system of differential equations with a considerable number of model parameters. Typically, model parameters that carry much uncertainty and are hard to derive *in vitro* or *in silico*, are adjusted so that the model could match the clinical observations. However, there are considerable methodological issues (i.e. structural and practical identifiability), hampering the successful implementation of this 'middle-out' approach. Methodological research and advances in computer sciences should enable this field to further develop as the middle-out approach integrates information from *in vitro* or *in silico* experiments together with information derived from observed clinical data [31, 34]. By combining the separate skill sets of the historically separated 'bottom-up and 'top-down' techniques, mechanistically sound models with clinical relevance should result [32].

Maybe one of the most important areas needing attention, is the communication between scientists involved in the broader context of physiologically-based PKPD modelling. Because of the highly-versatile

nature of these tools, scientists from many diverse disciplines in industry (experimentalists, biologists, epidemiologists, pharmacists, pharmacologists and mathematical modellers), who have traditionally been working apart, need to learn how to interact and communicate on a new level [17, 27]. At the same time, many pediatric prescribers from the clinical setting still dwell in the empiricism of the previous era. Modellers and care physicians need to be able to communicate at the same level in order for the patient to benefit from the innovation in pharmacological research [2]. From the moment different stakeholders in industry as well as in the clinic will be able to efficiently communicate with one another, only then will the true value of model-based pharmacological research emerge, yielding improved health in (pediatric) patients.

8

3 REFERENCES

1. Mahmood I. Dosing in children: a critical review of the pharmacokinetic allometric scaling and modelling approaches in paediatric drug development and clinical settings. Clin Pharmacokinet. 2014;53(4):327-46.

2. Cella M, Knibbe C, Danhof M, Della Pasqua O. What is the right dose for children? Br J Clin Pharmacol. 2010;70(4):597-603.

3. Johnson TN. The problems in scaling adult drug doses to children. Arch Dis Child. 2008;93(3):207-11.

4. Knibbe CA, Zuideveld KP, Aarts LP, Kuks PF, Danhof M. Allometric relationships between the pharmacokinetics of propofol in rats, children and adults. Br J Clin Pharmacol. 2005;59(6):705-11.

5. Johnson TN, Rostami-Hodjegan A. Resurgence in the use of physiologically based pharmacokinetic models in pediatric clinical pharmacology: parallel shift in incorporating the knowledge of biological elements and increased applicability to drug development and clinical practice. Paediatr Anaesth. 2011;21(3):291-301.

6. Edginton AN, Schmitt W, Voith B, Willmann S. A mechanistic approach for the scaling of clearance in children. Clin Pharmacokinet. 2006;45(7):683-704.

7. Barrett JS, Della Casa Alberighi O, Laer S, Meibohm B. Physiologically based pharmacokinetic (PBPK) modeling in children. Clin Pharmacol Ther. 2012;92(1):40-9.

8. Areberg J, Christophersen JS, Poulsen MN, Larsen F, Molz KH. The pharmacokinetics of escitalopram in patients with hepatic impairment. AAPS J. 2006;8(1):E14-9.

9. De Cock RF, Piana C, Krekels EH, Danhof M, Allegaert K, Knibbe CA. The role of population PK-PD modelling in paediatric clinical research. Eur J Clin Pharmacol. 2011;67 Suppl 1:5-16.

10. Krekels EH, Tibboel D, Knibbe CA. Pediatric pharmacology: current efforts and future goals to improve clinical practice. Expert Opin Drug Metab Toxicol. 2015;11(11):1679-82.

11. Sage DP, Kulczar C, Roth W, Liu W, Knipp GT. Persistent pharmacokinetic challenges to pediatric drug development. Front Genet. 2014;5:281.

12. Rowland M, Lesko LJ, Rostami-Hodjegan A. Physiologically Based Pharmacokinetics Is Impacting Drug Development and Regulatory Decision Making. CPT Pharmacometrics Syst Pharmacol. 2015;4(6):313-5.

13. Upreti VV, Wahlstrom JL. Meta-analysis of hepatic cytochrome P450 ontogeny to underwrite the prediction of pediatric pharmacokinetics using physiologically based pharmacokinetic modeling. J Clin Pharmacol. 2016;56(3):266-83.

14. Zhou SF. Polymorphism of Human Cytochrome P450 2D6 and Its Clinical Significance Part I. Clinical pharmacokinetics. 2009;48(11):689-723.

15. Collins FS, Varmus H. A new initiative on precision medicine. N Engl J Med. 2015;372(9):793-5.

16. Suzanne M. What You Need to Know about the Precision Medicine Initiative. The Roundtable: Our Thoughts About Model Based Drug Development. Certara website; 2015.

17. Jones H, Rowland-Yeo K. Basic concepts in physiologically based pharmacokinetic modeling in drug discovery and development. CPT Pharmacometrics Syst Pharmacol. 2013;2:e63.

18. Maharaj AR, Edginton AN. Physiologically based pharmacokinetic modeling and simulation in pediatric drug development. CPT Pharmacometrics Syst Pharmacol. 2014;3:e150.

19. Pade D. Precision Dosing Using PBPK Modeling. The Roundtable: Our Thoughts About Model Based Drug Development. Certara Website; 2015.

20. Sheiner LB. Learning versus confirming in clinical drug development. Clin Pharmacol Ther. 1997;61(3):275-91.

21. Leong R, Vieira MLT, Zhao P, Mulugeta Y, Lee CS, Huang SM, et al. Regulatory Experience With Physiologically Based Pharmacokinetic Modeling for Pediatric Drug Trials. Clin Pharmacol Ther. 2012.

22. Zhao P, Zhang L, Grillo JA, Liu Q, Bullock JM, Moon YJ, et al. Applications of physiologically based pharmacokinetic (PBPK) modeling and simulation during regulatory review. Clin Pharmacol Ther. 2011;89(2):259-67.

23. Berezhkovskiy LM. The Corrected Traditional Equations for Calculation of Hepatic Clearance that Account for the Difference in Drug Ionization in Extracellular and Intracellular Tissue Water and the Corresponding Corrected PBPK Equation. Journal of Pharmaceutical Sciences. 2011;100(3):1167-83.

24. EMA 5-year Progress Report. Better Medicines for Children From Concept to Reality: European Medicines Agency; 2013.

25. FDA Status Report to Congress. Best Pharmaceuticals for Children Act and Pediatric Research Equity Act: FDA; 2016.

26. Corny J, Lebel D, Bailey B, Bussieres JF. Unlicensed and Off-Label Drug Use in Children Before and After Pediatric Governmental Initiatives. J Pediatr Pharmacol Ther. 2015;20(4):316-28.

27. Jamei M. Recent Advances in Development and Application of Physiologically-Based Pharmacokinetic (PBPK) Models: a Transition from Academic Curiosity to Regulatory Acceptance. Curr Pharmacol Rep. 2016;2:161-9.

28. EMA Guidelines. Draft guideline on the qualification and reporting of physiologically based pharmacokinetic (PBPK) modelling and simulation. 2016 29-07-2016 [cited 24-08-2016]; EMA/CHMP/458101/2016]. Available from: http://www.ema.europa.eu/ema/doc_index.jsp?curl=pages/includes/document/document_detail.jsp?webContentId=WC500211315&murl=menus/document_library/document_library.jsp&mid=0b01ac058009a3dc

29. Allegaert K, Smits A, van den Anker JN. Physiologically based pharmacokinetic modeling in pediatric drug development: a clinician's request for a more integrated approach. J Biomed Biotechnol. 2012;2012:103763.

30. Turner MA, Mooij MG, Vaes WH, Windhorst AD, Hendrikse NH, Knibbe CA, et al. Pediatric microdose and microtracer studies using 14C in Europe. Clin Pharmacol Ther. 2015;98(3):234-7.

31. Li R, Barton HA, Yates PD, Ghosh A, Wolford AC, Riccardi KA, et al. A "middle-out" approach to human pharmacokinetic predictions for OATP substrates using physiologically-based pharmacokinetic modeling. J Pharmacokinet Pharmacodyn. 2014;41(3):197-209.

32. Tsamandouras N, Rostami-Hodjegan A, Aarons L. Combining the 'bottom up' and 'top down' approaches in pharmacokinetic modelling: fitting PBPK models to observed clinical data. Br J Clin Pharmacol. 2015;79(1):48-55.

33. Tylutki Z, Polak S, Wisniowska B. Top-down, Bottom-up and Middle-out Strategies for Drug Cardiac Safety Assessment via Modeling and Simulations. Curr Pharmacol Rep. 2016;2:171-7.

34. Feng S, Shi J, Parrott N, Hu P, Weber C, Martin-Facklam M, et al. Combining 'Bottom-Up' and 'Top-Down' Methods to Assess Ethnic Difference in Clearance: Bitopertin as an Example. Clin Pharmacokinet. 2016;55(7):823-32.

CURRICULUM VITAE

Huybrecht T'jollyn

Birth date & place: 24/04/1987, Gent

Address: Iepenstraat 78, 9000 Gent

E-mail: htjollyn@gmail.com

Phone: +32 499 38 74 57

Education

Bachelor in Pharmaceutical Sciences 2005-2008 (distinction)

Master in Pharmaceutical Sciences, Drug Development 2008-2010 (distinction)

Teaching experience

Organization of the practical exercises accompanying the course: "Medische biochemie" in the 3re bachelor of pharmaceutical sciences. 108 contact hours/year (2011 – 2016)

Organization of and conducting the exercise sessions accompanying the course "Pharmacokinetics" in the 2nd bachelor of pharmaceutical sciences. 12 contact hours/year (2014 – 2016)

Organization of and conducting the exercise sessions accompanying the course "PK-PD in drug development" in the 1st master of drug development, pharmaceutical sciences. 12 contact hours/year (2015 – 2016)

Pharmacology course for the 2nd and 3rd year Bachelor in Midwifery. 12 contact hours/year (2015 – present)

Pharmacology course for the Belgian Midwifes Association. 18 contact hours/year (2015 – present)

Supervised student dissertations

Hanne De Mildt: "*In vitro* metabolism of tramadol as input for physiologically-based pharmacokinetic modelling and simulating", 1st Master of Pharmaceutical Care, Feb-June 2012

Elien De Thaye: "Bioanalysis and pharmacokinetics of galantamine in plasma of rabbits", 1st Master of Drug Development, Feb-June 2013

Charlotte Hap: "Optimization of an UPLC-MSMS method for analysis of *in vitro* metabolism studies of propofol", MaNaMa Industrial Pharmacy Feb-May 2014

Somaya Ahalli: "LC/MS-MS method development of CYP2B6 substrates efavirenz, bupropion and their metabolites in HLM, 1st Master of Pharmaceutical Care, Feb-June 2015

Internship

At Model-Based Drug Development, Quantitative Sciences, Janssen Pharmaceutica NV, Beerse (June 2015 – Sept 2015)

1. Mechanistic modelling of hepatic transport from *in vitro* transporter assays
2. Integration of PopPK and viral kinetic modelling for a novel HepC compound

Communications

Scientific publications

T'jollyn H., Colin P., Van Bocxlaer J., Vermeulen A. A PBPK perspective on the clinical utility of albumin-based dose adjustments in critically ill patients. *Manuscript under review*

T'jollyn H., Snoeys J., Van Bocxlaer J., De Bock L., Annaert P., Cuyckens F., Van Peer A., Allegaert K., Mannens G., Vermeulen A., Boussery K. Strategies for determining correct CYP450 contributions in hepatic clearance predictions using a PBPK modelling approach. 2016//:1-7 (AOP).

T'jollyn H., Snoeys, J., Vermeulen A., Michelet R., Cuyckens F., Mannens G., Van Peer A., Annaert P., Allegaert K., Van Bocxlaer J., Boussery K. Physiologically Based Pharmacokinetic Predictions

of Tramadol Exposure Throughout Pediatric Life: an Analysis of the Different Clearance Contributors with Emphasis on CYP2D6 Maturation. *AAPS J* (2015) Nov; 17(6):1376-87.

T'jollyn H, Snoeys J, Colin P, Van Bocxlaer J, Annaert P, Cuyckens F, Vermeulen A, Van Peer A, Allegaert K, Mannens G, Boussery K. Physiology-Based IVIVE Predictions of Tramadol from *in vitro* Metabolism Data. *Pharm Res.* (2015) 32(1):260-74.

T'jollyn H., Boussery K., Mortishire-Smith R.J., Coe K., De Boeck B., Van Bocxlaer J.F., Mannens G. Evaluation of three state-of-the-art metabolite prediction software packages (Meteor, MetaSite, and StarDrop) through independent and synergistic use. *Drug Metabolism and Disposition* (2011) 39:11

Vercruysse J., T'jollyn H., De Thaye E., Tzachev C., Remon J.P., Vermeulen A., Van Bocxlaer J., Vervaet C. Pharmacokinetics of galantamine in plasma and brain for different intranasal formulations: an experimental *in vivo* study. *Manuscript under review*

Colin P., De Bock L., T'jollyn H., Boussery K., Van Bocxlaer J. Development and validation of a fast and uniform approach to quantify beta-lactam antibiotics in human plasma by solid phase extraction-liquid chromatography-electrospray-tandem mass spectrometry. *Talanta* 103 (2013) 285-293

De Bock L., Boussery K., Colin P., De Smet J., T'jollyn H., Van Bocxlaer J. Development and validation of a fast and sensitive UPLC-MS/MS method for the simultaneous quantification of six probe metabolites for the *in vitro* determination of cytochrome P450 activity. *Talanta* 89 (2012) 209-216

Poster presentations

T'jollyn, H; Colin, P; Van Bocxlaer, J; Vermeulen, A. Hypoalbuminaemia: new quantitative insights using PBPK simulations
Presented at the 24th PAGE meeting, June 2-5th, 2015, Hersonissos, Crete

T'jollyn, H; Snoeys, J; Mannens, G; Van Peer, A; Allegaert, K; Boussery, K; Van Bocxlaer, J; Vermeulen, A. Physiologically-based pharmacokinetic modeling and simulation can aid popPK model building in estimation of the CYP2D6 maturation clearance in early life. Presented at the 7th Systems Pharmacology Symposium , April 22-25th, 2014, Noorwijkerhout, The Netherlands

T'jollyn, H; Colin, P; Snoeys, J; Van Bocxlaer, J; Van Peer, A; Allegaert, K; Mannens, G; Boussery, K. Quantitative IVIVE-linked pediatric PBPK predictions: case study tramadol. Presented at Knowledge for Growth, May 30th, 2013, Gent, B

Oral presentations

"SAFE-PEDRUG Work Package 4: Physiology-based PK modelling" Presented at the SAFE-PEDRUG Stakeholder meeting. December 18th, 2014, Huis van de Toekomst, Vilvoorde, Belgium

"Quantitative *in vitro*-based PBPK predictions of tramadol: setting the correct CYP contributions" Presented at the Simcyp® webinar. November 20th, 2014

"Pharmacokinetics of galantamine in rabbits after single and multiple intranasal administration" Presented at the Bio-Analytical Meeting. February 14th, 2014, FFW, Gent, Belgium

"Quantitative *in vitro*-based pediatric PBPK predictions of tramadol: how close can we get?" Presented at Pharmacometrics Benelux meeting, edition Modeling and simulation in pediatric drug development. November 28th, 2013, Astellas, Leiden, The Netherlands

"PBPK model building and dose selection- case study tramadol" Presented at the 6th Juvenile Toxicity Symposium. May 16-17th, 2013. Janssen R&D, Beerse, Belgium

(International) Conferences & workshops attended

Annual BSMS Meeting on Mass Spectrometry. April 29, 2011. Mons, Belgium

Belgian Pediatric Clinical Research Network. September 9, 2011. Palace of the Academies, Brussels, Belgium

Simcyp® hands-on workshop: Incorporating population variability into mechanistic prediction of PK and modelling PK-PD- Part 1. September 19-21, 2011. Kenwood Hall, Sheffield, UK

Pharmacometrics Benelux: Pharmacometric concepts in the development of biological products for immunology disorders. November 22, 2012. MSD, Oss, The Netherlands.

The Sheiner/Rowland course. A one-week workshop on advanced methods in Pharmacokinetics/Pharmacodynamics. April 8-12, 2013. Children's Hospital, Philadelphia, USA.

Pharmacometrics Benelux: Translational Modeling - exemplifying the animal to human extrapolation. April 18, 2013, Antwerp University, Antwerp, Belgium.

Knowledge for Growth 2013. May 5th 2013. ICC, Gent, Belgium .

6th Juvenile Toxicity Symposium. May 16-17, 2013. Janssen R&D, Beerse, Belgium

Flames Summer School Methodology & Statistics. September 16-20, 2013. KU Leuven, Leuven, Belgium

Pharmacometrics Benelux: Modeling and simulation in pediatric drug development. 28/11/2013, Astellas, Leiden, The Netherlands.

7th Noordwijkerhout Symposium on Pharmacokinetics, Pharmacodynamics and Systems Pharmacology. April 23-25, 2013. Noordwijkerhout, The Netherlands.

Course on project management (organized by UGent Doctoral Schools, transferable skills section)

Simcyp focused workshop on PK/PD parameter estimation. September 22-23, 2014. Sheffield, UK.

Comprehensive course in Pharmacokinetics: Fundamental principles and Application to Contemporary Drug development. April 29-30, 2015. Campus Gasthuisberg, Leuven, Belgium

24th PAGE meeting. June 2-5, 2015, Hersonissos, Crete

25th PAGE meeting. June 7-10, 2016, Lisboa, Portugal